Investigating the Role of the Srs2 DNA Helicase during Meiosis in *S. cerevisiae*

Laura Jayne Hunt

A thesis submitted for the degree of:

Doctor of Philosophy

January 2018

University of Sheffield

Department of Molecular Biology and Biotechnology

Abstract

During cell division, duplicated chromosomes must be segregated faithfully to prevent aneuploidy in daughter cells. In meiosis, there are two rounds of division following a single round of DNA replication. In the first meiotic division, crossovers formed between homologous chromosomes, via homologous recombination, ensure correct DNA segregation. Homologous recombination is intitated by DNA double-strand breaks (DSBs), which are processed to form single-stranded DNA that can invade donor duplexes to effect repair. In yeast, formation of nucleoprotein-filaments (NPFs) by RecA homologues Rad51 and Dmc1 promotes strand invasion into sister chromatids or homologous chromosomes, respectively. I investigated the meiotic role of Srs2, a multi-functional DNA helicase that is thought to regulate mitotic strand invasion via promotion of Synthesis-Dependent Strand Annealing to prevent hyper-recombination.

To investigate meiotic phenotypes of *srs2* strains, including deficient meiotic progression and reduced spore viability, I analysed nuclear and spindle pole body (SPB) division of spread chromatin. I found a significant increase in single nucleus cells with divided SPBs in *srs2*, suggesting cells are attempting to progress into second meiosis despite the nucleus failing to divide. Using strains with integrated *TetO* repeats and TetR-GFP to observe division at a single chromosome level, I conclude that homologues and sister chromatids are moving apart even when the nucleus fails to divide. Immunofluorescence of Rad51, in *srs2* cells, revealed bright Rad51 foci appearing as aggregates under standard microscopy, which colocalise with RPA. These are dependent on *SPO11*, *NDT80* and Rad51 strand invasion activity, but independent of *MEK1* and *SAE2*, suggesting the meiotic phenotype is related to DSB formation and pachytene exit but independent of DSB resection or inter-homologue strand invasion. Interestingly, a partial rescue is observed when MRX complex formation is hindered. To determine whether Rad51 aggregation occurs at known recombination hotspots, I have prepared strains for ChIPSeq to analyse any alterations in the distribution of Rad51 along the DNA. Finally, the implications for the role of Srs2 during meiosis raised by these novel observations will be discussed.

Acknowledgements

I would like to thank a great many people for their contributions, great and small, without whom this thesis may never have occurred. Emily, a genuine inspiration who taught me so much about science and life. Tzu-Ling, whose wonderful energy brought so much life and light to the lab. Ta-Chung, who laid such excellent groundwork for this project and who was always happy to help. Emad, who taught me cytology and always pushed me to achieve. Hasan & Julia, who brought such life and joy to the lab at a crucial time in my studies, for which I may never be able to find the words to express my gratitude. Emma & Dan, for their cheery chats, encouragement and support. And everyone who worked in our labs over the years, for making them a much better place to be: Iliyana, Inam, Chris, Selina, James, Jess, Claudio, Thane, Stephen and more.

Enormous thanks are due to Alastair, without whom I could never have made it to this point. Bin, whose constant advice and teaching made me a better scientist. Pete, whose generous nature and expert knowledge has saved me countless times during this journey. John, Geoff, and Julie whose kind encouragement, each at different points during the very beginning of my scientific career, gave me more self-belief than they may ever know. And, importantly, the people with whom I really started my scientific journey, who have been there unfailingly ever since, the wonderful Katie, Klaudia, Louise, Hayley & Vicki; the sisters I never had.

I will be eternally grateful to those people who made Sheffield a better place to be just by their existence within it. My amazing friends Carla, Agata, and Ellie, and the unceasingly kind Claire who adopted me into Holly Hagg, the only place in Sheffield I ever felt truly relaxed. Everyone at MBB who helped make my time in the department so enjoyable and productive. And Matthew who transformed this city for me, filling it with warmth and laughter, into a place to call home.

Finally, most importantly, I wish to thank my family, Mum, Dad, Kasper & Naina, who moulded me into the person and the scientist that I am, for their constant, unwavering support and love, and for the knowledge that they would always catch me if ever I fell.

"Remember, kids, the only difference between screwing around and science is writing it down" – Adam Savage

Table of Contents

Abbreviations

ATP	Adenosine triphosphate
ADP	Adenosine diphosphate
bp	Base Pair
BSCR	Barrier to Sister Chromatid Repair
CO	Crossover
dAG	Diploid *S. cerevisiae* strain from the A. Goldman lab
DAPI	4',6-diamidino-2-phenylindole
dHJ	Double Holliday junction
dH_2O	Distilled water
ddH_2O	Deionised distilled water (a.k.a "MilliQ")
DNA	Deoxyribonucleic acid
dNTP	Deoxyribonucleotide triphosphate
DSB	Double-strand break
DSBR	Double-strand break repair
dsDNA	Double-stranded DNA
EDTA	Ethylenediaminetetraacetic acid
hAG	Haploid *S. cerevisiae* strain from the A. Goldman lab
HR	Homologous recombination
JM	Joint molecule
MI	Meiosis I
MII	Meiosis II
MRX	Complex of Mre11, Rad50 and Xrs2
NHEJ	Non-Homologous End Joining
NPF	Nucleoprotein-filament

nt	Nucleotide
NCO	Non-crossover
OD_x	Optical Density/Absorbance at x nm
OD_{600}	OD_{600} = 1 indicates a density of 1 OD of yeast cells/ml
1 OD of cells	Approximately 1-5 x 10^7 cells
pAG	Plasmid-containing *E. coli* strain from the A. Goldman lab
PCR	Polymerase chain reaction
PRR	Post-replicative repair
SC	Synaptonemal complex
SDSA	Synthesis-dependent strand annealing
ssDNA	Single-stranded DNA
SPB	Spindle pole body

Throughout this document, genes and proteins from *Saccharomyces cerevisiae* will be written as follows:

- Dominant allele: Italicised, all capitalised (*YFG1*)
- Recessive allele: Italicised, all lower case (*yfg1*)
- Wild-type protein: Non-italicised, first letter capitalised (Yfg1)

When referring to other species appropriate prefixes will be used for clarity. For example, proteins from *Homo sapiens* or *Schizosaccharomyces pombe* would be named hYfg1 or spYfg1, respectively.

Throughout this document, error bars represent the 95% Confidence Interval (i.e. 1.96x Standard Error of the Mean) unless otherwise stated.

Chapter 1 General Introduction

1.1 *Saccharomyces cerevisiae*

The budding yeast, *Saccharomyces cerevisiae*, is a unicellular eukaryote that shares many orthologous genes and processes with higher eukaryotes, many of which are highly conserved. Studying yeast can therefore be used both to understand unicellular organisms and to infer conclusions in higher organisms. As a model organism, *S. cerevisiae* is easy to grow, with a relatively short life cycle and requiring simple materials. It has a relatively small and well-mapped genome, and has been extensively studied, with a wide range of genotypic variants and resources available. Furthermore, budding yeasts exist in both haploid and diploid forms, making *S. cerevisiae* significantly more convenient for genetic manipulation than other model organisms (Figure 1.1).

Importantly for the purposes of this study, eukaryotic yeast models are valuable for the study of meiosis, which is evolutionarily conserved from fungi to humans (Mimitou and Symington, 2009). In particular, *S. cerevisiae* can be induced to undergo synchronised meiosis in the laboratory. Expression of the master regulator of gametogenesis, *IME1*, is inhibited by PKA and TORC1 signalling pathways which are active in the presence of glucose and nitrogen sources/amino acids, respectively (Weidberg *et al.*, 2016). Consequently, lack of these nutrients results in expression of *IME1* and entry into meiosis. This regulation can be exploited by culturing the yeast in a pre-sporulation media with a non-fermentable carbon source, lacking glucose, which synchronises the cells in G1 phase arrest (Honigberg and Purnapatre, 2003). Upon transfer to sporulation media, which lacks both glucose and nitrogen sources, cells enter meiosis synchronously allowing for consistent and comparable analyses of meiosis over the course of time.

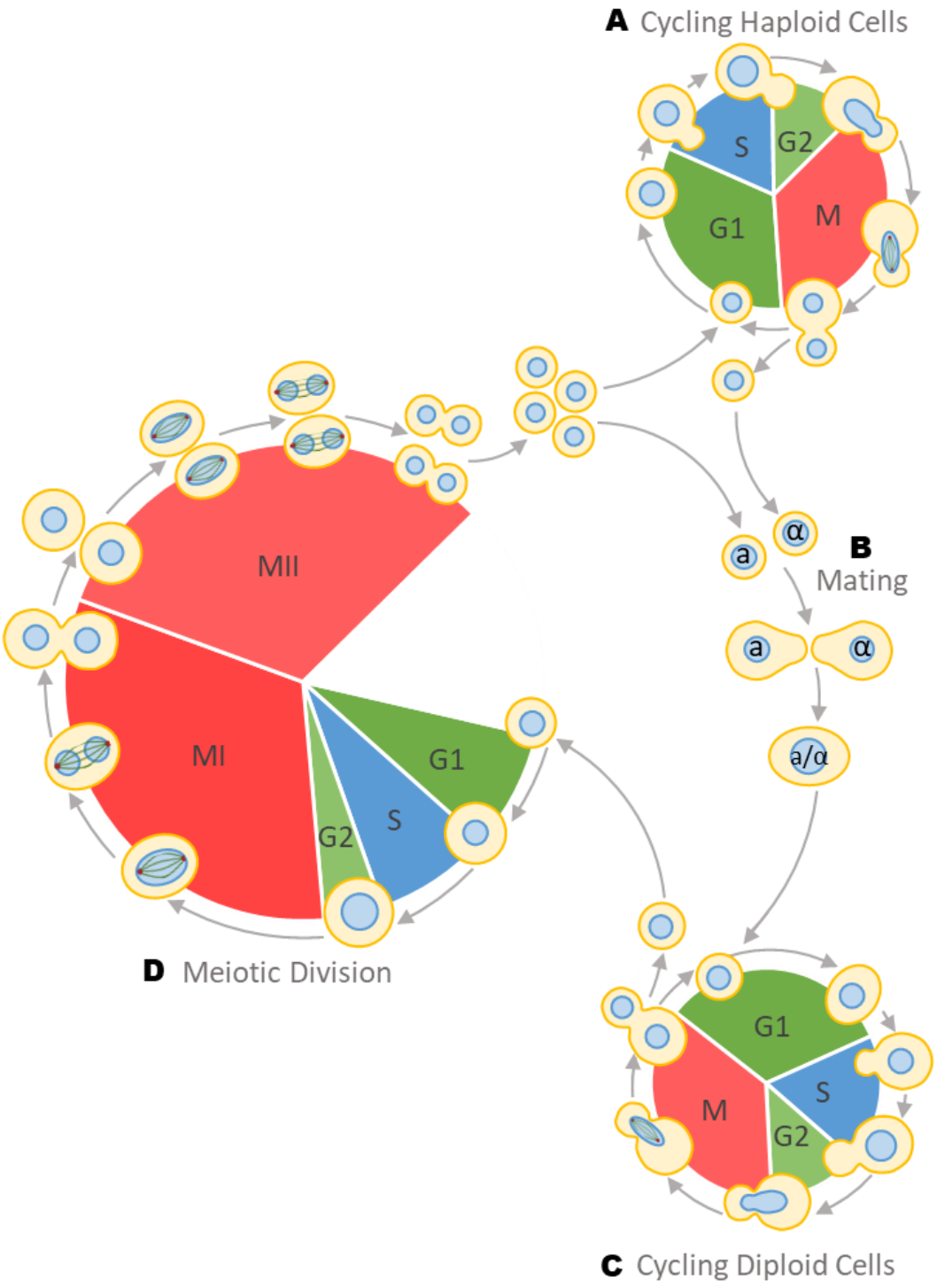

Figure 1.1 The life cycle of *Saccharomyces cerevisiae*. Budding yeast is a valuable model organism due to its natural ability to exist in a cycling haploid state (A) that can mate with a haploid of opposing mating type (**a** or α) to produce diploid cells (B). Diploid cells can also naturally exist in a cycling mitotic state (C) or undergo meiosis (D) to form haploid spore cells. The mitotic cycles and meiotic division process can be subdivided into several phases: G1 phase, in which the cells undergo growth; S phase, in which DNA is replicated; G2 phase, in which the cell prepares for division; and a division phase, either one mitotic division (M) or two rounds of meiotic division (MI + MII).

1.2 Mitosis and Meiosis

Eukaryotic organisms undergo two distinct modes of cell division to generate daughter cells from parental cells: mitosis and meiosis. Mitotic cell division is the process by which non-germline cells replicate and divide to produce genetically identical daughter cells (Figure 1.2). Faithful transmission of genetic information to the next generation of cells is essential for maintaining a healthy population of somatic cells, without which cells can lose heterozygosity and become predisposed to cancer. Mitotic DNA repair processes are therefore biased towards maintaining the original DNA sequence. Conversely, in meiosis, parental DNA is actively recombined during the repair of programmed DNA damage. In this way, meiosis produces daughter cells with unique genotypes, which allow for adaptation to the environment and the development of evolutionary advantages. However, this process increases the potential for errors during cell division. Following a single round of DNA replication, meiotic cells undergo two sequential rounds of DNA segregation, compared to only one during mitosis (Figures 1.2 & 1.3). In the first round of division, Meiosis I, the cells undergo reductional division in which homologues separate to opposite poles of the cell, producing two haploid cells, each containing two sister chromatids. These cells then divide again in Meiosis II, equationally, producing haploid gametes containing a single chromatid each. These haploid cells can then fuse with haploids of an opposite mating type, forming the next generation of diploid cells. To ensure that all the DNA segregates correctly at each stage, meiosis must be carefully controlled by a range of processes. Any missegregation of DNA during meiosis can generate daughter cells containing too many or too few chromosomes. In humans, such aneuploidy generally prevents formation of viable offspring and those that do survive may present severe phenotypes (Hassold and Hunt, 2001).

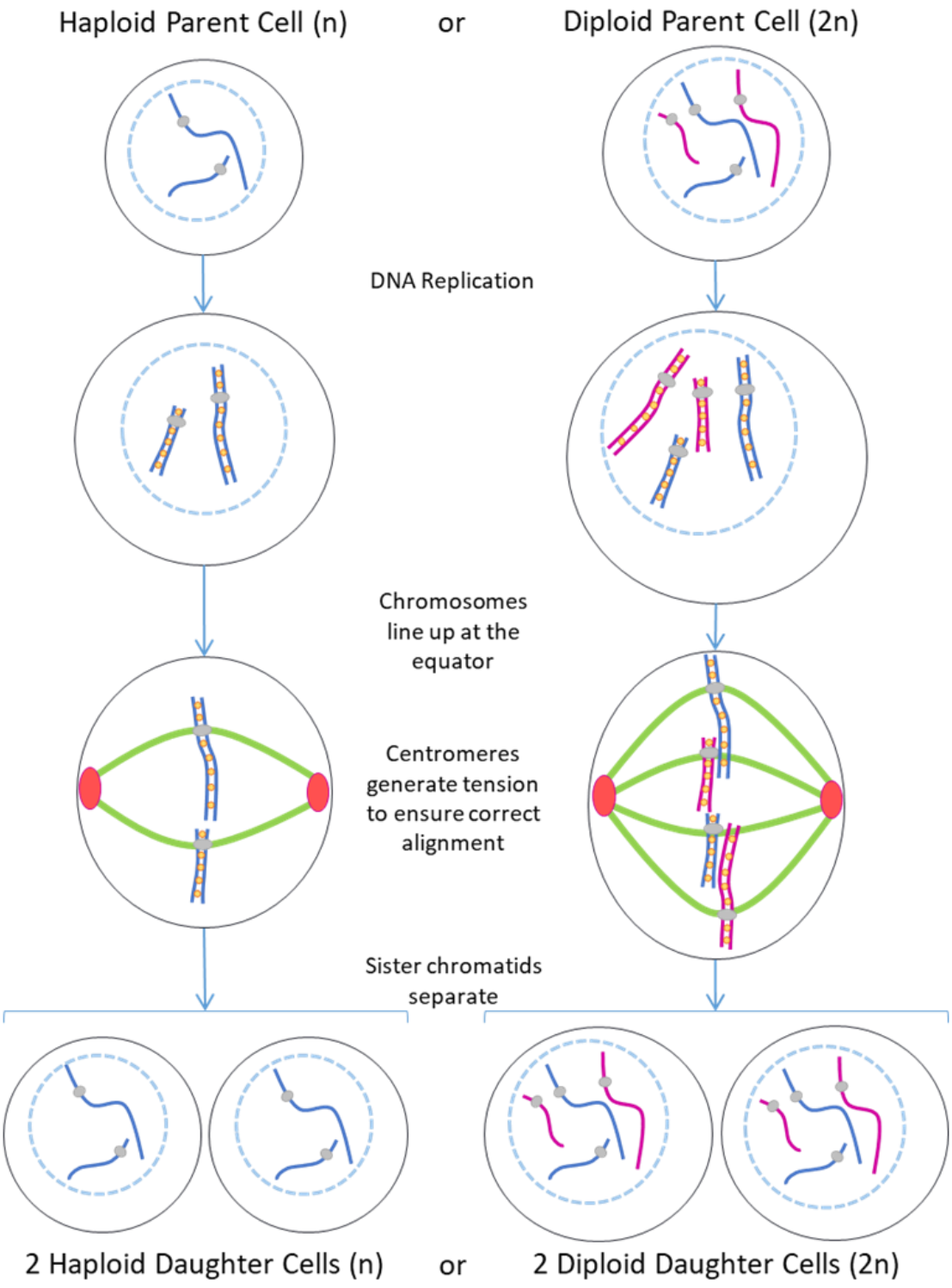

Figure 1.2 Mitotic division of haploid or diploid parent cells produce a genetically identical pair of haploid or diploid daughter cells, respectively, following DNA replication and cell division. Chromosomes (blue and pink) are replicated, then held together by sister chromatid cohesion (orange). Chromosomes are attached at their centromeres (grey) to tubulin spindles (green) and are held between spindle pole bodies (red) to ensure correct alignment and segregation.

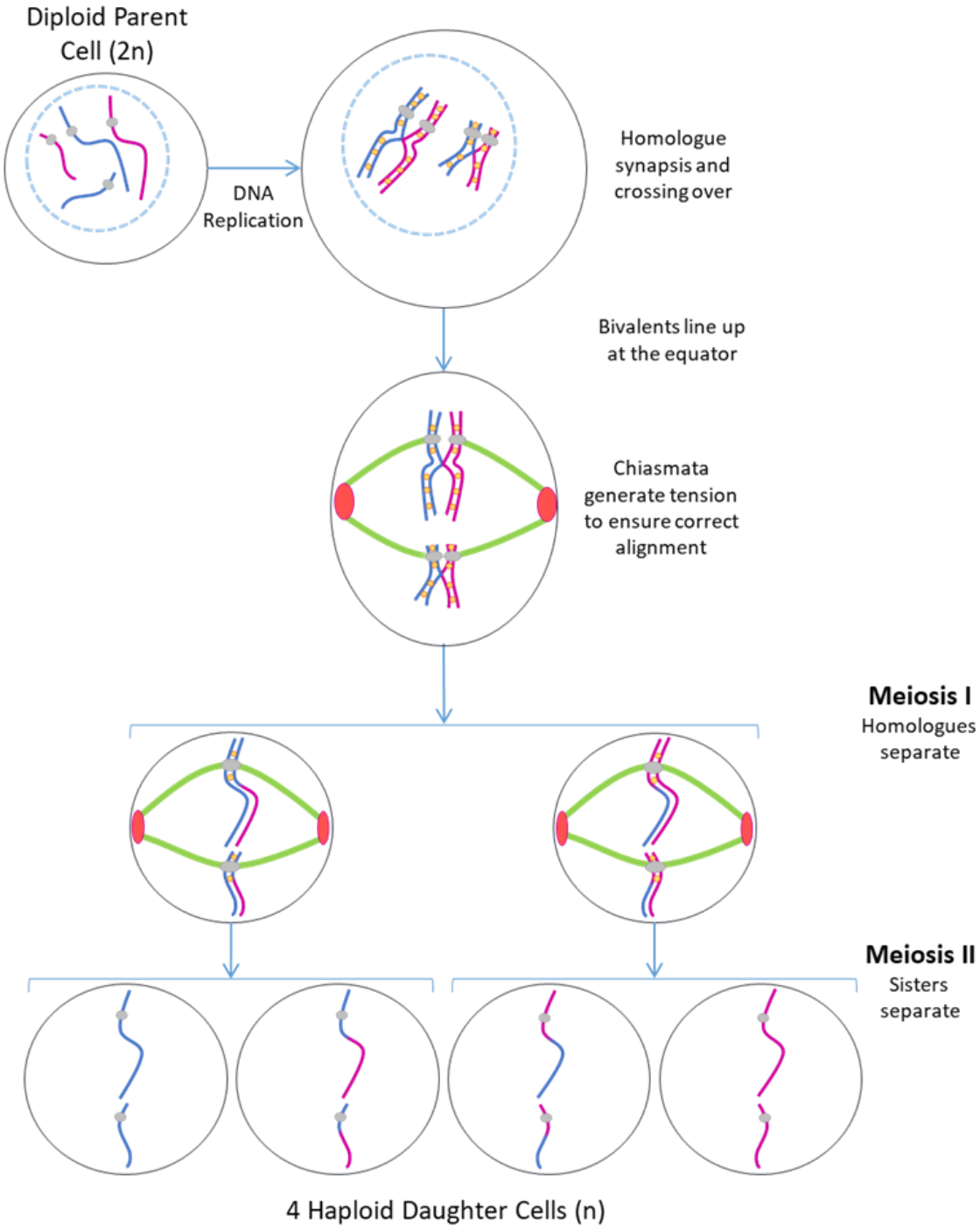

Figure 1.3 Meiotic division of diploid parent cells produces four genetically distinct haploid daughter cells following DNA replication, crossover formation, and two sequential rounds of division. Chromosomes (blue and pink) are replicated, then held together by sister chromatid cohesion (orange). Chromosomes are attached at their centromeres (grey) to tubulin spindles (green) and are held between spindle pole bodies (red) to ensure correct alignment and segregation. In Meiosis I this alignment is also dependent on crossovers between the homologues.

1.3 Meiotic Phases and Metaphase Alignment

Each stage of meiosis, Meiosis I and Meiosis II, can be subdivided into several phases: Prophase, Metaphase, Anaphase and Telophase. During Prophase I, the duplicated chromosomes condense and synapse, usually facilitated by the synaptonemal complex (SC), and form DNA crossovers. The SC is a tripartite, proteinaceous structure that forms along the length of homologues, providing a scaffold for interaction between the homologues (Gao and Colaiacovo, 2018). Once synapsed, the two homologues, each with a pair of sister chromatids, are collectively known as bivalents.

During cell division, accurate segregation of chromosomes is ensured by the positioning of chromosomes between poles and the requirement for checkpoint satisfaction before anaphase. In yeast Metaphase I, chromosomes line up along the equatorial plane of the cell, also known as the 'metaphase plate', due to pulling forces acting along tubulin spindles between the chromosomes and protein structures at the poles of the cell called 'spindle pole bodies' (SPB). The equivalent protein structures in higher eukaryotes, centrosomes, are generally only featured in mitosis and spermatogenesis. During oocyte meiosis, centromeres are dispensed with and tension along the spindles is instead generated between the chromosomes and crosslinked parallel microtubules at the spindle poles (Radford *et al.*, 2015).

Tubulin spindles are attached at the chromosome centromeres by kinetochore protein assemblies. During mitosis or the second meiotic division, sister chromatids held together with cohesin have bi-oriented kinetochores to produce the necessary tension, ensuring correct alignment and segregation segregation (Duro and Marston, 2015). In Meiosis I, sister chromatids of each homologue, held together by cohesion, must

segregate to the same daughter cell so their kinetochores are mechanically fused and mono-oriented towards the same pole during the first division (Sarangapani *et al.*, 2014). To generate the necessary spindle tension during the first meiotic division, most organisms use homologous recombination (HR), see Section 1.4, producing crossovers between the homologues that can be visualised as chiasmata. These crossovers ensure homologues align correctly in metaphase, remain associated until anaphase and then segregate to opposite daughter cells (Duro and Marston, 2015; Smith and Nicolas, 1998).

Once all bivalents are correctly aligned, checkpoints are satisfied by the presence of appropriate tubulin connections at the kinetochores and tension along the spindles, lifting inhibition of the anaphase promoting complex (APC) and allowing the cells progress through Anaphase I (Shonn *et al.*, 2000). As the chromosomes are pulled to opposite poles of the cell, sister chromatid cohesion is lost along chromosome arms and the chromatids move to towards their respective poles as the spindles shorten (Clift and Marston, 2011; Klein *et al.*, 1999). Pericentromeric cohesion, however, is retained as it will be required to ensure correct spindle tension and sister chromatid segregation during Metaphase II (Clift and Marston, 2011).

In Telophase I, cells undergo cytokinesis to form two separate cells, the nuclear envelopes reform and the chromatin decondenses. Meiosis II can then progress in the same manner, but instead of homologous chromosomes it is the sister chromatids that will separate during Anaphase II, producing four haploid daughter cells from one parental diploid.

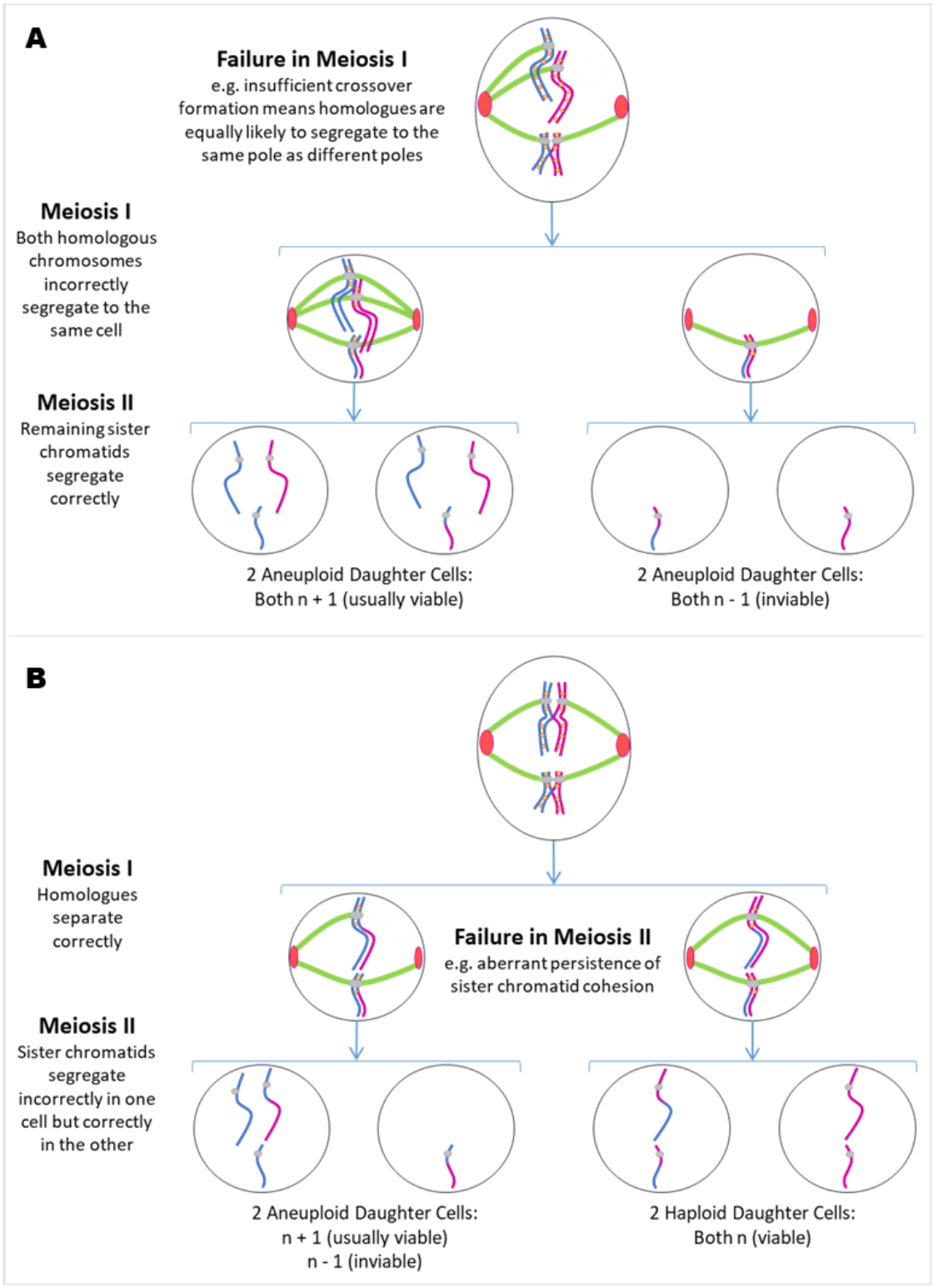

Figure 1.4 As yeast cells can generally tolerate the presence of extra chromosomes but not chromosomal loss, spore viability per tetrad can indicate the timing of the meiotic failure. (A) Failures in Meiosis I usually lead to the generation of 0 to 2 viable spores. (B) Failures in Meiosis II generally lead to 2 or 3 viable spores per tetrad. Chromosomes (blue and pink) are replicated, then held together by sister chromatid cohesion (orange). Chromosomes are attached at their centromeres (grey) to tubulin spindles (green) and are held between spindle pole bodies (red), without which alignment and segregation may fail.

In budding yeast, errors in segregation during Meiosis I or Meiosis II generate different patterns of spore viability, as budding yeast can generally tolerate additional chromosomes but not their loss (Parry and Cox, 1970). A segregation failure in Meiosis I would be unlikely to produce more than 2 viable spores whereas a failure during Meiosis II would be unlikely to produce fewer than 2 viable daughter cells (Figure 1.4).

The microtubule organising centres in *S. cerevisiae* are called Spindle pole bodies (SPBs). These are formed of multi-laminar structures that span the nuclear envelope and form nucleation sites for spindle microtubules and cytoplasmic microtubules, on the nuclear and cytoplasmic faces, respectively (Neiman, 2005). During each round of meiosis, the SPB of each cell must duplicate, divide and migrate to opposite poles of the cell in order for the dividing chromosomes to be correctly drawn along the tubulin spindles at anaphase (Figure 1.3). Duplicated SPBs are formed by the end of G1 phase, remaining physically connected by a bridge (Byers and Goetsch, 1975). Division of the SPBs during S-phase is controlled by activity of the cyclin-dependent kinase Cdc28/Cdk1, allowing the number of visible SPB signals to progress from 1 to 2 in Meiosis I then to 4 in Meiosis II (Jaspersen *et al.*, 2004). During the Meiosis I to Meiosis II transition, the SPBs must be relicensed for duplication, which is regulated by the Cdc14 phosphatase, without permitting DNA replication via re-licensing of DNA replication origins (Fox *et al.*, 2017). At the onset of Meiosis II, the SPBs are modified at the cytoplasmic face allowing them to act as nucleation sites for formation of prospore membranes (Neiman, 2005). As the duplication of SPBs is regulated by a cyclin dependent kinase in concert with cyclins and the cell cycle, analysis of SPB division can provide further insight into the nature of any defects introduced by a particular mutation in relation to the cell cycle.

1.4 An Overview of Homologous Recombination

Double strand breaks (DSBs) in DNA can be formed exogenously, e.g. by ionising radiation, or endogenously, e.g. at stalled replication forks or as programmed meiotic breaks initiated by the Spo11 transesterase. In each case, the break must be processed correctly to allow for faithful repair of the lost DNA. Two major pathways of DSB repair are Homologous Recombination (HR), in which a homologous template is used to repair the DNA break and any lost DNA sequence, and Non-homologous End Joining (NHEJ), which inherently loses information by directly religating the broken ends of DNA. The choice between NHEJ and HR pathways is influenced by the cell cycle stage: NHEJ mainly occurs in G1/early S phase while HR occurs in late S/G2 phase, when DNA duplication has generated a homologous repair template, or during meiosis. However, the pathway choice is not entirely cell-cycle dependent and can be influenced by other factors; for example, loss of the NHEJ DNA-binding protein heterodimer Ku70/80 enhances HR levels without increasing sister-chromatid exchange (Pierce *et al.*, 2001).

The initial step in homologous recombination is nucleolytic processing of the DNA break at the 5' end, see Chapter 1.5 and Figure 1.5. This process inhibits the NHEJ pathway and forms 3' single-stranded DNA (ssDNA) which is capable of homology search between the homologous chromosomes (Brandsma and Gent, 2012; Keeney *et al.*, 1997). Once an area of homology is found, the invading single strand displaces one of the strands in the homologous duplex to form a 'D-loop' (displacement loop). D-loops can collapse, causing gene-conversion when repaired, or be converted into a 'double Holliday junction' (dHJ), allowing successful crossover formation (Sung and Klein, 2006). Capture of the second ssDNA strand by the displaced loop stabilises the dHJ, the gaps in which

can then be filled in by DNA synthesis. Resolution of the dHJ by symmetrical or asymmetrical cleavage generates crossover or non-crossover products (Figure 1.5; Gray and Cohen, 2016). If the second end is not captured, the break can be repaired by synthesis-dependent strand annealing (SDSA) whereby the invading strand is extended by DNA polymerase but is instead then displaced from the homologue and reanneals to the second broken strand, forming exclusively noncrossover products (Chavdarova *et al.*, 2015; Jasin and Rothstein, 2013). In yeast meiosis, most non-crossover products are generated by SDSA or D-loop dissolution with stable joint molecules generating mostly crossover products (De Muyt *et al.*, 2012).

During meiosis, as with mitotic homologous recombination, the ssDNA may also find homology in its sister chromatid, which would not generate crossovers when used as a repair template (Cromie and Smith, 2007). As the generation of sufficient interhomologue crossovers is required to maintain tension along the meiotic spindle, allowing chromosomes to align on the metaphase plate and segregate correctly, cells must ensure that sufficient DSBs are formed and repaired through recombination with the homologous chromosome rather than the sister chromatid. This template choice is influenced by the recombinase proteins that form a nucleoprotein-filament (NPF) with the processed ssDNA to facilitate homology search, see Chapter 1.6, and a number of other proteins that will be discussed in Chapter 1.7.

The distribution of crossovers (COs) along a chromosome is also an important factor in ensuring correct segregation of chromosomes. For this reason, Spo11-DSBs are generated non-randomly across the genome at meiotic 'hotspots'. There at least 3,600 DSB hotspots in yeast but only 150-200 DSBs will be formed per cell during meiosis

(Cooper *et al.*, 2016). A hierarchical system of regulation ensures that primed hotspots are only able to form breaks where there are no neighbouring DSBs already. This DSB interference occurs in concert with CO interference such that, of a neighbouring cluster of DSBs, only one DSB enters the CO pathway (Cooper *et al.*, 2016).

As well as being well distributed, the number of COs must be tightly regulated. Too many COs pose a risk of missegregation and gross chromosomal rearrangements. As sister chromatid cohesion is disrupted around COs, excessive CO formation risks loss of cohesion. Due to the role of CO interference, this can potentially increase the risk of missegregation, e.g. crossover formation around centromeric regions negatively affects segregation, and the risk of aberrant chromosomal events, e.g. crossover formation at telomeric regions risks recombination occurring between non-homologous chromosomes (Martinez-Perez and Colaiacovo, 2009). Conversely, to ensure that sufficient COs occur during meiosis to maintain bivalent integrity at metaphase, an obligate CO level is maintained at the expense of non-crossover events when DSB numbers are reduced, a process termed crossover homeostasis (Martini *et al.*, 2006). Strains that are unable to undergo HR and CO formation at the required frequency will form a greater number of inviable spores due to aneuploidy, such as *spo11* mutant strains (which are unable to form meiotic breaks), *sae2* mutant strains (which are unable to resect breaks to perform meiotic recombination) and *dmc1* mutant strains (which are unable to generate crossovers) (Klapholz and Esposito, 1982; Neale *et al.*, 2005; Tsubouchi and Roeder, 2004).

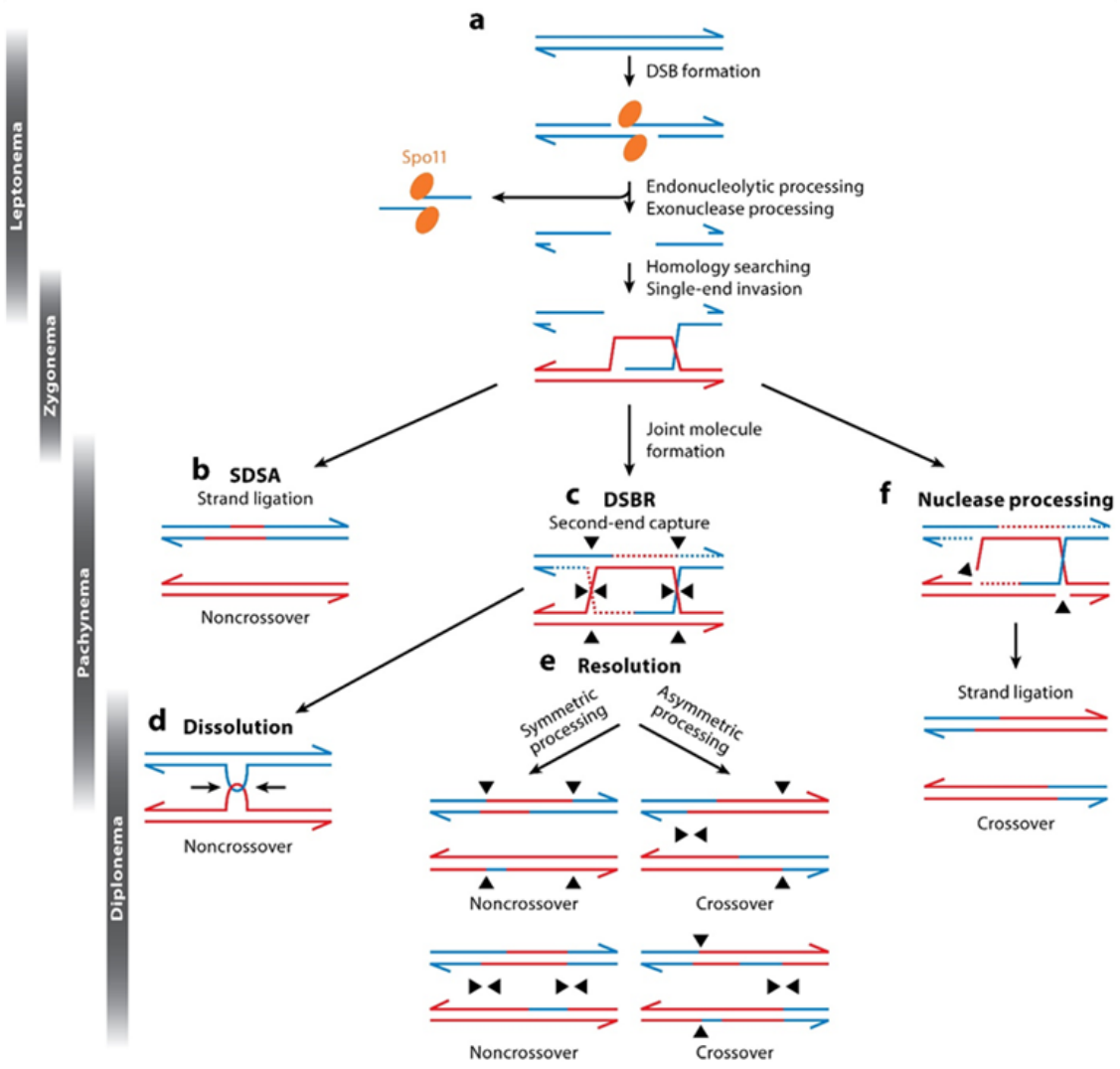

Gray S, Cohen PE. 2016.
Annu. Rev. Genet. 50:175–210

Figure 1.5 Schematic of repair routes for meiotic double strand breaks (DSBs). (a) DSBs are induced by Spo11 endonuclease and processed to leave 3' ssDNA strands. These can invade the neighbouring homologue, causing a D-loop, and search for regions of homology with the assistance of recombinases. (b) Following DNA synthesis and extension of the invading strand it can be displaced and reanneal to the other side of the DSB. It can then be used as the template for gap repair of its sister chromatid, resulting in a non-crossover event with gene conversion. (c) If the D-loop is extended sufficiently, second end capture can occur. Following DNA synthesis, this results in the formation of a double Holliday junction (dHJ). (d) Topoisomerase and helicase action can dissolve the dHJ by migration, resulting in non-crossover. (e) dHJs can also be cleaved asymmetrically to generate crossovers or symmetrically to generate non-crossovers. (f) Alternatively, following strand invasion, intermediate joint molecules can be processed by structure specific nucleases, leading to crossovers. Figure from Gray and Cohen, 2016.

1.5 DNA Double Strand Break Processing in Meiosis

In meiosis, the transesterase, Spo11, asymmetrically cleaves the duplex DNA and remains covalently bound to the 5' end of each chromatid. The initial step in processing the DSBs is the removal of short oligonucleotides bound to Spo11 by the MRX complex, in budding yeast, in concert with Sae2 (MRN and CtIP in mammals, respectively) (Neale *et al.*, 2005). The highly conserved MRX complex is formed of three components: the Mre11 nuclease, Rad50 and Xrs2 (Nbs1 in other eukaryotes). Mre11 has both endo- and exonuclease functions, dependent on the substrate, and interacts directly with two ATPase domains of Rad50 to form a DNA binding and processing core (Gobbini *et al.*, 2016; Hopfner *et al.*, 2001). Binding of ATP to Rad50 facilitates dsDNA binding, while hydrolysis of ATP by Rad50 induces conformational changes in the MRX complex that allow ssDNA to access the Mre11 nuclease site (Liu *et al.*, 2016). The slow rate at which Rad50 completes ATP-hydrolysis can be enhanced by Rif2, facilitating DSB resection and limiting repair by NHEJ (Cassani *et al.*, 2016). The coiled-coil region of Rad50 is able to dimerise via a zinc-mediated CXXC hook at its apex, which enables tethering of both broken DNA ends by the MRX complex in preparation for repair (Hopfner *et al.*, 2002). The Xrs2 (Nbs1) subunit of the complex facilitates nuclear localisation and protein-protein interactions (Tsukamoto *et al.*, 2005). The C-terminal region of Xrs2 binds to both Rif2 and the Tel1 kinase, which allows Rif2 to inhibit Tel1 binding and DSB repair signalling, particularly at telomeric DNA (Hirano *et al.*, 2009).

The Tel1 and Mec1 kinases (ATM and ATR in mammals, respectively) are serine/threonine kinases that regulate the cellular response to DNA damage. In response to double-stranded DNA damage, Tel1 coordinates checkpoint activation

leading to cell-cycle delay. Tel1 and Mec1 phosphorylate checkpoint mediators, which then activate downstream targets. Tel1 is localised to the site of DNA damage via interaction with the Xrs2 component of the MRX complex (Nakada *et al.*, 2003). This Tel1-MRX interaction at DNA ends stimulates Tel1 kinase activity, which has been found to increase further in *sae2Δ* or nuclease-deficient *mre11* strains when proteins are covalently attached to the DNA (Fukunaga *et al.*, 2011). Tel1 also promotes or stabilises the retention of MRX at DSBs, independently of its kinase activity, producing a positive feedback loop that facilitates the tethering of DSB ends (Cassani *et al.*, 2016; Gobbini *et al.*, 2016). Loss of Mre11 nuclease activity or Sae2 leads to persistence of MRX foci at DSBs, which enhances Tel1 activation (Clerici *et al.*, 2006).

Following phosphorylation by Cdk1, Sae2 stimulates the weak dsDNA endonuclease activity of Mre11 to generate nicks in the DNA, which are made preferentially on the 5'-terminated strand (Cannavo and Cejka, 2014; Huertas *et al.*, 2008). These nick sites can then provide access for nucleases to resect long tracts of DNA: the 5'-3' exonuclease Exo1 and the flap-endonuclease Dna2. Dna2 requires Sgs1 helicase activity, to unwind dsDNA forming a 5' flap substrate, and ATP hydrolysis to translocate in the 5'-3' direction (Miller *et al.*, 2017). In meiosis, these nicks generated by MRX/Sae2, in response to Cdk1-mediated phosphorylation of Sae2, are also required for the removal of Spo11 proteins covalently bound to the ends of the DNA break (Manfrini *et al.*, 2010). Exo1 is thought to be the major effector of meiotic DSB resection as these nicks are far more suitable substrates for Exo1 than Dna2-Sgs1, for which they are very poor substrates, and as the resection profile of *sgs1-mn* cells is indistinguishable from wild-type cells (Zakharyevich *et al.*, 2010). As well as providing entry sites for Exo1 and Dna2, the MRX complex facilitates recruitment of the nucleases to the DSB site, which occurs

independently of either its nuclease activity or the presence of Sae2 (Shim *et al.*, 2010). This may be achieved by competition with the NHEJ-promoting Ku heterodimer for binding the DNA ends, which would otherwise suppress Exo1 binding; *in vitro*, Ku is able to prevent Exo1-mediated resection at blunt and slightly resected DNA ends, up to 40nt of ssDNA, by localising to the ssDNA-dsDNA junction (Krasner *et al.*, 2015). Replication Protein A (RPA) binds to resected ssDNA preventing the DNA from reannealing and forming secondary structures. *In vitro*, once there is sufficient resected DNA to allow stable RPA binding, Ku binding is prevented, which allows Exo1 to complete long resection (Krasner *et al.*, 2015). Although RPA-coated ssDNA can stimulate nucleolytic activity, for example RPA targets Dna2 in the removal of RNA primers on Okazaki fragments, RPA actually protects the 3' ssDNA tails from nucleolytic degradation by reinforcing the 5' strand specificity of resection (Bae *et al.*, 2003; Chen *et al.*, 2013). *In vitro*, RPA stimulates 5'-DNA incision by Dna2 but attenuates 3'-DNA degradation in a dose dependent manner, with maximal inhibition corresponding to RPA-saturation of ssDNA (Cejka *et al.*, 2010; Niu *et al.*, 2010).

Following resection of the DNA to form 3' ssDNA filaments and RPA loading, Tel1 signalling is inhibited and Mec1 signalling is activated. A complex of Mec1-Ddc2 binds to RPA-coated ssDNA, signalling the presence of meiotic recombination intermediates; Ddc2 (orthologue of ATRIP in human) is a key checkpoint protein required for meiotic cell cycle delay and pachytene checkpoint signalling, without which cells may continue to divide despite unrepaired DSBs (Refolio *et al.*, 2011). RPA-coated ssDNA is also required to facilitate the loading of recombinases to ssDNA, generating nucleoprotein-filaments (NPFs) that can perform homology search and strand invasion, and without which DSB-induced recombinase foci are significantly reduced (Chen *et al.*, 2013).

1.6 Rad51 and Dmc1 Recombinases

Bacterial RecA is the prototypic recombinase protein that catalyses strand invasion of ssDNA into homologous DNA. It forms a right-handed helical sheath around the single stranded DNA, creating a nucleoprotein-filament (NPF) with specialised architecture that facilitates homology search (Masson and West, 2001). RecA contains two DNA binding sites: Site I for NPF polymerisation on ssDNA and Site II for weakly binding a second DNA strand during invasion and homology search (Muller *et al.*, 1990). The yeast RecA homologues, Dmc1 and Rad51, are both capable of forming similar NPFs on stretches of processed ssDNA for strand invasion (Krejci *et al.*, 2012). Deleting either of the RecA homologues leads to defects in recombination. While deleting *RAD51* produces severe mitotic and meiotic recombination defects, only meiotic recombination is deficient in *dmc1Δ* cells, which will accumulate DSBs and arrest in late meiotic prophase (Bishop *et al.*, 1992; Krejci *et al.*, 2012). It has been proposed that Rad51-NPFs favour inter-sister strand invasion for DSB repair, while Dmc1-NPFs favour using homologues as the repair template, therefore the disruption or promotion of the formation of either NPF would have repercussions on the choice of repair template and thus may affect segregation (Figure 1.6; Masson and West, 2001; Nimonkar *et al.*, 2012).

During meiosis, Rad51 and Dmc1 colocalise at the light microscope level and have been shown to interact with each other. Furthermore, *rad51* mutants do not form Dmc1 complexes or strand invade, while in *dmc1* mutants Rad51 complexes are indefinitely retained (Bishop, 1994). Strains containing the *rad51-II3A* allele, in which the second DNA binding pocket required for strand invasion has been mutated, cannot complete mitotic recombination but are capable of meiotic recombination in the presence of

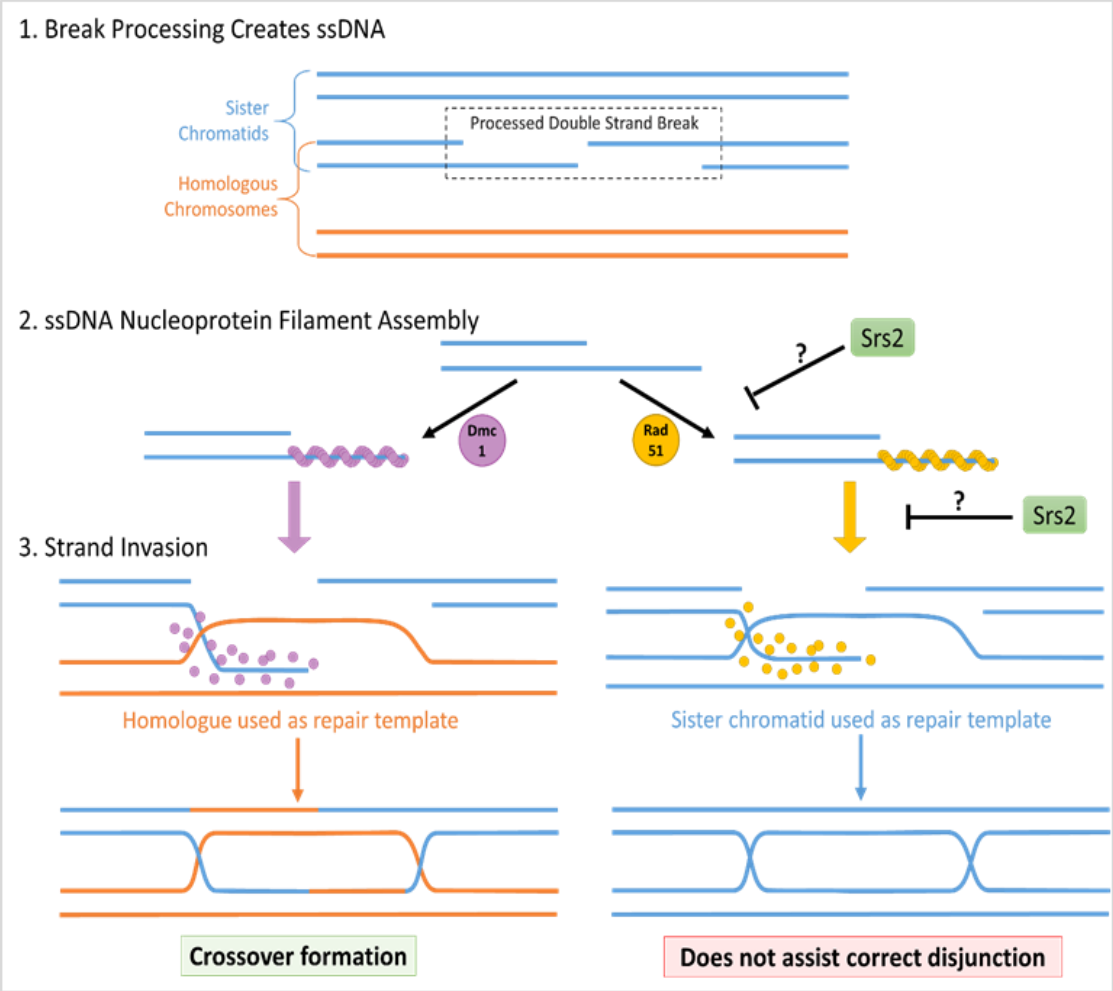

Figure 1.6 Which recombinase mediates strand invasion heavily influences the choice of repair template. Processed double strand breaks produce single stranded DNA that is loaded with a recombinase protein to facilitate strand invasion: Dmc1 promotes interhomologue strand invasion and repair, generating crossovers that assist the correct segregation of chromosomes, while Rad51 promotes repair from the sister chromatid and does not assist correct disjunction in meiosis. Mitotic and *in vitro* evidence suggests that Srs2 prevents loading of Rad51 and destabilises the protein nucleofilament once formed, however its meiotic role has not been fully characterised.

Dmc1. Conversely, *dmc1-II3A* cells are completely blocked from forming meiotic JMs or progressing through meiosis (Cloud *et al.*, 2012).

Together, these results suggest that Rad51 is a regulator of Dmc1 strand invasion activity. *In vitro* evidence suggests that Rad51 may regulate Dmc1 strand invasion activity by enhancing the Mei5-Sae3 complex stimulation of Dmc1, independently of Rad51's own strand invasion activity (Cloud *et al.*, 2012). This is consistent with cytological experiments that have shown deletion of *RAD51* greatly reduces the number of Mei5 foci observed (Hayase *et al.*, 2004).

In budding yeast, Mei5 and Sae3 are thought to form a complex that is required for loading of Dmc1 to ssDNA; loss of Dmc1 activity causes prophase arrest, DSB accumulation and poor spore viability, all of which are phenocopied by deletion of *MEI5* or *SAE3*. These phenotypes can largely be compensated for by overexpression of *RAD51*, as can the reduced crossover frequency observed in *dmc1Δ* strains (Hayase *et al.*, 2004; Tsubouchi and Roeder, 2003). *In vitro* assays have shown that Sae3-Mei5 acts as a mediator by binding to RPA and facilitating Dmc1-NPF formation and strand invasion by overcoming the inhibitory effect of RPA (Ferrari *et al.*, 2009). Deletion of *MEI5* and/or *SAE3* leads to Rad51 foci accumulation on meiotic chromosome that is consistent with DSB accumulation, indicating that Mei5 and Sae3 are required for the loading of Dmc1 but not of Rad51. Conversely, Dmc1 is required for the association of Mei5 and Sae3 with DNA (Hayase *et al.*, 2004). Budding yeast Sae3 shares 65% homology with the fission yeast protein spSwi5, which is known to interact with the spRad51-binding proteins spSwi2 and spSfr1 that also share significant homology to budding yeast Mei5. Furthermore, putative homologues of Sae3/spSwi5 and proteins that are potentially

homologous to Mei5/spSfr1 have been found in eukaryotes ranging from fish to humans, suggesting a conserved family of recombination and DNA repair proteins that function as RecA loading factors (Hayase *et al.*, 2004).

The Rad52 protein and a complex of the Rad55 and Rad57 paralogues of Rad51, facilitates Rad51 loading; the formation of Rad51 foci is dependent on *RAD52*, *RAD55* and *RAD57* while disappearance of RPA foci is dependent on *DMC1*, *RAD51*, *RAD55* and *RAD57* (Gasior *et al.*, 1998; Sung, 1997). It has been suggested that, during mitosis, the Rad55-Rad57 heterodimer stabilises the Rad51 filament, countering the antirecombinase activity of Srs2 by blocking its translocation (Liu *et al.*, 2011). Rad52 interacts with all three subunits of the RPA heterotrimer and alleviates its inhibitory effect, with Rad52 and Rad51 recruitment to ssDNA being attenuated in the absence of this interaction (Hays *et al.*, 1998; Lisby *et al.*, 2004; Shinohara and Ogawa, 1998). *In vitro* work also suggests that Rad52 acts with Rad51 to promote second end capture during homologous recombination, forming stabilised JMs (Nimonkar *et al.*, 2009). The role of Rad52 in Rad51 recruitment to ssDNA is performed by hBRCA2 in humans, a breast-cancer-associated tumour suppressor that physically interacts with hRAD51 to promote assembly and stability of the NPF and whose loss increases levels of broken or aberrant chromosomes (Pellegrini and Venkitaraman, 2004). Overexpression of hRAD51 has been found in several types of human cancer cells, increasing resistance to DNA damage-inducing treatments by improving the ability to repair by HR, making hRAD51 an attractive therapeutic target (Lv *et al.*, 2016).

Rad54 and Rdh54 (also known as Tid1) translocases are part of the Swi2/Snf2 helicase-like protein family that enhance Rad51- and Dmc1-mediated DSB repair

(Shinohara *et al.*, 1997). Rdh54 physically interacts with Dmc1, stabilising Dmc1-NPFs and stimulating JM formation while Rad54 interacts with Rad51, stabilising Rad51-NPFs (Nimonkar *et al.*, 2012). Rdh54 promotes dissociation of Dmc1 from non-productive sites on duplex chromatin, promoting its availability for assembly on ssDNA at DSBs (Holzen *et al.*, 2006). Similarly, Rad54 promotes dissociation of Rad51 from dsDNA NPFs via its ATPase-dependent translocation (Mazin *et al.*, 2010; Solinger *et al.*, 2002). Rdh54 shares some functional redundancy with Rad54. Deletion of *RAD54* reduces sporulation and spore viability, which is exacerbated by deletion of *RDH54* (Klein, 1997).

In vitro, hDMC1-NPFs were found to target nucleosome-depleted regions of chromatin (Kobayashi *et al.*, 2016). This is consistent with the observation that Dmc1 associates with recombination hotspots as nucleosome-depleted regions are often associated with transcription start sites and hotspots for meiotic recombination in budding yeast (Hayase *et al.*, 2004; Petes, 2001). hRAD51-NPFs, but not hDMC1-NPFs, were found to be strongly trapped by nucleosome binding, independently of DNA sequence, while removal of the histone tails improperly enhanced hDMC1-NPF binding to nucleosomes (Kobayashi *et al.*, 2016). Single molecule FRET has shown that hRAD51 can oligomerise onto dsDNA bound to nucleosomes, independently of DNA sequence, nucleating from the entry-exit region and allowing DNA to unwrap from the histone octamer in the presence of ATP (Senavirathne *et al.*, 2017). Observing single DNA molecules in nanofluidic channels suggests that, unlike RecA, hRAD51 forms inhomogeneous filaments with 'kinks' in the DNA where protein patches meet (Fornander *et al.*, 2016). It has been suggested that naked DNA in the filaments between discontinuous patches may release topological constraints during strand exchange.

Recently, two novel Rad51 paralogues, Psy3 and Csm2, have been shown to form a heterotetramer with Shu1 and Shu2, known as the PCSS or Shu complex (Martino and Bernstein, 2016). All four PCSS mutants are defective for spore viability and Rad51 assembly, with *in vitro* evidence suggesting that the PCSS complex stabilises Rad51 filaments (Sasanuma *et al.*, 2013b). Shu2 contains a zinc finger-like SWIM domain that is expected to facilitate DNA binding or protein-protein interactions (Godin *et al.*, 2015). Psy3 and Csm2 have significant structural homology to each other and to Rad51 with the Psy3-Csm2 dimer structure appearing strikingly similar to the Rad51 dimer subunit that forms NPFs (Sasanuma *et al.*, 2013b). The PCSS-mediated stimulation of Rad51 pre-synaptic assembly requires an interaction between Csm2 and Rad55, bridging an interaction between PCSS and Rad51 (Martino and Bernstein, 2016). As well as functioning in the repair of damaged replication forks, PCSS has been implicated in the interhomologue bias of meiotic repair with up to ten-fold more intersister JMs forming in *csm2Δ* cells than *CSM2* (Martino and Bernstein, 2016; Sasanuma *et al.*, 2013b).

1.7 Regulation of the Meiotic Interhomologue Bias of DSBR

In order to generate sufficient spindle tension to segregate chromosomes correctly during Meiosis I, cells must generate an appropriate numbers of inter-homologue crossovers during DSB repair. As homologous recombination can repair a DSB from any available homologous template, whether homologous chromosome or sister chromatid, template choice during meiosis must be highly regulated. To ensure the formation of sufficient chiasmata and prevent chromosome missegregation, the repair of DSBs in meiosis is strongly biased towards using the homologous chromosome as a repair

template (Hassold and Hunt, 2001). In yeast, this is heavily influenced by regulation of the RecA recombinases, Dmc1 and Rad51 (Figure 1.6; Schwacha and Kleckner, 1997). Additionally, several other factors contribute to the interhomologue bias to ensure tight regulation and will be discussed here (Figure 1.7).

1.7.1 Axis-associated Proteins Hop1, Red1 and Mek1

The inter-homologue bias for repairing DSBs during meiosis is active even when Rad51 is the only available recombinase; only significant overexpression of *RAD51* can alleviate the meiotic phenotypes of *dmc1Δ* (Tsubouchi and Roeder, 2003). In the absence of Dmc1, strand invasion following a DSB is prevented from occurring in the sister chromatid due to a "barrier to sister chromatid repair" (BSCR) (Niu *et al.*, 2005). A large component of this bias is dependent on the meiotic kinase Mek1, in complex with the axial elements Hop1 and Red1, that suppresses local HR machinery by phosphorylation of various targets (Humphryes and Hochwagen, 2014). Activation of the meiotic recombination checkpoint by DSB formation leads to phosphorylation of Hop1 by Mec1/Tel1 kinases. Mek1 is then recruited to the axis by Hop1 (Suhandynata *et al.*, 2016). Formation of the Hop1-Red1-Mek1 complex at chromosome axes then allows dimerisation and activation of Mek1 by autophosphorylation, in response to the DSB-dependent phosphorylation of Hop1 and Red1 (Niu *et al.*, 2007). Coupling Mek1 activation to DSB formation in this way ensures that it is only activated, and so only downregulates HR, in the immediate vicinity of a DSB, i.e. in the proximity of the sister chromatid (Humphryes and Hochwagen, 2014). If Mek1 is inactive, *dmc1Δ* cells rapidly

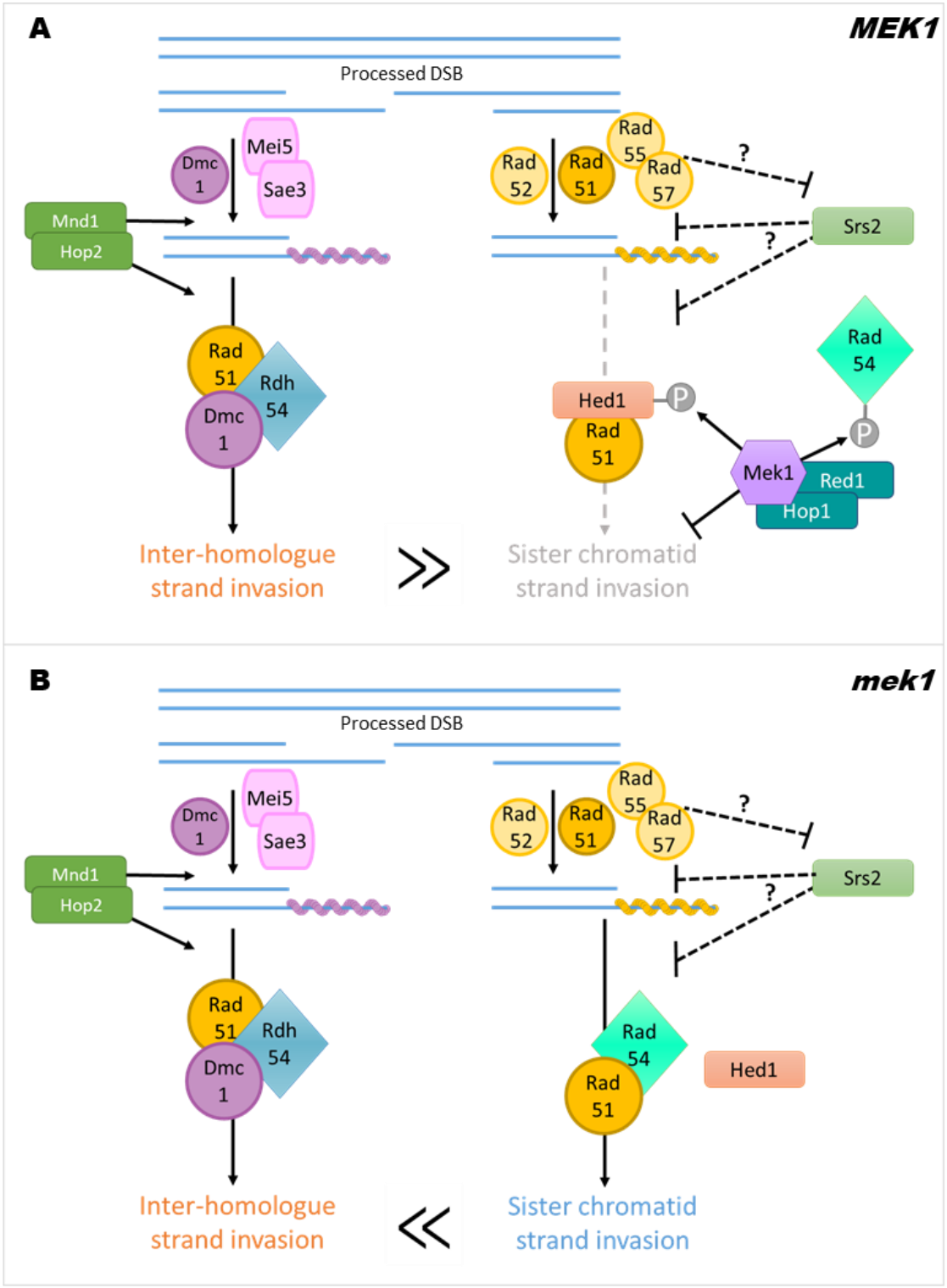

Figure 1.7 Mek1 promotes an interhomologue bias for meiotic repair by phosphorylation of Hed1 and Rad54. (A) In normal meiosis, in addition to any Srs2 activity, Mek1 phosphorylation of Hed1 and Rad54 prevents Rad51 from forming a complex with its accessory protein, Rad54. (B) In the absence of Mek1 activity, Hed1 inhibition of the Rad54-Rad51 interaction is lifted, as is the inhibition caused by phosphorylation of Rad54, allowing sister chromatid strand invasion. Although the Mnd1-Hop2 and Mei5-Sae3 complexes promote Dmc1-mediated strand invasion, in the absence of Mek1 activity Rad51-mediated repair occurs more rapidly, shifting the balance to intersister repair.

repair DSBs with Rad51-NPFs using the sister chromatids as a repair template (Niu *et al.*, 2005).

It has also been proposed that a Mek1-phosphorylated substrate, in combination with Rad51, provides structural support for the Dmc1-NPF, constraining it away from the sister chromatid and allowing the homologous chromosome to be preferentially targeted for strand invasion (Sheridan and Bishop, 2006). In possible support of this model, the functional orthologue of Red1 in humans, hSYCP3, has recently been shown to bind strongly to hRAD51 in pulldown assays but interacts only weakly with hDMC1. Consistently, hSYCP3 was shown to inhibit hRAD51-mediated, but not hDMC1-mediated, strand invasion (Kobayashi *et al.*, 2017).

1.7.2 Hed1 and Rad54 Phosphorylation

In *S. cerevisiae*, targets of Mek1 phosphorylation that contribute to the inter-homologue bias include Rad54 and Hed1, both of which events result in inhibition of Rad51-Rad54 complex formation. In complex, the accessory factor Rad54 stabilises Rad51-NPFs and stimulates Rad51-mediated strand invasion. Phosphorylation of Rad54 reduces both the formation of the complex and its stimulation of Rad51 strand-invasion activity (Niu *et al.*, 2009).

Hed1 is a meiosis-specific protein that prevents formation of the Rad51-Rad54 complex but not the assembly of Rad51-NPFs (Busygina *et al.*, 2008). Phosphorylation of Hed1 facilitates binding to Rad51, blocking access for Rad54 binding (Suhandynata *et al.*, 2016). Localisation of Hed1 to meiotic chromosomes is Rad51- and Spo11-dependent

(Tsubouchi and Roeder, 2006). Although Rdh54, which is related to Rad54, is primarily considered an accessory factor of Dmc1, it can also enhance strand invasion activity of Rad51-NPFs (Petukhova *et al.*, 2000). However, the Hed1-mediated inhibition of complex formation was found to be specific to the Rad51-Rad54 complex, with limited effect on Rad51-Rdh54 or Dmc1-Rad54 (Busygina *et al.*, 2008).

1.7.3 The Mnd1-Hop2 Complex

A complex of Mnd1 and Hop2 proteins promotes Dmc1 activity and homologous pairing (Tsubouchi and Roeder, 2002). In the absence of Hop2 or Mnd1, the cell cycle arrests at pachytene with unrepaired DSBs, accumulated Rad51 foci, which may no longer appear discrete, and aberrant synapsis, which is not only incomplete between homologous chromosomes but also occurs between nonhomologous chromosomes (Leu *et al.*, 1998; Tsubouchi and Roeder, 2002). The meiotic arrest of cells lacking Mnd1 activity is caused by a Mec1-mediated checkpoint response to hyperresected DSBs. This arrest can be relieved by deletion of *RED1* or *HOP1* (Zierhut *et al.*, 2004). This may relate to alleviation of the BSCR imposed by Mek1, allowing breaks to be repaired using the sister chromatid, or relief of a structural constraint imposed by Red1 and Hop1. Deletion of *DMC1*, but not *RAD51*, can also alleviate the cell-cycle arrest of *hop2* cells, while overexpression of Rad51 can alleviate the sporulation and spore viability defects of *hop2* and *mnd1* cells, particularly in the absence of Dmc1 (Tsubouchi and Roeder, 2003).

Using *ndt80* strains to observe near-complete homologue pairing, the *hop2* pairing defect was found to be at least partially due to Rad51 and Dmc1 activity: disruption of either recombinase gene increased the level of homologue pairing to approximately

rad51 HOP2 or *dmc1 HOP2* levels (Tsubouchi and Roeder, 2003). The loss of Hop2 function also greatly increases the proportion of cells with visible polycomplexes, which can be rescued by loss of Rad51 or Dmc1 activity (Tsubouchi and Roeder, 2002, 2003). Polycomplexes are thought to be aggregations of non-chromatin-associated synaptonemal complex proteins, possibly resulting from a failure in homologue pairing that reduces SC assembly efficiency (Loidl *et al.*, 1994). Recently, non-chromatin-associated hSYCP3, a component of the human SC, has been shown to compete with hHOP2-hMND1 for binding to hRAD51-ssDNA, suppressing activation of its strand invasion activity (Kobayashi *et al.*, 2017).

Crystal structure analysis of the Hop2-Mnd1 complex from *Giardia lamblia* identified winged-helix domains thought to represent a joint dsDNA interacting region, attached to long curved coiled-coil structure that fits into the helical groove of Dmc1-NPFs (Kang *et al.*, 2015). It has also been suggested that the hHOP2-hMND1 coiled-coil is structurally similar to hSYCP3 and, interestingly, to the yeast Mei5-Sae3 complex (Kobayashi *et al.*, 2017). *In vitro* work suggest that the stimulation of Dmc1 activity by Hop2-Mnd1 is due to both stabilisation of Dmc1-NPFs and facilitating the capture of duplex DNA by Dmc1-NPFs, thereby conjoining two DNA molecules (Pezza *et al.*, 2007). Similarly, Hop2-Mnd1 has been shown to stabilise Rad51-NPFs *in vitro* and enhance their ability to capture duplex DNA (Chi *et al.*, 2007). However, the stimulatory effect is not identical for both recombinases. An *in vitro* D-loop assay in the absence of Hop2-Mnd1 found that both recombinases required preincubation with ssDNA for D-loop formation. However, in the presence of Hop2-Mnd1, optimal Dmc1-mediated D-loop formation occurred without preincubation, while Rad51 still required preincubation, even when Hop2-Mnd1 was present at a ratio of 4:1 (Petukhova *et al.*, 2005).

1.7.4 Helicase Activity

Helicases, including Mph1, Sgs1 and Srs2, play an important role in the regulation of crossovers. The Mph1 helicase belongs to the FANCM family of helicases and has been shown to unwind D-loops *in vitro* via its helicase activity and can be recruited to HO breaks, where it unwinds D-loops formed by Rad51 to promote non-crossover events (Prakash *et al.*, 2009; Whitby, 2010). However, Mph1 is thought to function mainly at replication forks and in crossover avoidance during mitotic DSB repair, as its loss confers no significant meiotic phenotype (Lorenz, 2017).

The Sgs1 helicase, a RecQ orthologue, promotes dHJ dissolution to form non-crossover products (De Muyt *et al.*, 2012). The Srs2 helicase has been shown to unwind structures mimicking D-loop recombination intermediates *in vitro* but its function *in vivo* has yet to be fully elucidated, particularly during meiosis (Dupaigne *et al.*, 2008). Sgs1 and Srs2 will be discussed further in Section 1.8

1.8 RecQ, Sgs1 and Srs2 Helicases

In many species, disruption of Rad51 nucleoprotein-filaments (NPFs) can be performed by a subset of the highly-conserved RecQ helicases - a group of proteins that are central to genome stability through regulation of HR and the rescue of errant recombination events (Bugreev *et al.*, 2007; Cobb *et al.*, 2002). Loss of RecQ helicases can cause hyper-recombinant phenotypes and an increase in sister chromatid exchange. This can lead to clinical conditions including predisposition to cancer and genome instability syndromes, such as Werner's syndrome and Bloom's syndrome, resulting from the loss of activity of the human RecQ orthologues WRN and BLM, respectively (Ellis *et al.*, 2008). In *Drosophila melanogaster*, the RecQ helicase dmBLM, which is closely related to human BLM, is thought to reduce crossover formation by facilitating synthesis-dependent strand annealing (SDSA) (Andersen and Sekelsky, 2010; Kusano *et al.*, 1999). Mutating the single yeast RecQ helicase, Sgs1, also causes a hyper-recombination phenotype but Sgs1 does not display the translocase activity required for removal of Rad51 from DNA filaments (Rockmill *et al.*, 2003). In yeast, the Sgs1 helicase is thought to facilitate SDSA in complex with Top3 and Rmi1, by unwinding D-loops to disassemble strand invasion events before second end capture can occur (De Muyt *et al.*, 2012). The Sgs1-Top3-Rmi1 complex also facilitates convergent branch migration of dHJs and decatenation of the DNA to promote dissolution to non-crossover product (Cejka *et al.*, 2012). Sgs1 shares some functional redundancy with another yeast helicase, Srs2, and overexpression of either helicase can partially compensate for an absence of the other (Ira *et al.*, 2003; Krejci *et al.*, 2003). Loss of either helicase shortens the mean life-span of the cells while deletion of both *SGS1* and *SRS2* produces inviable spores or slow-growing colonies with an average life span of only three generations (McVey *et al.*, 2001).

1.8.1 Physical Properties of Srs2

Srs2 is 1,174 amino acid 3'-5' helicase related to the UvrD bacterial helicase, in the highly-conserved SF-1 superfamily. SF-1 helicases are non-hexameric enzymes that translocate along ssDNA in an ATP-dependent manner and are thought to unwind the DNA by promoting dsDNA destabilisation (Lohman *et al.*, 2008). Srs2 unwinds various substrates but preferentially acts on 3' overhangs of at least 10 nt. Other substrates include 5' overhangs, forks, flaps, D-loops and blunt end dsDNA (Marini and Krejci, 2010). *In vitro* studies have found that Srs2 translocates on naked ssDNA at approximately 300 nt/s, which is slowed to approximately 170 nt/s on RPA-ssDNA or approximately 200 nt/s in the presence of both Rad52 and RPA (Antony *et al.*, 2009; De Tullio *et al.*, 2017).

In mitosis, the expression of *SRS2* is induced during DNA replication or in response to DNA damaging agents during G2 phase (Heude *et al.*, 1995). Meiotic transcription of *SRS2* mRNA has been shown to be induced at 2-4h post induction with Srs2 levels reaching their peak after 5h, falling to undetectable levels after degradation of Rec8 and pachytene exit, around 9h (Sasanuma *et al.*, 2013a)

Srs2 has been shown to interact with a number of different proteins, with 166 potentials identified by 2-hybrid assay (Chiolo *et al.*, 2005). These include Cdc28, Dun1, Esc1, Mei5, Mlh2, Mms1, Mph1, Msl1, Mre11, Pol32, Rad2, Rad5, Rad14, Rad18, Rsc1, Sae2, Siz1, Siz2, Sgs1, Shu2, Slx5, Smt3, Top2, Ubc9, Ubp1, Ubp10, Ulp2 (Marini and Krejci, 2010).

Srs2 can be phosphorylated by Cdk1 with consensus sites at T604, S698, S879, S893, S938, S950 and S965 (Chiolo *et al.*, 2005). Srs2 can also be SUMOylated at K1081, K1089 and K1142 (Kolesar *et al.*, 2012). Several domains and regions of interaction have been

identified, as follows (Chavdarova *et al.*, 2015; Chiolo *et al.*, 2005; Marini and Krejci, 2010; Sasanuma *et al.*, 2013a):

- Residues between 1-845: DNA helicase domain, containing an ATP-binding/ATPase motif
- Residue K41: Walker type A motif
- Residues between 783-860: Mus81 (N-terminal) interaction domain
- Residues between 875-902: Rad51-interaction domain
- Residues between 848-1175: Mre11-interaction domain
- Residues between 1036-1174: Proliferating cell nuclear antigen (PCNA) and SUMO (small-ubiquitin-like-modifier)-interaction domains (PIM and SIM, respectively)

During the course of various studies, several variants of Srs2 have been utilised to dissect the phenotypes of interest, including:

- *srs2-101* (*srs2-P37L)*, *srs2-K41A* and *srs2-K41R* have been mutated at the ATP binding pocket, preventing translocase and helicase activity (Keyamura *et al.*, 2016; Nguyen *et al.*, 2017; Palladino and Klein, 1992). Notably, *srs2-K41R* can bind but not hydrolyse ATP while srs2-K41A can neither bind nor hydrolyse ATP (Burgess *et al.*, 2009)
- *srs2-Δ(875-902)* has a deletion of the Rad51 binding domain (Nguyen *et al.*, 2017)
- $srs2^{C\Delta6}$, $srs2^{C\Delta24}$, $srs2^{C\Delta136}$, $srs2^{C\Delta176}$ *(1-998)* and $srs2^{C\Delta276}$ *(1-898)* are C-terminal truncations that are deficient in PCNA interaction (Chavdarova *et al.*, 2015; Pfander *et al.*, 2005). As full-length Srs2 tends to aggregate *in vitro*, the C-terminal truncation mutant *srs2(1-898)* is frequently used for single molecule

and biochemical assays as it retains ATPase, DNA helicase and Rad51-strippase activities that are close to wild-type *SRS2* strains (De Tullio *et al.*, 2017).

- *srs2-ΔPIM* has lost amino acids 1,159-1,163 in the PCNA interaction domain (Kolesar *et al.*, 2016)
- *srs2-ΔSIM* has lost 5 amino acids from the SUMO interaction motif (Burgess *et al.*, 2009). *srs2-SIM** has amino acids 1,170-1,173 mutated to alanine in the SUMO interaction domain (Kolesar *et al.*, 2016)
- *srs2^{CΔ314} (1-860)* is a C-terminal truncation deficient in Rad51-binding, PCNA interaction and Mre11 interaction (Nguyen *et al.*, 2017)
- *srs2ΔN* is an N-terminal truncation deficient in helicase activity but capable of Rad51 binding (Pfander *et al.*, 2005)
- *srs2R1* contains an additional adenine at position 3,480, resulting in a protein that is 6 amino acids shorter and modified at the final 6 amino acids, and which is deficient for interaction with sumoylated PCNA (Pfander *et al.*, 2005)
- *srs2R3 (srs2-R337S)* has an amino acid substitution near helicase domain IV (310-321) and is attenuated for ATPase, helicase, DNA binding and Rad51 strippase activity (Pfander *et al.*, 2005)
- *srs2-7AV* has been mutated to be unphosphorylatable at putative Cdk1 phosphorylation sites (Chiolo *et al.*, 2005)
- *srs2-mn* is a meiotic null strain, generated during this study, in which *SRS2* is expressed under the mitotic-specific *CLB2* promoter, see Appendix A.1.1

1.8.2 Known Functions and Interactions of Srs2

Since identification, Srs2 has been implicated in a number of different roles, acting as a multifunctional protein that protects the cells from DNA instability. It is involved in post-replication repair, non-homologous end joining, DNA-damage checkpoint responses, maintenance of replication fork integrity, prevention of DNA triplet hairpins and homologous recombination (Marini and Krejci, 2010). Its action can be varied by post-translational modifications and interactions with key factors at DNA repair sites.

SRS2 (Suppressor of Rad6 2) was identified during a screen for mutations that would relieve the trimethoprim-mediated growth inhibition and UV sensitivity of *rad6* and *rad18* strains. The Rad6 and Rad18 proteins form a DNA-binding ubiquitin-conjugating heterodimer involved in post-replication repair (PRR), the process by which cells repair damage encountered during DNA replication (Bailly *et al.*, 1997; Lawrence and Christensen, 1979). Suppression of the PRR-deficient phenotype by *srs2* mutants was found to be dependent on the Rad52 recombinational repair pathway, while *srs2* single mutants were themselves found to be hyper-recombinant, suggesting a role for Srs2 in DNA repair and the suppression of homologous recombination (Rong *et al.*, 1991; Schiestl *et al.*, 1990). Loss of *SRS2* also sensitises wild-type cells to UV damage, as it is unable to remove toxic recombination intermediates. However, in the context of the highly UV-sensitive PRR-deficient cells, *rad6* and *rad18*, resistance to UV is increased by abrogation of the Srs2-mediated inhibition of recombinational repair (Le Breton *et al.*, 2008). Srs2 is recruited to replication forks by SUMOylated PCNA (Proliferating Cell Nuclear Antigen), where it promotes the *RAD6* repair pathway at stalled replication forks by inhibition of Rad51 association, preventing inappropriate formation of

recombinogenic filaments (Burgess *et al.*, 2009; Papouli *et al.*, 2005). Consistently, mutations in PCNA that prevent SUMOylation, or deletion of the SUMO-specific ligase Siz1, also improve *rad6*/*rad18* UV sensitivity, in a Rad52-dependent manner (Pfander *et al.*, 2005).

A subsequent screen for *srs2* mutants that are not UV sensitive themselves but can relieve the UV sensitivity of PRR-deficient strains, i.e. that are able to remove toxic recombination products but do not inhibit recombinational repair, identified *srs2R1* and *srs2R3*. Interestingly, these mutations were found in completely different regions of the gene: *srs2R1* is deficient for interaction with SUMOylated-PCNA but capable of Rad51-filament disruption, while *srs2R3* is capable of interaction with SUMOylated-PCNA but deficient in its biochemical functions (ATPase, helicase, Rad51-strippase and DNA-binding deficient) (Le Breton *et al.*, 2008). This suggests that the Srs2 interaction with SUMOylated PCNA is not required for the removal of toxic recombination intermediates, which is supported by the observation that a *siz1* single mutant is also not UV sensitive (Le Breton *et al.*, 2008; Pfander *et al.*, 2005). In *pol30-RR* strains, which encode non-SUMOylatable PCNA, S-phase Srs2 foci are drastically reduced but recombination foci are unaffected while the Srs2-ΔSIM protein, which has a deletion in the SUMO-interaction motif, still localises to recombination foci at wild-type levels (Burgess *et al.*, 2009; Le Breton *et al.*, 2008). Srs2 is also able to localise to HR foci in the absence of Rad51 but Siz1 is partially required for Srs2 recruitment, however the SUMOylatable Rad52 and Rad59 recombination proteins are not (Burgess *et al.*, 2009). Nej1, a regulator of NHEJ, has been shown to interact with Srs2, via two-hybrid and pulldown assays, and was shown to recruit Srs2 to HO-mediated DSBs. Furthermore, *in vitro*, the efficient repair of overhang substrates designed to represent the

Rad52-dependent process of single-strand annealing required both Srs2 and Nej1 (Carter *et al.*, 2009). Recently, *in vitro* work using Rad51 filaments containing randomly distributed RPA clusters has found a marked preference for RPA as a start site for initiation of Srs2 translocation, suggesting RPA may recruit Srs2 to the presynaptic complex (Kaniecki *et al.*, 2017). These results indicate that Srs2 is recruited differently to DNA replication forks and DNA repair centres.

A direct interaction was observed in a two-hybrid screen, between the C-terminal domain of Srs2 and Pol32 subunit of DNA polymerase δ, a yeast polymerase required during replication and repair. *In vitro* assays have also found that the human WRN RecQ helicase functionally interacts with Polδ, dependent on the Pol32 subunit, increasing the nucleotide incorporation rate of Polδ in the absence of PCNA (Kamath-Loeb *et al.*, 2000). Double mutation of *pol32Δ* and *srs2Δ* generates a strain that grows even more poorly than *pol32Δ* alone, which is cold sensitive although *srs2Δ* is not. Similarly, the double *pol32Δ srs2Δ* strain is more susceptible to exogenous DNA damage than *pol32Δ* and *srs2Δ* single mutants, which alone are only modestly susceptible to HU, UV and MMS treatment (Huang *et al.*, 2000). While these results might suggest a cooperative interaction between Srs2 and DNA polymerase δ, it has also been suggested that Srs2 competes with DNA polymerase δ for binding PCNA, or that the interaction of Srs2 with SUMO-PCNA triggers the release of Polδ from the DNA polymerising complex, and thereby promotes SDSA by disruption of the D-loops (Burkovics *et al.*, 2013; Liu *et al.*, 2017). Interestingly, *in vitro* work indicates that Srs2 exhibits a slight a preference for disrupting extending over unextended D-loops in the presence of SUMO-PCNA (Liu *et al.*, 2017). Srs2 is also required for viability in the absence of *RAD27,* a 5'-3' exonuclease and flap endonuclease involved in replication and repair, including Okazaki fragment

processing. This may reflect reversal of aberrant replicative DNA structures via the Srs2 interaction with Polδ or channelling of the structures to recombinational repair (Debrauwere *et al.*, 2001). Indeed, the repair of spontaneous S-phase damage in the absence of Rad27 requires phosphorylation of Srs2 at the Cdk1 consensus sites (Saponaro *et al.*, 2010).

In circumstances requiring mitotic HR for DNA repair, loss of the Srs2 SUMO-interaction domain (SIM), but not the PCNA-interaction domain (PIM), leads to cell death (Kolesar *et al.*, 2016). While binding of Srs2 to SUMO-PCNA at stalled replication forks promotes SDSA by disrupting D-loops, SUMOylation of Srs2 has been suggested to be inhibitory to SDSA, as SUMOylation of Srs2 reduces binding to SUMO-PCNA and the SDSA defects observed in non-phosphorylatable *srs2* cells can be rescued by mutation of the SUMOylation sites (Kolesar *et al.*, 2012; Saponaro *et al.*, 2010). It is thought that the SIM domain on its own promotes mitotic HR as mutation of the SIM domain causes decreased recombination levels and gene conversion *in vitro*, although the PIM domain had to first be deleted to observe this effect as interaction with SUMO-PCNA would otherwise inhibit HR (Kolesar *et al.*, 2016). As well as binding to SUMO-PCNA, the Srs2 SIM domain is required for SUMOylation of Srs2 via its interaction with SUMOylated Ubc9, a SUMO-conjugating ligase. This results in a reciprocal inhibition between the SUMOylation of Srs2 and the binding of Srs2 to SUMO-PCNA, as SUMO-PCNA binding at the SIM domain makes it unavailable for binding to Ubc9 (Kolesar *et al.*, 2012). In yeast two-hybrid assays, SUMOylation of Srs2 was shown to enhance the interaction with Rad51 (Kolesar *et al.*, 2016). Recently, the Uls1 SUMO-targeted ubiquitin ligase from the Swi2/Snf2 family, a paralogue of Rad54 and Rdh54, has been shown to interact with PCNA and Srs2, and promotes PCNA-Srs2 binding at replication forks by reducing the

level of Srs2 SUMOylation (Kramarz *et al.*, 2017). Interestingly, non-phopshorylatable *srs2* strains accumulate SUMOylated Srs2, suggesting that Cdk1 also plays an important role in preventing any unscheduled SUMOylation. Phosphorylation of Srs2 by Cdk1 has been shown to promote SDSA and control the turnover of Srs2 on invading strands but is not required for the removal of toxic Rad51-NPFs (Saponaro *et al.*, 2010). An assay of transformants containing plasmid-based SDSA or NHEJ products found that the promotion of SDSA by Srs2 was dependent upon its ATP hydrolysis, its interactions with Rad51 and SUMO-PCNA, and the *POL30* (PCNA), *SIZ1* and *RAD6* genes, which are required for PCNA SUMOylation and Ubiquitination (Miura *et al.*, 2013). Together these results suggest potential mechanisms for controlling Srs2 activity dependent on context by post-translational modification.

It has been proposed that Rad51 recruitment to stalled replication forks requires the Esc2 SUMO-like domain containing protein that locally down-regulates Srs2 activity by facilitating the binding of another protein to SUMO-PCNA, Elg1, locally inhibiting Srs2 binding. Esc2 has also been shown to interact with the SIM domain of Srs2 and with the Slx5-Slx8 complex, which it has been suggested promotes proteasome-dependent degradation of Srs2 (Urulangodi *et al.*, 2015).

Triplet repeats in DNA can form hairpin and other non-canonical DNA structures that block replication and other cellular processes, increasing instability, and have been implicated in a number of neurological disorders, such as Huntington's disease (Mirkin, 2007). Srs2 specifically unwinds hairpin-forming triplet repeats, relieving replication blockage, via its ATPase helicase activity and interaction with PCNA (Anand *et al.*, 2012). The helicase activity and interaction of Srs2 with PCNA is required to prevent breakage

of triplet repeats while recombination-dependent expansion or contraction of triplet repeats, which could generate genomic instability, is prevented by stripping Rad51 from nascent strands (Nguyen *et al.*, 2017). Without the action of Srs2 and its helicase activity triplet repeat expansion rates can increase up to 40-fold (Bhattacharyya and Lahue, 2004).

The structure-selective endonuclease Mus81, with its partner protein Mms4, processes a number of recombination and replication intermediates, especially in the absence of Sgs1, and is particularly active on branched duplex DNA and replication forks (Kaliraman *et al.*, 2001). In Meiosis I, Mus81-Mms4 is hyperactivated by cell cycle kinases Cdk/Cdc5 to ensure JM resolution and accurate segregation of chromosomes (Matos *et al.*, 2013). Mus81 has been shown to colocalise with Srs2 *in vivo* following DNA damage and *in vitro* to directly associate with Srs2. This interaction stimulates the nuclease activity of Mus81-Mms4, independently of Srs2's helicase activity or its SUMO/PCNA interaction domain, while the Srs2 strippase activity relieves Rad51-specific inhibition of Mus81 nuclease activity. Interestingly, Mus81 also prevents Srs2 from unwinding recombination or replication intermediates, suggesting a coordination of their activities to stabilise intermediate structures for resolution by Mus81-Mms4 (Chavdarova *et al.*, 2015). Notably, in the context of the synthetic lethality of *srs2 rad54* double mutation, a two-hybrid screen also identified an interaction between Mus81 and Rad54, possibly also in relation to targeting Mus81 to junction intermediates (Ceballos and Heyer, 2011).

Srs2 has been shown to physically interact with Mre11 and Sgs1 via two-hybrid analysis and co-immunoprecipitation. Furthermore, gel filtration chromatography has shown that Srs2, Sgs1 and Mre11 can be eluted in a single complex in wild-type, untreated cells.

Interestingly, following DNA damage induction the Srs2-Mre11 and Sgs1-Mre11 subcomplexes are eluted separately, dependent on Mec1- and Tel1-mediated checkpoint pathways and Cdk1-phosphorylation of Srs2 (Chiolo *et al.*, 2005; Liberi *et al.*, 2000).

Srs2 enhances Exo1 activity in order to reduce mutations caused by Top1 cleavage when RNaseH2 fails to remove misinserted ribonucleoside monophosphate (rNMP) residues (Potenski *et al.*, 2014). Sgs1 was also able to unwind DNA from a Top1-induced nick and was found to interact with Exo1 but did not enhance its activity (Niu *et al.*, 2016).

In mitosis, the Rad51 paralogue-containing PCSS complex has been shown to inhibit Srs2 localisation to DSBs and interacts with Srs2 in yeast two hybrid assays, however the mechanism behind this regulation has yet to be elucidated and does not occur in meiosis (Bernstein *et al.*, 2011; Martino and Bernstein, 2016). Interestingly, it has also been suggested that the dimer of the two Rad51 paralogues Rad55-Rad57 counters the anti-recombinase activity of Srs2 by blocking its translocation (Liu *et al.*, 2011).

Break-induced replication (BIR) is a potentially genomically unstable form of DSB repair that generally occurs where only one broken end can invade a homologue, such as at stalled replication forks or eroded telomeres. Recently, it has been shown that Srs2 is required during BIR bubble migration, without which long ssDNA can invade the donor chromosome and form toxic JMs, trapping the donor and recipient chromosomes (Elango *et al.*, 2017).

The anti-recombinase activity of Srs2 is thought to be dependent on both its interaction with Rad51 and its ATPase activity (Antony *et al.*, 2009; Krejci *et al.*, 2003). Truncations of Srs2 that have lost the Rad51 interaction domain show reduced ability to remove

Rad51 from ssDNA and reduced association with RPA-ssDNA, *in vitro* (Antony *et al.*, 2009; De Tullio *et al.*, 2017). Conversely, biochemical assays have determined that the mutant proteins Rad51-Y388H and Rad51-G393D, which are defective for interaction with Rad52, are also defective for interaction with Srs2 and that this renders them resistant to its strippase activity (Seong *et al.*, 2009).

In a strain that accumulates Rad51 due to impaired recombination, *mei5Δ*, induced overexpression of *SRS2* has been shown to reduce established Rad51 foci and aggregates after only 2h of induction (Sasanuma *et al.*, 2013a). In a strain that accumulates foci of both Rad51 and Dmc1, *rdh54Δ*, induced overexpression of *SRS2* resulted in only a reduction of Rad51 foci and not Dmc1 foci, indicating that once foci are formed the strippase activity of *SRS2* is recombinase specific (Holzen *et al.*, 2006; Sasanuma *et al.*, 2013a).

Although the interaction between Rad51 and Srs2 is required for disassembling the Rad51-NPFs on ssDNA *in vitro*, there is some debate regarding the role of this interaction at dsDNA. Dupaigne *et al* found that constructs of 3' tailed dsDNA were most efficiently unwound when exposed to increasing concentrations of Rad51, to the point that Rad51 coated the whole ssDNA-dsDNA construct, and suggest that Rad51-dsDNA enhances Srs2 activity (Dupaigne *et al.*, 2008). Conversely, Lytle *et al*, 2014, found that at dsDNA the interaction with Rad51 inhibits Srs2 activity, preventing it from unwinding dsDNA, and suggest that the context-dependent difference in the interaction between the two proteins may be influenced by phosphorylation. In this regard, it is of note that two of the Cdk1 consensus sites for phosphorylation on Srs2 are found within the Rad51 binding domain (Chiolo *et al.*, 2005). The key difference between these experiments

appears to be the length of incubation. Repeating their experiment with matched conditions, Lytle *et al*, 2014, found that Rad51-mediated inhibition of Srs2 activity at dsDNA occurred during the early stages of the reaction but was lost over time. They suggest that this represents Rad51 dissociation from the DNA over time, which relieves the inhibition. A separate *in vitro* analysis also suggests that the presence of Rad51 inhibits the NHEJ-promoting activity of Srs2 (Miura *et al.*, 2013).

Interestingly, two of three Rad51 mutant proteins identified by yeast two-hybrid assay as being defective for interaction with Rad52, also prevented interaction with Srs2 *in vitro*. Furthermore, the Srs2 interaction with Rad51 is also prevented by an excess of Rad52, suggesting that Srs2 and Rad52 may interact with Rad51 at similar or overlapping motifs (Seong *et al.*, 2009). In an *srs2Δ rad52Δ* strain, significantly more Rad51 and Rad54 foci are generated than in *rad52Δ* alone, suggesting that the promotion of Rad51 foci formation by Rad52 is less important when Srs2 is absent. However, those Rad51 foci that form in the absence of Rad52 may be defective for recombination as the increase in foci does not correspond to an increase in survival rates in response to radiation exposure (Burgess *et al.*, 2009).

Analysis of Srs2 unwinding activity on artificial substrates found that blunt-ended duplex DNA and 4-way junctions, equivalent to single Holliday junctions, are very poor substrates for Srs2 activity. However, forked DNA is efficiently unwound and a construct representing one end of a D-loop, a 'PX Junction', was unwound twice as efficiently as the forked DNA, which was not due to preferential binding (Dupaigne *et al.*, 2008). On ssDNA-dsDNA constructs *in vitro*, the length of the 3' ssDNA overhang has been found to determine Srs2 activity, with no ATPase or unwinding activity observed on substrates

with overhangs below 10 nt despite the ability of Srs2 to bind to this length, suggesting that assemblies of multiple Srs2 molecules are required for unwinding (Lytle *et al.*, 2014). *In vitro* experiments have shown that a single Srs2 monomer is sufficient for translocation activity which occurs at approximately 300 nt/s on naked ssDNA or approximately 200 nt/s when Rad52 and RPA are present (Antony *et al.*, 2009; De Tullio *et al.*, 2017). This is significantly faster than the rate of translocation observed by Antony *et al.*, 2009, during Rad51 clearance by Srs2, approximately 12 nt/s. However, in a separate study, Kaniecki *et al.*, 2017, observed that Srs2 translocation removes Rad51 at a rate of approximately 50 monomers per second, or approximately 140 nt/s; they suggest this difference is due to their use of longer ssDNA substrates and free RPA that enables assemblies of tandem Srs2 molecules The presence of Srs2 at ssDNA-dsDNA junctions observed by EM has been suggested to reflect Srs2 molecules travelling along RPA-coated ssDNA and accumulating at the junction awaiting sufficient oligomerisation to unwind the DNA (Dupaigne *et al.*, 2008).

1.8.3 Effects of Decreased or Increased Srs2 Activity

In mitosis, the loss of Srs2 activity leads to hyper-recombination and increased CO frequency, with a reduction in repair efficiency (Ira *et al.*, 2003; Rong *et al.*, 1991). The hyper-recombinant phenotype of *srs2* mutants is thought to relate to a failure in removing Rad51 from ssDNA, as susceptibility to DNA damaging agents in *srs2* and severe growth defects observed in the *sgs1Δ srs2Δ* double mutant can be alleviated by deletion of *RAD51* (Ira *et al.*, 2003; Krejci *et al.*, 2003). Overexpression of *RAD51* in the absence of Srs2 nearly eliminates NCOs (Ira *et al.*, 2003). In the absence of Srs2 activity,

cells are unable to pass the DNA damage checkpoint, even once the DNA has been repaired, and activity of the Rad53 checkpoint kinase persists (Vaze *et al.*, 2002).

Mutations in *srs2* are also lethal, or exhibit poor growth, in combination with *rad54Δ*, *rdh54Δ*, *rad50Δ*, *mre11Δ*, *xrs2Δ*, *rad27Δ* and *top3Δ.* However, many of these phenotypes can be rescued to an extent by mutation of recombination or checkpoint proteins, suggesting the formation of toxic recombination intermediates that can be sensed at the checkpoint stage (Klein, 2001; Palladino and Klein, 1992). Specifically, the lethality of *srs2 rad54Δ* double mutation is due to inappropriate recombination and can be rescued by loss of Rad51 activity, which it has been suggested implies a pro-recombination role for Srs2 that overlaps with Rad54 (Niu and Klein, 2017).

The absence of Srs2 activity causes accumulation of recombination foci in S-phase cells, as measured by increased Rad51 and Rad54 foci; *srs2Δ* and helicase-defective *srs2-K41A* and *srs2-K41R* strains, which cannot hydrolyse ATP, all form an increased number of Rad54 foci. Interestingly the *srs2-K41A* strain, which also cannot bind ATP, generated even more foci suggesting that its presence may block a different repair pathway or contribute to the accumulation of toxic intermediates (Burgess *et al.*, 2009).

In meiosis, the *srs2-101* strain in which the ATP-binding pocket required for translocase activity to remove Rad51 from ssDNA has been mutated, reduces spore viability and delays meiotic progression (Palladino and Klein, 1992). The presence of Srs2 during meiosis is also necessary to ensure efficient formation of COs and NCOs (Sasanuma *et al.*, 2013a).

Other effects of Srs2 activity loss include an increased rate of trinucleotide repeat expansions by up to 40-fold, which cannot be alleviated by overexpression of Sgs1

(Bhattacharyya and Lahue, 2004). Loss of Srs2 activity increases UV sensitivity and mitotic arrest that is dependent on Rad9, a component of the G2/M damage checkpoint (Le Breton *et al.*, 2008; McVey *et al.*, 2001). Interestingly, artificially increasing levels of Rad52 SUMOylation by overexpression of the sumo-ligase *SIZ2*, or replacement of Rad52 with a Rad52-SUMO fusion protein, can relieve the *srs2Δ* sensitivity to DNA damage, possibly by interfering with its action as a mediator of Rad51 and thus bypassing the requirement for Srs2 activity (Esta *et al.*, 2013). In the absence of Srs2, NHEJ is reduced for both sticky and blunt ends, although to a lesser extent than caused by loss of Rad50 (Hegde and Klein, 2000).

Overexpression of Srs2 is thought to specifically disrupt replication, independently of its interaction with Rad51 or its helicase activity, and produce toxic phenotypes via binding to SUMO-PCNA, with no toxicity observed when the *srs2-R1* allele is overexpressed (Leon Ortiz *et al.*, 2011). Furthermore, deletion of *ULS1*, which would otherwise favour PCNA-Srs2 binding by reduction of Srs2 SUMOylation levels, rescues the toxic effect of *SRS2* overexpression in mitosis (Kramarz *et al.*, 2017). Overexpression of Srs2 also largely eliminates mitotic crossover formation (Ira *et al.*, 2003).

In meiosis, overexpression of *SRS2* with different copy numbers under a *DMC1* promoter reduces spore viability in a dose-dependent manner, with no specific pattern of spore viability, and delays sporulation by approximately 2.5 h. Analysis of DSB resolution also indicated a reduction in recombination products (Sasanuma *et al.*, 2013a). SC perturbation was observed in cells overexpressing *SRS2*; Zip1 foci and Rec8 loading were observed slightly earlier but formation and disassembly of full-length SC is delayed, with an increase in the frequency of Zip1 polycomplexes (Sasanuma *et al.*, 2013a). Rad51 foci

were also disrupted by Srs2 overexpression, with delayed formation and turnover, independently of the Rad51-interacting domain, but Rad52, Dmc1 and RPA were not affected (Sasanuma *et al.*, 2013a).

1.8.4 Hypotheses Regarding the Action of Srs2 during Meiosis

In vitro evidence has suggested a role for Srs2 in the promotion of the SDSA pathway due to its ability to disrupt Rad51 presynaptic filaments *in vitro* (Andersen and Sekelsky, 2010). However, the precise role of Srs2 during meiosis is still yet to be fully elucidated.

One hypothesis regarding the mechanism for this clearance of Rad51 is stimulation by Srs2 of Rad51's intrinsic ATPase activity. Hydrolysis of ATP bound to RecA filaments has been shown to facilitate RecA dissociation from both ssDNA and dsDNA and promotes turnover of duplex DNA bound by microhomology in early recombination intermediates, with a possible role in homology search (Arenson *et al.*, 1999; Lee *et al.*, 2016). Formation of the Rad51-ssDNA nucleoprotein filament requires divalent cations and ATP binding (Fornander *et al.*, 2016). *In vitro*, the dose-dependent clearance of Rad51 from ssDNA by Srs2 was found to be dependent on hydrolysis of this ATP by Rad51: radiolabelled ATP was incorporated into Rad51-NPFs before addition of Srs2, plus unlabelled ATP to allow for the activity of Srs2, and then the rate of radiolabelled ADP generation analysed (Antony *et al.*, 2009). Single-molecule *in vitro* analysis and electron cryo-microscopy indicates that hRAD51-NPF with ATP incorporated at each interface becomes more compressed once the ATP is hydrolysed to ADP, making it less active for strand invasion (Robertson *et al.*, 2009; Short *et al.*, 2016).

Using truncations of Srs2, Antony *et al.*, 2009 observed that the Srs2 Rad51- and PCNA-binding domains were required for ATP hydrolysis-dependent Rad51 clearance by Srs2 *in vitro*, although they could not determine whether interaction at the Srs2 Rad51-binding domain would be required for engagement with Rad51 or for stimulation of its ATPase activity. Conversely, Rad51-Y388H and Rad51-G393D proteins, which are defective for interaction with Srs2 and Rad52 are resistant to *in vitro* clearance by Srs2 (Seong *et al.*, 2009). The presumed human orthologue of Srs2, PARI, which contains a UvrD-like helicase domain, preferentially interacts with SUMOylated PCNA and causes a hyperrecombinant phenotype when lost, has also been shown to interact with Rad51, disrupting Rad51 filaments *in vitro*, despite lacking the WalkerA/B domains required for the ATPase, and therefore helicase, activity observed in Srs2 (Moldovan *et al.*, 2012). However, *in vivo* work by Sasanuma *et al,* 2013a using overexpression of an *srs2* mutant lacking the Rad51 binding domain, *srs2-Δ(875-902),* found that Rad51 binding activity was not required for *in vivo* dismantling of Rad51-NPFs, although the mutant displayed reduced dismantling activity compared to overexpression of wild-type *SRS2*.

Instead, Sasanuma *et al.*, 2013a favour the model previously described by Krejci *et al.*, 2003 and Veaute *et al.*, 2003 that the ATP-hydrolysis and translocase activity of Srs2 is the principle method for removing Rad51 from ssDNA. Overexpressing a translocase deficient mutant, *srs2-K41A*, failed to remove Rad51 from meiotic chromosomes. Sasanuma *et al.*, 2013a found that while overexpression of wild-type *SRS2* disrupted Rad51 foci, Dmc1, Rad52 and RPA were not removed, suggesting that Srs2 translocation specifically affects Rad51. However, recent work by De Tullio *et al.*, 2017 using ssDNA curtains indicates that Rad52 and RPA are indeed removed by Srs2 as it translocates along ssDNA but that the naked DNA is rapidly repopulated after no more than a few

seconds due to the high affinity of RPA for ssDNA and of Rad52 for RPA-ssDNA. Interestingly, they also found that in the naked DNA wake of a leading Srs2 molecule, many new binding events occurred with trailing Srs2 molecules translocating far more rapily than the leading molecule (De Tullio *et al.*, 2017). This may indicate a *trans* mechanism of inhibition by Srs2, in which Rad52 and RPA are frequently recycled and redistributed, preventing Rad52 from functioning as an accessory factor for the loading of Rad51.

It has been proposed that following disruption of the Rad51-NPF by Srs2, reloading of Rad51 is prevented by Srs2 repetitively scrunching the DNA. Using single-molecule FRET and PIFE techniques, Qiu *et al.*, 2013 found that Rad51 binds 3 nt per monomer, requires 6 monomers for nucleation, and initiates assembly at the ssDNA-dsDNA junction. Interestingly, they observed a repetitive motion of Srs2 at the ssDNA-dsDNA junction, scrunching the ssDNA to disrupt Rad51 binding by periodically reeling in a range of approximately ~18-20 nts, approximately the length required for a stable nucleation of Rad51.

Finally, it has been suggested that Srs2 removal of Rad51 from a displaced extended strand in combination with direct Mus81-Mms4 stimulation could facilitate the resolution of intermediate structures by SDSA (Chavdarova *et al.*, 2015). This is supported by the observation that Srs2 may have a Rad51-independent influence on the promotion of SDSA: truncated Srs2 that cannot bind to Rad51 still reduces noncrossover frequency, although less so than a null mutant (Mitchel *et al.*, 2013).

1.9 Initial Aim of this Study

This study aims to investigate the molecular function of Srs2 during meiosis using cytological analysis. Much of the current knowledge of Srs2 function relies on *in vitro* assays, mitotic data and biochemical or structural analyses. Using cytological techniques on meiotic samples would provide further insight into the meiotic role of Srs2 *in vivo* via analysis of the effects of its absence on nuclear and chromosomal division, and on recombinase distribution.

Chapter 2 Materials and Methods

2.1 Media

2.1.1 Standard Media

Media solutions are made with distilled water, dH2O, and autoclaved

YPAD: 1% (w/v) Yeast extract (Difco), 2% (w/v) Peptone (Difco), 2% (w/v) D-glucose (Fisher), 4% (w/v) Adenine (Sigma) or 5% (w/v) YPAD Mix (Formedium)

YPG: 1% (w/v) Yeast extract (Difco), 2% (w/v) Peptone (Difco), 15% (v/v) Glycerol (Fisher)

K-Acetate: 1% (w/v) Potassium Acetate (Sigma)

BYTA: 1% (w/v) Yeast extract (Difco), 2% (w/v) Tryptone (Difco), 1% (w/v) Potassium Acetate (Sigma), 50 mM Potassium Phalate (Sigma)

SPM (Sporulation Media): 0.3% (w/v) Potassium Acetate (Sigma), 0.02% Raffinose (Sigma)

LB (L-Broth): 1% (w/v) NaCl (Fisher), 1% (w/v) Tryptone (Difco), 0.5% (w/v) Yeast extract (Difco) pH 7.5

SC (Leu^- Ura^- Drop-out) Media: 0.68% (w/v) Yeast Nitrogen Base without Amino Acids (Difco), 2% (w/v) D-glucose (Fisher), 0.087% (w/v) Amino Acid Master Mix Excluding Leucine and Uracil [Adenine 0.8 g, Arginine 0.8 g, Aspartic Acid 4.0 g, Histidine 0.8 g, Lysine 1.2 g, Methionine 0.8 g, Phenylalanine 2.0 g, Threonine 8.0 g, Tryptophan 0.8 g, Tyrosine 1.2 g, (all Sigma)]

Minimal Media: 0.68% (w/v) Yeast Nitrogen Base without Amino Acids (Formedium), 2% (w/v) D-glucose (Fisher), 2% (w/v) Agar (Difco)

2.1.2 Media Supplements

For Time Courses: 0.0025% (w/v) Leucine (Sigma) 0.0005% (w/v) [Uracil (Sigma); Tryptophan (Sigma); Arginine (Sigma); Histidine (Sigma); Adenine (Sigma)]

For Solid Media: 2% Agar (Difco)

For Antibiotic Selection (filter sterilised): 0.01% (w/v) Ampicillin (PanReac Applichem); 0.01% (w/v) Nourseothricin (Werner); 0.02% (w/v) G-418 (Melford); 0.03% (w/v) Hygromycin (Melford);

2.2 General Solutions

All solutions are made to volume with dH_2O, unless otherwise stated.

2.2.1 Electrophoresis Solutions

TAE: 40 mM Tris Base (Sigma), 0.11% (v/v) Glacial Acetic Acid (Fisher), 1 mM EDTA pH8.0 (Fisher)

SDS-PAGE Running Buffer: 10X Novex Tris-Glycine SDS Running Buffer (Invitrogen)

SDS-PAGE Semi-Dry Transfer Buffer: Pierce 1-Step Transfer Buffer (Thermo Scientific)

SDS-PAGE Wet Transfer Buffer: 0.025 M Tris Base (Sigma), 0.15 M Glycine (Melford), 2% (v/v) Methanol (Fisher)

2.2.2 Cytological Solutions

Stop Solution: 0.1 M MES (Sigma), 1 mM EDTA (Fisher), 0.5 mM $MgCl_2$ (BDH), 1 M D-Sorbitol (Sigma), pH 6.4

Fixative: 4.0% (w/v) Formaldehyde (Sigma), 3.8% (w/v) Sucrose (BDH), pH7.5

DTT (1,4-DiThioThreitol): 1 M DTT (Thermo Scientific)

Zymolyase Suspension: 10 mg/ml Zymolyase (MPBio), 10% (w/v) D-Glucose (Fisher)

PBS (Phosphate Buffered Saline): 1 PBS Tablet (Sigma) per 200 mL dH_2O

PBST: 1 PBS Tablet (Sigma) per 200 mL dH_2O, 0.1% (v/v) Tween-20 (Sigma)

2.2.3 Solutions for Generating Competent *E. coli*

TfbI: 30 mM Potassium Acetate (Sigma), 100 mM Rubidium Chloride (Sigma), 10mM Calcium Chloride (BDH), 50 mM Manganese Chloride (Fisons), 15% (v/v) Glycerol (Fisher), pH 5.8, Filter-sterilised

TfbII: 10 mM MOPS (Sigma), 75 mM Calcium Chloride (BDH), 10 mM Rubidium Chloride (Sigma), 15% (v/v) Glycerol (Fisher), pH 6.5, Filter-sterilised

2.2.4 Solutions for Extraction of DNA from Yeast

SCE: 1.0 M D-Sorbitol (Sigma), 0.1 M Sodium Citrate (Alfa Aesar), 0.06 mM EDTA (Fisher), pH 8.0

DNA Lysis Buffer: 2% (w/v) SDS (Fisher), 0.1 M Tris Base (Sigma), 0.05 mM EDTA (Fisher), pH 8.0

Zymolyase Suspension: 10 mg/ml Zymolyase (MPBio), 10% (w/v) D-Glucose (Fisher), made to volume in ddH_2O (deionised distilled water)

When extracting DNA by MasterPure DNA extraction kit, standard kit solutions were used instead.

2.2.5 Solutions for Extraction of Protein from Yeast

Buffer D: 1.85 M NaOH (Fisher), 7.5% (v/v) β-mercaptoethanol (Sigma)

Buffer H: 200 mM Tris-HCl pH6.5 (Sigma), 8 M Urea (GE Healthcare), 5% (w/v) SDS (Fisher), 1 mM EDTA (Fisher), 0.02% Bromophenol Blue (Sigma), 5% (v/v) β-mercaptoethanol (Sigma)

TCA: 55% Trichloroacetic acid (TCA) (Sigma)

Protein Lysis Buffer (Native): 50 mM Tris pH8.0 (Sigma), 75 mM Sodium Chloride (Fisher), 10% (v/v) Glycerol (Fisher), 1% (w/v) NP-40 (Sigma), 20 mM Sodium Pyrophosphate (Sigma), 30 mM Sodium Fluoride (Sigma), 60 mM Glycerophosphate (Sigma), 2 mM Sodium Orthovanadate (Sigma), 1 mM PMSF (Sigma), 1 Tablet per 20 ml Protease Inhibitors (Roche)

2.2.6 Chromatin Immunoprecipitation Solutions

ChIP Fixation Solution: 50 mM Tris-HCl pH8.0 (Sigma), 100 mM Sodium Chloride (Fisher), 0.5 mM EGTA (Sigma), 1mM EDTA (Fisher), 30% (w/v) Formaldehyde (Sigma)

ChIP Lysis Buffer: 50 mM HEPES Potassium Salt pH8.0 (Sigma), 140 mM Sodium Chloride (Fisher), 1mM EDTA (Fisher), 1% (v/v) Triton X-100 (Sigma), 0.1% (w/v) Sodium Deoxycholate (Sigma), 1 mM PMSF (Sigma), 1 Tablet per 25 ml Protease Inhibitors (Roche)

Glycine Solution: 2.5 M Glycine (Melford)

PBS (Phosphate Buffered Saline): 1 Tablet (Sigma) per 200 mL dH_2O

ChIP High-Salt Lysis Buffer: 50 mM HEPES Potassium Salt pH8.0 (Sigma), 500 mM Sodium Chloride (Fisher), 1 mM EDTA (Fisher), 1% (v/v) Triton X-100 (Sigma), 0.1% (w/v) Sodium Deoxycholate (Sigma), 1 mM PMSF (Sigma)

ChIP Wash Buffer: 10 mM Tris pH8.0 (Sigma), 0.25 M Lithium Chloride (Fisher), 0.5% (w/v) NP-40 (Sigma), 0.5% (w/v) Sodium Deoxycholate (Sigma), 1 mM EDTA (Fisher), 1 mM PMSF (Sigma)

TE Buffer: 10 mM Tris pH8.0 (Sigma), 1 mM EDTA (Fisher)

TES Buffer: 50 mM Tris pH8.0 (Sigma), 10 mM EDTA (Fisher), 1% (w/v) SDS (Fisher)

TES3 Buffer: 50 mM Tris pH8.0 (Sigma), 10 mM EDTA (Fisher), 3% (w/v) SDS (Fisher)

RNAseA: 1% (w/v) RNAseA (Sigma) in ddH_2O

Proteinase K: 2% (w/v) Proteinase K (Roche) in TE Buffer

2.3 Molecular Biology Techniques

2.3.1 SDS-PAGE Electrophoresis and Western Blotting

Protein samples were denatured at 95°C for 5 min in appropriate loading buffer and loaded into precast SDS-PAGE gels (Biorad) with an appropriate protein ladder (NEB). Gels were run at 40-50 mA or 140 V for 2-3 h in 1x running buffer.

Gels were sandwiched with Hybond C nitrocellulose membrane (Amersham) and Whatman 3MM blotting paper. The gel was then transferred by Semi-dry transfer, using Pearce 1-Step Transfer Buffer for 7 min, or by Wet transfer in 1x Wet Transfer Buffer at 150 mA for 2 h, or at 16V overnight.

The transferred membranes were rinsed in dH_2O. If necessary, the membrane was incubated in Ponceau, then washed in PBST. Membranes were incubated in 5% (w/v) skimmed milk in PBS at 4°C for 2-20 h, then incubated in 1° antibody in 1% (w/v) skimmed milk in PBS at an appropriate concentration for 2-20 h at 4°C. Membranes were washed 3x in PBS, 5 min each at RT, and incubated in 2° antibody in 1% (w/v) skimmed milk in PBS at an appropriate concentration for 30-120 min at RT. Membranes were washed 3x in PBS, 5 min each at RT, then 2 ml mixed high sensititivity ECL solution (Millipore) added and blots visualised on a gel documentation system.

2.3.2 Agarose Gel Electrophoresis

DNA products, such as PCR reaction products or DNA digested by restriction enzymes, were checked on 0.8%-1.5% Agarose gels at 85-130 V for 0.5-1.5 h, following addition of

6X loading dye. Band sizes were determined by comparison to a Generuler 1kB DNA Ladder (NEB).

2.3.3 PCR

Standard PCR mix: 2% (v/v) Genomic DNA or 1:50 to 1:200 Plasmid DNA, 20% (v/v) 5x HiFi PCR Buffer, 0.4-0.5 µM Forward Primer, 0.4-0.5 µM Reverse Primer, 1% (v/v) Taq Polymerase, [200 µM dNTPs if not included in the PCR Buffer]

Standard PCR programs were run as follows:

- 94-98°C for 2 min
- 18-35 cycles of:
    - 94-98°C for 30 s
    - 55-68°C for 30 s
    - 72°C for 30 s/kb
- 72°C for 5-10 min

Reactions were checked by DNA gel electrophoresis, with restriction digestion where necessary.

2.3.4 Restriction Digests

DNA was digested by addition of 4-10% (v/v) of appropriate restriction enzyme(s) (NEB) and 10% (v/v) 10x NEB Buffer. Digests were incubated at 37°C for 0.5-1.0 h. Digests were checked by DNA gel electrophoresis.

2.3.5 Restriction Cloning

Insert Generation: Genomic DNA was amplified by PCR using primers flanking the region of interest with restriction site sequences at each end. 130 µl of product was purified by GeneElute Kit, as per protocol except for elution with 57 µl ddH_2O. Inserts were digested overnight at the newly generated restriction sites.

Vector Generation: 10 µl of vector was digested for 1 h 40 min at 37°C (40 µl for CRISPR/Cas9 vector). As *Bam*HI-HF may be retained on the DNA ends, any such digests were additionally purified by GeneElute kit, as per protocol except for elution with 50 µl ddH_2O and 5.5µl of buffer. 1 µl rSAP (NEB) or Antarctic (NEB) alkaline phosphatase was added and incubated for a further 20 min at 37°C.

Purification: The processed insert and vector were run on agarose gel and purified by Qiagen or NEB Gel Extraction Kit, as per protocol except for additional incubation during the wash and elution steps to increase yield (5 min at room temperature) and elution in 10 µl ddH_2O.

Ligation: 2.5 µl each of gel-purified vector and insert were mixed with 5.0 µl of Ligation Solution I (Takara) and incubated at 16°C for 30 min. If necessary, concentrations were first determined by Nanodrop and volumes diluted appropriately to produce equimolar reactions.

Plasmid Recovery: 90 µl competent *E. coli* was transformed with the ligation mix and recovered by Qiagen or NEB Miniprep Kit, as per protocol except for elution with 65 µl ddH_2O. Plasmids were checked by digest and gel electrophoresis or sequencing (Source BioScience or MWG Eurofins), following concentration determination by Nanodrop.

CRISPR/Cas9 gRNA Linker Sequence Generation: Two antiparallel oligonucleotides targeting Rad51 were designed with overhanging sticky ends for *Sap*I and resuspended

to 100 µM. 10 µl of each oligonucleotide were annealed in a thermocycler at: 95°C for 30 seconds, 72°C for 2 min, 37°C for 2 min, 25°C for 2 min. The sequence was then ligated into an appropriately processed CRISPR/Cas9 plasmid, as described above.

The CRISPR/Cas9 plasmid with the gRNA target sequence insertion was subsequently used in a double transformation of wild-type *S. cerevisiae* along with a plasmid that contained a non-cuttable repair template of the desired sequence for insertion into the genomic DNA, see Appendix A.1.2

2.3.6 Overlapping PCR

Primers "1-4" were designed such that two overlapping primers (2 and 3) could be paired with either an upstream primer (1) or downstream primer (4) to amplify regions of interest by standard PCR, generating two separate DNA fragments with homologous overlapping ends. These two fragments were then run on an agarose gel and extracted with a Qiagen kit, as per standard kit protocol except for elution in 50 µl ddH_2O.

The overlapping fragments were diluted and added to a standard PCR mix, except for the absence of primers, and annealed in a thermocycler: 2% (v/v) 1:50 DNA fragment, 20% (v/v) 5x HiFi PCR Buffer, 1% (v/v) Taq Polymerase, [200 µM dNTPs if not included in the PCR Buffer]

The annealing program was run as follows:

- 98°C for 2 min
- 2 cycles of:
    - 98°C for 30 seconds
    - 68°C for 3 min

Primers 1 and 4 were added at 0.5 µM each and the program immediately continued with:

- 25 cycles of:
    - 98°C for 30 s
    - 55°C for 30 s
    - 72°C for 1 min
- 72°C for 10 min

Following size confirmation by gel electrophoresis, the product was purified by GeneElute Kit, as per protocol except for elution in 57 µl ddH_2O, and inserted into a vector as per standard restriction cloning.

2.4 Methods for Plasmid Amplification and Storage in *E. coli*

2.4.1 Generation of Competent *E. coli*

Frozen DH5α *E. coli* was streaked out on LB agar and grown overnight at 37°C. A colony was inoculated into 5 ml LB and grown at 37°C overnight. 3 ml of the starter culture was added to 200 ml LB, incubating at 37°C until OD_{550}=0.48. Cells were spun down for 5 min, resuspended in 50 ml ice-cold TfbI and incubated on ice for 10 min. Cells were spun down for 5 min, resuspended in 10 ml ice-cold TfbII and incubated on ice for 15 min. Cells were aliquoted and flash frozen in liquid nitrogen before storage at -80°C

2.4.2 *E.coli* Transformation

1 µl of 1:10 diluted plasmid DNA, 10 µl of restriction digest product or 10 µl of ligation reaction product was added to 50 to 90 µl of competent *E.coli* and incubated on ice for 40 min. Cells were heatshocked at 42°C for 90 seconds, mixed with 1 ml LB and incubated at 37°C for 1 h. Cells were spun down, resuspended in 100 µl LB and plated onto LB + ampicillin (100 µg/ml) then incubated overnight at 37°C. To recover plasmids, colonies were inoculated into 5 ml LB + ampicillin (100 µg/ml), grown overnight at 37°C and purified by Qiagen Miniprep Kit or NEB Miniprep Kit as per standard protocol, except for elution in 65 µl ddH_2O.

2.4.3 Plasmid Storage

Plasmids were archived within *E. coli* cells in pre-sterilised glass vials containing 1 ml 50% (v/v) Glycerol (Fisher) by addition of 1 ml LB liquid culture and storage at -80°C.

2.5 Methods for Culture and Genetic Manipulation of *S. cerevisiae*

2.5.1 Yeast Strain Storage

Yeast strains were archived in pre-sterilised glass vials containing 1ml 50% (v/v) Glycerol (Fisher) by addition of 1 ml YPAD liquid culture, or cells grown on YPAD solid media resuspended in 1 ml YPAD, and storage at -80°C.

2.5.2 General Yeast Recovery and Culture

Archive strains were patched onto YPG and grown at 30°C overnight. Cells were struck for single colonies onto YPAD plates, which were grown at 30°C for 2 days. A single colony was used to inoculate 10 ml YPAD, which was grown at 30°C overnight. Where exponential phase cells were required, the initial culture was diluted with volumes of YPAD that were calculated to give OD_{600}=0.5-0.8 after further growth at 30°C.

2.5.3 Yeast Mating

Cells from YPAD patches were mixed in a mating patch on YPAD and incubated for 3-4 h at 30°C. Cells were added to 0.5 ml ddH_2O, sonicated for 5 seconds if necessary, and 10 µl taken to a YPAD plate. Zygotes were selected by Singer Micromanipulator and incubated at 30°C for 2 days. Cells from the resultant colonies were visually inspected on the microscope, or sporulated on K-Acetate plates at 30°C overnight, for an initial indication of the success of the mating based on the presence of diploid cells. For confirmation of ploidy, cells from candidate colonies were patched to YPAD and incubated at 30°C overnight. Cells were then patched in a 'mating type test ladder' on YPAD plates in which the strains to be tested made up the horizontal 'rungs' of the ladder, along with *MATa* haploid, *MATα* haploid and diploid control strains (Figure 2.1). The vertical 'rails' of the ladder were then added using the edge of a clean microscope slide to replica patch particular *MATa* and *MATα* 'mating type tester' strains, which contain only one uncommon auxotrophic mutation not shared by any of the test or control strains. The completed ladder was incubated at 30°C overnight, then replica-plated with sterile velvet to minimal media plates and incubated for a further night at

30°C. The auxotrophic mutations in each individual strain prevented cells from any of the 'rungs' or 'rails' of the ladder from growing on the minimal media plates. Only strains that had been able to successfully complement their auxotrophies by mating with cells of an opposing mating type would be able to form successful diploid colonies at the intersections of the ladder. Test strains that failed to form colonies at both intersections, and therefore were unable to mate with either 'mating type tester' strain, were considered to be diploid.

2.5.4 Yeast Sporulation and Tetrad Dissection

The formation of tetrads of spores within asci provides a valuable method to directly observe the phenotypes of all daughter cells produced from a single meiotic event. Through enzymatic digestion of the ascus cell wall and micromanipulation, the spores from each tetrad can be dissected and transferred to a grid on an agar plate. Once grown to colonies, the percentage of viable spores produced by a particular strain can be determined, along with any pattern of spore viability. Cells were patched to 1% (w/v) Potassium Acetate plates and incubated at 30°C for 1-3 days. Cells from K-Acetate patches were added to tubes containing 5 µl 2.0 M D-Sorbitol (Sigma), 4 µl ddH_2O, 1 µl Zymolyase suspension and incubated at 30°C for 15 min. Cells were added to YPAD plates and dissected by Singer Micromanipulator into a grid, then incubated for 2 days at 30°C.

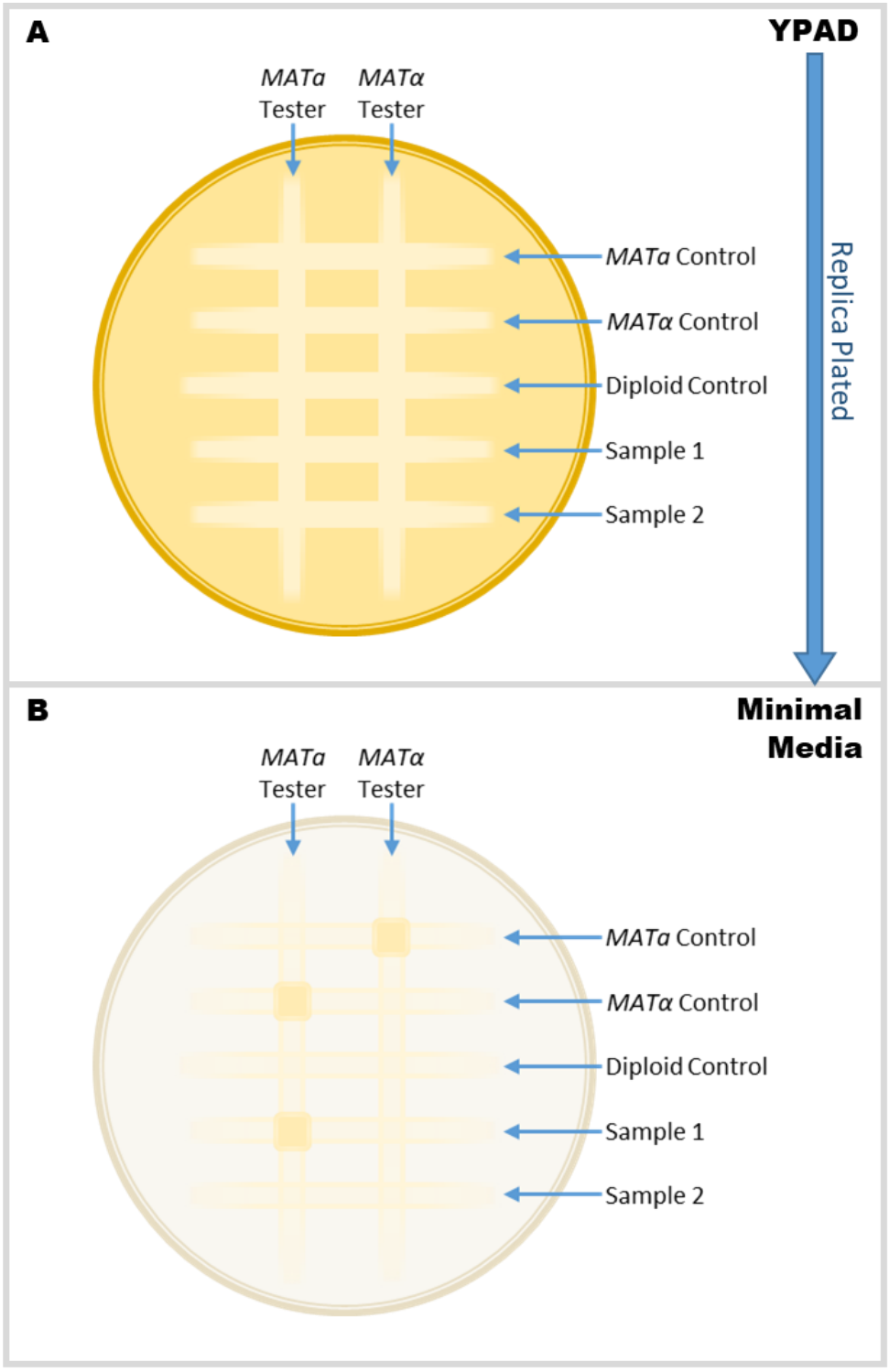

Figure 2.1 Mating type and ploidy test ladder schematic. (A) Mating type tester strains form the vertical 'rails' of the test ladder with 'rungs' being formed of both the samples to be tested and control haploid *MATa*, haploid *MATα* and diploid strains. The ladder is grown on YPAD overnight then replica plated to Minimal Media for overnight growth. (B) As all strains contain auxotrophic mutations they will be unable to grow on Minimal Media unless they have complemented their deficiencies by mating with a strain of the opposing mating type at the intersections of the ladder. The *MATa* and *MATα* controls will grow at the intersections with *MATα* and *MATa* test strains, respectively, while the diploid control will fail to grow at either intersection. In this example, Sample 1 would be expected to be haploid *MATα* and Sample 2 would be expected to be diploid.

2.5.5 Phenotypic Selection of Yeast

To identify auxotrophies or the presence of antibiotic markers, plated cells were replica plated using sterile velvet to appropriate drop-out plates or antibiotic plates and incubated at 30°C for 1 day.

To check mating types, cells from patches of *MATa* (hAG55/hBH216) or *MATα* (hAG56/hBH217) were resuspended in 100 µl ddH_2O, spread on Minimal Media plates and allowed to dry. Test strains were then replica plated on top using sterile velvets and incubated at 30°C for 2 days. Colonies surviving on *MATa* plates were considered to have mated successfully and so were identified as *MATα*. Conversely, colonies that survived on *MATα* plates were considered *MATa*.

2.5.6 Yeast Transformation

DNA for the transformation of *S. cerevisiae* was generated either by plasmid recovery from *E. coli*, and 1:10 dilution, or by generation of a PCR product with flanking homologous regions to the genomic region of interest. Cells were cultured to OD_{600}=0.8 spun down for 2 min and washed twice in 30 ml 100 mM lithium acetate (Sigma) before resuspension in 300-400 µl of 100 mM lithium acetate. Autoclaved 1% (w/v) salmon sperm DNA (Sigma) was denatured at 95°C for 5 min, sonicated and put on ice. 50 µl aliquots of cell suspension were incubated for 30 min at 30°C. To each aliquot, 240 µl 50% (w/v) PEG (Sigma), 35 µl 1 M lithium acetate (Sigma), 25 µl 1% (w/v) denatured salmon sperm DNA (Sigma) and 50 µl of DNA for transformation. Samples were incubated for 30 min at 30°C**,** heatshocked at 42°C for 15 to 45 min, spun down for 5 min and resuspended in 5 ml YPAD. Cells were incubated at 30°C for 90 min, spun down

for 2 min and washed in 5 ml sterile dH_2O. Finally, cells were resuspended in 100 µl sterile dH_2O, plated onto selective media and grown at 30°C for 2 days. Cells were streaked onto selective media and incubated at 30°C for 2 days. Single transformant colonies were patched onto YPAD and grown at 30°C overnight. Transformation was confirmed by DNA extraction and PCR or sequencing.

2.5.7 DNA Extraction of Yeast

Cells from YPAD patches were added to tubes containing 5 ml SCE, 250 µl Zymolyase suspension and 40 µl β-mercaptoethanol (Sigma) and incubated at 37°C for 1 h, shaking. 200 µl of DNA Lysis Buffer was added, mixed by inversion and incubated at 65°C for 5 min. 200 µl of 5M K-Acetate was added, mixed by inversion and incubated on ice for 30 min. Cells were spun down for 10 min and 300 µl of supernatant taken for addition to 800 µl ice-cold 100% Ethanol (Fisher). The tubes were mixed by inversion and spun down for 10 min.

Alternatively, DNA was extracted by MasterPure Kit (Cambio). The DNA pellet was washed twice in 100 µl 70% Ethanol, spinning 5 min after each, and dried in a vacuum centrifuge for 5-10 min at 65°C. The pellet was dissolved in 50-300 µl ddH_2O at 60°C and checked by PCR and DNA gel electrophoresis.

2.6 Meiotic Sampling and Analytical Methods

2.6.1 Meiotic Time-courses of *S. cerevisiae*

Archive strains were patched onto YPG and grown overnight. Cells were streaked onto YPAD plates and incubated for 2 days. A single colony was inoculated into 5-50 ml YPAD and grown overnight. This was used to inoculate 250 ml BYTA to approximately OD_{600}=0.3 which was incubated for 16 h. The BYTA culture was spun down, washed in 200 ml 1% K-Acetate. The cells were resuspended in 250 ml SPM at approximately OD_{600}=1.9, with appropriate supplements, and incubated, considering this time point as 0 h of the meiotic time course. All incubation steps were at 30°C.

Samples were taken hourly throughout the time course at volumes and times as required by the particular experiment. Usually, 0.5 ml samples for DAPI staining and 4-10 ml samples for either protein extraction or cytological spreading were taken at 0-9 h time points, plus 24 h.

2.6.2 DAPI Staining

The fluorescent probe 4',6-diamidino-2-phenylindole (DAPI) binds to the minor groove of DNA and is easily observed on a fluorescent microscope, which can then be used to observe the number of nuclei present within each ascus. 500 µl of meiotic culture was mixed with 750 µl 100% Ethanol and stored at -20°C. 1 µl 500 µg/ml DAPI (Sigma) was added and the sample incubated at room temperature for 30 seconds. Cells were spun down, resuspended in 200 µl 50% (v/v) glycerol and 4 µl placed on a microscope slide, sonicating first for 10 seconds, if needed. As DAPI staining was used to analyse the

progression of nuclear division, counts were made of the number of cells appearing to be mononucleate, binucleate, trinucleate or tetranucleate.

2.6.3 Cytological Methods

2.6.3.1 'Hard' Cytological Spreading for Aggregate Analysis

4.5 ml of meiotic culture was spun down on a bench centrifuge and resuspended to 500 µl with 1.0 M pH7.0 D-Sorbitol (Sigma). 12 µl of 1.0 M DTT (Sigma/Fermentas) and 7 µl 10 mg/ml Zymolyase (MPBio) was added and cells were spheroplasted by incubation at 37°C for 20 to 45 min with agitation. Spheroplasting success was determined by taking a few microliters to a microscope slide and adding an equivalent volume of 1.0% (w/v) Sodium N-Lauroylsarcosine (Sigma); most cells should lyse after a few seconds as the exposed membrane is disrupted by the detergent. After 3.5 ml of Stop Solution was added, cells were spun down and resuspended in 100 µl Stop Solution and distributed between 4 slides, which had been cleaned with ethanol. 20 µl of fixative was added to each slide followed by 40 µl of 1% Lipsol (Bibby Sterilin) and light mixing. 40 µl of fixative was added and the mixture spread across the slide. The spreads were incubated at room temperature (RT) for 30 min in damp conditions, then allowed to air-dry at RT. Once dry, slides were washed in 0.2% (v/v) PhotoFlo Wetting Agent (Kodak) then in dH_2O and allowed to air-dry slightly at RT. Slides were washed once in 0.025% Triton X-100 for 10 min at RT and twice in PBS for 5 min each at RT. Slides were blocked in 5% Skimmed Milk (Sigma) in PBS for 1-4 h at 37°C. Excess liquid was removed and slides laid horizontally in damp conditions. Primary α-Rad51 antibody (Santa Cruz), 150 µl per slide made up in 1% Skimmed Milk in PBS at 1:200, was added and the slides incubated at 4°C overnight. The slides were washed three times in PBS, 5 min each at RT, and incubated

in secondary AlexaFluor594 goat anti-mouse antibody (Life Technologies), 150 µl per slide made up in 1% Skimmed Milk in PBS at 1:1000, for 1-2 h at RT in damp conditions. Slides were washed three times with PBS, 5 min each at RT. Cover slips were affixed using Vectashield mounting medium with DAPI (VectorLabs), sealed with clear varnish and imaged on a DeltaVision microscope (z=12-15, Exposure times: RD-TP-RE=1.0 s, DAPI=0.05-1.0 s). Images were deconvolved by SoftWoRx software (standard settings) and the number of cells with No Signal, Rad51 Foci or Rad51 Aggregates counted. Aggregates were identified by pixel width using ImageJ software; this limit was generally 6 pixels = 0.39 µm, however due to potential variation in spreads performed on different days, the pixel limit was determined by visual inspection of several slides and then fixed for all timecourses spread under those same conditions.

2.6.3.2 'Gentle' Cytological Spreading for Spindle Pole Body (SPB) Analysis

In order to correlate the DAPI and SPB signals and to observe separation of *tetO*/TetR signals, a gentler spreading technique was employed to reduce the risk of the DAPI signal being disturbed by the spreading process. This process involved an additional initial step: 500 µl 37% (v/v) formaldehyde (Sigma) was added to 4.5 ml of meiotic culture and incubated at room temperature (RT) for 30 min. Cells were spun down and washed with 5 ml 1% (w/v) potassium acetate (Sigma). Cells were then spun down and treatment continued as per 'Hard' Spreading: cells were resuspended in Sorbitol, spheroplasted with DTT and Zymolyase, resuspended in stop solution and distributed over clean slides, fixative and lipsol were added and the mixture spread out, then slides were incubated in damp conditions, dried at RT, and washed in PhotoFlo Wetting Agent and dH_2O.

Cover slips were affixed using Vectashield mounting medium with DAPI (VectorLabs), sealed with clear varnish and imaged on a DeltaVision microscope, (z=12-24, Exposure times: FITC=1.0 s, RD-TP-RE=1.0 s, DAPI=0.05-1.0 s). Images were deconvolved by SoftWoRx software (standard settings) and analysed by counting the number of *tetO*/TetR signals or SPBs per cell, using GFP-tubulin as an additional signal where necessary, and the number of DAPI signals per cell.

2.6.4 Techniques for Protein Extraction from *S. cerevisiae*

2.6.4.1 TCA Protein Extraction

Samples containing 5-10 OD of cells were spun down, washed in 1 ml ddH_2O, and flash frozen in liquid nitrogen. The pellet was stored at -80°C for at least 2 h, then resuspended in 150 µl Buffer D and incubated on ice for 15 min. To each sample, 150 µl of 55% Trichloroacetic acid (TCA) (Sigma) was added and cells incubated for a further 10 min. Cells were spun down for 10 min then resuspended in 250 µl of Buffer H, with 10 µl 25x protease inhibitor stock (Roche). If necessary, 10 µl 1.5M Tris HCl pH8.8 was added to maintain pH, as shown by the blue indicator in the suspension. Cells were heat-shocked at 65°C for 10 min and spun down.

2.6.4.2 Native Protein Extraction

Samples containing 5-25 OD of cells were spun down, washed in 1ml Protein Lysis Buffer or ddH_2O, and flash-frozen in liquid nitrogen. The pellet was stored at -80°C for at least 2 h, then resuspended in 200 µl Protein Lysis Buffer. An equal volume of acid-washed glass beads (Sigma) was added to the suspension and the cells beaten on a Bead Beater for 3-5 cycles of 20-60 s, resting on ice for 5 min in between each cycle. The lysate was

separated from the beads by puncturing the base of each tube and centrifugation, collecting the flowthrough in fresh tubes. The lysate was spun down at 4°C for 10 min and the supernatant removed to a fresh tube. Protein concentration was determined by Bradford Assay.

2.6.4.3 Protein Concentration Determination by Bradford Assay

A standard protein sample, 10 mg/ml BSA (New England Biolabs), was diluted 1:10 then a range of volumes from 0-10 µl added to 1 ml filtered Bradford Assay Reagent (Biorad). Absorbances of the known standards were measured at 595 nm and a standard curve generated of Absorbance vs Concentration. Volumes of the unknown protein samples, produced by native extraction, were added to 1 ml Bradford Assay Reagent, their absorbances measured at 595 nm and the protein concentration determined using the equation generated from the gradient of the standard curve.

2.6.5 Immunoprecipitation (IP)

Following determination of Protein Concentration, e.g. by Bradford Assay, volumes of native protein extracts were calculated such that they contained a standard quantity of protein, between 0.5-2 mg, then each sample was made up to 200 µl volume with Protein Lysis Buffer.

Magnetic Dynabeads (Invitrogen), 50 µl per reaction, were washed 3 times in 200 µl Protein Lysis Buffer, using a magnetic rack. The beads were resuspended in 100 µl Protein Lysis Buffer with 5% (v/v) antibody and incubated at RT, rotating, for 0.6-2 h.

The beads were washed again, 3 times in 200 µl Protein Lysis Buffer on a magnetic rack, and incubated in the protein samples described above for 2 h – Overnight at 4°C, rotating.

The beads were washed 3 times in 200 µl Protein Lysis Buffer on a magnetic rack and resuspended in 48 µl 1x protein loading buffer, diluted from stock with lysis buffer. The beads were boiled for 5 min at 95°C, flash spun and returned to a chilled magnetic rack. The supernatant was analysed by SDS-PAGE gel and stored at -20°C.

2.6.6 Chromatin Immunoprecipitation (ChIP)

Liquid cultures of *S. cerevisiae* were grown to exponential phase and diluted to OD_{600}=0.3-0.4 in 45 ml volumes. To these, 4 ml 'ChIP Fixation Solution' was added and cells incubated at 18 °C for 30 min, shaking. To quench the crosslinking reaction, 2 ml 2.5 M glycine was added to reaction, the tubes inverted 5 times and incubated at room temperature for 5 min. The cells were spun down for 2 min at 4 °C and washed with 20 ml ice-cold PBS. Cells were spun down again at 4 °C for 2 min and resuspended in 1 ml ice-cold PBS. The OD_{600} was measured 15 OD of cells taken for resuspension in 300 µl '1x ChIP Lysis Buffer++'. An equivalent volume of acid-washed glass beads was added to each sample and the cells beadbeaten 3 times for 1 min, resting on ice for 5 min in between each.

The samples were sonicated in a pre-chilled Bioruptor at 4 °C for 6 cycles of [30 s sonication, 30 s off] at high level. Cells were spun down at maximum for 20 min at 4 °C and the supernatant transferred to new tubes, adjusting to 1 ml with 'ChIP Lysis Buffer++'. The supernatant was precleared with 30 µl Protein G Dynabeads, which had

been previously washed 6 times in 1 ml 'ChIP Lysis Buffer++', and incubated at 4 °C on a wheel for 1 h. The beads were pelleted and the supernatant transferred to new tubes, with 80 µl of each taken as the "Whole Cell Extract" (WCE) sample and stored at -80 °C. From the remaining supernatant, 880 µl was incubated with 5 µl antibody at 4 °C for 2 h (or Overnight), on a wheel. To immunoprecipitate, 50 µl of washed Protein G Dynabeads were added to each and incubated at 4 °C for 2 h (or Overnight), on a wheel. The beads were pelleted, discarding the supernatant by aspiration on a magnetic rack, and washed several times at 25 °C, shaking, for 5 min each: 2 washes in 1 ml 'ChIP Lysis Buffer++', 3 washes in 1 ml 'ChIP High-Salt Lysis Buffer', 2 washes in 1 ml 'ChIP Wash Buffer', and 1 wash in 1 ml 'TE Buffer'. To elute, the beads were incubated in 120 µl 'TES Buffer' at 65°C for 15 min. The beads were pelleted and the supernatant transferred to new tubes as the "IP sample".

To reverse crosslinking, the defrosted WCE samples with 40 µl 'TES3 Buffer' added to each, and the IP samples were incubated at 65 °C Overnight. The samples were incubated with 2 µl RNAse A (10 mg/ml) at 37 °C for 1 h, 900 rpm then incubated with 10 µl Proteinase K (20 mg/ml in TE) at 65 °C for 2 h, 900 rpm. The DNA was purified with a "ChIP DNA Clean & Concentrator" kit (Zymo Research), as per protocol except for elution of the DNA with 50µl Elution Buffer.

To prepare the qPCR reactions, WCE samples and IP samples were diluted 1:10 and the WCE samples were combined for the standard curve, serially diluting to 1:1, 1:10, 1:100 and 1:1,000. Each diluted sample was then added to a qPCR reaction mix with primer pairs targeting *FAB1*, *PAU5*, *SPB4* and *URA3*: 5 µl Diluted sample, 10 µl 2x Abgene SYBR Mix, 1.4 µl 1 µM Forward Primer, 1.4 µl 1 µM Reverse Primer, 2.2 µl dH_2O. The qPCR

reaction was programmed as follows: 95°C for 15min, 45 cycles of [95 °C for 10 s, 52°C for 20 s, 72 °C for 20s Acquiring on SYBR Channel] with a Melt Curve of 60 - 95 °C.

To analyse the qPCR data, C_t scores of the standard dilutions were taken from the linear section of the curve to generate an exponential equation. This was then used to determine the unknown concentration of the samples in arbitrary units corrected for the different volumes.

2.7 Strains Used in this Study

All strains are stored at -80°C in 1 ml 50% Glycerol plus 1 ml media (YPAD for *S. cerevisiae*, LB for *E. coli*). All strains of *S. cerevisiae* are in SK1 backgrounds.

2.7.1 Diploid *S. cerevisiae* Strains

Strain Number	Origin *Shortname*	*MATa* Genotype	*MATα* Genotype
dAG1668	T. Chou, (hAG1379 x hAG1847) *srs2Δ*	*MATa ura3 ho::hisG leu2::hisG,his4X arg4N, srs2Δ::KanMX4*	*MATα ho::LYS2/ho::hisG leu2::hisG/leu2¯(Xho1-Cla1) srs2Δ::KanMX4*
dAG1670	T. Chou, (hAG1856 x hAG1857) *srs2-101* TUB SPB	*MATa ho::LYS2 ura3 leu2? trp1::hisG his3::HIS3p-GFP-TUB1-HIS3 CNM67-3mCherry-NatMX4 srs2-101*	*MATα ho::LYS2 ura3 leu2? trp1::hisG his3::HIS3p-GFP-TUB1-HIS3 CNM67-3mCherry-NatMX4 srs2-101*
dAG1680	E. Strong, (hAG1886 x hAG1887) WT, *ura-*	*MATa ho::LYS2 TRP1 ura3 (VMA-201?)*	*MATα ho::LYS2 TRP1 ura3 (VMA-201?)*
dAG1681	T. Chou, (hAG1500 x hAG1695) *srs2-101*	*MATa ura3 lys2 ho::LYS2 leu2¯(Xho1-Cla1) trp1::hisG srs2-101*	*MATα ura3 lys2 ho::LYS2 leu2¯(Xho1-Cla1) trp1::hisG srs2-101*
dAG1692	T. Chou, (hAG1899 x hAG1845) WT TUB SPB	*MATa ho::LYS2 ura3 leu2? trp1::hisG his3::HIS3p-GFP-TUB1-HIS3 CNM67-3mCherry-NatMX4*	*MATα ho::LYS2 lys2 ura3 leu2::hisG his3-hisG trp1::hisG his3::HIS3p-GFP-TUB1-HIS3 CNM67-3mCherry-NatMX4*
dAG1735	E. Ahmed, (hAG1379 x hAG1845) *srs2Δ* TUB SPB	*MATa ho::LYS2 ura3 leu2? trp1::hisG his3::HIS3p-GFP-TUB1-HIS3 CNM67-3mCherry-NatMX4 srs2::KanMX*	*MATα ho::LYS2 ura3 leu2? trp1::hisG his3::HIS3p-GFP-TUB1-HIS3 CNM67-3mCherry-NatMX4 srs2::KanMX*
dAG1756	hAG2039 x hAG2040 WT*, ura- his- trp- leu-*	*ho::LYS2 ura3 leu2::hisG his3::hisG trp1::hisG*	*ho::LYS2 ura3 leu2::hisG his3::hisG trp1::hisG*
dAG1782	hAG2100 x hAG2101 *mek1Δ*	*ho::LYS2 lys2 ura3 leu2 mek1::LEU2*	*ho::LYS2 lys2 ura3 leu2 mek1::LEU2*
dAG1783	hAG2102 x hAG2103 *mek1Δ srs2-101*	*ho::LYS2 lys2 ura3 leu2 mek1::LEU2 srs2-101::HphMX his4x*	*ho::LYS2 lys2 ura3 leu2 mek1::LEU2 srs2-101::HphMX*
dAG1798	hAG2041 x hAG2122 *PK3-Rad51*	*ho::LYS2 lys2 ura3 leu2::hisG his3::hisG trp1::hisG PK3-Rad51*	*ho::LYS2 lys2 ura3 leu2 his3::hisG trp1::hisG PK3-RAD51*
dAG1799	hAG2120 x hAG2121 *PK3-Rad51 srs2-101*	*ho::LYS2 lys2 ura3 leu2 trp1::hisG PK3-RAD51 srs2-101::HphMX*	*ho::LYS2 lys2 ura3 leu2 his3::hisG trp1::hisG PK3-RAD51 srs2-101::HphMX*

Strain Number	Origin *Shortname*	*MATa* Genotype	*MATα* Genotype
dAG1805	hA2123 x hAG2124 *mek1Δ ZIP1-GFP srs2-101*	*ho::LYS2 lys2 ura3 leu2 mek1::LEU2 trp1::hisG ZIP1-GFP srs2-101::HphMX*	*ho::LYS2 lys2 ura3 leu2 mek1::LEU2 trp1::hisG ZIP1-GFP srs2-101::HphMX*
dAG1809	hAG2040 x hAG2041 WT *[PK3-RAD51]$_{+/-}$*	*ho::LYS2 lys2 ura3 leu2::hisG his3::hisG trp1::hisG PK3-Rad51*	*ho::LYS2 lys2 ura3 leu2::hisG his3::hisG trp1::hisG*
dAG1810	hAG2170 x hAG2182 *srs2-mn [PK3-RAD51]$_{+/-}$*	*ho::LYS2 lys2 ura3 leu2::hisG his3::hisG trp1::hisG pCLB2-3HA-SRS2::KANMX PK3-RAD51*	*ho::LYS2 lys2 ura3 leu2::hisG his3::hisG trp1::hisG pCLB2-3HA-SRS2::KANMX*
dAG1813	hAG2168 x hAG2169 *sae2Δ(Kan) srs2-mn*	*ho::LYS2 lys2 ura3 leu2 pCLB2-3HA-SRS2::KanMX sae2::KanMX6 trp1::hisG arg4-nsp,bgl*	*ho::LYS2 lys2 ura3 leu2 pCLB2-3HA-SRS2::KanMX sae2::KanMX6 trp1::hisG his3::hisG*
dAG1814	hAG2155 x hAG2170 *srs2-mn*	*ho::LYS2 lys2 ura3 leu2::hisG his3::hisG trp1::hisG pCLB2-3HA-SRS2::KanMX*	*ho::LYS2 lys2 ura3 leu2::hisG his3::hisG trp1::hisG pCLB2-3HA-SRS2::KANMX*
dAG1816	hAG2182 x hAG2183 *srs2-mn PK3-RAD51*	*ho::LYS2 lys2 ura3 leu2::hisG his3::hisG trp1::hisG pCLB2-3HA-SRS2::KANMX PK3-RAD51*	*ho::LYS2 lys2 ura3 leu2::hisG his3::hisG trp1::hisG pCLB2-3HA-SRS2::KANMX PK3-RAD51*
dAG1817	hAG1845 x hAG2145 SPB TUB *[TetO/R]$_{+/-}$*	*ho::LYS2 lys2 ura3 leu2::hisG trp1::hisG CNM67-3mCherry-NatMX4 his3::HIS3p-GFP-TUB1-HIS3 promURA3::tetR::GFP-LEU2,tetOx224-URA3*	*ho::LYS2 lys2 ura3 leu2::hisG trp1::hisG his3::HIS3p-GFP-TUB1-HIS3 CNM67-3mCherry-NatMX4*
dAG1818	hAG2180 x hAG2174 SPB TUB *srs2-mn [TetO/R]$_{+/-}$*	*ho::LYS2 lys2 ura3 leu2::hisG trp1::hisG CNM67-3mCherry-NatMX4 his3::HIS3p-GFP-TUB1-HIS3 promURA3::tetR::GFP-LEU2,tetOx224-URA3 pCLB2-3HA-SRS2::KANMX*	*ho::LYS2 lys2 ura3 leu2::hisG trp1::hisG his3::HIS3p-GFP-TUB1-HIS3 CNM67-3mCherry-NatMX4 pCLB2-3HA-SRS2::KANMX*
dAG1819	hAG2178 x hAG2148 SPB *[TetO/R]$_{+/-}$*	*ho::LYS2 lys2 ura3 leu2::hisG his3::hisG trp1::hisG CNM67-3mCherry-NatMX4*	*ho::LYS2 lys2 ura3 leu2::hisG promURA3::tetR::GFP-LEU2,tetOx224-URA3 trp1::hisG CNM67-3mCherry-NatMX4*
dAG1820	hAG2177 x hAG2172 SPB *srs2-mn [TetO/R]$_{+/-}$*	*ho::LYS2 lys2 ura3 leu2::hisG his3::hisG trp1::hisG CNM67-3mCherry-NatMX4 promURA3::tetR::GFP-*	*ho::LYS2 lys2 ura3 leu2::hisG his3::hisG trp1::hisG CNM67-3mCherry-NatMX4 pCLB2-3HA-SRS2::KANMX*

Strain Number	Origin *Shortname*	*MATa* Genotype	*MATα* Genotype
		LEU2,tetOx224-URA3 pCLB2-3HA-SRS2::KANMX	
dAG1821	hAG2200 x hAG2201 *sae2Δ(Kan)*	*ho::LYS2 lys2 ura3 leu2 his3::hisG trp1::hisG arg4-nsp,bgl sae2::KanMX6*	*ho::LYS2 lys2 ura3 leu2 his3::hisG trp1::hisG arg4-nsp,bgl sae2::KanMX6*
dAG1838	hAG2221 x hAG2222 *spo11-Y135F srs2-mn*	*ho::LYS2 lys2 ura3 leu2::hisG pCLB2-3HA-SRS2::KanMX spo11-Y135F-HA3-His6::KanMX4*	*ho::LYS2 lys2 ura3 leu2::hisG his3::hisG trp1::hisG pCLB2-3HA-SRS2::KanMX spo11-Y135F-HA3-His6::KanMX4*
dAG1845	hAG2238 x hAG2227 *sae2Δ(Hyg)*	*ho::LYS2 lys2 ura3 leu2::hisG his3::hisG trp1::hisG sae2Δ::HphMX*	*ho::LYS2 lys2 ura3 leu2::hisG his3::hisG trp1::hisG sae2Δ::HphMX*
dAG1846	hAG2228 x hAG2229 *sae2Δ(Hyg) srs2-mn*	*ho::LYS2 lys2 ura3 leu2::hisG his3::hisG trp1::hisG sae2Δ::HphMX pCLB2-3HA-SRS2::KanMX*	*ho::LYS2 lys2 ura3 leu2::hisG his3::hisG trp1::hisG sae2Δ::HphMX pCLB2-3HA-SRS2::KanMX*
dAG1847	hAG2234 x hAG2235 *rad51Δ*	ho::lys2 lys2 ura3 leu2::hisG ade2::LK trp1::hisG rad51Δ::HisG-URA3-hisG	ho::LYS2 lys2 ura3 leu2::hisG ade2::LK rad51Δ::HisG-URA3-hisG
dAG1865	hAG2250 x hAG2251 *tel1Δ srs2-mn sae2Δ*	*MATa ho::LYS2 lys2 ura3 leu2 his3::hisG trp1::hisG tel1Δ::HphMX sae2Δ::HphMX pCLB2-3HA-SRS2::KanMX*	*MATα ho::LYS2 lys2 ura3 leu2 his3::hisG trp1::hisG tel1Δ::HphMX sae2Δ::HphMX pCLB2-3HA-SRS2::KanMX*
dAG1868	hAG2268 x hAG2269 *mre11-58S srs2-mn sae2Δ*	*MATa ho::LYS2 lys2 ura3 leu2 his3::hisG trp1::hisG mre11-58S(H213Y) pCLB2-3HA-SRS2::KanMX sae2Δ::HphMX*	*MATα ho::LYS2 lys2 ura3 leu2 his3::hisG trp1::hisG mre11-58S(H213Y) pCLB2-3HA-SRS2::KanMX sae2Δ::HphMX*
dAG1870	hAG2278 x hAG2279 *mre11-H125N srs2-mn*	*MATa ho::LYS2 lys2 ura3 leu2 his3::hisG trp1::hisG mre11-H125N pCLB2-3HA-SRS2::KanMX*	*MATα ho::LYS2 lys2 ura3 leu2 his3::hisG trp1::hisG mre11-H125N pCLB2-3HA-SRS2::KanMX*
dAG1871	hAG2280 x hAG2281 *mre11-H125N srs2-mn sae2Δ*	*MATα ho::LYS2 lys2 ura3 leu2 his3::hisG trp1::hisG mre11-H125N sae2Δ::HphMX pCLB2-3HA-SRS2::KanMX*	*MATα ho::LYS2 lys2 ura3 leu2 his3::hisG trp1::hisG mre11-H125N sae2Δ::HphMX pCLB2-3HA-SRS2::KanMX*
dAG1877	hAG2285 x hAG2289 *RFA1-PK9 WT*	*MATa ho::LYS2 lys2 ura3 leu2::hisG his3::hisG trp1::hisG RFA1-PK9::KanMX*	*MATα ho::LYS2 lys2 ura3 leu2::hisG his3::hisG trp1::hisG RFA1-PK9::KanMX*
dAG1878	hAG2290 x hAG2291 *RFA1-PK9 srs2-mn*	*MATa ho::LYS2 lys2 ura3 leu2::hisG his3::hisG trp1::hisG RFA1-PK9::KanMX pCLB2-3HA-SRS2::KANMX*	*MATα ho::LYS2 lys2 ura3 leu2::hisG his3::hisG trp1::hisG RFA1-PK9::KanMX pCLB2-3HA-SRS2::KANMX*

Strain Number	Origin *Shortname*	*MATa* Genotype	*MATα* Genotype
dAG1882	hAG2305 x hAG2306 *RFA1-GFP*	*MATa ho::LYS2 lys2 ura3 leu2::hisG his3::hisG trp1::hisG RFA1-GFP::KanMX*	*MATα ho::LYS2 lys2 ura3 leu2::hisG his3::hisG trp1::hisG RFA1-GFP::KanMX*
dAG1883	hAG2292 x hAG2293 *RFA1-GFP srs2-mn*	*MATa ho::LYS2 lys2 ura3 leu2::hisG his3::hisG trp1::hisG RFA1-GFP::KanMX pCLB2-3HA-SRS2::KANMX*	*MATα ho::LYS2 lys2 ura3 leu2::hisG his3::hisG trp1::hisG RFA1-GFP::KanMX pCLB2-3HA-SRS2::KANMX*
dAG1884	hAG2294 x hAG2295 *RFA1-GFP srs2-mn sae2Δ*	*MATa ho::LYS2 lys2 ura3 leu2::hisG his3::hisG trp1::hisG RFA1-GFP::KanMX pCLB2-3HA-SRS2::KANMX sae2Δ::HphMX*	*MATα ho::LYS2 lys2 ura3 leu2::hisG his3::hisG trp1::hisG RFA1-GFP::KanMX pCLB2-3HA-SRS2::KANMX sae2Δ::HphMX*
dAG1885	hAG2309 x hAG2310 *mre11-58S srs2-mn*	*MATa ho::LYS2 lys2 ura3 leu2 his3::hisG trp1::hisG mre11-58S(H213Y) pCLB2-3HA-SRS2::KanMX*	*MATα ho::LYS2 lys2 ura3 leu2 his3::hisG trp1::hisG mre11-58S(H213Y) pCLB2-3HA-SRS2::KanMX*
dAG1887	hAG2299 x hAG2300 *ndt80Δ srs2-mn*	*MATa ho::LYS2 lys2 ura3 leu2::hisG arg4Δ(eco47III-hpaI) trp1::hisG his3::hisG ndt80Δ(Eco47III-BseRI)::KanMX6 pCLB2-3HA-SRS2::KanMX*	*MATα ho::LYS2 lys2 ura3 arg4Δ(eco47III-hpaI) leu2::hisG ndt80Δ(Eco47III-BseRI)::KanMX6 pCLB2-3HA-SRS2::KanMX*
dAG1892	hAG2173 x hAG2174 *srs2-mn* SPB TUB	*MATa ho::LYS2 lys2 ura3 leu2::hisG trp1::hisG his3::HIS3p-GFP-TUB1-HIS3 CNM67-3mCherry-NatMX4 pCLB2-3HA-SRS2::KANMX*	*MATα ho::LYS2 lys2 ura3 leu2::hisG trp1::hisG his3::HIS3p-GFP-TUB1-HIS3 CNM67-3mCherry-NatMX4 pCLB2-3HA-SRS2::KANMX*
dAG1898	hAG2350 x hAG2351 *spo11-Y135F sae2Δ*	*MATa ho::LYS2 lys2 ura3 leu2::hisG trp1::hisG spo11-Y135F-HA3-His6::KanMX4 sae2Δ::HphMX*	*MATα ho::LYS2 lys2 ura3 leu2::hisG spo11-Y135F-HA3-His6::KanMX4 sae2Δ::HphMX*

2.7.2 Haploid *S. cerevisiae* Strains

Strain Number	Origin *Shortname*	Genotype
hAG55	*Mating type tester, MATa*	*MATa ura2*
hAG56	*Mating type tester, MATα*	*MATα ura2*
hBH216	B. Hu *Mating type tester, MATa*	*MATa his1*
hBH217	B. Hu *Mating type tester, MATα*	*MATα his1*
hAG707	N. Hollingsworth *mek1Δ*	*MATa ho::LYS2 lys2 ura3 leu2ΔhisG his4x mek1::LEU2 ade2-bglII*
hAG1500	L. Hulme *srs2-101*	*MATα ura3 lys2 ho::LYS2 leu2¯(Xho1-Cla1) trp1::hisG srs2-101*
hAG1743	T. Chou *ZIP1-GFP*	*MATα ura3 lys2 ho::LYS2 leu2¯(Xho1-Cla1) trp1::hisG ZIP1-GFP*
hAG1801	T. Chou *rad51-II3A*	*MATα ho::hisG, leu2::hisG, ura3(ΔSma-Pst), his4-X::LEU2-(NgoMIV;+ori)-URA3, RAD51-R188A,K361A,K371A-KanMX6*
hAG1802	T. Chou *rad51-II3A*	*MATa ho::hisG, leu2::hisG, ura3(ΔSma-Pst), HIS4-X::LEU2-(BamHI;+ori)-ura3, RAD51-R188A,K361A,K371A-KanMX6*
hAG1845	T. Chou *TUB SPB*	*MATα ho::LYS2 lys2 ura3 leu2::hisG his3-hisG trp1::hisG his3::HIS3p-GFP-TUB1-HIS3 CNM67-3mCherry-NatMX4*
hAG1886	E. Strong *WT, ura-*	*MATa ho::LYS2 ura3 (VMA-201?)*
hAG1887	E. Strong *WT, ura-*	*MATα ho::LYS2 ura3 (VMA-201?)*
hAG2015	hAG1801::(pBH173-M13F/R) *rad51-II3A(NatMX)*	*MATα ho::hisG, leu2::hisG, ura3(ΔSma-Pst), his4-X::LEU2-(NgoMIV;+ori)-URA3, RAD51-R188A,K361A,K371A-NatMX*
hAG2016	hAG1500::(pBH43-LJH013/014) *srs2-101::HphMX*	*MATα ho::LYS2 lys2 leu2¯(Xho1-Cla1) ura3 trp1::hisG srs2-101::HphMX*
hAG2031	hAG2014 x hAG2015 dissection *srs2-mn rad51-II3A*	*MATa ho::LYS2 TRP1 ura3 (VMA-201?) pCLB2::SRS2::KANMX ho::hisG, leu2::hisG, ura3(ΔSma-Pst), his4-X::LEU2-(NgoMIV;+ori)-URA3, RAD51-R188A,K361A,K371A-NatMX*
hAG2032	hAG2014 x hAG2015 dissection *srs2-mn rad51-II3A*	*MATα ho::LYS2 TRP1 ura3 (VMA-201?) pCLB2::SRS2::KANMX ho::hisG, leu2::hisG, ura3(ΔSma-Pst), his4-X::LEU2-(NgoMIV;+ori)-URA3, RAD51-R188A,K361A,K371A-NatMX*
hAG2039	BH26 dissection WT, *leu- his- trp- ura-*	*MATa ho::LYS2 lys2 ura3 leu2::hisG his3::hisG trp1::hisG*
hAG2040	BH26 dissection WT, *leu- his- trp- ura-*	*MATα ho::LYS2 lys2 ura3 leu2::hisG his3::hisG trp1::hisG*
hAG2041	hAG2039::pAG469(Cas9) & pAG470 (template) *PK3-RAD51*	*MATa ho::LYS2 lys2 ura3 leu2::hisG his3::hisG trp1::hisG PK3-RAD51*
hAG2100	hAG707 x hAG2016 dissection *mek1Δ*	*MATa ho::LYS2 lys2 ura3 leu2 mek1::LEU2*

Strain Number	Origin *Shortname*	Genotype
hAG2101	hAG707 x hAG2016 dissection *mek1Δ*	*MATα ho::LYS2 lys2 ura3 leu2 mek1::LEU2*
hAG2102	hAG707 x hAG2016 dissection *mek1Δ srs2-101*	*MATa ho::LYS2 lys2 ura3 leu2 mek1::LEU2 srs2-101::HphMX his4x*
hAG2103	hAG707 x hAG2016 dissection *mek1Δ srs2-101*	*MATα ho::LYS2 lys2 ura3 leu2 mek1::LEU2 srs2-101::HphMX*
hAG2120	hAG2041 x hAG2016 dissection *PK3::RAD51 srs2-101*	*MATa ho::LYS2 lys2 ura3 leu2 trp1::hisG PK3-RAD51 srs2-101::HphMX*
hAG2121	hAG2041 x hAG2016 dissection *PK3::RAD51 srs2-101*	*MATα ho::LYS2 lys2 ura3 leu2 his3::hisG trp1::hisG PK3-RAD51 srs2-101::HphMX*
hAG2122	hAG2041 x hAG2016 dissection *PK3::RAD51*	*MATα ho::LYS2 lys2 ura3 leu2 his3::hisG trp1::hisG PK3-RAD51*
hAG2123	hAG2116 x hAG2016 dissection *mek1Δ ZIP1-GFP srs2-101*	*MATa ho::LYS2 lys2 ura3 leu2 mek1::LEU2 trp1::hisG ZIP1-GFP srs2-101::HphMX*
hAG2124	hAG2116 x hAG2016 dissection *mek1Δ ZIP1-GFP srs2-101*	*MATα ho::LYS2 lys2 ura3 leu2 mek1::LEU2 trp1::hisG ZIP1-GFP srs2-101::HphMX*
hAG2145	hAG1979 x hAG1845 dissection *TetO/R* SPB TUB	*MATa ho::LYS2 lys2 ura3 leu2::hisG promURA3::tetR::GFP-LEU2,tetOx224-URA3 trp1::hisG CNM67-3mCherry-NatMX4 his3::HIS3p-GFP-TUB1-HIS3*
hAG2148	hAG2147 x hAG2016 dissection *TetO/R* SPB	*MATα ho::LYS2 lys2 ura3 leu2::hisG promURA3::tetR::GFP-LEU2,tetOx224-URA3 trp1::hisG CNM67-3mCherry-NatMX4*
hAG2155	hAG2039 ::(pAG335-LJH025/26) *SRS2::pCLB2/srs2-mn*	*MATa ho::LYS2 lys2 ura3 leu2::hisG his3::hisG trp1::hisG pCLB2-3HA-SRS2::KanMX*
hAG2168	hAG287 x hAG2155 dissection *srs2-mn sae2Δ(Kan)*	*MATa ho::LYS2 lys2 ura3 leu2 pCLB2-3HA-SRS2::KanMX sae2::KanMX6 trp1::hisG arg4-nsp,bgl*
hAG2169	hAG287 x hAG2155 dissection *srs2-mn sae2Δ(Kan)*	*MATα ho::LYS2 lys2 ura3 leu2 pCLB2-3HA-SRS2::KanMX sae2::KanMX6 trp1::hisG his3::hisG*
hAG2170	hAG1845 x hAG2155 dissection *srs2-mn*	*MATα ho::LYS2 lys2 ura3 leu2::hisG his3::hisG trp1::hisG pCLB2-3HA-SRS2::KANMX*
hAG2172	hAG1845 x hAG2155 dissection *srs2-mn* SPB	*MATα ho::LYS2 lys2 ura3 leu2::hisG his3::hisG trp1::hisG CNM67-3mCherry-NatMX4 pCLB2-3HA-SRS2::KANMX*
hAG2173	hAG1845 x hAG2155 dissection *srs2-mn* SPB TUB	*MATa ho::LYS2 lys2 ura3 leu2::hisG trp1::hisG his3::HIS3p-GFP-TUB1-HIS3 CNM67-3mCherry-NatMX4 pCLB2-3HA-SRS2::KANMX*
hAG2174	hAG1845 x hAG2155 dissection *srs2-mn* SPB TUB	*MATα ho::LYS2 lys2 ura3 leu2::hisG trp1::hisG his3::HIS3p-GFP-TUB1-HIS3 CNM67-3mCherry-NatMX4 pCLB2-3HA-SRS2::KANMX*

Strain Number	Origin *Shortname*	Genotype
hAG2177	hAG2147 x hAG2172 dissection *srs2-mn TetO/R* SPB	*MATa ho::LYS2 lys2 ura3 leu2::hisG his3::hisG trp1::hisG CNM67-3mCherry-NatMX4 promURA3::tetR::GFP-LEU2,tetOx224-URA3 pCLB2-3HA-SRS2::KANMX*
hAG2178	hAG2147 x hAG2172 dissection SPB	*MATa ho::LYS2 lys2 ura3 leu2::hisG his3::hisG trp1::hisG CNM67-3mCherry-NatMX4*
hAG2180	hAG2145 x hAG2174 dissection *srs2-mn TetO/R* SPB TUB	*MATa ho::LYS2 lys2 ura3 leu2::hisG trp1::hisG CNM67-3mCherry-NatMX4 his3::HIS3p-GFP-TUB1-HIS3 promURA3::tetR::GFP-LEU2,tetOx224-URA3 pCLB2-3HA-SRS2::KANMX*
hAG2182	hAG2041 x hAG2170 dissection *srs2-mn PK3-RAD51*	*MATa ho::LYS2 lys2 ura3 leu2::hisG his3::hisG trp1::hisG pCLB2-3HA-SRS2::KANMX PK3-RAD51*
hAG2183	hAG2041 x hAG2170 dissection *srs2-mn PK3-RAD51*	*MATα ho::LYS2 lys2 ura3 leu2::hisG his3::hisG trp1::hisG pCLB2-3HA-SRS2::KANMX PK3-RAD51*
hAG2200	hAG287 x hAG2039 dissection *sae2Δ(Kan)*	*MATa ho::LYS2 lys2 ura3 leu2 his3::hisG trp1::hisG arg4-nsp,bgl sae2::KanMX6*
hAG2201	hAG287 x hAG2039 dissection *sae2Δ(Kan)*	*MATα ho::LYS2 lys2 ura3 leu2 his3::hisG trp1::hisG arg4-nsp,bgl sae2::KanMX6*
hAG2221	hAG946 x hAG2155 dissection *srs2-mn spo11-Y135F*	*MATa ho::LYS2 lys2 ura3 leu2::hisG pCLB2-3HA-SRS2::KanMX spo11-Y135F-HA3-His6::KanMX4*
hAG2222	hAG946 x hAG2155 dissection *srs2-mn spo11-Y135F*	*MATα ho::LYS2 lys2 ura3 leu2::hisG his3::hisG trp1::hisG pCLB2-3HA-SRS2::KanMX spo11-Y135F-HA3-His6::KanMX4*
hAG2227	hAG2226 x hAG2155 dissection *sae2Δ(Hyg)*	*MATα ho::LYS2 lys2 ura3 leu2::hisG his3::hisG trp1::hisG sae2Δ::HphMX*
hAG2228	hAG2226 x hAG2155 dissection *sae2Δ(Hyg) srs2-mn*	*MATα ho::LYS2 lys2 ura3 leu2::hisG his3::hisG trp1::hisG sae2Δ::HphMX pCLB2-3HA-SRS2::KanMX*
hAG2229	hAG2226 x hAG2155 dissection *sae2Δ(Hyg) srs2-mn*	*MATa ho::LYS2 lys2 ura3 leu2::hisG his3::hisG trp1::hisG sae2Δ::HphMX pCLB2-3HA-SRS2::KanMX*
hAG2234	hAG2170 x hAG316 dissection *rad51Δ*	*MATa ho::lys2 lys2 ura3 leu2::hisG ade2::LK trp1::hisG rad51Δ::HisG-URA3-hisG*
hAG2235	hAG2170 x hAG316 dissection *rad51Δ*	*MATα ho::LYS2 lys2 ura3 leu2::hisG ade2::LK rad51Δ::HisG-URA3-hisG*
hAG2238	hAG2227 x hAG2039 dissection *sae2Δ(Hyg)*	*MATa ho::LYS2 lys2 ura3 leu2::hisG his3::hisG trp1::hisG sae2Δ::HphMX*
hAG2250	hAG2167 x hAG2229 dissection *tel1Δ sae2Δ srs2-mn*	*MATa ho::LYS2 lys2 ura3 leu2 his3::hisG trp1::hisG tel1Δ::HphMX sae2Δ::HphMX pCLB2-3HA-SRS2::KanMX*

Strain Number	Origin *Shortname*	Genotype
hAG2251	hAG2167 x hAG2229 dissection *tel1Δ sae2Δ srs2-mn*	*MATα ho::LYS2 lys2 ura3 leu2 his3::hisG trp1::hisG tel1Δ::HphMX sae2Δ::HphMX pCLB2-3HA-SRS2::KanMX*
hAG2268	hAG2159 x hAG2229 dissection *mre11-58S srs2-mn sae2*	*MATa ho::LYS2 lys2 ura3 leu2 his3::hisG trp1::hisG mre11-58S(H213Y) pCLB2-3HA-SRS2::KanMX sae2Δ::HphMX*
hAG2269	hAG2159 x hAG2229 dissection *mre11-58S srs2-mn sae2*	*MATα ho::LYS2 lys2 ura3 leu2 his3::hisG trp1::hisG mre11-58S(H213Y) pCLB2-3HA-SRS2::KanMX sae2Δ::HphMX*
hAG2278	hAG2161 x hAG2229 dissection *mre11-H125N srs2-mn*	*MATa ho::LYS2 lys2 ura3 leu2 his3::hisG trp1::hisG mre11-H125N pCLB2-3HA-SRS2::KanMX*
hAG2279	hAG2161 x hAG2229 dissection *mre11-H125N srs2-mn*	*MATα ho::LYS2 lys2 ura3 leu2 his3::hisG trp1::hisG mre11-H125N pCLB2-3HA-SRS2::KanMX*
hAG2280	hAG2161 x hAG2229 dissection *mre11-H125N srs2-mn sae2*	*MATα ho::LYS2 lys2 ura3 leu2 his3::hisG trp1::hisG mre11-H125N sae2Δ::HphMX pCLB2-3HA-SRS2::KanMX*
hAG2281	hAG2161 x hAG2229 dissection *mre11-H125N srs2-mn sae2*	*MATα ho::LYS2 lys2 ura3 leu2 his3::hisG trp1::hisG mre11-H125N sae2Δ::HphMX pCLB2-3HA-SRS2::KanMX*
hAG2285	hAG2039::[pBH245 fragment] *RFA1-PK9* WT	*MATa ho::LYS2 lys2 ura3 leu2::hisG his3::hisG trp1::hisG RFA1-PK9::KanMX*
hAG2289	hAG2040 x hAG2285 dissection *RFA1-PK9* WT	*MATα ho::LYS2 lys2 ura3 leu2::hisG his3::hisG trp1::hisG RFA1-PK9::KanMX*
hAG2290	hAG2170 x hAG2285 dissection *RFA1-PK9 srs2-mn*	*MATa ho::LYS2 lys2 ura3 leu2::hisG his3::hisG trp1::hisG RFA1-PK9::KanMX pCLB2-3HA-SRS2::KANMX*
hAG2291	hAG2170 x hAG2285 dissection *RFA1-PK9 srs2-mn*	*MATα ho::LYS2 lys2 ura3 leu2::hisG his3::hisG trp1::hisG RFA1-PK9::KanMX pCLB2-3HA-SRS2::KANMX*
hAG2292	hAG2228 x hAG2284 dissection *RFA1-GFP srs2-mn*	*MATa ho::LYS2 lys2 ura3 leu2::hisG his3::hisG trp1::hisG RFA1-GFP::KanMX pCLB2-3HA-SRS2::KANMX*
hAG2293	hAG2228 x hAG2284 dissection *RFA1-GFP srs2-mn*	*MATα ho::LYS2 lys2 ura3 leu2::hisG his3::hisG trp1::hisG RFA1-GFP::KanMX pCLB2-3HA-SRS2::KANMX*
hAG2294	hAG2228 x hAG2284 dissection *RFA1-GFP srs2-mn sae2*	*MATa ho::LYS2 lys2 ura3 leu2::hisG his3::hisG trp1::hisG RFA1-GFP::KanMX pCLB2-3HA-SRS2::KANMX sae2Δ::HphMX*
hAG2295	hAG2228 x hAG2284 dissection *RFA1-GFP srs2-mn sae2*	*MATα ho::LYS2 lys2 ura3 leu2::hisG his3::hisG trp1::hisG RFA1-GFP::KanMX pCLB2-3HA-SRS2::KANMX sae2Δ::HphMX*
hAG2299	hAG1688 x hAG2155 dissection *ndt80Δ srs2-mn*	*MATa ho::LYS2 lys2 ura3 leu2::hisG arg4Δ(eco47III-hpaI) trp1::hisG his3::hisG ndt80Δ(Eco47III-BseRI)::KanMX6 pCLB2-3HA-SRS2::KanMX*

Strain Number	Origin *Shortname*	Genotype
hAG2300	hAG1688 x hAG2155 dissection *ndt80Δ srs2-mn*	*MATα ho*::*LYS2 lys2 ura3 arg4Δ(eco47III-hpaI) leu2*::*hisG ndt80Δ(Eco47III-BseRI)*::*KanMX6 pCLB2-3HA-SRS2*::*KanMX*
hAG2305	hAG2040 x hAG2284 dissection RFA1-GFP WT	*MATa ho*::*LYS2 lys2 ura3 leu2*::*hisG his3*::*hisG trp1*::*hisG RFA1-GFP*::*KanMX*
hAG2306	hAG2040 x hAG2284 dissection *RFA1-GFP WT*	*MATα ho*::*LYS2 lys2 ura3 leu2*::*hisG his3*::*hisG trp1*::*hisG RFA1-GFP*::*KanMX*
hAG2309	hAG2039 x hAG2267 dissection *srs2-mn mre11-58S*	*MATa ho*::*LYS2 lys2 ura3 leu2 his3*::*hisG trp1*::*hisG mre11-58S(H213Y) pCLB2-3HA-SRS2*::*KanMX*
hAG2310	hAG2039 x hAG2267 dissection *srs2-mn mre11-58S*	*MATα ho*::*LYS2 lys2 ura3 leu2 his3*::*hisG trp1*::*hisG mre11-58S(H213Y) pCLB2-3HA-SRS2*::*KanMX*
hAG2350	hAG946 x hAG2238 dissection *spo11-Y135F sae2Δ*	*MATa ho*::*LYS2 lys2 ura3 leu2*::*hisG trp1*::*hisG spo11-Y135F-HA3-His6*::*KanMX4 sae2Δ*::*HphMX*
hAG2351	hAG946 x hAG2238 dissection *spo11-Y135F sae2Δ*	*MATα ho*::*LYS2 lys2 ura3 leu2*::*hisG spo11-Y135F-HA3-His6*::*KanMX4 sae2Δ*::*HphMX*

2.7.3 Plasmids, stored in *E. coli* Strains

Strain Ref.	Genotype	Source
YCplac33	Yeast centromeric plasmid; AmpR, URA3	B. Hu
YEplac195	Yeast episomal plasmid; AmpR, URA3	B. Hu
pAG468 [DH5α]	YCplac33 with RAD51 N-terminal section (cut site inserted after Rad51 start codon, Silent mutation in CRISPR site guided by pAG469); AmpR, URA3, KpnI	This Study
pAG469 [DH5α]	Cas9/CRISPR plasmid with N-terminal RAD51 guide sequence; AmpR, LEU2	This Study
pAG470 [DH5α]	pAG468::PK3; AmpR, URA3, Tag inserted at the KpnI site	This Study
pAG471 [DH5α]	YEplac195::RAD51 (i.e. RAD51OE); AmpR, URA3, includes promRAD51 & termRAD51	This Study
pBH43	HphMX plasmid; AmpR, HpHMX	B. Hu
pBH150	PK3 tag plasmid; AmpR, KanMX	B. Hu
pBH173	NatMX plasmid; AmpR, NatMX	B. Hu
pKT127	GFP plasmid; AmpR, KanMX	B. Hu

Chapter 3 Srs2 Function is Required for Normal Meiotic Progression

3.1 Introduction

Loss of Srs2 activity during meiosis has previously been shown to cause defects (Niu and Klein, 2017). These phenotypes include delayed progression, a reduction in the proportion of cells that successfully produce spores and a reduction in the percentage of those spores that can form viable colonies (Palladino and Klein, 1992). These phenotypes were confirmed in three *srs2* mutant backgrounds by analysis of nuclear division during meiotic timecourses, and spore viability following tetrad dissection. The strains used were *srs2Δ*, a complete deletion of *SRS2* by a KanMX marker, the *srs2-101* strain, which has been mutated at the ATP binding pocket thus preventing translocase and helicase activity, and the *srs2-mn* strain, which was generated during this study to be expressed only during mitosis under a *CLB2* promoter. To characterise these phenotypes further, cytological analysis was performed on meiotic samples in strains with fluorescently-tagged proteins in order to observe the division of spindle pole bodies (SPBs) as an indicator of cell cycle progression.

3.2 Sporulation is Delayed and Reduced in *srs2* Mutants

The programmed division of chromosomes between daughter cells can be easily observed in budding yeast and used to identify any perturbations in meiotic progression in mutant backgrounds of interest. After diploid yeast cell undergoes meiosis, haploid spores are formed within the plasma membrane of the mother cell, which then forms

an ascus around the mature spores. Staining the cells with DAPI and quantifying the number of visible signals over the duration of a meiotic time course can therefore allow direct observation of the rate of sporulation and provides insight into whether, and when, nuclear division has been affected (Figure 3.1, A).

A reduction of sporulation in wild-type and *srs2* strains was confirmed by DAPI analysis, over a meiotic time-course. The percentage of wild-type cells completing sporulation by 9 h post induction of meiosis was 93.5% while sporulation in *srs2* strains is reduced by approximately 34% to 59.5%, 59.0% and 60.0%, respectively in cells homozygous for *srs2-mn, srs2-101* and *srs2Δ* (Figure 3.1, B-E). Additionally, a delay of approximately 1 h was observed in the progression of meiosis in all *srs2* strains: in wild-type cells, 40% were completing Meiosis II by 5.9 h post meiotic induction, while in *srs2* strains it took approximately 6.9 h to reach the same level of 40% sporulation (Figure 3.1, B-E). This is consistent with previous work in our lab (E. Ahmed, unpublished data; Chou, 2014). Studies in non-SK1 backgrounds, which sporulate more slowly, have found a more pronounced delay in *srs2* sporulation, although the final values are consistent, reaching approximately 60% sporulation after 24h (Palladino and Klein, 1992).

3.3 Spore Viability is Reduced in *srs2* Mutants

Tetrad dissection confirmed a significant reduction in spore viability in *srs2* strains, from 98.3% in wild-type to 68.0%, 63.3% and 63.6%, respectively in cells homozygous for *srs2-mn, srs2-101* and *srs2Δ* (Figure 3.2). This is consistent with previous work in our lab and others (E. Ahmed, unpublished data; Palladino and Klein, 1992). The number of viable spores produced by each meiotic event can provide further information about the

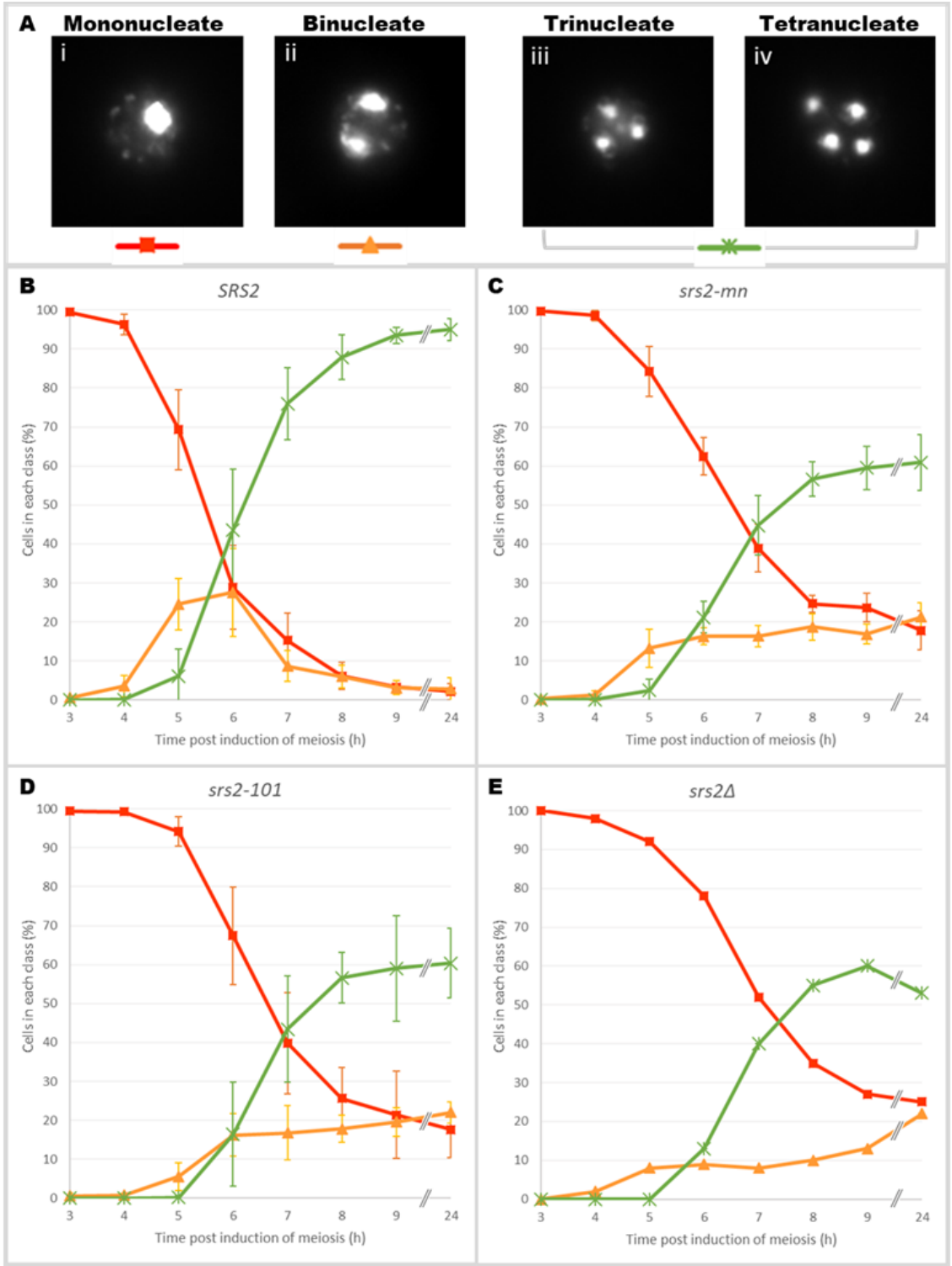

Figure 3.1 DAPI analysis of meiotic progression reveals sporulation defects when Srs2 activity is lost. (A) Examples of (i) Mono-, (ii) Bi- , (iii) Tri- and (iv) Tetra-nucleate cells). (B) In wild-type *SRS2* strains, 93.5% of cells progress through two nuclear divisions by 9h (n=7). (C-E) When Srs2 activity is lost, sporulation is reduced by 33.5-34.5% compared to wild-type (srs2-*mn*, n=7; *srs2-101*, n=5; *srs2Δ*, n=1). Loss of Srs2 activity also delays meiotic progression by approximately 1h, relative to wild-type, and leads to the persistence of binucleate cells.

timing of meiotic failure as *S. cerevisiae* can generally tolerate additional chromosomes but not their loss (Parry and Cox, 1970). Therefore, a failure in segregation during Meiosis I would be unlikely to produce more than 2 viable spores whereas a failure during Meiosis II would be unlikely to produce fewer than 2 viable daughter cells (Figure 1.4). Analysis of the number of viable products generated by each tetrad did not show any particular pattern in the viability of the spores, suggesting that the meiotic failure is not specific to Meiosis I nor Meiosis II alone (Figure 3.2, C).

3.4 Cytological Analysis of Meiotic Progression

SPB analysis of the meiotic delay observed in *S. cerevisiae srs2* mutants was performed by cytological spreading of strains with fluorescently-tagged proteins, over meiotic time courses. Strains expressing tagged proteins at the SPB (*CNM67-mCherry*) and tubulin spindle (*GFP-TUB1*) were analysed by observing division of DAPI-stained nuclei to ensure that the tags themselves did not affect meiosis (Figure 3.3). Subsequently, cells from meiotic time courses were spread and images were analysed for SPB division in the absence of Srs2 activity. Cells were classified by number of SPB signals, comparable to the classes used in nuclear division analysis (Figure 3.4).

In wild-type cells, meiotic progression as observed by SPB signals followed a similar pattern to the progression of meiosis as observed by nuclear division, although approximately 1 h advanced as expected due to SPB division preceding nuclear division, with 96.2% of cells completing two SPB divisions by 9 h post induction of meiosis (Figure 3.5, A). In the *srs2-101* strain, however, the pattern of SPB division was found to be significantly different to the pattern of nuclear division with the proportion of cells with

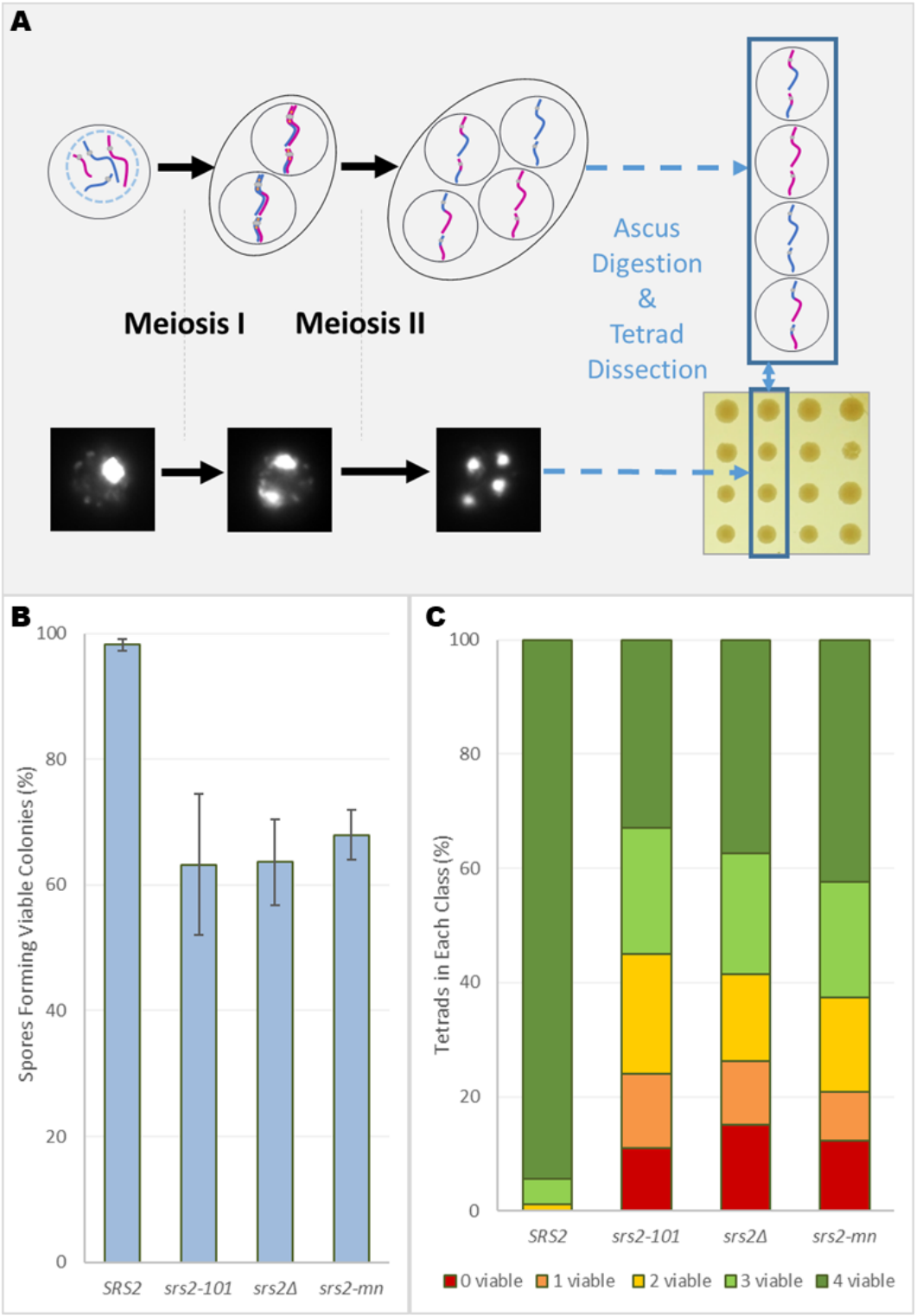

Figure 3.2 Spore viability analysis reveals non-specific defects in spore viability following loss of Srs2 activity. (A) Schematic overview of spore viability analysis: during meiosis, tetrads of spores form within protective asci. Following digestion of each ascus, spores are dissected and arranged into grids enabling phenotypic observation of all products formed from a single meiotic event. (B) Loss of Srs2 activity reduces spore viability from 98.3% in wild-type strains (n=6, 636 spores) to 63.3%, 63.6% and 68.0% in *srs2-101* (n=3, 396 spores), *srs2Δ* (n=3, 400 spores) and srs2-mn (n=5, 556 spores), respectively. (C) No discernible pattern was observed in the number of inviable spores produced per tetrad, suggesting the meiotic is failure is not specific to a particular meiotic phase.

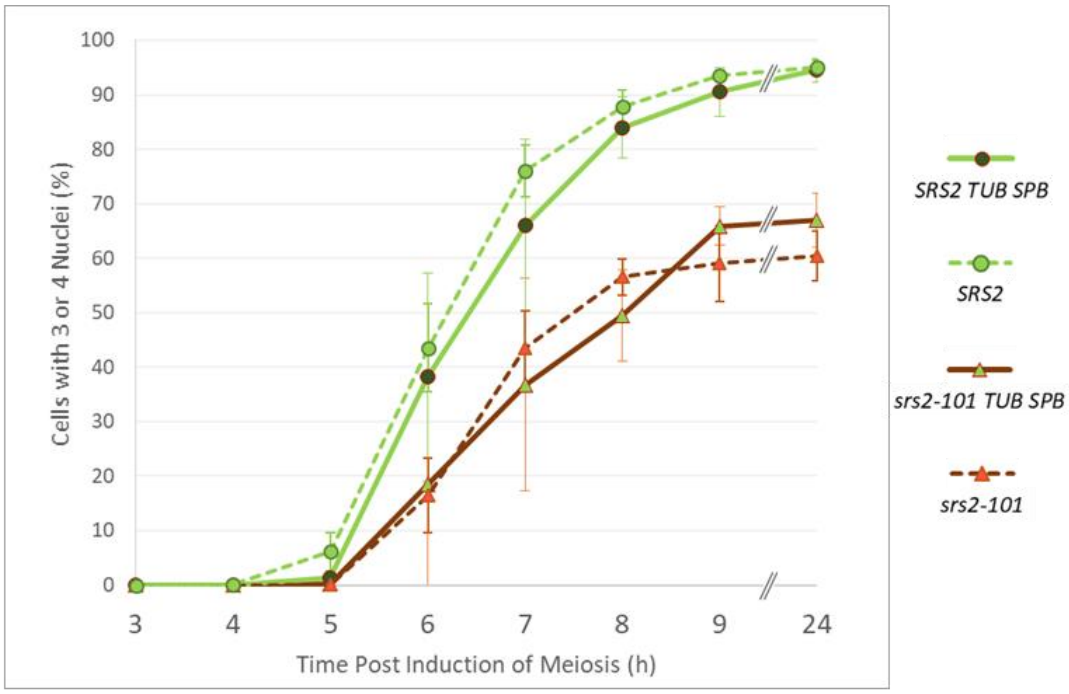

Figure 3.3 Nuclear division analysis shows no significant defect in meiotic progression caused by tagging the spindle pole body or tubulin spindle. The percentage of cells with 3 or 4 nuclear signals measured by DAPI in *SRS2* and *srs2-101* tagged strains was found to be within reasonable margins of their corresponding untagged strains. [SPB = *CNM67-mCherry*, TUB = *GFP-TUB1*. *SRS2 TUB SPB*, n=6; *SRS2*, n=7; *srs2-101 TUB SPB*, n=4; *srs2-101*, n=5]

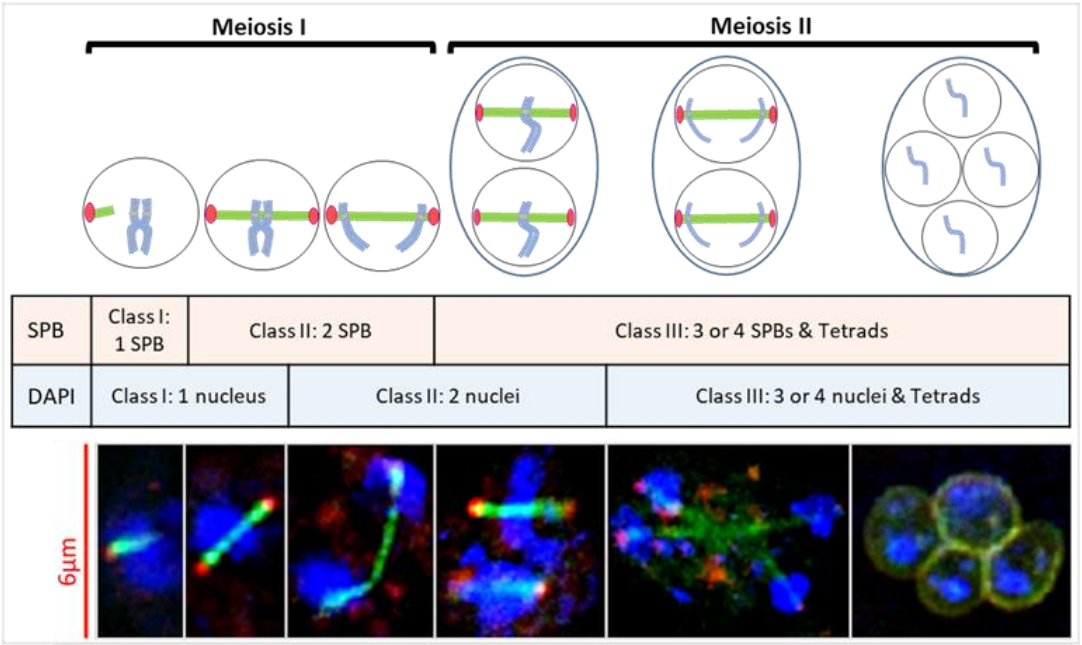

Figure 3.4 Comparison of the classifications used during analysis of spindle pole body (SPB) division and nuclear division (DAPI), with representative images. As SPB division precedes nuclear division, meiotic progression as analysed by SPB division is expected to appear slightly advanced in comparison to previous DAPI analysis.

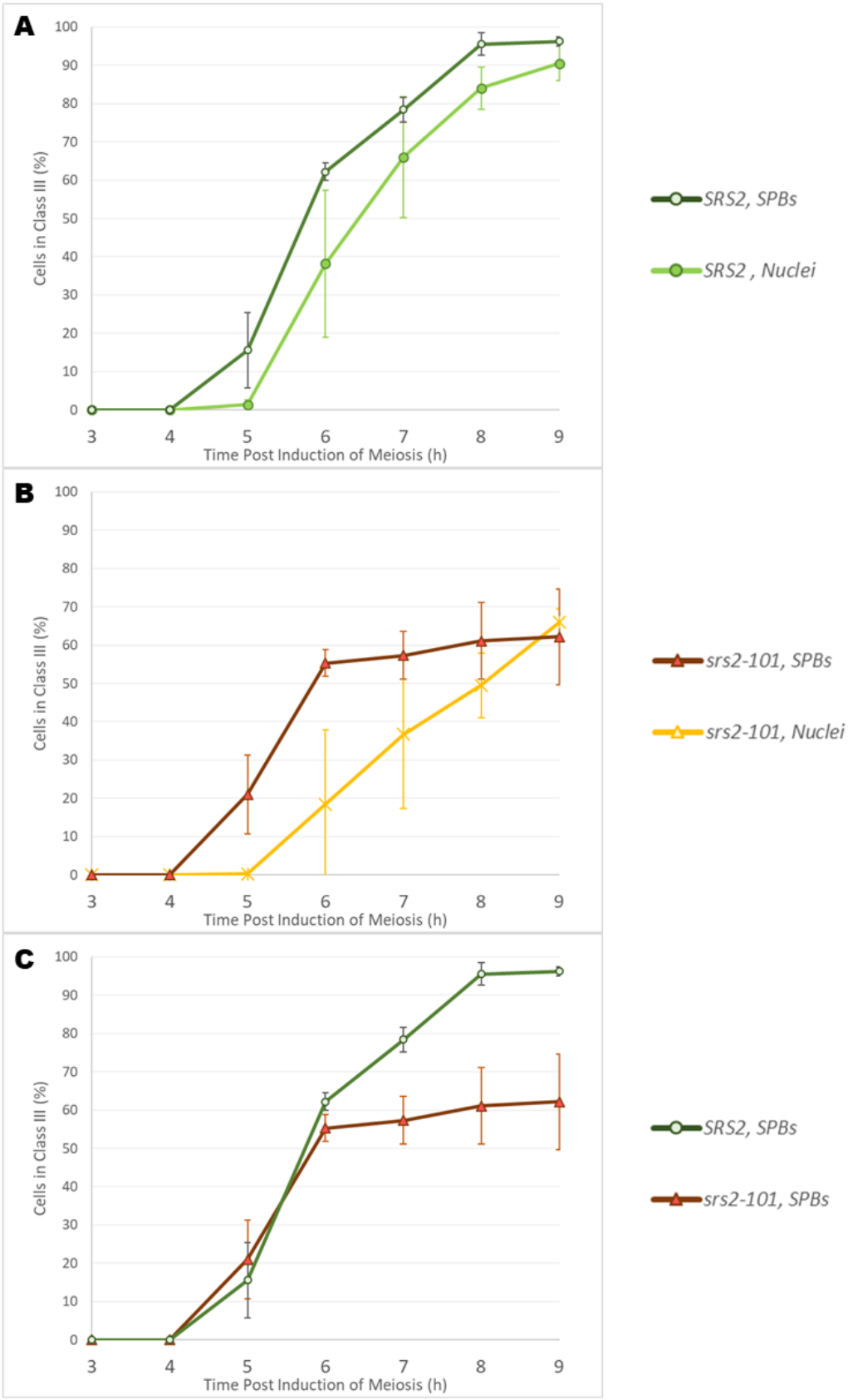

Figure 3.5 Comparison of meiotic progression analyses using SPB and nuclear division. (A) SPB division precedes nuclear division in *SRS2* by ~1h (SPBs, n=3; Nuclei, n=6). (B) In *srs2-101*, the delay between SPB division and nuclear division is greatly increased, although eventually reaching similar proportions of fully divided SPBs and nuclei by 9h (SPBs, n=2; Nuclei, n=4). (C) In *srs2-101*, SPB division is less delayed than nuclear division and occurs at a similar rate to wild-type until 6h.

divided SPBs being normal until 6 h (Figure 3.5 C). However, between 6 h and 9 h, the proportion of cells with correctly divided SPBs increased by only 6.8% such that, by 9 h, the proportion of cells that had failed to produce 4 SPBs was similar to the proportion of cells that fail to produce 4 nuclei, 37.8% and 34.1% respectively (Figure 3.5, B).

3.5 Cells with Failed Nuclear Division Can Continue to Divide Spindle Pole Bodies

As SPB division initially appears to proceed normally in *srs2* strains, even during time points in which a delay in nuclear division can already be observed, individual cells from each strain were scored for both criteria. Cytological spreads of wild-type and *srs2* strains expressing fluorescently tagged SPB proteins were analysed over meiotic time courses, and classified according to both their SPB score and their DAPI signal score, as per Figure 3.4.

This analysis revealed a further sub-classification within the population of cells previously termed Class III: "3 or 4 SPBs, & tetrads". Cells with divided SPBs and the expected 2 or more nuclear signals were termed Class IIIa (Figure 3.6 A), and those cells with divided SPBs but only a single, undivided nuclear signal were termed Class IIIb (Figure 3.6 B). A small number of cells were also found with 4 SPB signals but failed second nuclear division and these were included within Class IIIb.

Significantly, the proportion of Class IIIb cells was found to be greatly increased in *srs2* strains compared to the wild-type strain (Figure 3.6 C). The proportion of cells with this phenotype peaks at 6 h post induction of meiosis for *srs2-101* and *srs2Δ* strains, with

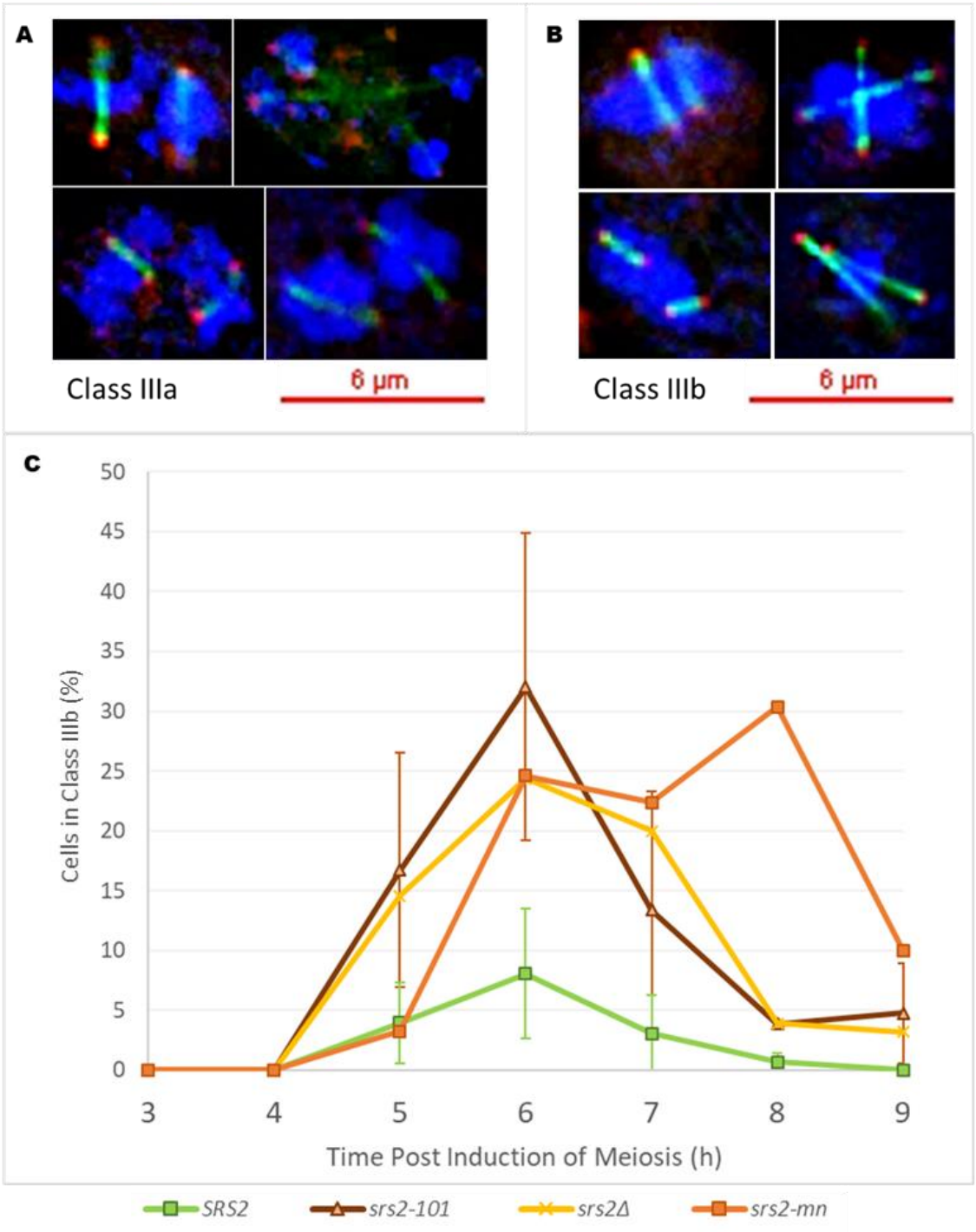

Figure 3.6 Further analysis of cells within Class III revealed two distinct subcategories of cells. (A) Class IIIa: cells with divided nuclei, as anticipated for cells with divided SPBs. (B) Class IIIb: cells with only 1 nuclear DAPI signal, despite having divided SPB signals. (C) Analysing both SPB division and nuclear division for each cell across meiotic timecourses revealed a marked increase in cells with divided SPB signals but only 1 nucleus in the *srs2* mutant strains compared to wild-type *SRS2*. (*SRS2*, n=3; *srs2-101*, n=2; *srs2Δ*, n=1; *srs2-mn*, n=1)

32.0% and 24.3%, respectively compared to 8.0% in wild-type. Unexpectedly, in cells that were homozygous for the meiotic-null allele *srs2-mn*, the proportion of cells that were found to be in Class IIIb was found to peak slightly later, at 8 h with 30.3%, leading us to question whether *srs2-101* and *srs2Δ* strains could retain mitotic or replication faults, giving the appearance of a slightly more severe meiotic phenotype. Later experiments therefore primarily focused on the *srs2-mn* allele.

3.6 Discussion

Following confirmation of the meiotic delay and the reduction in spore viability and sporulation caused by *srs2* mutation, an in-depth cytological analysis was performed. Observing the duplication and division of SPBs during meiosis allows analysis of meiotic progression in the context of the cell cycle. Interestingly, the loss of Srs2 activity was found to impede nuclear division at an earlier stage of meiosis compared to SPB division, leading to a significant population of cells failing to divide their nucleus but presenting 4 SPB signals. The presence of cells with divided SPBs but undivided nuclei suggests that cells are attempting to progress to Meiosis II despite the nucleus failing to divide correctly in Meiosis I. Interestingly, loss of the related Fbh1 helicase in *S. pombe* has also been shown to cause segregation failures during meiosis (Sun *et al.*, 2011).

As Srs2 is able to dismantle Rad51 NPFs *in vitro* and is thought to promote SDSA during mitotic repair, we considered that loss of Srs2 activity may permit increased strand invasion events by Rad51 that could cause DNA entanglement during meiosis. Analysis of the distribution of Rad51 in *srs2* mutants may therefore elucidate potential causes of the observed nuclear division failure.

Chapter 4 Loss of Srs2 Function in Meiosis Leads to Rad51 Aggregation

4.1 Introduction

Loss of Srs2 function causes sporulation failures, meiotic delay and a reduction in spore viability. Evidence presented in Chapter 3 suggests that this may be related to a failure in nuclear division that does not initially arrest the cell cycle. As Srs2 is thought to promote non-crossovers during mitotic repair by removing Rad51 from ssDNA nucleoprotein filaments and allowing repair by SDSA (Andersen and Sekelsky, 2010), I hypothesised that the nuclear division failure of *srs2* cells may be due to entanglement of DNA through inappropriate Rad51 activity. We therefore performed an immunofluorescent study of cytological spreads to observe the influence of Srs2 on the quantity and distribution of Rad51.

4.2 Immunofluorescent Study of Rad51

To investigate whether the distribution of Rad51 protein during meiosis is affected by the *srs2* mutations, cells from meiotic time courses were cytologically spread and then incubated in α-Rad51 primary antibody followed by a fluorescently-tagged secondary antibody. Analysing this immunofluorescence, three classes of cells were observed: cells with no Rad51 signal, cells with small foci of Rad51 signal and cells with much larger and brighter Rad51 signals, which we here refer to as 'Rad51 aggregates' (Figure 4.1, A). Scoring for Rad51 aggregates in the *srs2* strains revealed a significant increase in the

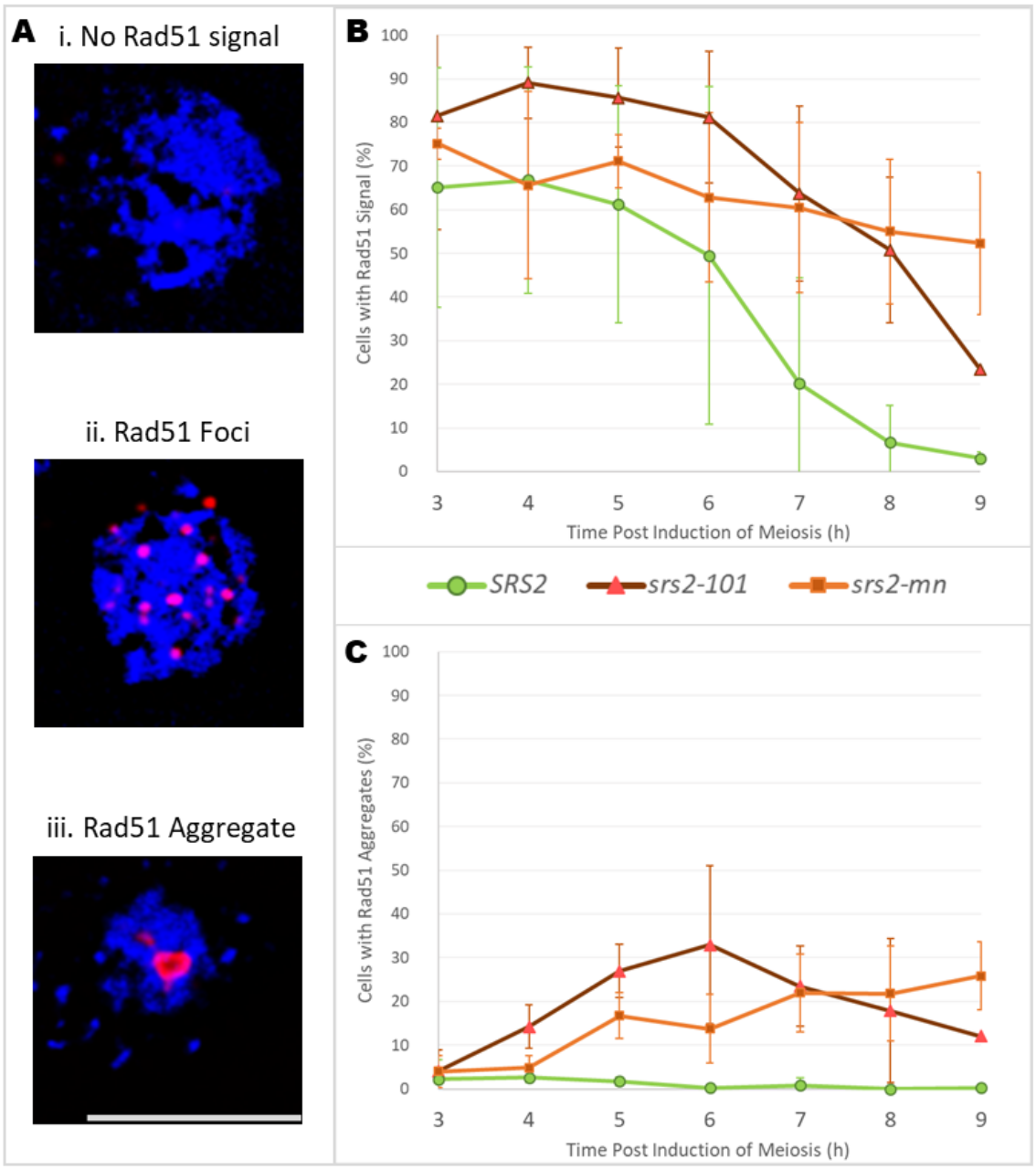

Figure 4.1 Immunofluorescence of cytological spreads with α-Rad51 antibody (Blue=DAPI/DNA, Red=α-Rad51). (A) Cells were categorised in the following classifications: (i) cells with no Rad51 signal, (ii) cells with Rad51 foci, (iii) cells with large Rad51 aggregates, scale bar = 5µm. (B) The *srs2* mutant strains show a persistence of Rad51 signal (foci or aggregates) at later time points in comparison to wild-type. (C) Significantly more cells contain Rad51 aggregates in *srs2* mutant strains compared to wild-type *SRS2*. (*SRS2*, n=3; *srs2-101*, n=3; *srs2-mn*, n=5)

proportion of cells with Rad51 aggregates and a persistence of Rad51 signals at later time points, compared to wild-type (Figure 4.1, B & C).

Like the SPB phenotype (see Figure 3.6, C), the aggregation phenotype appears more significant at later time points in the *srs2-mn* strain compared to *srs2-101*. Again, I hypothesise that this difference may be due to the retention of mitotic or replication defects in the *srs2-101* strain that are avoided by using the meiotic null allele. Notably, there was no evidence of any increase in Rad51 signal at 0 h in *srs2-mn* compared to wild-type.

4.3 RPA colocalises with Rad51 aggregation

Following resection of a DSB, ssDNA is coated with Replication Protein A (RPA), a heterotrimeric complex comprised of Rfa1, Rfa2 and Rfa3 subunits in yeast (hRPA1-3 in human), all of which are essential for viability (Brill and Stillman, 1991; Chen *et al.*, 2013). To determine if the Rad51 aggregates colocalised with ssDNA, Rfa1 was tagged with a C-terminal GFP marker and the distribution of Rfa1-GFP compared to Rad51 distribution in cytological spreads.

The Rad51 loading factor Rad52 is known to interact with all three subunits of the RPA heterotrimer and extensively colocalises with RPA during meiosis, although its colocalisation with Rad51 is more limited because Rad51 is loaded onto DNA in the place of RPA (Gasior *et al.*, 1998; Hays *et al.*, 1998). It was therefore expected that RPA and Rad51 foci would appear proximal but not colocalised in cytological analysis. An initial analysis performed across a meiotic timecourse, in *srs2-mn* and *SRS2* strains, and scored for both RPA and Rad51 signals confirmed that RPA foci do not generally colocalise with

Rad51 foci, even in the *srs2* mutant (Figure 4.2 A & B). Interestingly, however, aggregates of RPA or Rad51 were clearly found to frequently colocalise with at least a focus of the other protein and most frequently with an aggregate (Figure 4.2 C & D). It should be noted that the timecourses of strains expressing GFP-tagged Rfa1 unexpectedly produced lower levels of Rad51 signal compared to strains that lack the tagged protein, however this reduction was not observed in subsequent time courses of strains expressing another tagged Rfa1 protein, PK3-Rfa1 (Figure 7.3) suggesting that this effect may be due to differences in experimental conditions or the size of the GFP tag.

This analysis was used to select an appropriate time point for a more detailed focus-by-focus analysis in each cell, at 5 h post induction of meiosis. This detailed analysis confirmed the previous observations: 89.2% and 86.4% of Rfa1 and Rad51 foci were not colocalised, respectively, in cells homozygous for *SRS2* and *srs2-mn*, while 90.0% and 84.8% of aggregates were found to colocalise, respectively, in cells homozygous for *SRS2* and *srs2-mn* (Figure 4.3).

4.4 Super-Resolution Microscopy of Rad51 Aggregates

To determine whether the Rad51 aggregates observed in *srs2* strains contained any substructure or other pertinent information that might contribute to the formation of a model, cytological spreads of *srs2-mn* cells were prepared and analysed by super-resolution Structured Illumination Microscopy (SIM). The SoftWoRx program was used for reconstruction and image registration of the SIM data The SIMCheck plugin for Fiji/ImageJ was then used to determine the suitability of the SIM images for analysis, by

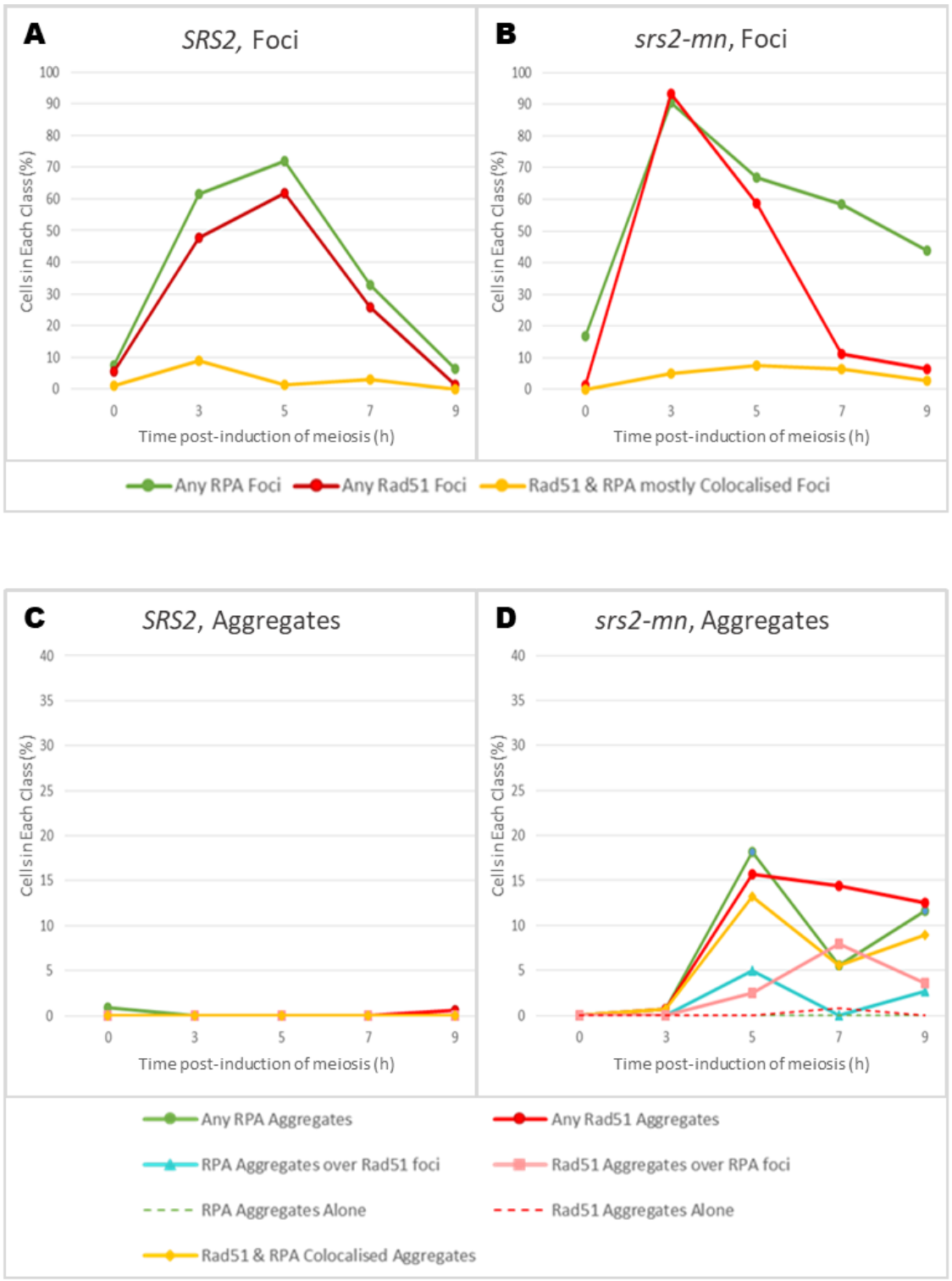

Figure 4.2 Colocalisation analysis of Rad51 immunofluorescence and fluorescently-tagged RPA. (A & B) Broad-scale analysis of cells with Rad51 and RPA foci did not show significant colocalisation of signals in either *SRS2* or *srs2-mn*. (C & D) In *srs2-mn* cells, aggregates of Rad51 or RPA frequently colocalise with at least a focus, and usually with an aggregate, of the other protein.

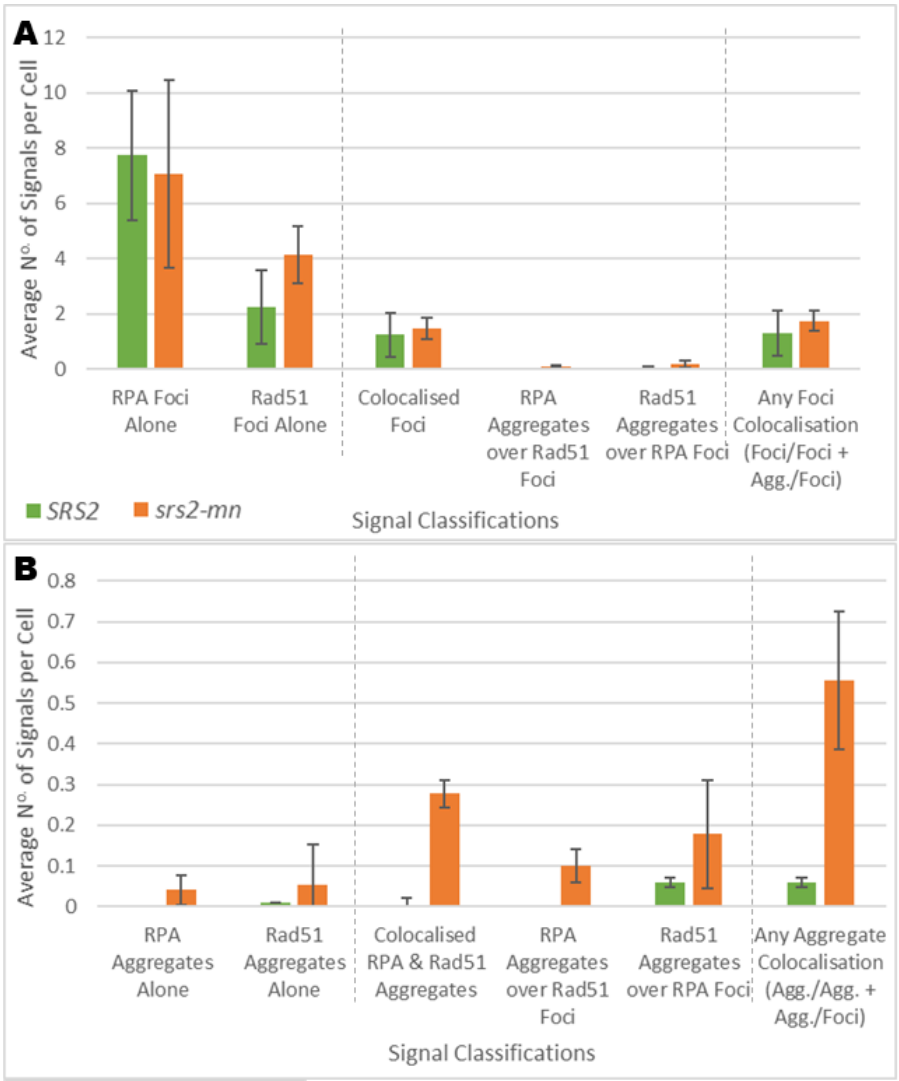

Figure 4.3 Detailed colocalisation analysis of Rad51 immunofluorescence and fluorescently-tagged RPA at 5h post induction of meiosis. (A) Average number of foci signals per cell, by classification, n=87. (B) Average number of aggregate signals per cell, by classification, n=78. (C) Analysis of colocalised foci as a percentage of all foci signals in each strain revealed a significant majority of foci of Rad51 and RPA were not colocalised: 89.2% and 86.4% of foci in *SRS2* and *srs2-mn*, respectively. (D) Analysis of colocalised aggregates as a percentage of all aggregate signals in each strain revealed that a significant majority of aggregates of Rad51 and RPA were colocalised: 90.0% and 84.8% of aggregates in *SRS2* and *srs2-mn*, respectively. Error bars represent variation between images analysed from the same time course.

intensity decay, and to process the images, by conversion to 16-bit, discarding negative values. SoftWoRx was additionally used to reconstitute a Widefield image equivalent to standard high-resolution DeltaVision microscopy, from the raw data, which was then deconvolved as standard for comparison to the SIM images.

Comparison of aggregates from the reconstituted DeltaVision (DV) images to the same cell in the SIM images revealed that the large aggregates of Rad51 that had previously been observed were generally comprised of several smaller foci of Rad51 (Figure 4.4).

4.5 Aggregates are Present in Cells Lacking Zip1

To gain further insight about the timing of aggregate formation, immunofluorescence of Rad51 was combined with observation of the synaptonemal complex (SC) using Zip1-GFP. The SC is a tripartite structure that forms along the length of homologous chromosomes during meiotic prophase and is thought to provide a framework that assists the process of homologous recombination (HR) (Heyting, 1996; Yang and Wang, 2009). Once HR has been completed, the SC dissolves leaving the chiasmata formed by HR to maintain the connection between the homologues (Zickler and Kleckner, 1999, 2016). Rad51 functions in meiotic HR as a loading factor for Dmc1 and is often observed in spread samples as punctate foci at meiotic DSBs in co-foci pairs with Dmc1 (Brown *et al.*, 2015).

In line with its role as a Dmc1 loading factor, it was expected that Rad51 foci would not be observed in cells that had completed HR and disassembled the SC. Indeed, immunofluorescence of wild-type cells revealed no observable Rad51 signal in cells

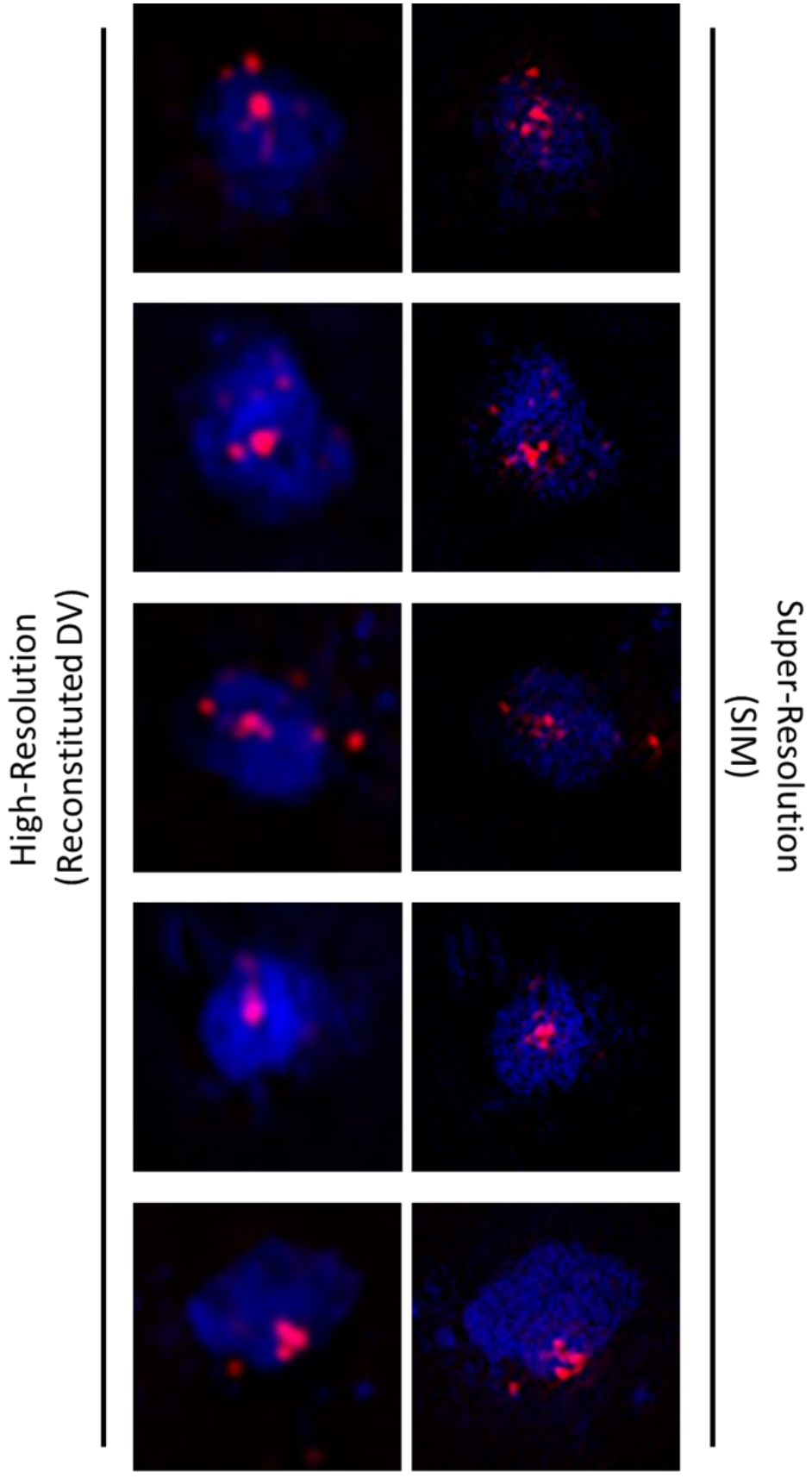

Figure 4.4 Analysis of *srs2-mn* spreads by Super-Resolution Microscopy (Structured Illumination Microscopy, SIM) reveals that the Rad51 aggregates observed by High-Resolution Microscopy (Deltavision, DV) are formed of smaller Rad51 foci. Samples from 6 h post induction of meiosis. Scale bar = 5µm

lacking any SC signal, as determined by expression of a fluorescently-tagged SC protein, Zip1-GFP (E. Ahmed, personal communication). However, in *srs2* mutant strains, immunofluorescence revealed clear Rad51 aggregate signals in cells that lacked any SC signal (Figure 4.5; E. Ahmed, unpublished data). From this analysis alone, however, it was unclear whether these cells had yet to form a SC or had completed SC dissolution.

4.6 Discussion

Immunofluorescent study of cytological spreads in the absence of Srs2 activity, identified aggregates of Rad51 protein. The combination of α-Rad51 immunofluorescence with expression of a fluorescently tagged RPA subunit, Rfa1-GFP, allowed for analysis of aggregate formation in the context of RPA-coated ssDNA. It was discovered that although foci of Rad51 and RPA rarely colocalise, most aggregates of Rad51 or RPA do colocalise with at least a focus of the other protein, but more often with an aggregate, suggesting that Rad51 aggregates occur at sites of ssDNA. Foci of RPA, and Rad52, have previously been observed to persist in mutants that are unable to complete recombination (*rad51*, *rad55*, *rad57* and *dmc1*), becoming larger and spherical or ellipsoid over time in *rad51*, *rad55* and *rad57* strains but remaining punctate in *dmc1* (Gasior *et al.*, 1998). The involvement of ssDNA at sites of Rad51 aggregation led us to question whether the meiotic delay caused by loss of Srs2 activity was due to errant strand invasion events or a failure in recombination and joint molecule resolution during DSB repair. To investigate this possibility further, several aspects of DSB repair were next investigated, including DSB formation, interhomologue strand invasion and chromatid separation, see Chapter 5.

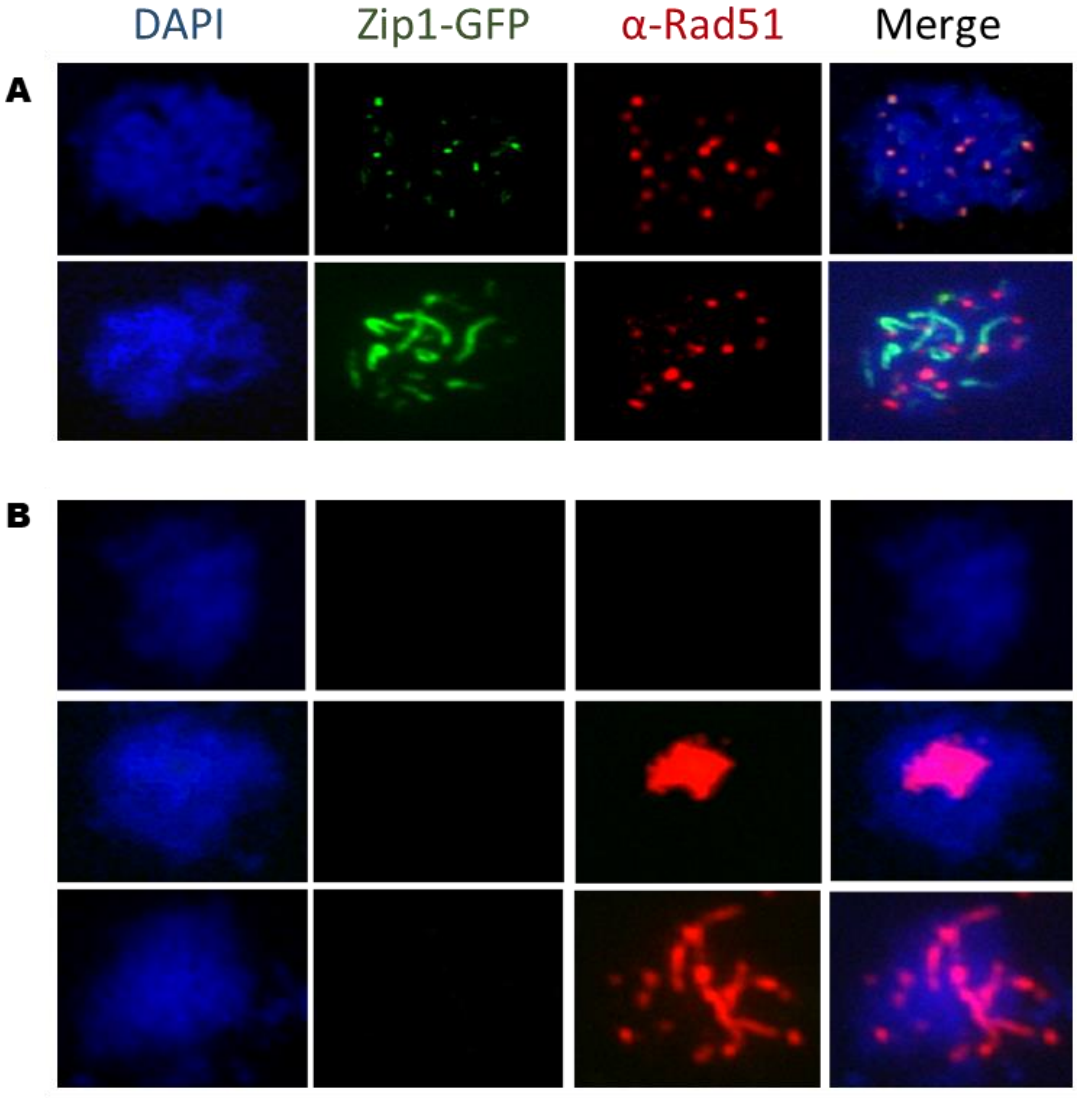

Figure 4.5 Analysis of Rad51 aggregates in cells expressing Zip1-GFP, a synaptonemal complex protein. (A) Representative images of *srs2-101* cells with punctate or elongated Zip1-GFP signals (3 h and 5 h, respectively) with clear Rad51 foci. (B) Representative images of Zip1-negative *srs2-101* cells at 5 h. Cells can be classified as having no Rad51 signal, large aggregates of Rad51 or elongated thread-like aggregates of Rad51. Aggregates of Rad51 can be observed in *srs2-101* cells in the absence of a Synaptonemal Complex. (E. Ahmed, unpublished data).

Curiously, a preliminary investigation into Rad51 and RPA colocalisation in *srs2-mn sae2Δ* strains, which are not expected to perform normal strand resection to produce stretches of ssDNA, also indicated the presence of colocalised RPA and Rad51 aggregates at later time points of the meiotic timecourse, suggesting that aggregate colocalisation is still occurring at ssDNA despite loss of normal resection activity. This is consistent with observations in the mutant *rad50S* strain, which is DSB proficient but deficient for DSB resection, that RPA foci are retained in 98% of cells at 8h post induction of meiosis and Rad51 foci in 26%, with the RPA foci formed in S-phase being Spo11-independent (Gasior *et al.*, 1998).

Rad51 aggregates were also imaged by SIM super-resolution microscopy and found to be formed of clusters of smaller Rad51 foci. Preliminary SIM images of GFP-tagged RPA with Rad51 immunofluorescence suggests that, at the super-resolution level, the Rad51 and RPA aggregates that had previously been observed as colocalised may actually represent RPA-GFP signals surrounded by two or more dots of Rad51, sometimes appearing as a broken circle. However, insufficient images were collected in the initial analysis to be certain of this result and as such the microscopy would need repeating before drawing any conclusions.

Through the combination of α-Rad51 immunofluorescence with observation of the fluorescently tagged synaptonemal complex (SC) protein, Zip1-GFP, we found that Rad51 aggregates are present in the absence of SC signal. This leads to the question of whether this is a population of cells being observed prior to SC formation or whether they are cells that have already completed Prophase I and disassembled the SC. To

address this question, a strain that cannot exit pachytene due to loss of the critical transcription factor, Ndt80, was next analysed for aggregate formation, see Section 5.3.

Chapter 5 Meiotic Phenotypes of *srs2* Depend on DSB Formation but not Interhomologue Recombination

5.1 Introduction

Nuclear division is hindered during meiosis in *srs2* strains and Rad51 aggregates are formed that colocalise with RPA, implying a role for ssDNA. A persistence of large spherical or ellipsoid foci of RPA has also been observed in *rad51*, *rad55* & *rad57* mutants that are unable to complete recombination (Gasior *et al.*, 1998). We therefore considered whether loss of Srs2 activity might lead to entanglement of DNA due to a failure in joint molecule resolution during DSB repair. We have also shown that the Rad51 aggregates are present in *srs2* cells in the absence of the synaptonemal complex (SC) but it was not clear whether these were cells that had yet to form a SC or were cells that had already completed Prophase I, and the SC had subsequently dissolved.

We first analysed the dependency of the aggregation phenotype on the formation of DSBs, using a *spo11* strain that cannot form DSBs. The timing of aggregation formation was assessed with an *ndt80* strain that arrests in pachytene with full-length SC. Having established that the observed meiotic phenotypes are dependent on both DSB formation and exit from pachytene, we next assessed the effect of *srs2* mutation on DSB repair kinetics, interhomologue recombination events and sister chromatid separation.

5.2 Rad51 Aggregation is Dependent on Spo11

The formation of DSBs during meiosis is critically dependent on Spo11 transesterase activity. As Spo11 forms a phosphodiester bond between the DNA 5' end and its catalytic residue, Tyrosine 135, mutation of this residue to Phenylalanine abolishes its ability to

form DSBs through loss of the reactive –OH group. Whereas complete deletion of Spo11 has multiple effects, including reduction in the length of meiotic S-phase, this *spo11-Y135F* mutant retains normal S-phase length and DSB-independent meiotic homologue pairing while precisely preventing formation of DSBs and the SC (Cha *et al.*, 2000). Using the *spo11-Y135F* allele in combination with *srs2-mn* therefore enabled analysis of the DSB-dependency of the previously observed meiotic phenotypes. Both the sporulation defect and aggregate formation phenotypes of *srs2-mn* were found to be dependent on DSB formation as they were rescued by the *spo11-Y135F* mutation (Figure 5.1).

5.3 Rad51 Aggregation is Dependent on Ndt80

The Ndt80 transcription factor is responsible for activating a range of sporulation-specific genes required for meiotic division and spore formation, in response to signalling by the early meiotic regulator, Ime1 (Chu and Herskowitz, 1998). Deletion or mutation of *NDT80* causes cells to arrest in pachytene, with fully synapsed homologues and duplicated but unseparated SPBs (Xu *et al.*, 1995).

As would be expected from cells that arrest in pachytene, sporulation was abolished in the s*rs2-mn ndt80Δ* double mutant strain (Figure 5.1, A). Significantly, immunofluorescent analysis of the *srs2-mn ndt80Δ* strain revealed that the formation of Rad51 aggregates was rescued by deletion of *NDT80* (Figure 5.1, B). As Rad51 foci still form in *ndt80Δ* cells, although at lower levels, it is unlikely that the rescue of aggregation by *ndt80Δ* is due to an affect on the early steps of recombination (Hayase *et al.*, 2004). This result suggests that aggregate formation occurs after the cells exit from pachytene.

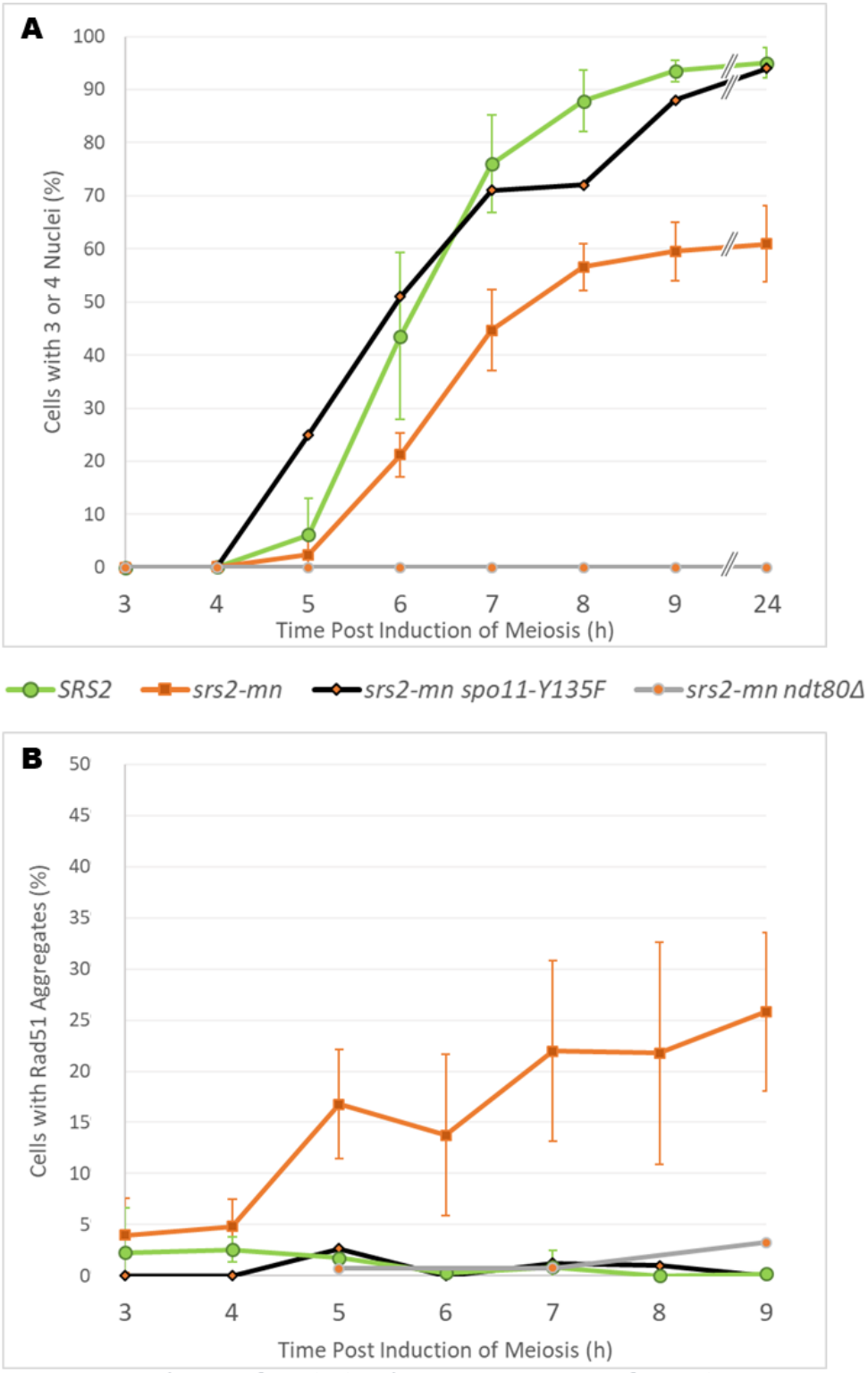

Figure 5.1 Dependency of meiotic phenotypes on DSB formation, *SPO11*, and pachytene exit, *NDT80*. (A) The reduction in sporulation caused by loss of Srs2 activity is rescued by preventing DSB formation through mutation of Spo11. As expected from the pachytene arrest caused by loss of the Ndt80 transcription factor, *srs2-mn ndt80Δ* cells do not sporulate. (B) The Rad51 aggregation phenotype of *srs2* cells is dependent on both *SPO11* and *NDT80,* suggesting aggregate formation requires DSB formation and exit from pachytene. (Aggregate analysis: *SRS2*, n=3; *srs2-mn*, n=5; *srs2-mn spo11-Y135F*, n=1; *srs2-mn ndt80Δ*, n=1. Nuclei analysis: *SRS2*, n=7; *srs2-mn*, n=7; *srs2-mn spo11-Y135F*, n=1; *srs2-mn ndt80Δ*, n=1.)

5.4 Rad51 Aggregation is Independent of Mek1

The increased proportion of *srs2* mutant cells found with 3 or 4 SPB signals but only 1 nucleus suggests that these cells are attempting to progress into second meiosis even though the nucleus has not divided in first meiosis. Furthermore, the Rad51 aggregation phenotype is dependent on both the formation of DSBs and the exit from pachytene. I therefore considered whether the delay in *srs2* meiotic progression may be due to a failure to resolve recombination intermediates and therefore homologous chromosomes in the first meiotic division, preventing progression into second meiosis. In wild-type cells, the repair of meiotic DSBs is preferentially completed by using the homologous chromosome as a repair template in order to ensure the formation of sufficient crossovers, see Section 1.7. A significant component of this interhomologue bias and the Barrier to Sister Chromatid Repair (BSCR) is the Mek1 kinase (Niu *et al.*, 2005).

To determine whether aggregation of Rad51 in *srs2* cells is due to failure in the resolution of interhomologue joint molecules, a double mutant strain was generated in the *mek1Δ* background, removing the interhomologue bias of strand invasion and allowing meiotic DSBs instead to be rapidly repaired using the sister chromatid as a template. Interestingly, although a minor rescue of sporulation was observed, the deletion of *MEK1* did not rescue aggregate formation in *mek1Δ srs2-101* cells compared to *srs2-101* as measured by Rad51 immunofluorescence (Figure 5.2). This suggests that aggregate formation is not dependent on interhomologue strand invasion, which in turn suggests that Rad51 aggregates are not caused by a failure in the normal resolution of interhomologue crossovers.

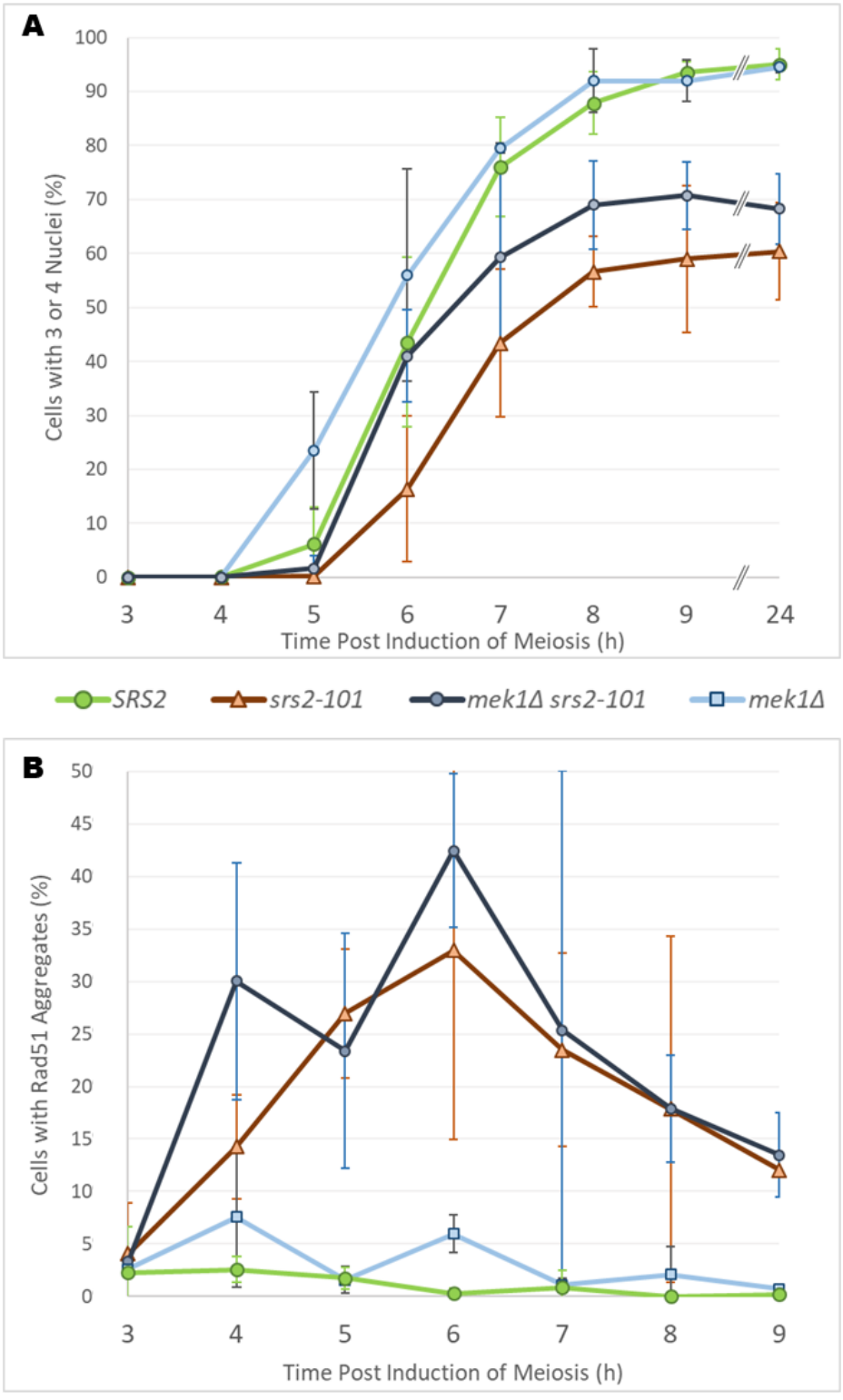

Figure 5.2 Analysis of the *srs2-101 mek1Δ* strain, which is able to complete DSB repair by using the sister chromatid as a template. (A) Deletion of *MEK1* allows earlier sporulation due to inter-sister DSB repair. Only a small sporulation rescue is observed in *mek1Δ srs2-101* compared to *srs2-101*. (B) The deletion of *MEK1* does not rescue aggregate formation in *mek1Δ srs2-101 compared to srs2-101* suggesting aggregate formation is independent of normal interhomologue strand invasion. (Aggregate analysis: *SRS2*, n=3; *srs2-101*, n=3; *srs2-101 mek1Δ*, n=2; *mek1Δ*, n=2. Nuclei analysis: *SRS2*, n=7; *srs2-101*, n=5; *srs2-101 mek1Δ*, n=3; *mek1Δ*, n=2.)

5.5 Chromatids Move Apart Despite Failures in Nuclear Division

Previous work by Chou, 2014 and Hulme, 2009, using Southern analysis of DSB levels at the *ARE1* hotspot, has shown much lower levels of observable DSBs in *srs2-101* strains compared to *SRS2* during meiotic time courses. However, in an *sae2Δ* background, which accumulates unrepaired DSBs, both *srs2-101* and *SRS2* accumulate DSBs to similar levels suggesting that the lower level of DSBs observed in *srs2-101* may be due to faster repair (Chou, 2014; Hulme, 2009). We hypothesised that this potentially faster repair may be due to use of the sister chromatid as a repair template. As Rad51 aggregation in the absence of Srs2 activity is dependent on DSB formation and exit from pachytene but not on the resolution of interhomologue joint molecules, we further considered that an errant strand invasion event between sister chromatids occurring at a position that was distal to an interhomologue crossover could prevent normal segregation of the bivalent. This could generate DNA entanglement and failure in nuclear division.

To investigate this possibility, we took advantage of a bacterial operon and its repressor. In *Escherichia coli*, when tetracycline antibiotic is absent, the Tet Repressor (TetR) protein binds to the Tn10 Tet Operon (*TetO*) with high specificity, repressing transcription of resistance genes (Gossen and Bujard, 1992). Strains of *S. cerevisiae* were generated with 224 repeats of the Tet Operon inserted around 40kB from the *URA3* locus on Chromosome V, which also express a TetR-GFP fusion protein under a *URA3* promoter. Using a heterozygous diploid in which only one homologue carries the *TetO* repeats and expresses TetR-GFP, we observed the separation of the *tetO*/TetR signals across meiosis as a proxy for sister chromatid separation. During normal meiosis in this heterozygous system, a single signal is visible until the binucleate stage. During

metaphase II, this signal divides into two signals, which then separate into different nuclei in the tetranucleate stage (Figure 5.3, A).

Cells in each strain were scored individually for their SPB separation, nuclear division and *tetO*/TetR signal count across meiotic time courses. Cells with divided SPBs but failed nuclear division (Class IIIb cells from Figure 3.6, B) were then analysed for *tetO*/TetR signal separation, both as a percentage of all cells counted (Figure 5.4, A), and as a percentage of only those cells with failed nuclear division (Figure 5.4, B). In the mutant *srs2-mn* strain, the proportion of cells with failed nuclear division that had separated signals was similar to or greater than in the wild-type strain, although the total number of wild-type cells with failed nuclear division was small. Indeed, at every time point in which *srs2-mn* cells with failed nuclear division were observed, over 70% had divided signal (Figure 5.3, B). This suggests that even when the nucleus is undivided, the majority of sister chromatids are separating correctly, at least where measured, close to pericentromeric DNA on Chromosome V.

5.6 Discussion

Discovery of Rad51 aggregates that are associated with RPA in meiotic *srs2* cells, and the failure of *srs2* cells to complete nuclear division observed in Chapter 4, raised further questions about whether the Rad51 aggregations were symptomatic of entangled DNA resulting from poor DSB repair. We first confirmed that the phenotypes were dependent on DSB formation by the Spo11 transesterase and the exit from pachytene, as controlled by the Ndt80 transcription factor. This indicates that the Zip1-negative strains observed

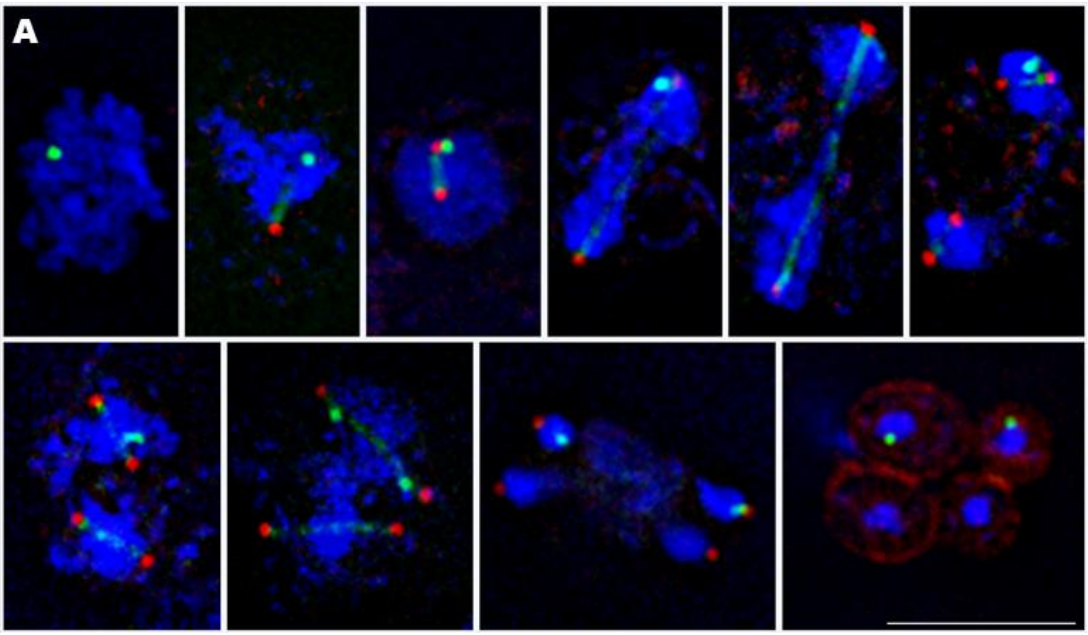

Red: Spindle Pole Body (Cnm67-mCherry)
Linear Green: Tubulin spindles (Tub1-GFP)
Punctate Green: Sister chromatids (TetR-GFP at *tetO* repeats on Chr. V)
Blue: Nuclear DNA (DAPI)

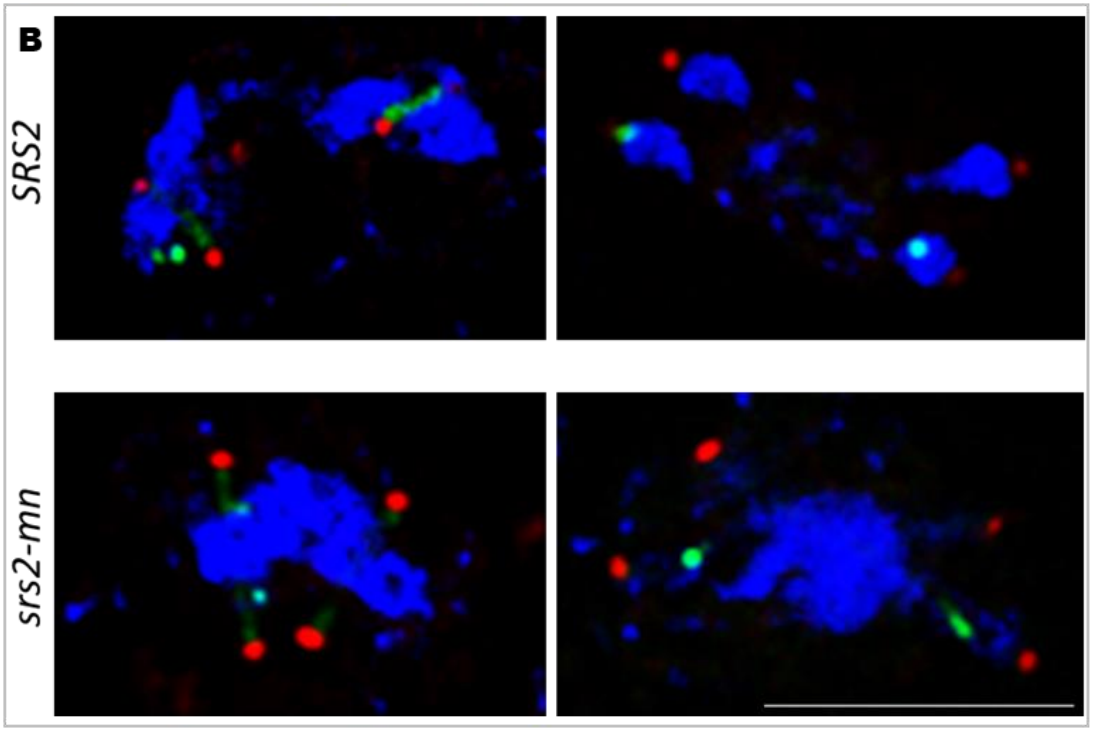

Figure 5.3 Sister chromatid separation observed during meiosis using *tet* Operon repeats heterozygously inserted at the *URA3* locus on chromosome V in cells expressing a Tet Repressor GFP fusion protein. (A) Representative images of the expected progression of sister chromatid segregation through meiosis. in Wild-type cells. Scale bar = 5µm. (B) Representative images of *SRS2* (6h & 7h) and *srs2-mn* (6h & 8h) cells with divided spindle pole bodies. Even when the nucleus fails to divide in *srs2-mn* cells, separated *tetO*/TetR signals can be observed suggesting sister chromatids have separated. Scale bar = 5µm.

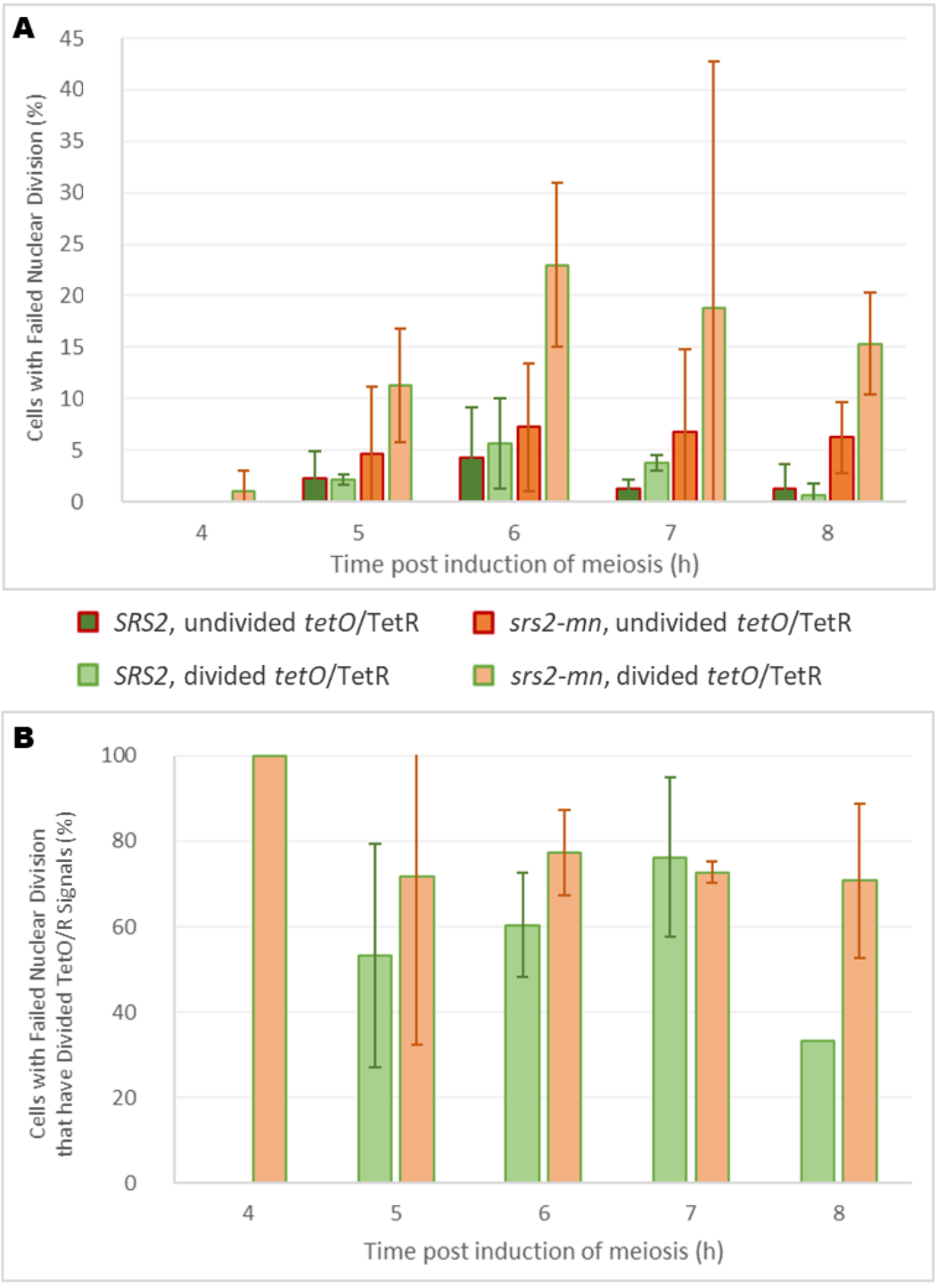

Figure 5.4 Sister chromatid separation analysis of cells with *tet* Operon repeats heterozygously inserted at the *URA3* locus on chromosome V in cells expressing a Tet Repressor GFP fusion protein. (A) Cells with failed nuclear division (Class IIIb, see Figure 3.7, B) classified by the number of signals visible per cell, as a percentage of total cells counted at each time point, n=2. (B) Cells with divided signals as a percentage of those cells with failed nuclear division (Class IIIb, see Figure 3.7, B), n=2 except for *srs2-mn* at 4h and *SRS2* at 8h where n=1 due to Class IIIb cells only being present in one repeat of each. Analysis indicates that even when the nucleus fails to divide in *srs2-mn* cells, signals separate in over 70% of cells suggesting that sister chromatids continue to separate when nuclear DNA does not.

to contain Rad51 aggregates in Section 4.4 must represent cells that have already dismantled their synaptonemal complex (SC).

As joint molecules (JMs) are formed in *ndt80* cells but are not resolved, and Rad51 aggregates are absent in *ndt80* but present following dissolution of the SC, it was hypothesised that JMs formed in Prophase I may not be correctly resolved in *srs2* cells, causing DNA entanglement (Allers and Lichten, 2001). To remove the requirement for interhomologue JM resolution, strains were generated that lacked the Mek1 kinase, a major effector in establishing the interhomologue bias of DSB repair. This allowed DSBs to be rapidly repaired by using the sister chromatid as a repair template, bypassing the need for interhomologue JM formation and resolution. However, deletion of *MEK1* did not rescue the *srs2-101* meiotic failure, as the *mek1Δ srs2-101* strains produced similar levels of Rad51 aggregates.

The aggregation phenotype of *srs2* strains has been shown to be independent of interhomologue JMs, and previous work has identified a possible faster rate of DSB repair in *srs2-101* cells compared to *SRS2*, suggesting that intersister interactions may be involved in the *srs2* phenotypes. The separation of sister chromatids during meiosis was therefore analysed in *srs2* cells using a heterozygous diploid expressing a Tet Repressor GFP fusion protein with *tet* Operon repeats inserted near the centromere of Chromosome V. However, over 70% of those *srs2* cells that fail to divide their nucleus did successfully divide the TetO/R signals, suggesting that sister chromatids are separating, at least at the pericentromeric region. Similar analysis of a homozygous strain also indicates that 4 signals can be observed in *srs2* strains, suggesting that both

sister chromatids and homologous chromosomes are separated (E. Ahmed, unpublished observations).

To elucidate the nature of the *srs2* phenotypes, further mutations were next analysed to dissect the phenotype by intermediate stages.

Chapter 6 Further Dissection of the Meiotic Phenotypes of *srs2*

6.1 Introduction

As the cytological analyses described in Chapters 3, 4 and 5, had yet to yield a cohesive model, intermediate stages were next analysed to elucidate the observed phenotypes further. As the aggregates of Rad51 appear to be dependent on the exit from pachytene, when joint molecules (JMs) are resolved, but not dependent on interhomologue strand invasion, the dependency of aggregate formation on the strand invasion activity of Rad51 was next analysed and a JM assay was performed at the *LEU2* hotspot. As aggregates of Rad51 appear to form near ssDNA, and be dependent on DSB formation, their dependency on DSB resection and processing was also analysed, using *sae2* and *mre11* mutants.

6.2 Aggregation is Rescued by the *rad51-II3A* Mutation

If the phenotypes being observed in *srs2* mutants are due to an inability of Srs2 to remove Rad51 from nucleoproteinfilaments (NPFs) in such a way that errant Rad51-mediated strand-invasion events occur, then utilising *rad51-II3A*, which is mutated at the second DNA binding site responsible for strand invasion, should abolish the phenotype (Cloud *et al.*, 2012). Double mutants of *rad51-II3A* and *srs2-101* or *srs2Δ* in diploid strains were found to be synthetically lethal during mitotic growth, so experiments were performed with the meiotic null allele of *srs2*.

The *srs2-mn rad51-II3A* strain was analysed by immunofluorescence for Rad51 aggregates at selected time points post induction of meiosis, finding only approximately

4% of cells with aggregates at each time point (Figure 6.1; E. Ahmed, unpublished data). This represents a significant rescue of aggregate formation, approaching wild-type levels and suggests that formation of Rad51 aggregates is dependent on its ability to bind a second strand of DNA. This may implicate Rad51-mediated strand invasion plays a role in the generation of aggregates, however, this suggestion must be made with caution.

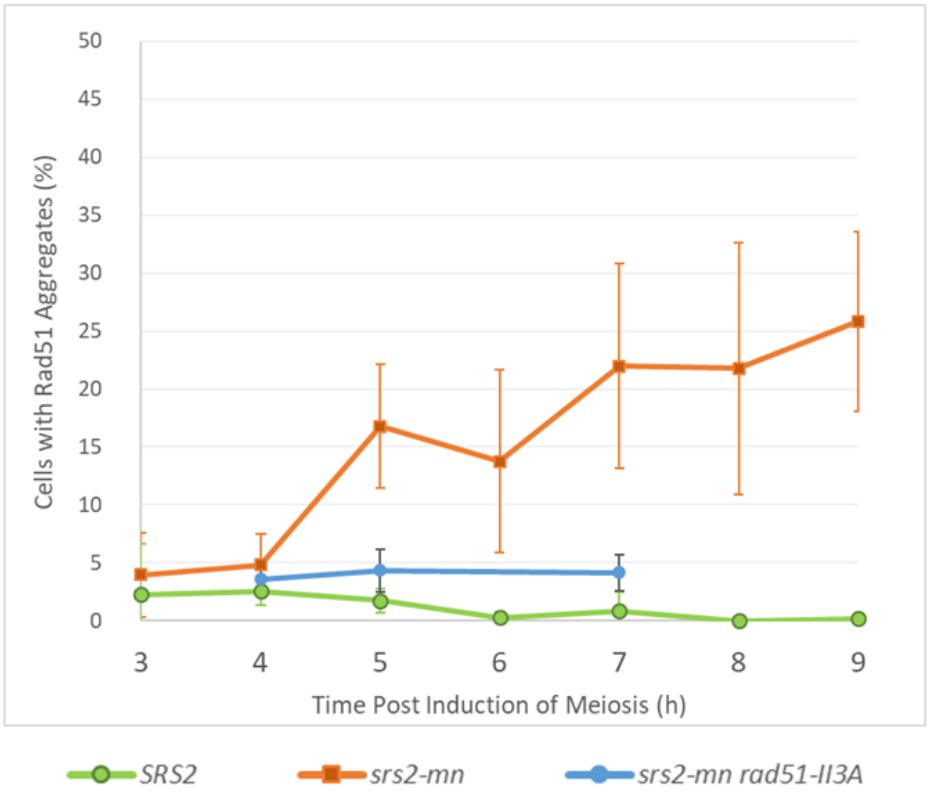

Figure 6.1 Aggregate analysis of the *srs2-mn rad51-II3A* strain. Aggregate formation is rescued by the *rad51-II3A* mutation that prevents binding of Rad51 to a second strand of DNA, which is required for its strand invasion activity, n=3 (E. Ahmed, unpublished data).

6.3 Recombination Intermediates are More Labile in *srs2*

Joint molecule (JM) analysis performed by our collaborators, in the laboratory of Michael Lichten, using Southern analysis at the *LEU2* hotspot found a significant decrease in JM formation in *srs2* and an increase in non-crossover events (NCOs) compared to wild-type, with levels of crossover events (COs) similar to wild-type. However, when repeating the JM assay with an initial crosslinking step, JMs were observed at approximately wild-type levels, accompanied by a reduction in both CO and NCO products compared to non-crosslinked samples, suggesting that the JMs in *srs2* are in some way more labile than normal (Figure 6.2; M. Lichten, unpublished data). To determine whether JM formation is being disturbed by errant Rad51-mediated strand invasion events, the JM molecule analysis is being repeated using the *rad51-II3A* allele, as well as further characterisation of the nature of the JMs by 2D gel analysis.

6.4 Rad51 Aggregation is Independent of Sae2

Both the meiotic delay of *srs2* mutants and the formation of aggregates are *SPO11*-dependent, indicating that these phenotypes are dependent on the normal formation of DSBs. The colocalisation of Rad51 aggregates with RPA and the rescue of aggregation by the *rad51-II3A* allele suggested an errant strand invasion event might be responsible for the aggregation phenotype. To test this hypothesis, Rad51 immunofluorescence and aggregate analysis was performed in a double mutant *srs2-mn sae2Δ* strain. As Sae2 is required for the normal programmed resection of Spo11-induced DSBs prior to recombinase-mediated strand invasion, it was anticipated that Rad51 aggregates should be abolished by deletion of *SAE2*. However, no such rescue was observed, with

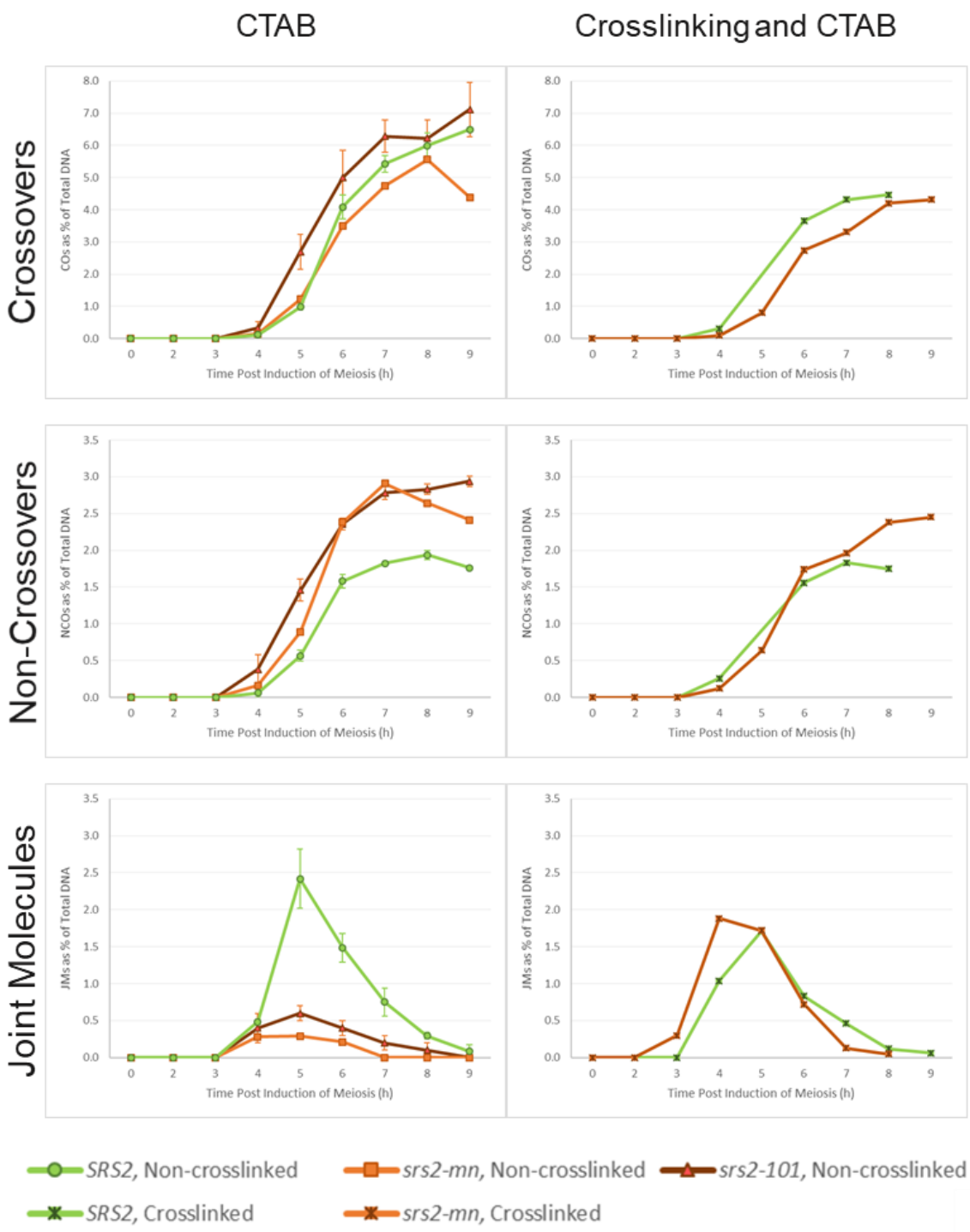

Figure 6.2 Joint molecule (JM) analysis at the *LEU2* hotspot suggests that recombination intermediates formed in *srs2* cells may be more labile than normal. Initial joint molecule analysis of meiotic DNA, extracted by CTAB, found fewer JMs as a proportion of total DNA in *srs2* cells than in Wild-type. However, following an additional cross-linking step before DNA extraction, *srs2* cells were found to have similar levels of JMs as wild-type, accompanied by a reduction in crossover and non-crossover products compared to the *srs2* non-crosslinked samples (M. Lichten, unpublished data). Error bars for *SRS2* and *srs2-101* non-crosslinked samples represent standard deviation.

aggregates reaching a greater level in the *srs2-mn sae2Δ* double mutant than in *srs2-mn* alone, although this was not found to be statistically significant (Figure 6.3, A). In an attempt to dissect the phenotype between *SPO11*-dependence and *SAE2*-independence, *TEL1* was additionally deleted yet did not provide any rescue beyond *srs2-mn* levels.

Unexpectedly, a small number of aggregates were observed in the *sae2Δ* single strain at later time points that were also dependent on Spo11 (Figure 6.3, B). Although aggregation levels in *srs2-mn* and *srs2-mn sae2Δ* were not found to be significantly different statistically, it is potentially curious that summing the proportion of cells with aggregates observed in the two individual *srs2-mn* and *sae2Δ* single mutant strains matched closely with the proportion of cells with aggregates observed in the *srs2-mn sae2Δ* double deletion mutant. If this were to represent a cumulative effect it could suggest there are two populations of aggregates: one formed due to loss of Srs2 activity and one due to loss of Sae2 activity. It is also interesting that at the later time points of 8 and 9h, when aggregates become most apparent in the *sae2Δ* single mutant, the proportion of cells with aggregates observed in the *srs2-mn sae2Δ tel1Δ* strain appears to match more closely the proportion of cells with aggregates observed in the *srs2-mn* strain than in the *srs2-mn sae2Δ* strain. It is therefore tempting to hypothesise that a population of *sae2Δ*-dependent aggregates might have been rescued by *TEL1* deletion, however, as the *srs2-mn sae2Δ tel1Δ* has not been repeated, further analysis would be necessary before making any such conclusions.

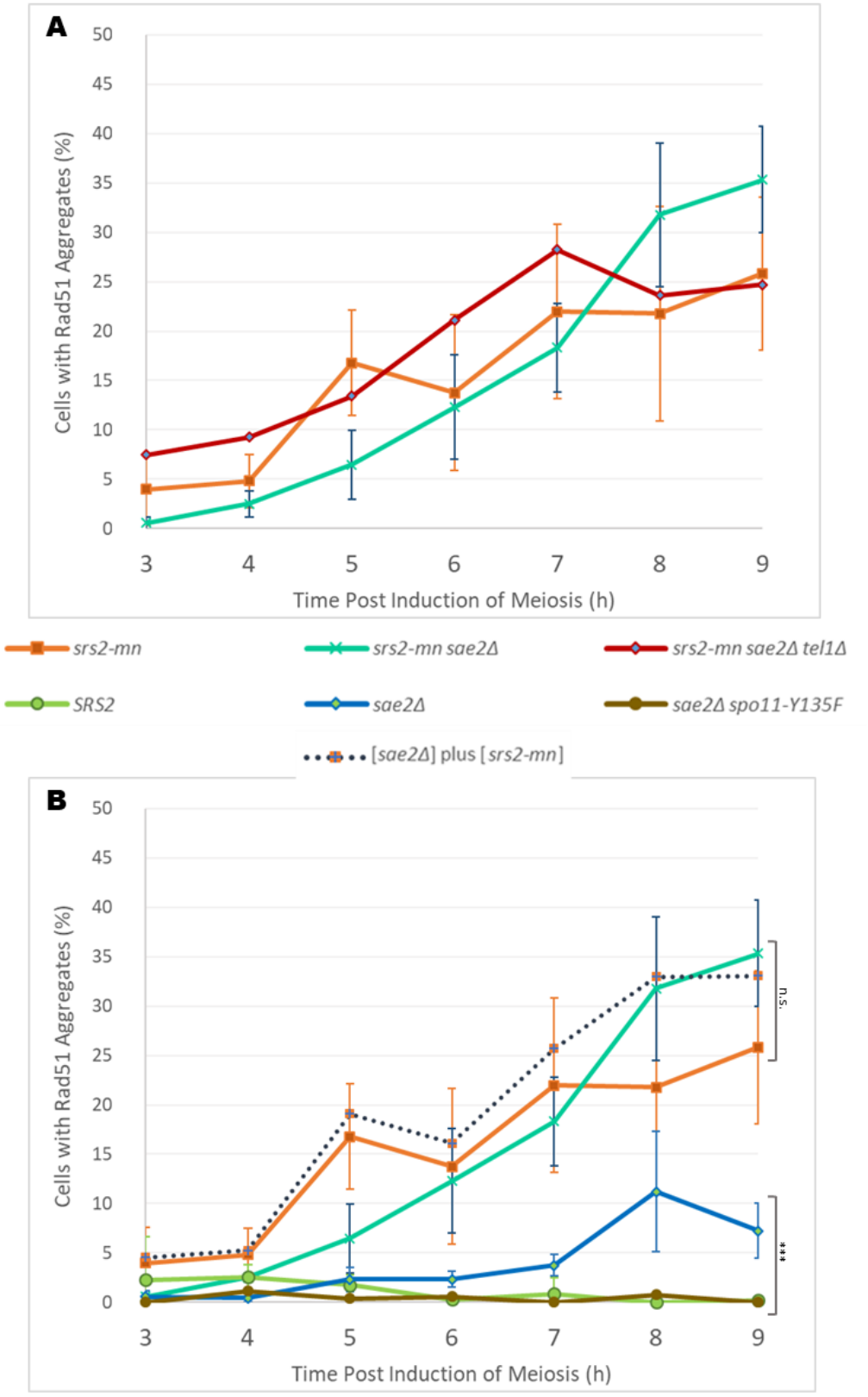

Figure 6.3 Aggregate analysis with *sae2Δ* strains. (A) Deletion of *SAE2* does not rescue aggregate formation in *srs2-mn sae2Δ*, nor does additional deletion of *TEL1*. (B) A small proportion of *sae2Δ* cells form aggregates at later time points and these were also found to be *SPO11*-dependent. Interestingly, the sum of the *srs2-mn* aggregates and *sae2* aggregates closely matches the aggregate values in the *srs2-mn sae2Δ* double mutant strain. suggesting a possible cumulative effect. (*SRS2*, n=3; *srs2-mn*, n=5; *srs2-mn sae2Δ*, n=4; *srs2-mn sae2Δ tel1Δ*, n=1; *sae2Δ*, n=3; *sae2Δ spo11-Y135F*, n=1). Fisher's Exact test for significance *** P<0.00001.

6.5 Separation of Function Alleles of *mre11* have Surprising Effects on Aggregation

As the inability of the *SAE2* deletion to rescue *srs2-mn* phenotypes was largely unexpected, we next considered whether some residual resection or transient unwinding was occurring in the *srs2-mn sae2Δ* cells that could allow aggregate formation at sites of ssDNA. Deletion of *sae2Δ* is expected to prevent DSB resection, however, Ddc2 foci, which bind to RPA-coated ssDNA as part of pachytene checkpoint signalling, have been observed in *sae2Δ* cells suggesting the presence of some ssDNA (Refolio *et al.*, 2011). As both Sae2 and the MRX complex are involved in removal of Spo11 from meiotic DSBs and the initiation of resection, the aggregate analysis was performed with *srs2-mn sae2Δ mre11* triple mutant strains to determine whether aggregates were present when normal programmed resection was completely inhibited.

It has been suggested that MRX complexes are retained at DSB ends when Sae2 or Mre11 activity is lost. Deletion of *SAE2* prolongs the presence of Mre11 foci, while overexpression reduces foci retention, and a Rad50 mutant that cannot interact with Sae2 causes recombination defects similar to *sae2Δ*, with both being unable to override DSB-induced cell-cycle arrest (Clerici *et al.*, 2006). To determine whether MRX complex retention affects the formation of Rad51 aggregates, and because meiotic DSBs do not form in *mre11Δ* cells, it was decided to perform aggregate analysis using two separation of function alleles: *mre11-H125N* is nuclease deficient, while *mre11-58S (H213Y)* is unable to form the MRX complex (Moreau *et al.*, 1999; Tsubouchi and Ogawa, 1998; Usui *et al.*, 1998).

Interestingly, both double *mre11 srs2-mn* mutants provided a partial rescue of the *srs2-mn* aggregation phenotype but the triple *mre11 srs2-mn sae2Δ* mutants of each allele had opposing effects (Figure 6.4). Deletion of *SAE2* in the *mre11-58S srs2-mn* background further increased the level of rescue, to less than half the *srs2-mn* level of aggregation, but in the *mre11-H125N srs2-mn* background, *sae2Δ* abolished the rescue, returning the level of aggregation to *srs2-mn* levels.

6.6 Discussion

In Chapters 3, 4 and 5, evidence has been presented of novel meiotic phenotypes caused by the loss of Srs2 activity. These include a failure in meiotic nuclear division, which is at least initially separate from cell cycle progression and which does not prevent chromatid separation, and formation of Rad51 aggregates, which are DSB dependent, present at sites of ssDNA and dependent on exit from pachytene but are independent of interhomologue recombination. To investigate these phenotypes further, a series of analyses were performed to address intermediate stages of meiosis to those that had previously been observed.

As the Rad51 aggregates are dependent on exit from pachytene, when joint molecules (JMs) are resolved, but are not dependent on interhomologue strand invasion, the strand invasion activity of Rad51 was analysed, utilising the *rad51-II3A* allele. This mutation produces a mutated rad51 protein that can form NPFs but is unable to bind a second strand of DNA at its second binding site, thus preventing strand invasion activity. This loss of binding was found to rescue the aggregation phenotype significantly; the

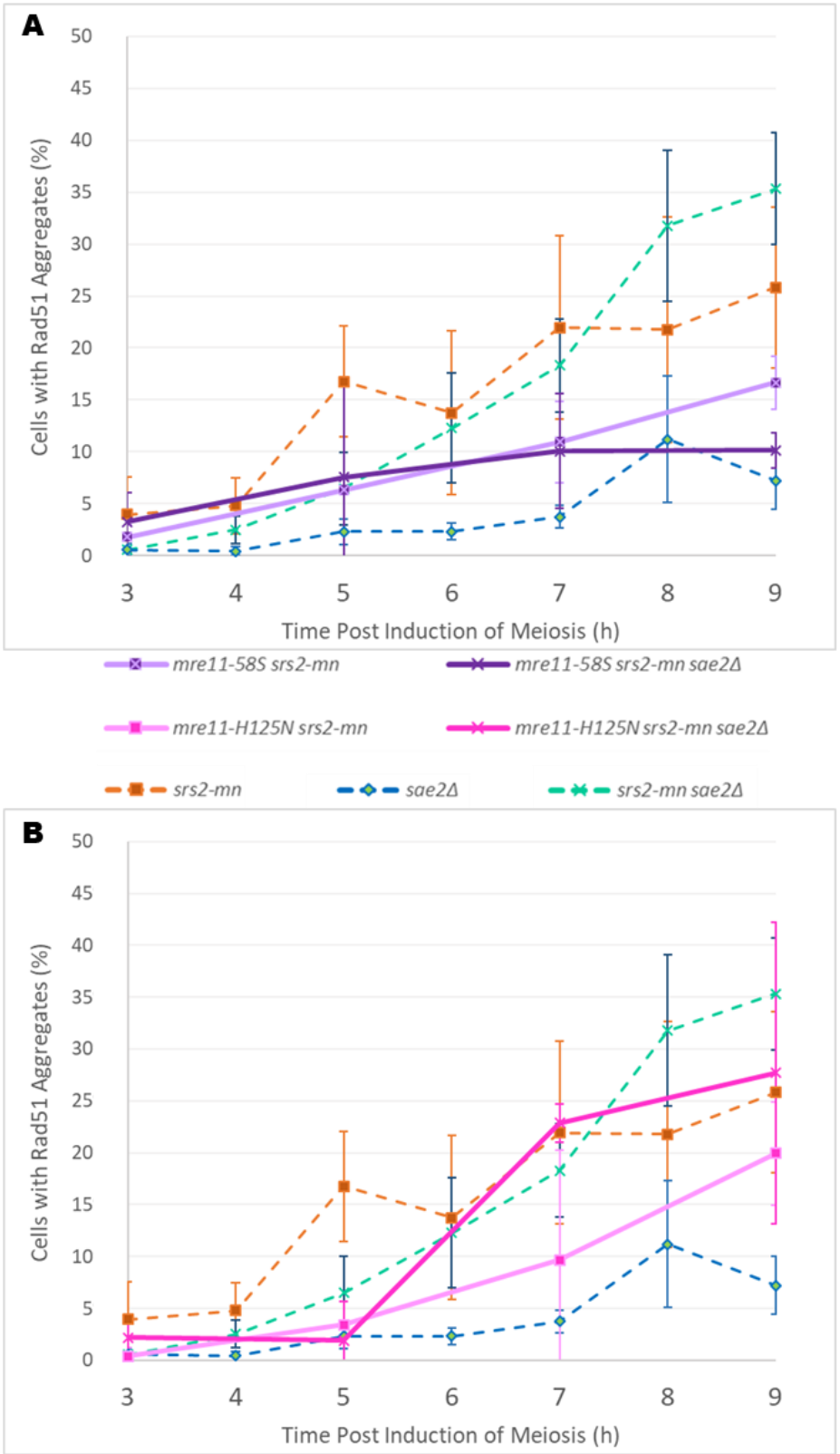

Figure 6.4 Aggregate analysis in *mre11* double and triple mutants. (A) The non complex-forming *mre11-58S* allele provided a partial rescue of Rad51 aggregation in the *mre11-58S srs2-mn* strain, which was increased further in the triple *mre11-58S srs2-mn sae2Δ* mutant. (B) The nuclease dead *mre11-H125N* allele again provided a partial rescue of aggregates in the *mre11-H125N srs2-mn* double mutant but this was abolished in the triple *mre11-H125N srs2-mn sae2Δ*, which generated *srs2-mn* levels of aggregates. (*SRS2*, n=3; *srs2-mn*, n=5; *srs2-mn sae2Δ*, n=4; *mre11-58S srs2-mn*, n=2; *mre11-58S srs2-mn sae2Δ*, n=2; *mre11-H125N srs2-mn*, n=2; *mre11-H125N srs2-mn sae2Δ*, n=2)

rad51-II3A srs2-mn strain was found to produce extremely low levels of aggregation compared to *srs2-mn*, although slightly above *SRS2* levels.

Analysis of JM formation by Southern analysis at the *LEU2* hotspot found a reduction in JM levels in *srs2* strains with an increase in the levels of non-crossover (NCO) products, while the level of crossover (CO) products remained similar to wild-type. However, following an additional crosslinking stage, the formation of JMs was found to occur at similar levels in *srs2-mn* to wild-type, accompanied by a reduction in the levels of both CO and NCO products relative to the non-crosslinked *srs2* samples. Together these results suggest that the JMs formed in *srs2* cells are more labile. The increase in NCO products before crosslinking and the observation that the crosslinked *srs2* samples reach peak levels of JMs approximately 1h earlier than in *SRS2* cells, further support the hypothesis that JMs in *srs2* cells may involve intersister strand invasion, which generally occurs more rapidly than interhomologue invasion. However, 2D-gel analysis would be required to investigate this further.

The dependency of the aggregate phenotype on DSB formation and the ability of Rad51 to bind a second strand of DNA, along with the colocalisation of the aggregates with RPA, could lead to a hypothesis that Rad51 aggregation should also be dependent on DSB resection. Surprisingly, however, deletion of *SAE2* did not rescue the formation of aggregates. Due to the surprising nature of this *sae2Δ* result, an entirely new deletion of *sae2Δ* was generated and analysed, corroborating the observed results.

To address the unexpected lack of rescue conferred by deletion of *SAE2*, aggregate analysis was repeated in triple mutant strains lacking mre11 function, in order to ensure full inhibition of normal DSB resection. This was also performed using separation of

function alleles to determine whether the nuclease function of Mre11 or the formation of the MRX complex might play a particular role in aggregate formation, as MRX complexes may be retained at DSB ends when Sae2 or Mre11 activity is lost. Both of the double *mre11 srs2-mn* mutants provided a partial rescue of the *srs2-mn* aggregation phenotype but the triple *mre11 srs2-mn sae2Δ* mutants of each allele had opposing effects. Deletion of *SAE2* in the *mre11-58S srs2-mn* background, which is unable to form the MRX complex, further increased the level of rescue, to less than half the *srs2-mn* level of aggregation, but deletion of *SAE2* in the *mre11-H125N srs2-mn* background, in which mre11 nuclease activity is lost, abolished the rescue, returning the level of aggregation to *srs2-mn* levels.

Although improbable statistically, if the potential cumulative effect of the *sae2Δ* and *srs2-mn* mutations were to be indicative of separate populations of aggregates, the observation that *mre11-H125N srs2-mn sae2Δ* matches more closely the *srs2-mn* levels of aggregates than *srs2-mn sae2Δ*, could suggest that the lack of Mre11 nuclease function may rescue an *sae2Δ*-dependent population of aggregates. However, this hypothesis would need to be confirmed by aggregate analysis in the *mre11-H125N sae2Δ* double mutant.

The difference in the effects of the *mre11* alleles in the triple mutants may be connected to the recruitment of Exo1. Mre11 has been shown to be involved in Exo1 recruitment at HO-induced DSBs, and the prevention of Ku binding, independently of its nuclease function but dependent on MRX complex formation (Shim *et al.*, 2010). It has also been suggested that Srs2 enables access for Exo1 to complete long strand resection by enlarging the gap, as well as preventing Rad51 binding that could inhibit Exo1 activity.

Using affinity pulldown, a physical interaction between Srs2 and Exo1 has been established and *in vitro* data indicate that the Exo1 endonucleolytic cleavage of gapped 5'-Flap DNA, a constructed substrate that resembles DNA unwound from a nick by Srs2, was specifically enhanced by Srs2 in an ATP-dependent manner, while cleavage by Dna2 was not (Potenski *et al.*, 2014). These considerations will be discussed in further detail in Chapter 8.

To investigate an intermediate step between DSB formation and DSB resection, aggregate analysis was repeated following deletion of *TEL1*, as phosphorylation of Sae2 during the meiotic cycle requires the Tel1 and Mec1 kinases (Cartagena-Lirola *et al.*, 2006). Deletion of *TEL1* did not rescue aggregation suggesting Rad51 aggregation is not dependent on Tel1 activity. Although not statistically significant, it is curious that the level of aggregates observed in the *tel1Δ srs2-mn sae2Δ* triple mutant appeared to match more closely with *srs2-mn* levels of aggregation. In a similar manner to the *mre11-H125N srs2-mn sae2Δ* result, it is tempting to hypothesise that the deletion of *TEL1* may have rescued an *sae2Δ*-dependent population of aggregates but this would again need much more analysis and to be confirmed by aggregate analysis in the double mutant, *tel1Δ sae2Δ*. The possibility that loss of either Tel1 or Mre11 activity could rescue a phenotype conferred by *SAE2* deletion would itself be of interest as it may implicate the involvement of checkpoint signalling. It has been suggested that the recombination checkpoint release caused by Mec1-/Tel1-phosphorylation of Sae2 is due to inhibition of MRX-dependent signalling, as the presence of Mre11 foci at DSBs is prolonged by *SAE2* deletion and reduced by *SAE2* overexpression (Cartagena-Lirola *et al.*, 2006; Clerici *et al.*, 2006).

Chapter 7 Genome-Wide Analysis of Rad51 Distribution

7.1 Introduction

As the *srs2* phenotypes that have been observed are dependent on DSB formation, we considered whether the observed Rad51 aggregates were forming at hotspots for meiotic recombination or whether they might be randomly distributed across the chromosomes. To examine this possibility, we began testing strains for suitability for analysis by ChIP-seq and are awaiting the results of ChIP-seq analysis.

7.2 Rad51 Antibody Binding is Insufficiently Sensitive for ChIP Analysis

To establish the suitability of Rad51 as a target for ChIP-seq in meiotic cells, ChIP-qPCR was first performed on mitotic cells. Wild-type were treated with the damage-inducing agent Bleomycin to enrich for Rad51 repair foci, with *rad51Δ* cells as a negative control. Enrichment was confirmed by immunofluorescent analysis, which found a greater than 3-fold increase in the average number of Rad51 foci per cell and a greater than 4-fold increase in the maximum number of Rad51 foci per cell in wild-type cells that had been treated with Bleomycin (Figure 7.1, A & B).

Chromatin Immunoprecipitation (ChIP) was performed on bleomycin-treated and untreated cells of each strain. Purified ChIP samples were used to perform qPCR with known primer pairs (targeting *FAB1*, *PAU5*, *SPB4* and *URA3*) and the DNA quantified as a percentage of the DNA from the pre-IP Whole-Cell Extract. However, no DNA enrichment was observed over background levels with any of the primer pairs (Figure 7.1, C). It was concluded that the Rad51 antibody was insufficiently sensitive for use in

ChIP-seq analysis. Instead, the Rad51 protein was tagged at the N-terminus with a PK/V5 epitope tag for which strong antibodies were available.

7.3 Tagged Rad51 Partially Rescues *srs2* Mutant Phenotypes

As the Rad51 antibody was insufficiently sensitive for ChIP-seq analysis, a strain was generated that would express an N-terminally tagged Rad51 protein construct, as C-terminal tags are thought to interfere with Rad51 function. In order to use this PK-tagged *RAD51* strain for ChIP-seq analysis of the aggregates formed when Srs2 activity is lost, it was first necessary to determine whether the tag itself caused any phenotypic effects. Unfortunately, the tagged Rad51 strain proved to be unusable.

Tagging Rad51 at the N-terminal with a PK3 tag rescued the spore viability of *srs2-101* to near wild-type levels. The spore viability of the untagged strains was found to be 63.3% and 98.3% for *srs2-101* and *SRS2*, respectively. In the tagged PK3-RAD51 background, however, spore viability increased to 91.3% for *srs2-101*, compared to 95.8% in *SRS2*. The *srs2* sporulation defect was also rescued by tagging Rad51. Notably, this rescue occurs in a dose-dependent manner: when Rad51 is homozygously tagged, *srs2-mn* sporulation approaches wild-type levels of sporulation, but when Rad51 is heterozygously tagged, sporulation is only rescued to an intermediate level (Figure 7.2).

In addition to this apparent undesired rescue of the *srs2* meiotic phenotypes that were observed in tagged Rad51 strains, it was also difficult to confirm reasonable levels of immunofluorescent colocalisation of the α-Rad51 signal and the α-PK/V5 signal, even in

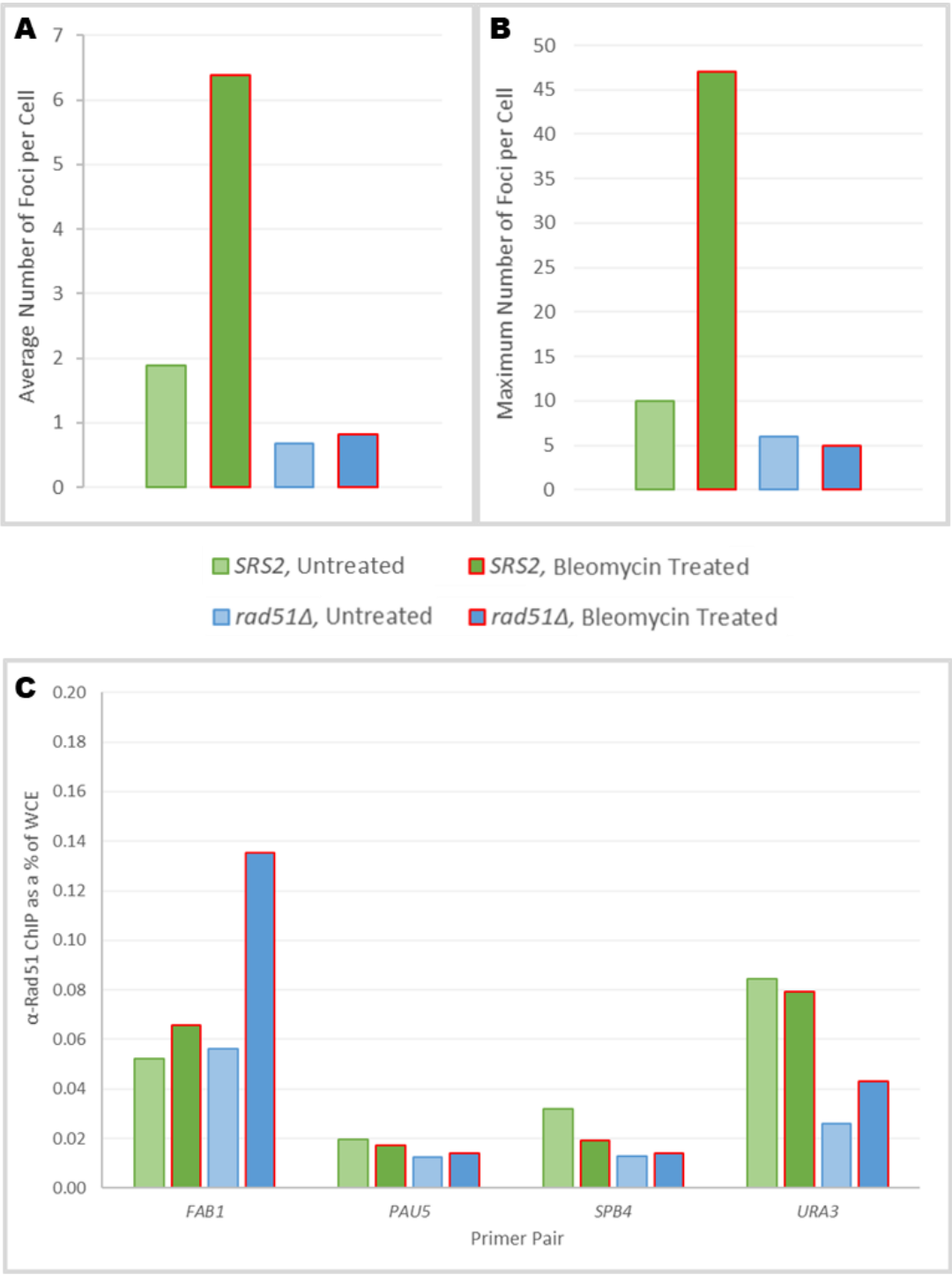

Figure 7.1 Although bleomycin treatment significantly enriches for Rad51 foci, DNA retrieved by ChIP was not specifically enriched. Immunofluorescence following bleomycin treatment revealed a 3-fold increase in the average number of Rad51 foci per cell (A) and a 4-fold increase in the maximum number of Rad51 foci per cell (B). (C) ChIP-qPCR found no significant enrichment of DNA pulled down with any primer pair in response to Bleomycin treatment, relative to the whole-cell extract.

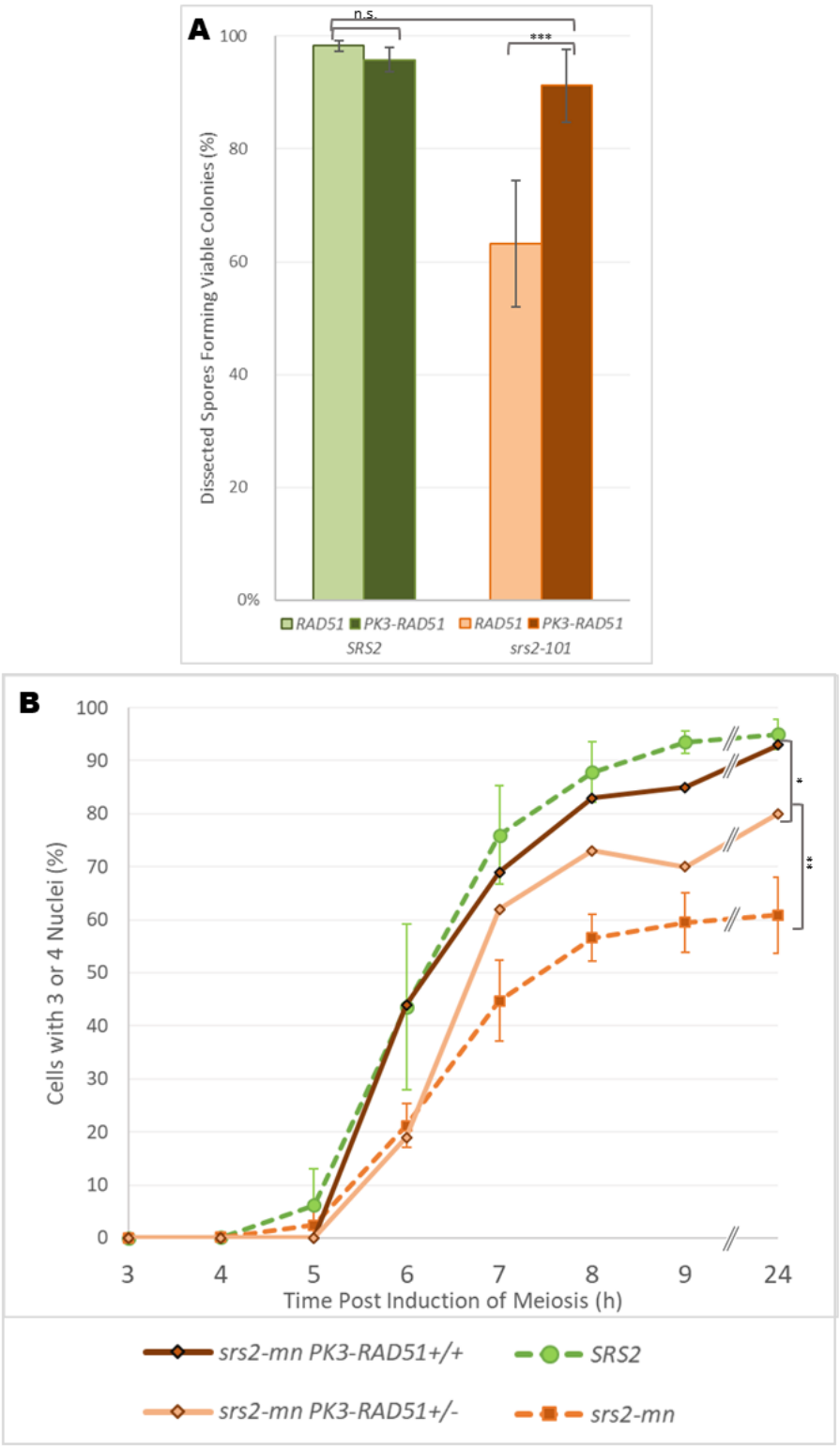

Figure 7.2 A PK/V5 tag at the N-terminal of Rad51 rescues meiotic phenotypes caused by Srs2 loss. (A) The reduction of spore viability in *srs2* strains is rescued to near wild-type levels by the N-terminal PK3-Rad51 tag. (*SRS2*, n=6, 636 spores; *SRS2 PK3-RAD51 +/+*, n=3, 240 spores; *srs2-101*, n=3, 400 spores; *srs2-101 PK3-RAD51 +/+*, n=3, 240 spores) (B) The reduction in sporulation observed in *srs2* strains is rescued by the tagged Rad51 in a dose-dependent manner: the *srs2-mn* strain that is homozygously tagged at Rad51 reaches almost wild-type levels of sporulation while the heterozygously tagged sporulates at an intermediate level. (*SRS2*, n=7; *srs2-mn*, n=7; *srs2-mn PK3-RAD51 +/+*, n=1; *srs2-mn PK3-RAD51 +/-*, n=1) Fisher's Exact test for significance * P<0.05, ** P<0.01, *** P<0.00001.

the homozygously-tagged strain. It was therefore decided utilise a different strategy for ChIP-seq analysis using a tagged RPA strain instead.

7.4 Tagged RPA Partially Rescues Sporulation but not Aggregation

As shown in Chapter 4.3 in immuofluorescent analysis of spread cells, the RPA component Rfa1 tagged with GFP at the C-terminus colocalises well with aggregates of Rad51 but not with foci of Rad51. This suggested that tagged RPA could be a valuable candidate for ChIP-seq analysis as a proxy for Rad51 distribution, by subtraction of the non-aggregate related ChIP-seq data obtained from wild-type controls.

A strain was generated that expressed C-terminally tagged Rfa1-PK9 and analysed to determine whether the tag would interfere with the observed *srs2* phenotypes. A partial rescue of sporulation was observed in the *srs2-mn RFA1-PK9* strain compared to the untagged *srs2-mn* strain (Figure 7.3, A). The level of potential sporulation rescue caused by tagged Rfa1 was much less significant than the rescue caused by tagged Rad51: Fisher's Exact test was used to determine whether values at 24h were significantly different to *srs2-mn* and returned P values of 0.098, 0.003 and <0.00001 for *srs2-mn RFA1-PK9, srs2-mn PK3-RAD51+/-* and *srs2-mn PK3-RAD51+/+*, respectively. Although sporulation rate appeared slightly elevated in *srs2-mn RFA1-PK9* it did not reach statistical significance and so aggregate analysis was performed. No rescue in the proportion of cells containing Rad51 aggregates was found in *srs2-mn RFA1-PK9*, which remained at approximately untagged levels (Figure 7.3, B). Although aggregate levels in both the tagged and untagged timecourses on this occasion involved an unusual level of variation between time points, the proportions of cells with aggregates at each

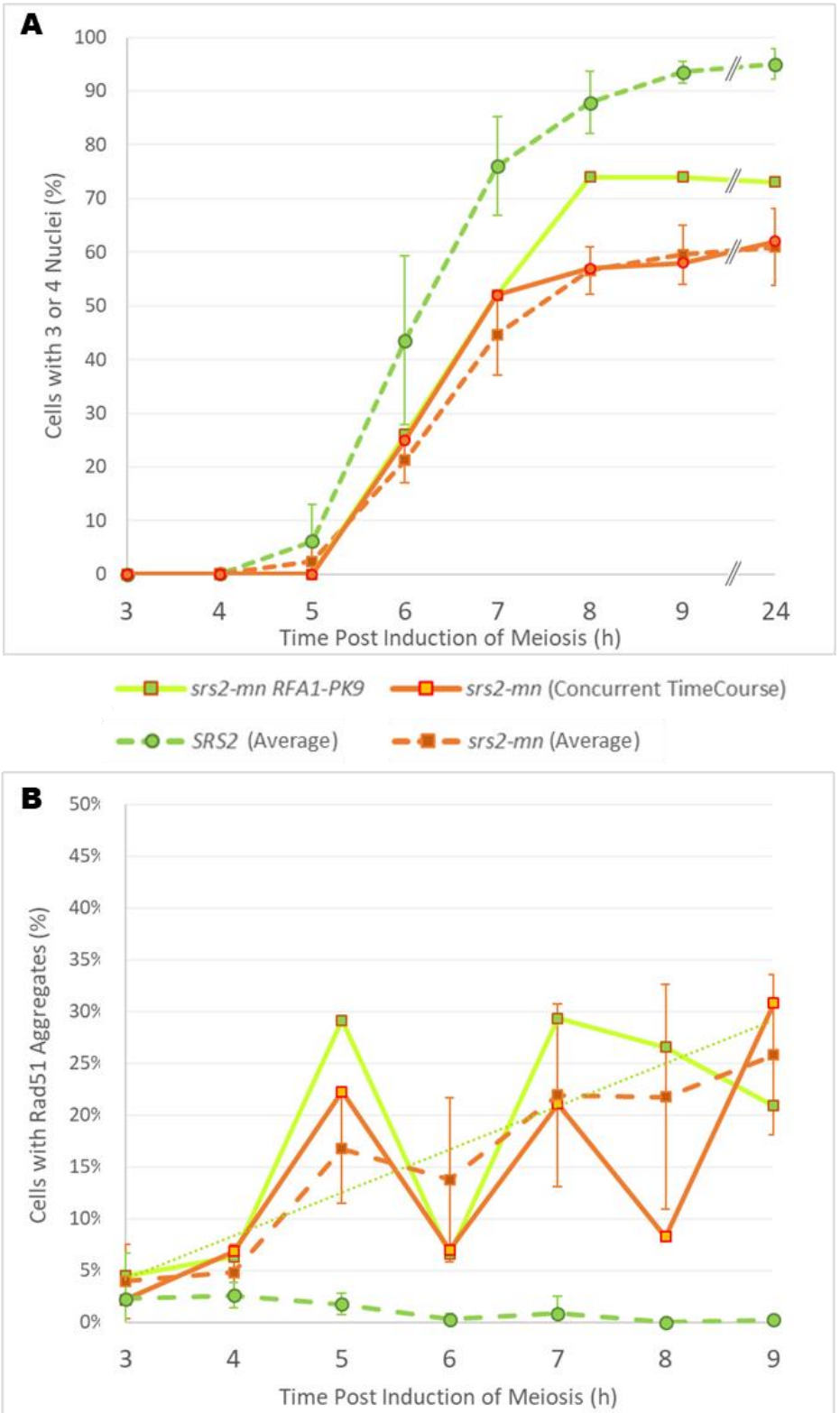

Figure 7.3 A PK/V5 tag at the C-terminal of Rfa1 (RPA subunit) does not prevent Rad51 aggregation in *srs2* cells. (A) The reduction of sporulation observed in *srs2* strains is partially rescued by the RPA tag. (B) The RPA tag does not, however, rescue the Rad51 aggregation observed in *srs2-mn* cells. In the RPA-tagged strain, aggregate levels at individual time points correlate well with the concurrent untagged *srs2-mn* time course, while its linear trendline correlates with the averaged *srs2-mn* data.

individual time point correlated well between the two strains. Furthermore, the linear trendline generated from the RPA-tagged *srs2-mn* strain data correlated well with the overall *srs2-mn* average data.

7.5 Discussion

The meiotic phenotypes of *srs2* strains are dependent on the formation of meiotic DSBs. Specifically, aggregates of Rad51 have been found to form during meiosis in a *SPO11*-dependent manner. It would therefore be of considerable interest to determine whether these aggregates are forming solely at hotspots for meiotic recombination, i.e. sites with increased probability of meiotic DSBs, or whether only their initiation is dependent on DSBs, with aggregate formation occurring away from the break site, either randomly or non-randomly.

To address this question, strains were tested and analysed in preparation for ChIP-seq analysis. Unfortunately, Rad51 proved problematic as a direct target for ChIP-seq due to the poor sensitivity of the α-Rad51 antibody, as determined through ChIP-qPCR of mitotic samples following Rad51 foci enrichment through damage induction. Tagging Rad51 in order to use a more sensitive antibody was additionally unsuitable as the tag itself caused intolerable levels of rescue to the *srs2* phenotypes that were to be analysed, and did so a dose-dependent manner. Although the rescue caused by the heterozgyously tagged strain was only partial, colocalisation between tagged and untagged Rad51 was difficult to establish in immunofluorescence analysis. Together, these concerns prevented progression of the tagged Rad51 line of investigation due to

the possibility that ChIP-seq of tagged Rad51 in a heterozygous strain might not be representative of the distribution of untagged Rad51.

Having previously observed that Rad51 aggregates, but not foci, colocalise with GFP-tagged Rfa1, a PK-tagged Rfa1 strain was generated and tested. Although a slight increase in sporulation was observed in the tagged strain compared to the untagged it was not found to be significant and no significant rescue was observed in the Rad51 aggregation phenotype. We therefore intend to perform ChIP-seq analysis on meiotic samples of *SRS2* and *srs2-mn* using PK-tagged Rfa1, subtracting the non-colocalised foci background data from the wild-type analysis, to determine the sequence distribution of Rad51 aggregates in *srs2*.

Chapter 8 General Discussion

The control of recombinatorial repair during meiosis is critical to maintaining genomic stability. The multifunctional *S. cerevisiae* helicase Srs2 has been implicated in a number of mitotic roles, including promoting DNA repair via the non-recombinatorial synthesis-dependent strand annealing (SDSA) pathway (Andersen and Sekelsky, 2010; Marini and Krejci, 2010). Furthermore, loss of Srs2 activity causes hyperrecombination phenotypes (Rong *et al.*, 1991). This project aimed to elucidate the meiotic role of Srs2 during DSB repair.

8.1 Srs2 Loss Causes Failures in Separation of Nuclear DNA but not Chromatids

Loss of Srs2 activity causes a meiotic delay, reduction in spore viability and reduced sporulation (Palladino and Klein, 1992). Following confirmation of these phenotypes, an in-depth cytological analysis was performed revealing that a significantly increased population of *srs2* cells compared to wild-type have divided spindle pole bodies (SPBs) but a single nucleus, suggesting that the cells are attempting to progress to Meiosis II despite the nucleus failing to divide correctly in Meiosis I. Although a population of *srs2* cells never correctly divide their SPBs, the initial stages of SPB separation in *srs2* occurs with similar kinetics to wild-type. Together, these results suggest that cell-cycle progression is not the primary cause for meiotic delay in *srs2* but that the nuclear DNA is failing to separate. However, chromatid separation analysis found no obvious failures in the separation of sister chromatids or homologous chromosomes s in *srs2* cells.

8.2 Srs2 Loss Results in *SPO11*- & *NDT80*-Dependent Rad51 Aggregation

Immunofluorescent analysis of Rad51 distribution identified aggregates of Rad51 signal in *srs2* mutants. Using cells with fluorescently-tagged RPA (*RFA1-GFP*) suggested that Rad51 aggregates occur at sites of ssDNA. Aggregates were found to be dependent on *SPO11* and is therefore expected to be dependent on meiotic DSB formation. Using cells with a fluorescently-tagged synaptonemal complex (SC) component protein (*ZIP1-GFP*), aggregates were observed in cells that lacked a SC signal. Rescue of aggregate formation by deletion of *NDT80* indicated that cells with aggregates which lack a SC are post-pachytene cells that have disassembled the SC, rather than pre-prophase cells observed before SC assembly. Super-resolution microscopy indicated that aggregates may be clusters of smaller Rad51 foci. Preliminary work suggests colocalised Rad51 and RPA may be formed of two or more Rad51 foci flanking GFP-RPA signals but more microscopy would be needed before further comment due to the small number of images available.

8.3 Inter-sister Strand Invasion and Joint Molecules may be Increased in the Absence of Srs2

Strains lacking the Mek1 kinase, a major effector in establishing the interhomologue bias of DSB repair and without which DSBs repair rapidly from the sister chromatid template, were generated and analysed (Niu *et al.*, 2005). No rescue was observed suggesting that aggregate formation is independent of *MEK1* and interhomologue recombination.

Aggregates were analysed in combination with the *rad51-II3A* allele that prevents Rad51 from binding to a second strand of DNA, as is required for strand invasion activity, but

does not affect NPF formation (Cloud *et al.*, 2012). This allele rescued the aggregation phenotype indicating that the ability of Rad51 to bind DNA at the second binding site is required for the formation of aggregates. It is tempting to infer from this that Rad51-mediated strand invasion activity is required for aggregate formation, but it may be that binding two DNA strands is sufficient without canonical strand invasion.

Joint molecule analysis initially revealed a reduction in JMs in *srs2* strains compared to wild-type, however, following an additional crosslinking stage, JMs were found at similar levels in *srs2-mn* to wild-type, suggesting that JMs are more labile in *srs2* cells. This supports previous work from our group which found no deficiency in the frequency of DSB formation at the *ARE1* hotspot but an increased rate of DSB repair in *srs2-101* cells than in *SRS2* (Chou, 2014; Hulme, 2009).

These results suggest that JMs in *srs2* cells may involve relatively more intersister strand invasion and lends credence to the hypothesis that *rad51-II3A* rescues the aggregation phenotype via lack of strand invasion activity rather than its inability to simply bind two DNA strands. However, as sister chromatids move apart, even when the nuclear mass is unable to divide, a relative increase in inter-sister JMs may not always generate aggregates but may contribute to a situation where aggregation is more probable.

8.4 Further Aggregate Characterisation Generated Unexpected Results

If Rad51 aggregates are present at sites of ssDNA and dependent on DSB formation, pachytene exit, and the ability of Rad51 to bind of a second strand of DNA, although independent of interhomologue recombination, they might be expected to be dependent on the formation of inter-sister joint molecules which requires DSB

resection. However, two independently generated *srs2-mn sae2* strains revealed that deletion of *SAE2* did not rescue aggregate formation in *srs2-mn sae2Δ*., suggesting aggregates are independent of normal strand invasion.

In order to ensure full inhibition of normal DSB resection, aggregate analysis was repeated in *mre11 sae2 srs2* triple mutant strains using separation of function alleles to investigate any specific effects caused by the loss of Mre11 nuclease activity (*mre11-H125N*) or MRX complex formation (*mre11-58S*), however these results were surprising and complex. Both double *mre11 srs2-mn* mutants partially rescued aggregates levels compared to *srs2-mn*. Unexpectedly, the effects of the triple *mre11 srs2-mn sae2Δ* mutants on levels of aggregation were very different between the two *mre11* alleles. Deletion of *SAE2* in the non-complex forming *mre11-58S srs2-mn* background further rescued the aggregate phenotype to less than half the *srs2-mn* level of aggregation, but deletion of *SAE2* in the nuclease-dead *mre11-H125N srs2-mn* background abolished the partial rescue observed in the double mutant, returning aggregation to *srs2-mn* levels.

8.5 Observations from Related Helicases

Srs2 belongs to a group of UvrD-like helicases, which is a highly conserved group with at least one representative in most organisms (Lorenz, 2017). There is a sequence homologue of *SRS2* in *S. pombe* whose loss also causes a hyperrecombinant phenotype and DNA damage sensitivity, however spSrs2 is not required for post-replicative repair and loss of spSrs2 does not cause any meiotic phenotypes (Lorenz, 2017; Marini and Krejci, 2010). Conversely, loss of another Srs2-like protein found in *S. pombe*, spFbh1, causes significant meiotic defects with reduced spore viability and, significantly,

accumulation of spRad51 (Sun *et al.*, 2011). As with Srs2 in budding yeast, spFbh1 is thought to suppress crossover formation and remove spRad51 from ssDNA, dependent on its helicase/translocase activity (Lorenz *et al.*, 2009; Tsutsui *et al.*, 2014). Loss of spFbh1 also causes a failure in segregation of chromosomes during meiosis, however this is not thought to be related to unresolved joint molecules or processing at DNA junctions during HR (Sun *et al.*, 2011). Interestingly, spFbh1 appears to promote ubiquitination of Rad51 in addition to its helicase-dependent activity (Tsutsui *et al.*, 2014).

The human homologue of spFbh1, hFBH1, has a helicase domain which is highly conserved with budding yeast Srs2. Furthermore, hFBH1 has been shown to repress recombination defects and DNA damage sensitivity of *srs2* yeast strains (Chiolo *et al.*, 2007).

Another possible human orthologue of Srs2 is PARI, which contains a UvrD-like helicase domain, preferentially interacts with SUMOylated PCNA and causes a hyperrecombinant phenotype when lost. PARI has also been shown to interact with hRad51, disrupting hRad51 filaments *in vitro*, despite lacking the WalkerA/B domains required for the ATPase, and therefore helicase, activity observed in Srs2 (Moldovan *et al.*, 2012). Instead, it is thought that PARI regulates the frequency of HR events via inhibition of D-loop extenstion by DNA polymerase δ, with the UvrD-like helicase domain of PARI being dispensible for inhibtion (Burkovics *et al.*, 2016).

The human RecQ helicase hBLM has been suggested to have an Srs2-like anti-recombinase role via reversing the formation of hRad51-NPFs (Patel *et al.*, 2017). Conversely, the antirecombinase role of SPAR-1 in *Caenorhabditis elegans*, and its

counterpart SPAR1/RTEL1 in humans, is thought to be due to disruption of D-loops rather than via disruption of Rad51-NPFs (Barber *et al.*, 2008). RTEL1 is thought to play an anti-recombinase role in telomere maintenance and, in *C. elegans*, enforces CO interference and homeostasis via its D-loop disassembly capability (Uringa et al., 2011).

8.6 Implications for the Role of Srs2

The observed rescue of *srs2* sporulation and spore viability by tagging Rad51 at the N-terminal may support the suggestion that Srs2 stimulates the intrinsic ATP-ase activity of Rad51 (Antony *et al.*, 2009). ADP-bound hRAD51-NPFs are thought to have a slightly altered helical pitch than active ATP-bound filaments making them more compact (Short *et al.*, 2016). It has been suggested that the extended form of the NPFs are more active for strand exchange and that a conformational shift of the Rad51 N-terminal domain is involved in regulating the ATPase activity (Galkin *et al.*, 2006; Robertson *et al.*, 2009). If an N-terminal tag similarly emulated such an architectural change it may make the filament less suitable for strand invasion, compensating for the lack of Srs2 activity and rescuing the phenotypes.

The different effects of the *mre11* separation of function alleles were unexpected and need further consideration. The difference could relate to the retention of MRX complexes. When Sae2 or Mre11 activity is lost, MRX complexes are retained at DSB ends, meaning the ends remained tethered. This would not be the case in the *mre11-58S* strains, as the MRX complex does not form stably, potentially explaining the partial rescue of aggregates observed in these strains.

We considered whether the difference in the effects of the *mre11* alleles may relate to its interaction with Exo1. At HO-induced breaks, Mre11 recruits Exo1 and prevents Ku binding, independently of its nuclease function but dependent on MRX complex formation (Shim *et al.*, 2010). Affinity pulldown has also revealed a direct interaction between Exo1 and Srs2. *In vitro* evidence suggests that Srs2 enhances Exo1 activity and enables access for it to complete resection by enlarging the gap and preventing Rad51 binding: Exo1-mediated endonucleolytic cleavage of a construct resembling nicked DNA unwound by Srs2 (gapped 5'-Flap DNA) was specifically enhanced by Srs2 in an ATP-dependent manner, while cleavage by Dna2 was not (Potenski *et al.*, 2014). It is therefore possible that Srs2 unwinds DNA at nicks generated by Mre11/Sae2 allowing access for Exo1 and enhancing its activity.

In the absence of Sgs1/Dna2 or Exo1 resection at HO-induced breaks, the MRX complex with Sae2 can resect a few hundred nucleotides in the vicinity of the DSB end, dependent on Mre11 nuclease activity, which notably can be sufficient for gene conversion (Shim *et al.*, 2010; Zhu *et al.*, 2008). Furthermore, the mitotic cell cycle arrest in response to DSBs is inefficient in the absence of Exo1 and Sgs1-Dna2 resection, potentially allowing minimally resected DSBs to bypass arrest (Zhu *et al.*, 2008). If the meiotic checkpoint is similarly inefficient in the absence of long resection, and the absence of Srs2 reduces Exo1 activity, minimally resected DSBs that are still sufficient for strand invasion may erroneously pass through checkpoints. This could lead to unresolved JMs and a failure in DNA division as the cell attempts to continue through the cell cycle, possibly explaining why SPBs continue to divide in *srs2* strains. However, if the lack of Exo1 enhancement by Srs2 was the main cause of aggregation, the relative ability of *mre11-H125N* and *mre11-58S* to recruit Exo1 should be largely irrelevant as

neither would be able perform the minimal resection described, meaning aggregation should be rescued fully rather than partially.

While considering the relationship between Exo1 and Srs2, it may be of note that mitotic Exo1-dependent resection can occur when the initiation of resection is impaired, in *rad50Δ*, *mre11Δ* or *sae2Δ* cells, although the yield is lower, and that Exo1- or Dna2-mediated resection close to HO-induced breaks in the absence of MRX can be largely rescued by deletion of Ku (Mimitou and Symington, 2008; Shim *et al.*, 2010; Zhu *et al.*, 2008). In meiosis, when MRX is absent Spo11 is retained on the ends of DSB, preventing exonuclease access. Perhaps Srs2 functions in a backup process in case of inefficient MRX activity, enhancing Exo1 endonucleolytic activity and facilitating Exo1 entry into otherwise inaccessible DNA.

It is also possible that the different alleles of *mre11* may affect the interactions between Mre11, Srs2 and Sgs1. Srs2, Sgs1 and Mre11 have been shown to coimmunoprecipitate in unperturbed mitotic cells and may form Srs2-Mre11 and Sgs1-Mre11 subcomplexes following damage induction and damage checkpoint activation (Chiolo *et al.*, 2005). As overexpression of *SGS1* is able to partly compensate for the loss of Srs2 activity in certain circumstances, it is possible that the poor complex-forming ability of *mre11-58S* alters the interaction with Sgs1. However, this might be expected to exacerbate the Srs2 phenotypes whereas *mre11-58S* appears to reduce aggregate formation.

Finally, the unexpected *mre11* and *sae2* results could imply a connection to the pachytene checkpoint, which delays meiotic division. This delay is mediated by the Mek1 kinase preventing entry into Meiosis I until DSBs have been repaired. Furthermore, deletion of *MEK1* can abolish the meiotic delay even in strains that are deficient for DSB

resection and repair, such as *rad50S* (Xu *et al.*, 1997). As DSBs are repaired, Mek1 activity reduces below a threshold allowing Ndt80 activation. This leads to Red1 degradation and further Mek1 inactivation, following which Rad51-mediated repair can tidy up leftover DSBs (Prugar *et al.*, 2017).

In response to DSB formation, Mec1 and Tel1 phosphorylate Sae2, while its dephosphorylation can be prevented by persistent checkpoint activation, for example due to accumulation of DSBs in *dmc1Δ*, (Cartagena-Lirola *et al.*, 2006). As the presence of Mre11 foci at DSBs is prolonged by *SAE2* deletion and reduced by *SAE2* overexpression, it has been suggested that checkpoint regulation by Sae2 involves modulation of MRX-dependent signalling (Cartagena-Lirola *et al.*, 2006; Clerici *et al.*, 2006). When Sae2 is absent, or is non-phosphorylatable, cells accumulate unresected DSBs, fail to complete meiotic recombination and division, and display persistent Mek1 phosphorylation, as required to maintain the checkpoint arrest (Cartagena-Lirola *et al.*, 2006). Interestingly, checkpoint activation and DNA damage sensitivity observed in *sae2Δ* cells is suppressed by *mre11* alleles that dissociate more readily from DSB ends (Chen *et al.*, 2015). As the *mre11-58S* allele does not form stable MRX complexes, this could facilitate escape from the *sae2Δ*-mediated checkpoint activation. However, whereas *mre11-58S* partially rescues aggregate levels in *mre11-58S srs2*, bypassing DNA damage checkpoints might more intuitively be expected to increase aggregate formation.

An alternative connection to the Mek1 pachytene checkpoint may be via Ddc1. During prophase, the Ddc1 checkpoint protein localises to chromosomes and is phosphorylated by Mek1, becoming increasingly hyperphosphorylated in arrested cells dependent on

arrest severity. Ddc1 also promotes Mek1 function and Mek1-dependent phosphorylation of Red1 in a positive feedback loop (Hong and Roeder, 2002). Ddc1 has structural homology to PCNA and is expected to form part a heterotrimeric Rad17/Ddc1/Mec3 sliding clamp complex (also known as the 9-1-1 complex) upstream of Mec1 activation in the DNA damage checkpoint activation (de la Torre-Ruiz *et al.*, 1998; Venclovas and Thelen, 2000). It would be interesting to determine whether Srs2 is able to interact with Ddc1 via its PCNA binding domain. However, mitotic *srs2R1* cells, in which srs2 disrupts Rad51-NPFs but cannot interact with SUMOylated-PCNA, only show around half the increase in crossover level observed in *srs2Δ*, suggesting that the promotion of SDSA and the removal of toxic recombination intermediates by Srs2 is only partially dependent on its recruitment by SUMOylated PCNA (Le Breton *et al.*, 2008). Significantly, Vaze and coworkers observed that *srs2Δ* and *srs2-K41A* cells fail to recover from the mitotic DNA damage checkpoint, and that this can be suppressed by deletion of *MEC1* to prevent checkpoint initiation (Vaze *et al.*, 2002).

This project initially aimed to investigate the molecular role of Srs2 during meiosis. Although a cohesive model remains elusive, novel phenotypes have been observed with interesting implications for future experiments.

8.7 Future Directions

As aggregates of Rad51 have been found to form during meiosis in a *SPO11*-dependent manner it would be of considerable interest to determine whether these aggregates are forming solely at hotspots for meiotic recombination, i.e. sites with increased probability of meiotic DSBs, or whether only their initiation is dependent on DSBs, with aggregate

formation occurring away from the break site, either randomly or non-randomly. To address this question, strains have been tested and analysed in preparation for ChIP-seq analysis (Chapter 7). Unfortunately, Rad51 has proven problematic as a direct target for ChIP-seq due to the poor sensitivity of the α-Rad51 antibody and tagging of the Rad51 protein rescues *srs2-mn* phenotypes, even when the tag is expressed heterozygously. Instead, strains expressing the tagged PK9-Rfa1 subunit of RPA have been designed for use in ChIP-seq as it colocalises with Rad51 aggregates and does not significantly rescue the *srs2* aggregation phenotype. We therefore intend to perform α-PK ChIP-seq analysis on meiotic samples of *SRS2* and *srs2-mn* in the *PK9-RFA1* background, subtracting the non-colocalised foci background data from the wild-type analysis, to determine the sequence distribution of Rad51 aggregates in *srs2-mn*.

As the *tetO*/TetR separation analysis was performed with *tetO* inserts in a pericentromeric region, it would be interesting to repeat the experiment with *tetO* repeats inserted further along chromosome arms or in peritelomeric regions. Since SPB division in *srs2* cells has been shown to continue despite failures in nuclear separation, and given that the spindle tubules pulling the chromosomes toward the SPBs attach at the centromeres, it would be reasonable to expect the pericentomeric regions to be pulled out of the nuclear mass first, while the chromosome arms could theoretically remain entangled. Therefore, a repeat of the chromatid separation experiment in which the *tetO* insertions are made further along the chromosomes or at peritelomeric regions would be of significant interest to determine whether the signals continue to divide to the same extent. This would provide further insight into whether the apparently successful chromatid separation observed in cells with failed nuclear division holds true along the length of the chromosomes.

To determine whether the increased, unregulated presence of Rad51 due to the loss of Srs2 strippase activity is the major cause of the Rad51 aggregation phenotype, rather than loss of the Srs2 helicase activity or Srs2-mediated enhancement of Exo1 activity, it would be of interest to determine whether the Rad51 aggregation in *srs2* can be phenocopied in wild-type cells by overexpression of Rad51.

The surprising potential for a cumulative effect of aggregate levels observed in *srs2-mn sae2Δ* cells and the potential rescue of an *sae2Δ*-dependent population of aggregates by deletion of *TEL1* or loss of Mre11 nuclease activity should be investigated further. Double mutant strains of *sae2Δ tel1Δ* and *sa2Δ mre11-H125N* should therefore be analysed for aggregate formation. The potential connection to the Mek1 pachytene checkpoint raised by the *mre11* and *sae2* results raises several questions for potential lines of enquiry.

It would be of interest to observe whether aggregates occur during mitosis or whether the phenomenon is meiosis-specific. This could be achieved with DSB-inducing agents or by utilising the HO endonuclease naturally expressed in G1 phase. HO-induced DSBs at *MAT* loci are usually repaired by gene conversion using one of two unexpressed heterochromatin sites as a donor, *HMLa* or *HMRα*, to allow mating type switching (Haber, 2002). Cells that have already divided can then mate with the recently generated daughter cell to produce diploids, whereupon, the *Mata1-Matα2* corepressor causes a non-mating phenotype by altering gene expression (Haber, 2012). As laboratory strains are generally mutated at the HO gene to prevent its expression, the gene would need to be introduced on a plasmid or under an inducible promoter. Although HO would behave in a more predictable manner, DSB-inducing agents have advantages such as a

significantly increased number of DSBs formed per cell. DSB-inducing agents could also be used in *spo11 srs2* strains to observe whether aggregates are formed at non-programmed breaks during meiosis.

In vitro evidence has shown that Srs2 stimulates the structure-selective nuclease activity of Mus81-Mms4, independently of its helicase activity or its SUMO/PCNA interaction domain, and relieves Rad51-mediated inhibition of Mus81. Mus81 was also found to prevent Srs2 from unwinding recombination or replication intermediates, suggesting a coordination of their activities to stabilise intermediate structures for resolution by Mus81-Mms4 (Chavdarova *et al.*, 2015). It would therefore be of interest to repeat aggregate analysis in strains lacking Mms4, with and without Rad51 strand invasion activity.

In vitro evidence has been found that hRad51-NPFs were more likely to be trapped by nucleosomes than hDmc1-NPFs (Kobayashi *et al.*, 2016). A Co-IP would therefore be of interest to determine whether the aggregation phenotype may relate to histone binding.

Although meiotic expression of *SRS2* has been largely avoided in these experiments by using the mitotic-only *CLB2* promoter, it is possible that the observed phenotypes could be affected by the absence of Srs2 during S-phase. It would therefore be of interest to generate a strain in which *SRS2* expression could be controlled more finely.

Finally, it has been suggested that toxic joint molecules forming during Break-Induced Replication (BIR) of collapsed replication forks or eroded telomeres are rescued by Srs2 activity (Elango *et al.*, 2017). It would be of significant interest to observe Rad51

aggregation in the context of telomeres by colocalisation analysis with a tagged telomeric protein.

Appendices

A.1 Strains Generated during this Study

All strains are stored at -80°C in 1ml 50% Glycerol plus 1ml media (YPAD for *S. cerevisiae*, LB for *E.coli*). All strains of *S. cerevisiae* are in SK1 backgrounds.

A.1.1 Generation of *srs2-mn*

To avoid potential for retaining mitotic or replicative issues, and to be able to use the *rad51-II3A* allele, which is synthetically lethal with mitotic *srs2* mutation, a meiotic null allele of Srs2 was generated in which *SRS2* is under the control of the mitotic-only promoter, *pCLB2*. During mitosis, Srs2 is readily produced but upon entry into meiosis, Srs2 will be degraded without further transcription and produce an effectively doubly mutated strain. A section of *CLB2* promoter region DNA was amplified from a vector with primers to include regions of homology upstream of *SRS2*. This was then transformed into wild-type haploid yeast and its lack of meiotic expression confirmed by Western analysis (Figure A.1)

A.1.2 Generation of N-terminal Tagged *PK3-RAD51*

Previous studies have indicated that a C-terminal tag interferes with the function of Rad51 and so the CRISPR/Cas9 system was instead used to tag Rad51 at the N-terminal. Sticky-ended oligonucleotides, complementary to a target sequence in *RAD51* were annealed to form a gRNA insert specific to *RAD51* and cloned into a CRISPR/Cas9 plasmid. Mutagenesis primers were designed across the target site in *RAD51* that would introduce a silent mutation resistant to cutting by the Cas9 endonuclease.

A section of *RAD51* immediately downstream from the start codon was amplified by PCR and cloned into a centromeric vector, with cut sites introduced by PCR. A section of the promoter region of *RAD51* up to and including the start codon was amplified by PCR and cloned into the same vector, with cut sites introduced by PCR. This plasmid containing both consecutive *RAD51* insertions, separated by a restriction site immediately after the start codon, was then amplified by Overlapping PCR using the overlapping mutagenesis primers and cloned into a new centromeric vector. A PK3 tag was then cloned into the mutagenised Rad51 vector using cut sites introduced by PCR to match the N-terminal restriction site in the Rad51 vector.

Haploid wild-type yeast was simultaneously transformed with the CRISPR/Cas9 plasmid, targeting genomic *RAD51*, and the template plasmid, containing a non-cuttable *RAD51* section with the PK3 tag inserted at the N-terminal.

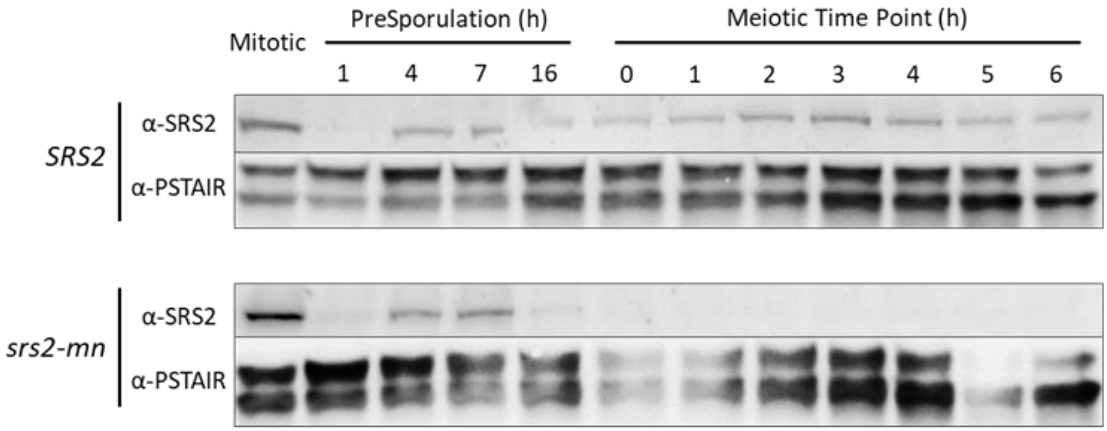

Figure A.1 Confirmation of the meiotic null allele of *SRS2*. Wild-type *SRS2* is visibly expressed throughout the meiotic time course. Conversely, in the *srs2-mn* strain, expression is clearly reduced toward the end of the presporulation incubation and is not visible during meiotic time points. *SRS2* expression was not observable in either strain following 1h incubation in presporulation media as the culture had been inoculated with non-exponential cells, however expression was subsequently clearly observed in both presporulation cultures. (17h Presporulation = 0h Meiotic Time Point)

A.1.3 Generation of C-terminal Tagged *RFA1-GFP* and *RFA1-PK9*

Fragments were amplified from vectors containing *PK9* and *GFP* sequences, with primers to introduce regions of homology to the C-terminal of *RFA1*. These were then transformed into wild-type yeast. Localisation of *RFA1-GFP* to the nucleus visually confirmed by microscopy and *RFA1-PK9* expression confirmed by Western analysis.

A.1.4 Diploid *S. cerevisiae* Strains

Strain Number	Origin *Shortname*	MATa Genotype	MATα Genotype
dAG1756	hAG2039 x hAG2040 WT, *ura- his- trp- leu-*	*ho::LYS2 ura3 leu2::hisG his3::hisG trp1::hisG*	*ho::LYS2 ura3 leu2::hisG his3::hisG trp1::hisG*
dAG1768	dAG1756::pAG471 WT *RAD51OE*	*ho::LYS2 ura3 leu2::hisG his3::hisG trp1::hisG [pAG471 (YEplac195 + Rad51)]*	*ho::LYS2 ura3 αeu2::hisG his3::hisG trp1::hisG*
dAG1769	dAG1681::pAG471 *srs2-101 RAD51OE*	*ura3 lys2 ho::LYS2 leu2⁻(Xho1-Cla1) trp1::hisG srs2-101*	*ura3 lys2 ho::LYS2 leu2⁻(Xho1-Cla1) trp1::hisG srs2-101 [pAG471 (YEplac195 + Rad51)]*
dAG1782	hAG2100 x hAG2101 *mek1Δ*	*ho::LYS2 lys2 ura3 leu2 mek1::LEU2*	*ho::LYS2 lys2 ura3 leu2 mek1::LEU2*
dAG1783	hAG2102 x hAG2103 *mek1Δ srs2-101*	*ho::LYS2 lys2 ura3 leu2 mek1::LEU2 srs2-101::HphMX his4x*	*ho::LYS2 lys2 ura3 leu2 mek1::LEU2 srs2-101::HphMX*
dAG1791	hAG2116 x hAG2117 *mek1Δ ZIP1-GFP*	*ho::LYS2 lys2 ura3 leu2 mek1::LEU2 trp1::hisG ZIP1-GFP*	*ho::LYS2 lys2 ura3 leu2 mek1::LEU2 ZIP1-GFP*
dAG1792	dAG1681::pAG472 *srs2-101* Empty OE vector	*ura3 lys2 ho::LYS2 leu2⁻(Xho1-Cla1) trp1::hisG srs2-101*	*ura3 lys2 ho::LYS2 leu2⁻(Xho1-Cla1) trp1::hisG srs2-101 [pAG472 (YEplac195 + pIME2)]*
dAG1793	dAG1681::pAG473 *srs2-101 RAD51OE*	*ura3 lys2 ho::LYS2 leu2⁻(Xho1-Cla1) trp1::hisG srs2-101*	*ura3 lys2 ho::LYS2 leu2⁻(Xho1-Cla1) trp1::hisG srs2-101 [pAG473 (YEplac195 + pIME2::RAD51)]*
dAG1798	hAG2041 x hAG2122 *PK3-Rad51*	*ho::LYS2 lys2 ura3 leu2::hisG his3::hisG trp1::hisG PK3-Rad51*	*ho::LYS2 lys2 ura3 leu2 his3::hisG trp1::hisG PK3-RAD51*

Strain Number	Origin *Shortname*	MATa Genotype	MATα Genotype
dAG1799	hAG2120 x hAG2121 *PK3-Rad51 srs2-101*	*ho::LYS2 lys2 ura3 leu2 trp1::hisG PK3-RAD51 srs2-101::HphMX*	*ho::LYS2 lys2 ura3 leu2 his3::hisG trp1::hisG PK3-RAD51 srs2-101::HphMX*
dAG1800	hAG2118 x hAG2119 *PK3-Rad51 srs2Δ*	*ho::hisG lys2 ura3 leu2 PK3-Rad51 srs2Δ::KanMX4*	*ho::LYS2/ho::hisG lys2?(If lys2, ho::LYS2) ura3 leu2 his3::hisG PK3-Rad51 srs2Δ::KanMX4*
dAG1803	(hAG2039::pAG472) x hAG2040 WT Empty OE vector	*ho::LYS2 lys2 ura3 leu2::hisG his3::hisG trp1::hisG [pAG472 (YEplac195 + pIME2)]*	*ho::LYS2 lys2 ura3 leu2::hisG his3::hisG trp1::hisG*
dAG1804	(hAG2039::pAG473) x hAG2040 WT *RAD51OE*	*ho::LYS2 lys2 ura3 leu2::hisG his3::hisG trp1::hisG [pAG473 (YEplac195 + pIME2::RAD51)]*	*ho::LYS2 lys2 ura3 leu2::hisG his3::hisG trp1::hisG*
dAG1805	hA2123 x hAG2124 *mek1Δ ZIP1-GFP srs2-101*	*ho::LYS2 lys2 ura3 leu2 mek1::LEU2 trp1::hisG ZIP1-GFP srs2-101::HphMX*	*ho::LYS2 lys2 ura3 leu2 mek1::LEU2 trp1::hisG ZIP1-GFP srs2-101::HphMX*
dAG1809	hAG2040 x hAG2041 WT *[PK3-RAD51]$_{+/-}$*	*ho::LYS2 lys2 ura3 leu2::hisG his3::hisG trp1::hisG PK3-Rad51*	*ho::LYS2 lys2 ura3 leu2::hisG his3::hisG trp1::hisG*
dAG1810	hAG2170 x hAG2182 *srs2-mn [PK3-RAD51]$_{+/-}$*	*ho::LYS2 lys2 ura3 leu2::hisG his3::hisG trp1::hisG pCLB2-3HA-SRS2::KANMX PK3-RAD51 (Confirmed by PCR)*	*ho::LYS2 lys2 ura3 leu2::hisG his3::hisG trp1::hisG pCLB2-3HA-SRS2::KANMX*
dAG1811	hAG1847 x hAG2118 *srs2Δ [PK3-RAD51]$_{+/-}$*	*ho::hisG lys2 ura3 leu2 PK3-Rad51 srs2Δ::KanMX4*	*ho::LYS2/ho::hisG leu2 srs2Δ::KanMX4*
dAG1812	hAG2145 x hAG2146 *TetO/R* SPB TUB	*ho::LYS2 lys2 ura3 leu2::hisG promURA3::tetR::GFP-LEU2,tetOx224-URA3 trp1::hisG CNM67-3mCherry-NatMX4 his3::HIS3p-GFP-TUB1-HIS3*	*ho::LYS2 lys2 ura3 leu2::hisG promURA3::tetR::GFP-LEU2,tetOx224-URA3 trp1::hisG CNM67-3mCherry-NatMX4 his3::HIS3p-GFP-TUB1-HIS3*
dAG1813	hAG2168 x hAG2169 *sae2Δ(Kan) srs2-mn*	*ho::LYS2 lys2 ura3 leu2 pCLB2-3HA-SRS2::KanMX sae2::KanMX6 trp1::hisG arg4-nsp,bgl*	*ho::LYS2 lys2 ura3 leu2 pCLB2-3HA-SRS2::KanMX sae2::KanMX6 trp1::hisG his3::hisG*
dAG1814	hAG2155 x hAG2170 *srs2-mn*	*ho::LYS2 lys2 ura3 leu2::hisG his3::hisG trp1::hisG pCLB2-3HA-SRS2::KanMX*	*ho::LYS2 lys2 ura3 leu2::hisG his3::hisG trp1::hisG pCLB2-3HA-SRS2::KANMX*
dAG1816	hAG2182 x hAG2183 *srs2-mn PK3-RAD51*	*ho::LYS2 lys2 ura3 leu2::hisG his3::hisG trp1::hisG pCLB2-3HA-SRS2::KANMX PK3-RAD51 (Confirmed by PCR)*	*ho::LYS2 lys2 ura3 leu2::hisG his3::hisG trp1::hisG pCLB2-3HA-SRS2::KANMX PK3-RAD51 (Confirmed by PCR)*

Strain Number	Origin *Shortname*	MATa Genotype	MATα Genotype
dAG1817	hAG1845 x hAG2145 SPB TUB *[TetO/R]$_{+/-}$*	*ho::LYS2 lys2 ura3 leu2::hisG trp1::hisG CNM67-3mCherry-NatMX4 his3::HIS3p-GFP-TUB1-HIS3 promURA3::tetR::GFP-LEU2,tetOx224-URA3*	*ho::LYS2 lys2 ura3 leu2::hisG trp1::hisG his3::HIS3p-GFP-TUB1-HIS3 CNM67-3mCherry-NatMX4*
dAG1818	hAG2180 x hAG2174 SPB TUB *srs2-mn [TetO/R]$_{+/-}$*	*ho::LYS2 lys2 ura3 leu2::hisG trp1::hisG CNM67-3mCherry-NatMX4 his3::HIS3p-GFP-TUB1-HIS3 promURA3::tetR::GFP-LEU2,tetOx224-URA3 pCLB2-3HA-SRS2::KANMX*	*ho::LYS2 lys2 ura3 leu2::hisG trp1::hisG his3::HIS3p-GFP-TUB1-HIS3 CNM67-3mCherry-NatMX4 pCLB2-3HA-SRS2::KANMX*
dAG1819	hAG2178 x hAG2148 SPB *[TetO/R]$_{+/-}$*	*ho::LYS2 lys2 ura3 leu2::hisG his3::hisG trp1::hisG CNM67-3mCherry-NatMX4*	*ho::LYS2 lys2 ura3 leu2::hisG promURA3::tetR::GFP-LEU2,tetOx224-URA3 trp1::hisG CNM67-3mCherry-NatMX4*
dAG1820	hAG2177 x hAG2172 SPB *srs2-mn [TetO/R]$_{+/-}$*	*ho::LYS2 lys2 ura3 leu2::hisG his3::hisG trp1::hisG CNM67-3mCherry-NatMX4 promURA3::tetR::GFP-LEU2,tetOx224-URA3 pCLB2-3HA-SRS2::KANMX*	*ho::LYS2 lys2 ura3 leu2::hisG his3::hisG trp1::hisG CNM67-3mCherry-NatMX4 pCLB2-3HA-SRS2::KANMX*
dAG1821	hAG2200 x hAG2201 *sae2Δ(Kan)*	*ho::LYS2 lys2 ura3 leu2 his3::hisG trp1::hisG arg4-nsp,bgl sae2::KanMX6*	*ho::LYS2 lys2 ura3 leu2 his3::hisG trp1::hisG arg4-nsp,bgl sae2::KanMX6*
dAG1832	hAG2204 x hAG2205 *mek1Δ*	*ho::LYS2 lys2 ura3 leu2 mek1::LEU2*	*ho::LYS2 lys2 ura3 leu2 mek1::LEU2 trp1::hisG*
dAG1833	hAG2206 x hAG2207 *mek1Δ srs2-mn*	*ho::LYS2 lys2 ura3 leu2 mek1::LEU2 pCLB2-3HA-SRS2::KANMX ade2-bglII trp1::hisG*	*ho::LYS2 lys2 ura3 leu2 mek1::LEU2 pCLB2-3HA-SRS2::KANMX trp1::hisG*
dAG1834	hAG2208 x hAG2209 *dmc1Δ*	*ho::LYS2 lys2 ura3 leu2::hisG trp1::hisG dmc1Δ::KanMX4*	*ho::LYS2 lys2 ura3 leu2::hisG his3::hisG dmc1Δ::KanMX4*
dAG1835	hAG2210 x hAG2212 *dmc1Δ srs2-mn*	*ho::LYS2 lys2 ura3 leu2::hisG his3::hisG pCLB2-3HA-SRS2::KanMX dmc1Δ::KanMX4*	*ho::LYS2 lys2 ura3 leu2::hisG his3::hisG trp1::hisG pCLB2-3HA-SRS2::KanMX dmc1Δ::KanMX4*
dAG1838	hAG2221 x hAG2222 *spo11-Y135F srs2-mn*	*ho::LYS2 lys2 ura3 leu2::hisG pCLB2-3HA-SRS2::KanMX spo11-Y135F-HA3-His6::KanMX4*	*ho::LYS2 lys2 ura3 leu2::hisG his3::hisG trp1::hisG pCLB2-3HA-SRS2::KanMX spo11-Y135F-HA3-His6::KanMX4*

Strain Number	Origin *Shortname*	MATa Genotype	MATα Genotype
dAG1845	hAG2238 x hAG2227 *sae2Δ(Hyg)*	*ho*::*LYS2 lys2 ura3 leu2*::*hisG his3*::*hisG trp1*::*hisG sae2Δ*::*HphMX*	*ho*::*LYS2 lys2 ura3 leu2*::*hisG his3*::*hisG trp1*::*hisG sae2Δ*::*HphMX*
dAG1846	hAG2228 x hAG2229 *sae2Δ(Hyg) srs2-mn*	*ho*::*LYS2 lys2 ura3 leu2*::*hisG his3*::*hisG trp1*::*hisG sae2Δ*::*HphMX pCLB2-3HA-SRS2*::*KanMX*	*ho*::*LYS2 lys2 ura3 leu2*::*hisG his3*::*hisG trp1*::*hisG sae2Δ*::*HphMX pCLB2-3HA-SRS2*::*KanMX*
dAG1847	hAG2234 x hAG2235 *rad51Δ*	*ho*::*lys2 lys2 ura3 leu2*::*hisG ade2*::*LK trp1*::*hisG rad51Δ*::*HisG-URA3-hisG*	*ho*::*LYS2 lys2 ura3 leu2*::*hisG ade2*::*LK rad51Δ*::*HisG-URA3-hisG*
dAG1848	hAG2236 x hAG2237 *rad51Δ srs2-mn*	*ho*::*lys2 lys2 ura3 leu2*::*hisG ade2*::*LK trp1*::*hisG rad51Δ*::*HisG-URA3-hisG pCLB2-3HA-SRS2*::*KANMX*	*ho*::*LYS2 lys2 ura3 leu2*::*hisG rad51Δ*::*HisG-URA3-hisG pCLB2-3HA-SRS2*::*KANMX*
dAG1849	hAG2147 x hAG2148 *TetO/R* SPB WT	*ho*::*LYS2 lys2 ura3 leu2*::*hisG promURA3*::*tetR*::*GFP-LEU2,tetOx224-URA3 his3*::*hisG trp1*::*hisG CNM67-3mCherry-NatMX4*	*ho*::*LYS2 lys2 ura3 leu2*::*hisG promURA3*::*tetR*::*GFP-LEU2,tetOx224-URA3 trp1*::*hisG CNM67-3mCherry-NatMX4*
dAG1850	hAG2177 x hAG2276 *TetO/R* SPB *srs2-mn*	*MATa ho*::*LYS2 lys2 ura3 leu2*::*hisG his3*::*hisG trp1*::*hisG CNM67-3mCherry-NatMX4 promURA3*::*tetR*::*GFP-LEU2,tetOx224-URA3 pCLB2-3HA-SRS2*::*KANMX*	*MATα ho*::*LYS2 lys2 ura3 leu2*::*hisG his3*::*hisG trp1*::*hisG CNM67-3mCherry-NatMX4 pCLB2-3HA-SRS2*::*KANMX promURA3*::*tetR*::*GFP-LEU2,tetOx224-URA3*
dAG1863	hAG2272 x hAG2273 *tel1Δ*	*MATa ho*::*LYS2 lys2 ura3 leu2 his3*::*hisG trp1*::*hisG tel1Δ*::*HphMX*	*MATα ho*::*LYS2 lys2 ura3 leu2 his3*::*hisG trp1*::*hisG tel1Δ*::*HphMX*
dAG1864	hAG2274 x hAG2275 *tel1Δ srs2-mn*	*MATa ho*::*LYS2 lys2 ura3 leu2 his3*::*hisG trp1*::*hisG tel1Δ*::*HphMX pCLB2-3HA-SRS2*::*KanMX*	*MATα ho*::*LYS2 lys2 ura3 leu2 his3*::*hisG trp1*::*hisG tel1Δ*::*HphMX pCLB2-3HA-SRS2*::*KanMX*
dAG1865	hAG2250 x hAG2251 *tel1Δ srs2-mn sae2Δ*	*MATa ho*::*LYS2 lys2 ura3 leu2 his3*::*hisG trp1*::*hisG tel1Δ*::*HphMX sae2Δ*::*HphMX pCLB2-3HA-SRS2*::*KanMX*	*MATα ho*::*LYS2 lys2 ura3 leu2 his3*::*hisG trp1*::*hisG tel1Δ*::*HphMX sae2Δ*::*HphMX pCLB2-3HA-SRS2*::*KanMX*
dAG1866	hAG2264 x hAG2265 *mre11-58S*	*MATa ho*::*LYS2 lys2 ura3 leu2 his3*::*hisG trp1*::*hisG mre11-58S(H213Y confirmed by seq)*	*MATα ho*::*LYS2 lys2 ura3 leu2 his3*::*hisG trp1*::*hisG mre11-58S(H213Y confirmed by seq)*
dAG1868	hAG2268 x hAG2269 *mre11-58S srs2-mn sae2Δ*	*MATa ho*::*LYS2 lys2 ura3 leu2 his3*::*hisG trp1*::*hisG mre11-58S(H213Y confirmed by seq) pCLB2-*	*MATα ho*::*LYS2 lys2 ura3 leu2 his3*::*hisG trp1*::*hisG mre11-58S(H213Y confirmed by seq) pCLB2-*

Strain Number	Origin *Shortname*	MATa Genotype	MATα Genotype
		3HA-SRS2::KanMX sae2Δ::HphMX	*3HA-SRS2::KanMX sae2Δ::HphMX*
dAG1869	hAG2277 x hAG2161 *mre11-H125N*	*MATa ho::LYS2 lys2 ura3 leu2 his3::hisG trp1::hisG mre11-H125N (confirmed by seq)*	*MATα ho::LYS2 lys2 ura3 leu2::hisG his3::hisG trp1::hisG mre11-H125N (seq)*
dAG1870	hAG2278 x hAG2279 *mre11-H125N srs2-mn*	*MATa ho::LYS2 lys2 ura3 leu2 his3::hisG trp1::hisG mre11-H125N (confirmed by seq) pCLB2-3HA-SRS2::KanMX*	*MATα ho::LYS2 lys2 ura3 leu2 his3::hisG trp1::hisG mre11-H125N (confirmed by seq) pCLB2-3HA-SRS2::KanMX*
dAG1871	hAG2280 x hAG2281 *mre11-H125N srs2-mn sae2Δ*	*MATα ho::LYS2 lys2 ura3 leu2 his3::hisG trp1::hisG mre11-H125N (confirmed by seq) sae2Δ::HphMX pCLB2-3HA-SRS2::KanMX*	*MATα ho::LYS2 lys2 ura3 leu2 his3::hisG trp1::hisG mre11-H125N (confirmed by seq) sae2Δ::HphMX pCLB2-3HA-SRS2::KanMX*
dAG1877	hAG2285 x hAG2289 *RFA1-PK9 WT*	*MATa ho::LYS2 lys2 ura3 leu2::hisG his3::hisG trp1::hisG RFA1-PK9::KanMX*	*MATα ho::LYS2 lys2 ura3 leu2::hisG his3::hisG trp1::hisG RFA1-PK9::KanMX*
dAG1878	hAG2290 x hAG2291 *RFA1-PK9 srs2-mn*	*MATa ho::LYS2 lys2 ura3 leu2::hisG his3::hisG trp1::hisG RFA1-PK9::KanMX pCLB2-3HA-SRS2::KANMX*	*MATα ho::LYS2 lys2 ura3 leu2::hisG his3::hisG trp1::hisG RFA1-PK9::KanMX pCLB2-3HA-SRS2::KANMX*
dAG1882	hAG2305 x hAG2306 *RFA1-GFP*	*MATa ho::LYS2 lys2 ura3 leu2::hisG his3::hisG trp1::hisG RFA1-GFP::KanMX*	*MATα ho::LYS2 lys2 ura3 leu2::hisG his3::hisG trp1::hisG RFA1-GFP::KanMX*
dAG1883	hAG2292 x hAG2293 *RFA1-GFP srs2-mn*	*MATa ho::LYS2 lys2 ura3 leu2::hisG his3::hisG trp1::hisG RFA1-GFP::KanMX pCLB2-3HA-SRS2::KANMX*	*MATα ho::LYS2 lys2 ura3 leu2::hisG his3::hisG trp1::hisG RFA1-GFP::KanMX pCLB2-3HA-SRS2::KANMX*
dAG1884	hAG2294 x hAG2295 *RFA1-GFP srs2-mn sae2Δ*	*MATa ho::LYS2 lys2 ura3 leu2::hisG his3::hisG trp1::hisG RFA1-GFP::KanMX pCLB2-3HA-SRS2::KANMX sae2Δ::HphMX*	*MATα ho::LYS2 lys2 ura3 leu2::hisG his3::hisG trp1::hisG RFA1-GFP::KanMX pCLB2-3HA-SRS2::KANMX sae2Δ::HphMX*
dAG1885	hAG2309 x hAG2310 *mre11-58S srs2-mn*	*MATa ho::LYS2 lys2 ura3 leu2 his3::hisG trp1::hisG mre11-58S(H213Y confirmed by seq) pCLB2-3HA-SRS2::KanMX*	*MATα ho::LYS2 lys2 ura3 leu2 his3::hisG trp1::hisG mre11-58S(H213Y confirmed by seq) pCLB2-3HA-SRS2::KanMX*
dAG1886	hAG2301 x hAG2302 *ndt80Δ*	*MATa ho::LYS2 lys2 ura3 leu2::hisG trp1::hisG arg4Δ(eco47III-hpaI)*	*MATα ho::LYS2 lys2 ura3 ndt80Δ(Eco47III-BseRI)::KanMX6*

Strain Number	Origin *Shortname*	MATa Genotype	MATα Genotype
		ndt80Δ(Eco47III-BseRI)::KanMX6	
dAG1887	hAG2299 x hAG2300 *ndt80Δ srs2-mn*	*MATa ho::LYS2 lys2 ura3 leu2::hisG arg4Δ(eco47III-hpaI) trp1::hisG his3::hisG ndt80Δ(Eco47III-BseRI)::KanMX6 pCLB2-3HA-SRS2::KanMX*	*MATα ho::LYS2 lys2 ura3 arg4Δ(eco47III-hpaI) leu2::hisG ndt80Δ(Eco47III-BseRI)::KanMX6 pCLB2-3HA-SRS2::KanMX*
dAG1892	hAG2173 x hAG2174 *srs2-mn* SPB TUB	*MATa ho::LYS2 lys2 ura3 leu2::hisG trp1::hisG his3::HIS3p-GFP-TUB1-HIS3 CNM67-3mCherry-NatMX4 pCLB2-3HA-SRS2::KANMX*	*MATα ho::LYS2 lys2 ura3 leu2::hisG trp1::hisG his3::HIS3p-GFP-TUB1-HIS3 CNM67-3mCherry-NatMX4 pCLB2-3HA-SRS2::KANMX*
dAG1897	hAG2348 x hAG2349 *RFA1-GFP sae2Δ*	*MATa ho::LYS2 lys2 ura3 leu2::hisG his3::hisG trp1::hisG RFA1-GFP::KanMX sae2Δ::HphMX*	*MATα ho::LYS2 lys2 ura3 leu2::hisG his3::hisG trp1::hisG RFA1-GFP::KanMX sae2Δ::HphMX*
dAG1898	hAG2350 x hAG2351 *spo11-Y135F sae2Δ*	*MATa ho::LYS2 lys2 ura3 leu2::hisG trp1::hisG spo11-Y135F-HA3-His6::KanMX4 sae2Δ::HphMX*	*MATα ho::LYS2 lys2 ura3 leu2::hisG spo11-Y135F-HA3-His6::KanMX4 sae2Δ::HphMX*

A.1.5 Haploid *S. cerevisiae* Strains

Strain Number	Origin *Shortname*	Genotype
hAG2014	hAG1886::(pAG335-LJH025/26) *SRS2::pCLB2/srs2-mn*	*MATa ho::LYS2 TRP1 ura3 (VMA-201?) pCLB2-3HA-SRS2::KanMX*
hAG2015	hAG1801::(pBH173-M13F/R) *rad51-II3A::NatMX/rad51-II3A*	*MATα ho::hisG, leu2::hisG, ura3(ΔSma-Pst), his4-X::LEU2-(NgoMIV;+ori)-URA3, RAD51-R188A,K361A,K371A-NatMX*
hAG2016	hAG1500::(pBH43-LJH013/014) *srs2-101::HphMX*	*MATα ho::LYS2 lys2 leu2⁻(Xho1-Cla1) ura3 trp1::hisG srs2-101::HphMX*
hAG2029	hAG2014 x hAG2015 dissection *srs2-mn*	*MATα ho::LYS2 TRP1 ura3 (VMA-201?) pCLB2-3HA-SRS2::KanMX*
hAG2031	hAG2014 x hAG2015 dissection *srs2-mn rad51-II3A*	*MATa ho::LYS2 TRP1 ura3 (VMA-201?) pCLB2::SRS2::KANMX ho::hisG, leu2::hisG, ura3(ΔSma-Pst), his4-X::LEU2-(NgoMIV;+ori)-URA3, RAD51-R188A,K361A,K371A-NatMX*

Strain Number	Origin *Shortname*	Genotype
hAG2032	hAG2014 x hAG2015 dissection *srs2-mn rad51-II3A*	*MATα ho::LYS2 TRP1 ura3 (VMA-201?) pCLB2::SRS2::KANMX ho::hisG, leu2::hisG, ura3(ΔSma-Pst), his4-X::LEU2-(NgoMIV;+ori)-URA3, RAD51-R188A,K361A,K371A-NatMX*
hAG2039	BH26 dissection *WT, leu- his- trp- ura-*	*MATa ho::LYS2 lys2 ura3 leu2::hisG his3::hisG trp1::hisG*
hAG2040	BH26 dissection *WT, leu- his- trp- ura-*	*MATα ho::LYS2 lys2 ura3 leu2::hisG his3::hisG trp1::hisG*
hAG2041	hAG2039::pAG469(Cas9) & pAG470 (template) *PK3-RAD51*	*MATa ho::LYS2 lys2 ura3 leu2::hisG his3::hisG trp1::hisG PK3-RAD51*
hAG2074	hAG2016 x hAG2053 dissection	*MATa srs2-101::HphMX slx1::KanMX yen1::HphMX KanMX::pCLB2::3HA::MMS4 (this is mms4-mn) (possibly [ura3Δ(hind3-Sma1) lys2hi::LYS2 arg4Δ(eco47III-hpa1) cyh-z leu2-R::URA3rev-tel-ARG4] and [ura3 lys2 ho::LYS2 leu2⁻(Xho1-Cla1) trp1::hisG])*
hAG2075	hAG2016 x hAG2053 dissection	*MATα srs2-101::HphMX slx1::KanMX yen1::HphMX KanMX::pCLB2::3HA::MMS4 (this is mms4-mn) (possibly [ura3Δ(hind3-Sma1) lys2hi::LYS2 arg4Δ(eco47III-hpa1) cyh-z leu2-R::URA3rev-tel-ARG4] and [ura3 lys2 ho::LYS2 leu2⁻(Xho1-Cla1) trp1::hisG])*
hAG2100	hAG707 x hAG2016 dissection *mek1Δ*	*MATa ho::LYS2 lys2 ura3 leu2 mek1::LEU2*
hAG2101	hAG707 x hAG2016 dissection *mek1Δ*	*MATα ho::LYS2 lys2 ura3 leu2 mek1::LEU2*
hAG2102	hAG707 x hAG2016 dissection *mek1Δ srs2-101*	*MATa ho::LYS2 lys2 ura3 leu2 mek1::LEU2 srs2-101::HphMX his4x*
hAG2103	hAG707 x hAG2016 dissection *mek1Δ srs2-101*	*MATα ho::LYS2 lys2 ura3 leu2 mek1::LEU2 srs2-101::HphMX*
hAG2110	hAG2100 x hAG1845 dissection *mek1Δ* SPB TUB	*MATa ho::LYS2 lys2 ura3 leu2 mek1::LEU2 his3-hisG? his3::HIS3p-GFP-TUB1-HIS3 CNM67-3mCherry-NatMX4 trp1::hisG*
hAG2111	hAG2100 x hAG1845 dissection *mek1Δ* SPB TUB	*MATα ho::LYS2 lys2 ura3 leu2 mek1::LEU2 his3-hisG? his3::HIS3p-GFP-TUB1-HIS3 CNM67-3mCherry-NatMX4*
hAG2116	hAG2100 x hAG1743 dissection *mek1Δ ZIP1-GFP*	*MATa ho::LYS2 lys2 ura3 leu2 mek1::LEU2 trp1::hisG ZIP1-GFP*
hAG2117	hAG2100 x hAG1743 dissection *mek1Δ ZIP1-GFP*	*MATα ho::LYS2 lys2 ura3 leu2 mek1::LEU2 ZIP1-GFP*
hAG2118	hAG2041 x hAG1847 dissection *PK3::RAD51 srs2Δ*	*MATa ho::hisG lys2 ura3 leu2 PK3-Rad51 srs2Δ::KanMX4*
hAG2119	hAG2041 x hAG1847 dissection *PK3::RAD51 srs2Δ*	*MATα ho::LYS2/ho::hisG lys2?(lys2 only possible if ho::LYS2) ura3 leu2 his3::hisG PK3-Rad51 srs2Δ::KanMX4*
hAG2120	hAG2041 x hAG2016 dissection *PK3::RAD51 srs2-101*	*MATa ho::LYS2 lys2 ura3 leu2 trp1::hisG PK3-RAD51 srs2-101::HphMX*
hAG2121	hAG2041 x hAG2016 dissection *PK3::RAD51 srs2-101*	*MATα ho::LYS2 lys2 ura3 leu2 his3::hisG trp1::hisG PK3-RAD51 srs2-101::HphMX*

Strain Number	Origin *Shortname*	Genotype
hAG2122	hAG2041 x hAG2016 dissection *PK3*::*RAD51*	*MATα ho*::*LYS2 lys2 ura3 leu2 his3*::*hisG trp1*::*hisG PK3-RAD51*
hAG2123	hAG2116 x hAG2016 dissection *mek1Δ ZIP1-GFP srs2-101*	*MATa ho*::*LYS2 lys2 ura3 leu2 mek1*::*LEU2 trp1*::*hisG ZIP1-GFP srs2-101*::*HphMX*
hAG2124	hAG2116 x hAG2016 dissection *mek1Δ ZIP1-GFP srs2-101*	*MATα ho*::*LYS2 lys2 ura3 leu2 mek1*::*LEU2 trp1*::*hisG ZIP1-GFP srs2-101*::*HphMX*
hAG2145	hAG1979 x hAG1845 dissection *TetO/R* SPB TUB	*MATa ho*::*LYS2 lys2 ura3 leu2*::*hisG promURA3*::*tetR*::*GFP-LEU2,tetOx224-URA3 trp1*::*hisG CNM67-3mCherry-NatMX4 his3*::*HIS3p-GFP-TUB1-HIS3*
hAG2146	hAG1979 x hAG1845 dissection *TetO/R* SPB TUB	*MATα ho*::*LYS2 lys2 ura3 leu2*::*hisG promURA3*::*tetR*::*GFP-LEU2,tetOx224-URA3 trp1*::*hisG CNM67-3mCherry-NatMX4 his3*::*HIS3p-GFP-TUB1-HIS3*
hAG2147	hAG1979 x hAG1845 dissection *TetO/R* SPB	*MATa ho*::*LYS2 lys2 ura3 leu2*::*hisG promURA3*::*tetR*::*GFP-LEU2,tetOx224-URA3 his3*::*hisG trp1*::*hisG CNM67-3mCherry-NatMX4*
hAG2148	hAG2147 x hAG2016 dissection *TetO/R* SPB	*MATα ho*::*LYS2 lys2 ura3 leu2*::*hisG promURA3*::*tetR*::*GFP-LEU2,tetOx224-URA3 trp1*::*hisG CNM67-3mCherry-NatMX4*
hAG2149	hAG2147 x hAG2016 dissection *TetO/R SPB srs2-101*	*MATa ho*::*LYS2 lys2 ura3 leu2 trp1*::*hisG promURA3*::*tetR*::*GFP-LEU2,tetOx224-URA3 his3*::*hisG CNM67-3mCherry-NatMX4 srs2-101*::*HphMX*
hAG2150	hAG2147 x hAG2016 dissection *TetO/R SPB srs2-101*	*MATα ho*::*LYS2 lys2 ura3 leu2 trp1*::*hisG promURA3*::*tetR*::*GFP-LEU2,tetOx224-URA3 his3*::*hisG CNM67-3mCherry-NatMX4 srs2-101*::*HphMX*
hAG2151	hAG2145 x hAG2016 dissection *TetO/R* SPB TUB *srs2-101*	*MATa ho*::*LYS2 lys2 ura3 leu2 promURA3*::*tetR*::*GFP-LEU2,tetOx224-URA3 trp1*::*hisG CNM67-3mCherry-NatMX4 srs2-101*::*HphMX his3*::*HIS3p-GFP-TUB1-HIS3*
hAG2152	hAG2145 x hAG2016 dissection *TetO/R* SPB TUB *srs2-101*	*MATα ho*::*LYS2 lys2 ura3 leu2 promURA3*::*tetR*::*GFP-LEU2,tetOx224-URA3 trp1*::*hisG CNM67-3mCherry-NatMX4 srs2-101*::*HphMX his3*::*HIS3p-GFP-TUB1-HIS3*
hAG2153	hAG288 x hAG2016 dissection *sae2Δ(Kan) srs2-101*	*MATa ho*::*LYS2 lys2 ura3 leu2 srs2-101*::*HphMX sae2*::*KanMX6 trp1*::*hisG arg4-nsp,bgl*
hAG2154	hAG288 x hAG2016 dissection *sae2Δ(Kan) srs2-101*	*MATα ho*::*LYS2 lys2 ura3 leu2 srs2-101*::*HphMX sae2*::*KanMX6 trp1*::*hisG arg4-nsp,bgl*
hAG2155	hAG2039 ::(pAG335-LJH025/26) *SRS2*::*pCLB2/srs2-mn*	*MATa ho*::*LYS2 lys2 ura3 leu2*::*hisG his3*::*hisG trp1*::*hisG pCLB2-3HA-SRS2*::*KanMX*
hAG2168	hAG287 x hAG2155 dissection *srs2-mn sae2Δ(Kan)*	*MATa ho*::*LYS2 lys2 ura3 leu2 pCLB2-3HA-SRS2*::*KanMX sae2*::*KanMX6 trp1*::*hisG arg4-nsp,bgl*

Strain Number	Origin *Shortname*	Genotype
hAG2169	hAG287 x hAG2155 dissection *srs2-mn sae2Δ(Kan)*	*MATα ho::LYS2 lys2 ura3 leu2 pCLB2-3HA-SRS2::KanMX sae2::KanMX6 trp1::hisG his3::hisG*
hAG2170	hAG1845 x hAG2155 dissection *srs2-mn*	*MATα ho::LYS2 lys2 ura3 leu2::hisG his3::hisG trp1::hisG pCLB2-3HA-SRS2::KANMX*
hAG2171	hAG1845 x hAG2155 dissection *srs2-mn* SPB	*MATa ho::LYS2 lys2 ura3 leu2::hisG his3::hisG trp1::hisG CNM67-3mCherry-NatMX4 pCLB2-3HA-SRS2::KANMX*
hAG2172	hAG1845 x hAG2155 dissection *srs2-mn* SPB	*MATα ho::LYS2 lys2 ura3 leu2::hisG his3::hisG trp1::hisG CNM67-3mCherry-NatMX4 pCLB2-3HA-SRS2::KANMX*
hAG2173	hAG1845 x hAG2155 dissection *srs2-mn* SPB TUB	*MATa ho::LYS2 lys2 ura3 leu2::hisG trp1::hisG his3::HIS3p-GFP-TUB1-HIS3 CNM67-3mCherry-NatMX4 pCLB2-3HA-SRS2::KANMX*
hAG2174	hAG1845 x hAG2155 dissection *srs2-mn* SPB TUB	*MATα ho::LYS2 lys2 ura3 leu2::hisG trp1::hisG his3::HIS3p-GFP-TUB1-HIS3 CNM67-3mCherry-NatMX4 pCLB2-3HA-SRS2::KANMX*
hAG2177	hAG2147 x hAG2172 dissection *srs2-mn TetO/R* SPB	*MATa ho::LYS2 lys2 ura3 leu2::hisG his3::hisG trp1::hisG CNM67-3mCherry-NatMX4 promURA3::tetR::GFP-LEU2,tetOx224-URA3 pCLB2-3HA-SRS2::KANMX*
hAG2178	hAG2147 x hAG2172 dissection SPB	*MATa ho::LYS2 lys2 ura3 leu2::hisG his3::hisG trp1::hisG CNM67-3mCherry-NatMX4*
hAG2179	hAG2147 x hAG2172 dissection SPB	*MATα ho::LYS2 lys2 ura3 leu2::hisG his3::hisG trp1::hisG CNM67-3mCherry-NatMX4*
hAG2180	hAG2145 x hAG2174 dissection *srs2-mn TetO/R* SPB TUB	*MATa ho::LYS2 lys2 ura3 leu2::hisG trp1::hisG CNM67-3mCherry-NatMX4 his3::HIS3p-GFP-TUB1-HIS3 promURA3::tetR::GFP-LEU2,tetOx224-URA3 pCLB2-3HA-SRS2::KANMX*
hAG2181	hAG2145 x hAG2174 dissection *srs2-mn TetO/R* SPB TUB	*MATα ho::LYS2 lys2 ura3 leu2::hisG trp1::hisG CNM67-3mCherry-NatMX4 his3::HIS3p-GFP-TUB1-HIS3 promURA3::tetR::GFP-LEU2,tetOx224-URA3 pCLB2-3HA-SRS2::KANMX*
hAG2182	hAG2041 x hAG2170 dissection *srs2-mn PK3-RAD51*	*MATa ho::LYS2 lys2 ura3 leu2::hisG his3::hisG trp1::hisG pCLB2-3HA-SRS2::KANMX PK3-RAD51 (Confirmed by PCR)*
hAG2183	hAG2041 x hAG2170 dissection *srs2-mn PK3-RAD51*	*MATα ho::LYS2 lys2 ura3 leu2::hisG his3::hisG trp1::hisG pCLB2-3HA-SRS2::KANMX PK3-RAD51 (Confirmed by PCR)*

Strain Number	Origin *Shortname*	Genotype
hAG2200	hAG287 x hAG2039 dissection *sae2Δ(Kan)*	*MATa ho::LYS2 lys2 ura3 leu2 his3::hisG trp1::hisG arg4-nsp,bgl sae2::KanMX6*
hAG2201	hAG287 x hAG2039 dissection *sae2Δ(Kan)*	*MATα ho::LYS2 lys2 ura3 leu2 his3::hisG trp1::hisG arg4-nsp,bgl sae2::KanMX6*
hAG2202	hAG287 x hAG2039 dissection WT, *leu- his- trp- ura-, arg-*	*MATa ho::LYS2 lys2 ura3 leu2 his3::hisG trp1::hisG arg4-nsp,bgl*
hAG2203	hAG287 x hAG2039 dissection WT, *leu- his- trp- ura-, arg-*	*MATα ho::LYS2 lys2 ura3 leu2 his3::hisG trp1::hisG arg4-nsp,bgl*
hAG2204	hAG707 x hAG2170 dissection *mek1Δ*	*MATa ho::LYS2 lys2 ura3 leu2 mek1::LEU2*
hAG2205	hAG707 x hAG2170 dissection *mek1Δ*	*MATα ho::LYS2 lys2 ura3 leu2 mek1::LEU2 trp1::hisG*
hAG2206	hAG707 x hAG2170 dissection *mek1Δ srs2-mn*	*MATa ho::LYS2 lys2 ura3 leu2 mek1::LEU2 pCLB2-3HA-SRS2::KANMX ade2-bglII trp1::hisG*
hAG2207	hAG707 x hAG2170 dissection *mek1Δ srs2-mn*	*MATα ho::LYS2 lys2 ura3 leu2 mek1::LEU2 pCLB2-3HA-SRS2::KANMX trp1::hisG*
hAG2208	hAG1699 x hAG2039 dissection *dmc1Δ*	*MATa ho::LYS2 lys2 ura3 leu2::hisG trp1::hisG dmc1Δ::KanMX4*
hAG2209	hAG1699 x hAG2039 dissection *dmc1Δ*	*MATα ho::LYS2 lys2 ura3 leu2::hisG his3::hisG dmc1Δ::KanMX4*
hAG2210	hAG1699 x hAG2155 dissection *dmc1Δ srs2-mn*	*MATa ho::LYS2 lys2 ura3 leu2::hisG his3::hisG pCLB2-3HA-SRS2::KanMX dmc1Δ::KanMX4*
hAG2211	hAG1699 x hAG2155 dissection *dmc1Δ srs2-mn hop1*	*MATα ho::LYS2 lys2 ura3 leu2::hisG trp1::hisG pCLB2-3HA-SRS2::KanMX dmc1Δ::KanMX4 hop1Δ::LEU2 hop1-S298A::URA3*
hAG2212	hAG2209 x hAG2155 dissection *dmc1Δ srs2-mn*	*MATα ho::LYS2 lys2 ura3 leu2::hisG his3::hisG trp1::hisG pCLB2-3HA-SRS2::KanMX dmc1Δ::KanMX4*
hAG2221	hAG946 x hAG2155 dissection *srs2-mn spo11-Y135F*	*MATa ho::LYS2 lys2 ura3 leu2::hisG pCLB2-3HA-SRS2::KanMX spo11-Y135F-HA3-His6::KanMX4*
hAG2222	hAG946 x hAG2155 dissection *srs2-mn spo11-Y135F*	*MATα ho::LYS2 lys2 ura3 leu2::hisG his3::hisG trp1::hisG pCLB2-3HA-SRS2::KanMX spo11-Y135F-HA3-His6::KanMX4*
hAG2223	hAG2040::(pBH43-LJH050/051) *sae2Δ(Hyg)*	*MATα ho::LYS2 lys2 ura3 leu2::hisG his3::hisG trp1::hisG sae2Δ::HphMX*
hAG2226	hAG2223 restreaked for health *sae2Δ(Hyg)*	*MATα ho::LYS2 lys2 ura3 leu2::hisG his3::hisG trp1::hisG sae2Δ::HphMX*
hAG2227	hAG2226 x hAG2155 dissection *sae2Δ(Hyg)*	*MATα ho::LYS2 lys2 ura3 leu2::hisG his3::hisG trp1::hisG sae2Δ::HphMX*
hAG2228	hAG2226 x hAG2155 dissection *sae2Δ(Hyg) srs2-mn*	*MATα ho::LYS2 lys2 ura3 leu2::hisG his3::hisG trp1::hisG sae2Δ::HphMX pCLB2-3HA-SRS2::KanMX*
hAG2229	hAG2226 x hAG2155 dissection *sae2Δ(Hyg) srs2-mn*	*MATa ho::LYS2 lys2 ura3 leu2::hisG his3::hisG trp1::hisG sae2Δ::HphMX pCLB2-3HA-SRS2::KanMX*

Strain Number	Origin *Shortname*	Genotype
hAG2234	hAG2170 x hAG316 dissection *rad51Δ*	*MATa ho::lys2 lys2 ura3 leu2::hisG ade2::LK trp1::hisG rad51Δ::HisG-URA3-hisG*
hAG2235	hAG2170 x hAG316 dissection *rad51Δ*	*MATα ho::LYS2 lys2 ura3 leu2::hisG ade2::LK rad51Δ::HisG-URA3-hisG*
hAG2236	hAG2170 x hAG316 dissection *rad51Δ srs2-mn*	*MATa ho::lys2 lys2 ura3 leu2::hisG ade2::LK trp1::hisG rad51Δ::HisG-URA3-hisG pCLB2-3HA-SRS2::KANMX*
hAG2237	hAG2170 x hAG316 dissection *rad51Δ srs2-mn*	*MATα ho::LYS2 lys2 ura3 leu2::hisG rad51Δ::HisG-URA3-hisG pCLB2-3HA-SRS2::KANMX*
hAG2238	hAG2227 x hAG2039 dissection *sae2Δ(Hyg)*	*MATa ho::LYS2 lys2 ura3 leu2::hisG his3::hisG trp1::hisG sae2Δ::HphMX*
hAG2249	hAG2167 x hAG2229 dissection *tel1Δ sae2Δ*	*MATα ho::LYS2 lys2 ura3 leu2 his3::hisG trp1::hisG tel1Δ::HphMX sae2Δ::HphMX*
hAG2250	hAG2167 x hAG2229 dissection *tel1Δ sae2Δ srs2-mn*	*MATa ho::LYS2 lys2 ura3 leu2 his3::hisG trp1::hisG tel1Δ::HphMX sae2Δ::HphMX pCLB2-3HA-SRS2::KanMX*
hAG2251	hAG2167 x hAG2229 dissection *tel1Δ sae2Δ srs2-mn*	*MATα ho::LYS2 lys2 ura3 leu2 his3::hisG trp1::hisG tel1Δ::HphMX sae2Δ::HphMX pCLB2-3HA-SRS2::KanMX*
hAG2264	hAG2159 x hAG2229 dissection *mre11-58S*	*MATa ho::LYS2 lys2 ura3 leu2 his3::hisG trp1::hisG mre11-58S(H213Y confirmed by seq)*
hAG2265	hAG2159 x hAG2229 dissection *mre11-58S*	*MATα ho::LYS2 lys2 ura3 leu2 his3::hisG trp1::hisG mre11-58S(H213Y confirmed by seq)*
hAG2268	hAG2159 x hAG2229 dissection *mre11-58S srs2-mn sae2*	*MATa ho::LYS2 lys2 ura3 leu2 his3::hisG trp1::hisG mre11-58S(H213Y confirmed by seq) pCLB2-3HA-SRS2::KanMX sae2Δ::HphMX*
hAG2269	hAG2159 x hAG2229 dissection *mre11-58S srs2-mn sae2*	*MATα ho::LYS2 lys2 ura3 leu2 his3::hisG trp1::hisG mre11-58S(H213Y confirmed by seq) pCLB2-3HA-SRS2::KanMX sae2Δ::HphMX*
hAG2272	hAG2167 x hAG2229 dissection *tel1Δ*	*MATa ho::LYS2 lys2 ura3 leu2 his3::hisG trp1::hisG tel1Δ::HphMX*
hAG2273	hAG2167 x hAG2229 dissection *tel1Δ*	*MATα ho::LYS2 lys2 ura3 leu2 his3::hisG trp1::hisG tel1Δ::HphMX*
hAG2274	hAG2167 x hAG2229 dissection *tel1Δ srs2-mn*	*MATa ho::LYS2 lys2 ura3 leu2 his3::hisG trp1::hisG tel1Δ::HphMX pCLB2-3HA-SRS2::KanMX*
hAG2275	hAG2167 x hAG2229 dissection *tel1Δ srs2-mn*	*MATα ho::LYS2 lys2 ura3 leu2 his3::hisG trp1::hisG tel1Δ::HphMX pCLB2-3HA-SRS2::KanMX*
hAG2276	dAG1820 dissection *srs2-mn TetO/R* SPB	*MATα ho::LYS2 lys2 ura3 leu2::hisG his3::hisG trp1::hisG CNM67-3mCherry-NatMX4 pCLB2-3HA-SRS2::KANMX promURA3::tetR::GFP-LEU2,tetOx224-URA3*
hAG2277	hAG2161 x hAG2229 dissection *mre11-H125N*	*MATa ho::LYS2 lys2 ura3 leu2 his3::hisG trp1::hisG mre11-H125N (confirmed by seq)*

Strain Number	Origin *Shortname*	Genotype
hAG2278	hAG2161 x hAG2229 dissection *mre11-H125N srs2-mn*	*MATa ho::LYS2 lys2 ura3 leu2 his3::hisG trp1::hisG mre11-H125N (confirmed by seq) pCLB2-3HA-SRS2::KanMX*
hAG2279	hAG2161 x hAG2229 dissection *mre11-H125N srs2-mn*	*MATα ho::LYS2 lys2 ura3 leu2 his3::hisG trp1::hisG mre11-H125N (confirmed by seq) pCLB2-3HA-SRS2::KanMX*
hAG2280	hAG2161 x hAG2229 dissection *mre11-H125N srs2-mn sae2*	*MATα ho::LYS2 lys2 ura3 leu2 his3::hisG trp1::hisG mre11-H125N (confirmed by seq) sae2Δ::HphMX pCLB2-3HA-SRS2::KanMX*
hAG2281	hAG2161 x hAG2229 dissection *mre11-H125N srs2-mn sae2*	*MATα ho::LYS2 lys2 ura3 leu2 his3::hisG trp1::hisG mre11-H125N (confirmed by seq) sae2Δ::HphMX pCLB2-3HA-SRS2::KanMX*
hAG2284	hAG2039::[pKT127 fragment] *RFA1-GFP* WT	*MATa ho::LYS2 lys2 ura3 leu2::hisG his3::hisG trp1::hisG RFA1-GFP::KanMX*
hAG2285	hAG2039::[pBH245 fragment] *RFA1-PK9* WT	*MATa ho::LYS2 lys2 ura3 leu2::hisG his3::hisG trp1::hisG RFA1-PK9::KanMX*
hAG2286	hAG2039::[pBH245 fragment] *RFA1-PK6?* WT	*MATa ho::LYS2 lys2 ura3 leu2::hisG his3::hisG trp1::hisG RFA1-PK?::KanMX (PCR fragment used in transformation should have been PK9 but the checking PCR fragment was 100-200bp too small suggesting some loss of PK repeats)*
hAG2288	hAG2040 x hAG2284 dissection *RFA1-GFP* WT	*MATα ho::LYS2 lys2 ura3 leu2::hisG his3::hisG trp1::hisG RFA1-GFP::KanMX*
hAG2289	hAG2040 x hAG2285 dissection *RFA1-PK9* WT	*MATα ho::LYS2 lys2 ura3 leu2::hisG his3::hisG trp1::hisG RFA1-PK9::KanMX*
hAG2290	hAG2170 x hAG2285 dissection *RFA1-PK9 srs2-mn*	*MATa ho::LYS2 lys2 ura3 leu2::hisG his3::hisG trp1::hisG RFA1-PK9::KanMX pCLB2-3HA-SRS2::KANMX*
hAG2291	hAG2170 x hAG2285 dissection *RFA1-PK9 srs2-mn*	*MATα ho::LYS2 lys2 ura3 leu2::hisG his3::hisG trp1::hisG RFA1-PK9::KanMX pCLB2-3HA-SRS2::KANMX*
hAG2292	hAG2228 x hAG2284 dissection *RFA1-GFP srs2-mn*	*MATa ho::LYS2 lys2 ura3 leu2::hisG his3::hisG trp1::hisG RFA1-GFP::KanMX pCLB2-3HA-SRS2::KANMX*
hAG2293	hAG2228 x hAG2284 dissection *RFA1-GFP srs2-mn*	*MATα ho::LYS2 lys2 ura3 leu2::hisG his3::hisG trp1::hisG RFA1-GFP::KanMX pCLB2-3HA-SRS2::KANMX*
hAG2294	hAG2228 x hAG2284 dissection *RFA1-GFP srs2-mn sae2*	*MATa ho::LYS2 lys2 ura3 leu2::hisG his3::hisG trp1::hisG RFA1-GFP::KanMX pCLB2-3HA-SRS2::KANMX sae2Δ::HphMX*
hAG2295	hAG2228 x hAG2284 dissection *RFA1-GFP srs2-mn sae2*	*MATα ho::LYS2 lys2 ura3 leu2::hisG his3::hisG trp1::hisG RFA1-GFP::KanMX pCLB2-3HA-SRS2::KANMX sae2Δ::HphMX*
hAG2299	hAG1688 x hAG2155 dissection *ndt80Δ srs2-mn*	*MATa ho::LYS2 lys2 ura3 leu2::hisG arg4Δ(eco47III-hpaI) trp1::hisG his3::hisG ndt80Δ(Eco47III-BseRI)::KanMX6 pCLB2-3HA-SRS2::KanMX*

Strain Number	Origin *Shortname*	Genotype
hAG2300	hAG1688 x hAG2155 dissection *ndt80Δ srs2-mn*	*MATα ho::LYS2 lys2 ura3 arg4Δ(eco47III-hpaI) leu2::hisG ndt80Δ(Eco47III-BseRI)::KanMX6 pCLB2-3HA-SRS2::KanMX*
hAG2301	hAG1688 x hAG2039 dissection *ndt80Δ*	*MATa ho::LYS2 lys2 ura3 leu2::hisG trp1::hisG arg4Δ(eco47III-hpaI) ndt80Δ(Eco47III-BseRI)::KanMX6*
hAG2302	hAG1688 x hAG2039 dissection *ndt80Δ*	*MATα ho::LYS2 lys2 ura3 ndt80Δ(Eco47III-BseRI)::KanMX6*
hAG2305	hAG2040 x hAG2284 dissection RFA1-GFP WT	*MATa ho::LYS2 lys2 ura3 leu2::hisG his3::hisG trp1::hisG RFA1-GFP::KanMX*
hAG2306	hAG2040 x hAG2284 dissection *RFA1-GFP WT*	*MATα ho::LYS2 lys2 ura3 leu2::hisG his3::hisG trp1::hisG RFA1-GFP::KanMX*
hAG2309	hAG2039 x hAG2267 dissection *srs2-mn mre11-58S*	*MATa ho::LYS2 lys2 ura3 leu2 his3::hisG trp1::hisG mre11-58S(H213Y confirmed by seq) pCLB2-3HA-SRS2::KanMX*
hAG2310	hAG2039 x hAG2267 dissection *srs2-mn mre11-58S*	*MATα ho::LYS2 lys2 ura3 leu2 his3::hisG trp1::hisG mre11-58S(H213Y confirmed by seq) pCLB2-3HA-SRS2::KanMX*
hAG2344	hAG2285 x hAG2227 dissection *RFA1-PK9 sae2Δ*	*MATa ho::LYS2 lys2 ura3 leu2::hisG his3::hisG trp1::hisG RFA1-PK9::KanMX sae2Δ::HphMX*
hAG2345	hAG2285 x hAG2227 dissection *RFA1-PK9 sae2Δ*	*MATα ho::LYS2 lys2 ura3 leu2::hisG his3::hisG trp1::hisG RFA1-PK9::KanMX sae2Δ::HphMX*
hAG2346	hAG2284 x hAG2227 dissection *RFA1-GFP sae2Δ*	*MATa ho::LYS2 lys2 ura3 leu2::hisG his3::hisG trp1::hisG RFA1-GFP::KanMX sae2Δ::HphMX*
hAG2347	hAG2284 x hAG2227 dissection *RFA1-GFP sae2Δ*	*MATα ho::LYS2 lys2 ura3 leu2::hisG his3::hisG trp1::hisG RFA1-GFP::KanMX sae2Δ::HphMX*
hAG2348	hAG2305 x hAG2227 dissection *RFA1-GFP sae2Δ*	*MATa ho::LYS2 lys2 ura3 leu2::hisG his3::hisG trp1::hisG RFA1-GFP::KanMX sae2Δ::HphMX*
hAG2349	hAG2305 x hAG2227 dissection *RFA1-GFP sae2Δ*	*MATα ho::LYS2 lys2 ura3 leu2::hisG his3::hisG trp1::hisG RFA1-GFP::KanMX sae2Δ::HphMX*
hAG2350	hAG946 x hAG2238 dissection *spo11-Y135F sae2Δ*	*MATa ho::LYS2 lys2 ura3 leu2::hisG trp1::hisG spo11-Y135F-HA3-His6::KanMX4 sae2Δ::HphMX*
hAG2351	hAG946 x hAG2238 dissection *spo11-Y135F sae2Δ*	*MATα ho::LYS2 lys2 ura3 leu2::hisG spo11-Y135F-HA3-His6::KanMX4 sae2Δ::HphMX*

A.1.6 Plasmids, stored in *E. coli* Strains

Strain Number	Origin *Shortname*	Description
pAG468 in DH5α	YCplac33::(Overlapped PCR [WT Genomic, LJH002/006] x [WT Genomic, LJH005/007) *RAD51 Section for Tagging*	[Rad51 Promoter region & N-terminal section (PstI - EcoRI), KpnI site after ATG, silent mutation at the gRNA target of pAG469] inserted into YCplac33, URA3, AmpR
Pag469 in DH5α	pBH257::(Annealed LJH003/LJH004) *RAD51-Targeting Cas9*	[gRNA sequence targeting Rad51 N-terminal region] inserted into a Cas9/CRISPR plasmid, LEU, AmpR
pAG470 in DH5α	pAG468::(KpnI digested pBH150) *PK3-RAD51*	[Rad51 Promoter region & N-terminal section (PstI - EcoRI), PK3-Tag after ATG, silent mutation at the gRNA target of pAG469] inserted into YCplac33, URA3, AmpR
pAG471 in DH5α	YEplac195::(WT Genomic, LJH030/031) *RAD51-OE*	[Rad51 inc. promoter & terminator regions (PstI-KpnI)] inserted into YEplac195, URA3, AmpR
pAG472 in XL1-Blue	YEplac195::(WT Genomic, LJH037/042) *Meiotic Only OE Vector*	[pIME2 region (SphI-BamHI)] inserted into YEplac195, URA3, AmpR
pAG473 in XL1-Blue	pAG472::(WT Genomic, LJH040/041) *Meiotic Only RAD51-OE*	[pIME2::RAD51 plus RAD51 terminator region (SphI-KpnI)] inserted into YEplac195, URA3, AmpR
pAG474 in XL1-Blue	pAG468::(pKT127, LJH043/044) *GFP-RAD51*	[Rad51 Promoter region & N-terminal section (PstI - EcoRI), GFP after ATG, silent mutation at the gRNA target of pAG469] inserted into YCplac33, URA3, AmpR

A.2 Primers Generated during this Study

All primers were generated by MWG Eurofins. Primers were shipped in a lyophilised format and resuspended in ddH_2O upon arrival, storing at -20°C.

Primer Number	Name	Sequence (5' → 3')
LJH001	Rad51F_Kpn1	GAGAGAGGTACCTCTCAAGTTCAAGAACAACATATATC
LJH002	Rad51R_Pst1	GAGAGACTGCAGTTTAGCAACTTATCTGCCTTAG
LJH003	Rad51Cas9F	ATCGCCACCATCGCCGGAGCCGT
LJH004	Rad51Cas9R	AACACGGCTCCGGCGATGGTGGC
LJH005	Rad51mutF	CATCGCCGGAGCCGTTAGTGGCCTCAATATCTTCG
LJH006	Rad51mutR	CGAAGATATTGAGGCCACTAACGGCTCCGGCGATG
LJH007	Rad51proF_EcoR1	GAGAGAGAATTCGTCGATACAGCCGATTAGGTCG
LJH008	Rad51proR_Kpn1	GAGAGAGGTACCCATATGACGATAACAAATTAGTAG
LJH009	PK3Check_For	GCAGACGTAGTTATTTGTTAAAGGC
LJH010	PK3Check_Rev	TCGTATGCTTCATCCTCCATTTCAC
LJH011	PK3Check_1KB_Rev	TTGGTTAGTAACGACGACTGCAACA
LJH012	PK3andCas9_CHK	GTTTAGCAACTTATCTGCCTTAG
LJH013	SRS2ChroKantagF	CGAAAAAAAAGTCAAAATTAAACAACGGTGAAATCATAGTC ATCGATTAGGGCGCGCCACTTCTAAATAAGCG
LJH014	SRS2ChroKantagR	AAATTATAAACCGCCTCCAATAGTTGACGTAGTCAGGCATGA AAGTGCTACATCGATGAATTCGAGCTCG
LJH015	Clb2proseq1	TCATTCGCTCGTTTGTCAG
LJH016	Clb2proseq2	TAATACTCTGTATAGATCG
LJH017	SRS2intF	GATGACACTACAGTTGACAATCG
LJH018	SRS2intR	TATGGACAATACTGTTGATGGTG
LJH019	Rad51overR	GTTTAGCAACTTATCTGCCTTAG
LJH020	Rad51overF	AGGTATATCGGAAGCTAAGGCAG
LJH021	Rad61proF_NotI	GAGAGAGCGGCCGCAAGAAACGCACTCTACTTCG
LJH022	Rad51TerR_BamH1	GAGAGAGGATCCATCGCATCCTCACCAATAG
LJH023	Rad51TerF_HindII	AGAGAGAAGCTTACGAGTAGGTATTTGGTCTCTTG
LJH024	Rad51TerF_SalI	GAGAGAGTCGACCAGTATTGACGAACTTCTGG
LJH025	Srs2Clb2ptagF	GAGTATCATTCCAATTTGATCTTTCTTCTACCGGTACTTAGGG ATAGCAATCGATGAATTCGAGCTCG
LJH026	Srs2Clb2ptagR	GTATTTAACTGGGATACTAAATGCAACCAAAGATCATTGTTC GACGACATGCACTGAGCAGCGTAATCTG
LJH027	Srs2intR	TCTTTCTGTAGATCCACCAAGTG
LJH028	Rad51TerR2_BamH1	GAGAGAGGATCCTGCAGGAGGAAGTAGTCATCG
LJH029	Rad51ProF_PstI	agagCTGCAGAGAAACGCACTCTACTTCG
LJH030	Rad51TerR_forPst	TAAGAGGATGGCGACATATCAG
LJH031	Rad51ProF_KpnI	agagGGTACCAGAAACGCACTCTACTTCG
LJH032	IMEOverlap1IMEPF	agagagaGGTACCTGTATAGCCTATCGGTTATTCGATC

Primer Number	Name	Sequence (5' → 3')
LJH033	IMEOverlap2IMEPR	TGTTCTTGAACTTGAGACATAAATGACCTATTAAGTTAAGCTTAGTACTCTTCTTTTATTACG
LJH034	IMEOverlap3Rad51	GCTTAACTTAATAGGTCATTTATGTCTCAAGTTCAAGAACAACATATATCAGAGTCACAG
LJH035	IME2CheckPIME	CATCAGGCGCCATTCGCCATTCAGG
LJH036	IME2CheckRad51	ATTAAGGTAGCAACTCACCGGTCTG
LJH037	IMEProF_SphI	agagagaGCATGCTGTATAGCCTATCGGTTATTCGATC
LJH038	IMEProR_SalI	agagagaGTCGACAAATGACCTATTAAGTTAAGCTTAGTAC
LJH039	Rad51CodF_SalI	AGAGAGAGTCGACATGTCTCAAGTTCAAGAACAACATATATCAG
LJH040	Rad51TerR_KpnI	agagagaGGTACCAACCGTACTTCTCTTGCTGTTAG
LJH041	Rad51CodF_BamHI	agagagaGGATCCATGTCTCAAGTTCAAGAACAACATATATCAG
LJH042	IMEProR_BamHI	agagagaGGATCCAAATGACCTATTAAGTTAAGCTTAGTAC
LJH043	pKT127GFP-KpnF	gagagaGGTACCatgtctaaaggtgaagaattattcac
LJH044	pKT127GFP-KpnR	gagagaGGTACCttatttgtacaattcatccatacc
LJH045	ZIPGFPCheck_Rev	CTATTTGTATAGTTCATC
LJH046	ZIPGFPCheck_For	ATGAGTAAAGGAGAA
LJH047	PK3atRAD51Chk_F	CATATGGGTACCGGTATTCCTAACC
LJH048	GFP_For	AGTAAAGGAGAAGAACTTTTCAC
LJH049	GFP_Rev	CTATTTGTATAGTTCATCCATGC
LJH050	sae::HygF	ATACCTGCATTTCCATCCATGCTGTAAGCCATTAGGTGTTTGTATGTGAGGGCGCGCCACTTCTAAATAAGCG
LJH051	sae::HygR	AAAATGTATTTGAAGTAATGAATAAAGAATGATGATCGCTGGCGTCATCGATGAATTCGAGCTCG
LJH052	SAE2upstrF	CACCATTCGAGTCTTGAGAACAACTTT
LJH053	HygChkIntR	GAGAGCCTGCGCGACGGACGCACTGAC
LJH054	telUpstrHphChk	ATCACATGATATTATGAGCGTGATAG
LJH055	HygInt_OppTel	ACACTACATGGCGTGATTTCATATGC
LJH056	HygInt_SameTel	GCATATGAAATCACGCCATGTAGTGT
LJH057	MRE11_For	GAGATTATGTTGCATGGGTGACAAG
LJH058	MRE11_Rev	AGCTACAGATGAACCTGGTTGTAATAC
LJH059	RFAChrGFP_F	GGGCTGAAGCCGACTATCTTGCCGATGAGTTATCCAAGGCTTTGTTAGCTGGTGACGGTGCTGGTTTA
LJH060	RFAChrGFP_R	TTTCTCATATGTTACATAGATTAAATAGTACTTGATTATTTGATACATTATCGATGAATTCGAGCTCG
LJH061	RFAChrPK_F	GGGCTGAAGCCGACTATCTTGCCGATGAGTTATCCAAGGCTTTGTTAGCTTCCGGTTCTGCTGCTAGAG
LJH062	RFAChrPK_R	TTTCTCATATGTTACATAGATTAAATAGTACTTGATTATTTGATACATTAAGGCCAGAAGACTAAGAGGT
LJH063	RFA1TagChkF	AGCAAGCCCTTGATTTCAACCTTCCTGAAG

References

Allers, T., and Lichten, M. (2001). Differential timing and control of noncrossover and crossover recombination during meiosis. Cell *106*, 47-57.

Anand, R.P., Shah, K.A., Niu, H., Sung, P., Mirkin, S.M., and Freudenreich, C.H. (2012). Overcoming natural replication barriers: differential helicase requirements. Nucleic Acids Res *40*, 1091-1105.

Andersen, S.L., and Sekelsky, J. (2010). Meiotic versus mitotic recombination: two different routes for double-strand break repair: the different functions of meiotic versus mitotic DSB repair are reflected in different pathway usage and different outcomes. Bioessays *32*, 1058-1066.

Antony, E., Tomko, E.J., Xiao, Q., Krejci, L., Lohman, T.M., and Ellenberger, T. (2009). Srs2 disassembles Rad51 filaments by a protein-protein interaction triggering ATP turnover and dissociation of Rad51 from DNA. Mol Cell *35*, 105-115.

Arenson, T.A., Tsodikov, O.V., and Cox, M.M. (1999). Quantitative analysis of the kinetics of end-dependent disassembly of RecA filaments from ssDNA. J Mol Biol *288*, 391-401.

Bae, K.H., Kim, H.S., Bae, S.H., Kang, H.Y., Brill, S., and Seo, Y.S. (2003). Bimodal interaction between replication-protein A and Dna2 is critical for Dna2 function both in vivo and in vitro. Nucleic Acids Res *31*, 3006-3015.

Bailly, V., Lauder, S., Prakash, S., and Prakash, L. (1997). Yeast DNA repair proteins Rad6 and Rad18 form a heterodimer that has ubiquitin conjugating, DNA binding, and ATP hydrolytic activities. J Biol Chem *272*, 23360-23365.

Barber, L.J., Youds, J.L., Ward, J.D., McIlwraith, M.J., O'Neil, N.J., Petalcorin, M.I., Martin, J.S., Collis, S.J., Cantor, S.B., Auclair, M., *et al.* (2008). RTEL1 maintains genomic stability by suppressing homologous recombination. Cell *135*, 261-271.

Bernstein, K.A., Reid, R.J., Sunjevaric, I., Demuth, K., Burgess, R.C., and Rothstein, R. (2011). The Shu complex, which contains Rad51 paralogues, promotes DNA repair through inhibition of the Srs2 anti-recombinase. Mol Biol Cell *22*, 1599-1607.

Bhattacharyya, S., and Lahue, R.S. (2004). Saccharomyces cerevisiae Srs2 DNA helicase selectively blocks expansions of trinucleotide repeats. Mol Cell Biol *24*, 7324-7330.

Bishop, D.K. (1994). Reca Homologs Dmc1 and Rad51 Interact to Form Multiple Nuclear-Complexes Prior to Meiotic Chromosome Synapsis. Cell *79*, 1081-1092.

Bishop, D.K., Park, D., Xu, L., and Kleckner, N. (1992). DMC1: a meiosis-specific yeast homolog of E. coli recA required for recombination, synaptonemal complex formation, and cell cycle progression. Cell *69*, 439-456.

Brandsma, I., and Gent, D.C. (2012). Pathway choice in DNA double strand break repair: observations of a balancing act. Genome Integr *3*, 9.

Brill, S.J., and Stillman, B. (1991). Replication factor-A from Saccharomyces cerevisiae is encoded by three essential genes coordinately expressed at S phase. Genes Dev *5*, 1589-1600.

Brown, M.S., Grubb, J., Zhang, A., Rust, M.J., and Bishop, D.K. (2015). Small Rad51 and Dmc1 Complexes Often Co-occupy Both Ends of a Meiotic DNA Double Strand Break. PLoS Genet *11*, e1005653.

Bugreev, D.V., Yu, X., Egelman, E.H., and Mazin, A.V. (2007). Novel pro- and anti-recombination activities of the Bloom's syndrome helicase. Genes Dev *21*, 3085-3094.

Burgess, R.C., Lisby, M., Altmannova, V., Krejci, L., Sung, P., and Rothstein, R. (2009). Localization of recombination proteins and Srs2 reveals anti-recombinase function in vivo. J Cell Biol *185*, 969-981.

Burkovics, P., Dome, L., Juhasz, S., Altmannova, V., Sebesta, M., Pacesa, M., Fugger, K., Sorensen, C.S., Lee, M.Y., Haracska, L.*, et al.* (2016). The PCNA-associated protein PARI negatively regulates homologous recombination via the inhibition of DNA repair synthesis. Nucleic Acids Res *44*, 3176-3189.

Burkovics, P., Sebesta, M., Sisakova, A., Plault, N., Szukacsov, V., Robert, T., Pinter, L., Marini, V., Kolesar, P., Haracska, L., *et al.* (2013). Srs2 mediates PCNA-SUMO-dependent inhibition of DNA repair synthesis. EMBO J *32*, 742-755.

Busygina, V., Sehorn, M.G., Shi, I.Y., Tsubouchi, H., Roeder, G.S., and Sung, P. (2008). Hed1 regulates Rad51-mediated recombination via a novel mechanism. Genes Dev *22*, 786-795.

Byers, B., and Goetsch, L. (1975). Behavior of spindles and spindle plaques in the cell cycle and conjugation of Saccharomyces cerevisiae. J Bacteriol *124*, 511-523.

Cannavo, E., and Cejka, P. (2014). Sae2 promotes dsDNA endonuclease activity within Mre11-Rad50-Xrs2 to resect DNA breaks. Nature *514*, 122-125.

Cartagena-Lirola, H., Guerini, I., Viscardi, V., Lucchini, G., and Longhese, M.P. (2006). Budding Yeast Sae2 is an In Vivo Target of the Mec1 and Tel1 Checkpoint Kinases During Meiosis. Cell Cycle *5*, 1549-1559.

Carter, S.D., Vigasova, D., Chen, J., Chovanec, M., and Astrom, S.U. (2009). Nej1 recruits the Srs2 helicase to DNA double-strand breaks and supports repair by a single-strand annealing-like mechanism. Proc Natl Acad Sci U S A *106*, 12037-12042.

Cassani, C., Gobbini, E., Wang, W., Niu, H., Clerici, M., Sung, P., and Longhese, M.P. (2016). Tel1 and Rif2 Regulate MRX Functions in End-Tethering and Repair of DNA Double-Strand Breaks. PLoS Biol *14*, e1002387.

Ceballos, S.J., and Heyer, W.D. (2011). Functions of the Snf2/Swi2 family Rad54 motor protein in homologous recombination. Biochim Biophys Acta *1809*, 509-523.

Cejka, P., Cannavo, E., Polaczek, P., Masuda-Sasa, T., Pokharel, S., Campbell, J.L., and Kowalczykowski, S.C. (2010). DNA end resection by Dna2-Sgs1-RPA and its stimulation by Top3-Rmi1 and Mre11-Rad50-Xrs2. Nature *467*, 112-116.

Cejka, P., Plank, J.L., Dombrowski, C.C., and Kowalczykowski, S.C. (2012). Decatenation of DNA by the S. cerevisiae Sgs1-Top3-Rmi1 and RPA complex: a mechanism for disentangling chromosomes. Mol Cell *47*, 886-896.

Cha, R.S., Weiner, B.M., Keeney, S., Dekker, J., and Kleckner, N. (2000). Progression of meiotic DNA replication is modulated by interchromosomal interaction proteins, negatively by Spo11p and positively by Rec8p. Genes Dev *14*, 493-503.

Chavdarova, M., Marini, V., Sisakova, A., Sedlackova, H., Vigasova, D., Brill, S.J., Lisby, M., and Krejci, L. (2015). Srs2 promotes Mus81-Mms4-mediated resolution of recombination intermediates. Nucleic Acids Res *43*, 3626-3642.

Chen, H., Donnianni, R.A., Handa, N., Deng, S.K., Oh, J., Timashev, L.A., Kowalczykowski, S.C., and Symington, L.S. (2015). Sae2 promotes DNA damage resistance by removing the Mre11-Rad50-Xrs2 complex from DNA and attenuating Rad53 signaling. Proc Natl Acad Sci U S A *112*, E1880-1887.

Chen, H., Lisby, M., and Symington, L.S. (2013). RPA coordinates DNA end resection and prevents formation of DNA hairpins. Mol Cell *50*, 589-600.

Chi, P., San Filippo, J., Sehorn, M.G., Petukhova, G.V., and Sung, P. (2007). Bipartite stimulatory action of the Hop2-Mnd1 complex on the Rad51 recombinase. Genes Dev *21*, 1747-1757.

Chiolo, I., Carotenuto, W., Maffioletti, G., Petrini, J.H., Foiani, M., and Liberi, G. (2005). Srs2 and Sgs1 DNA helicases associate with Mre11 in different subcomplexes following checkpoint activation and CDK1-mediated Srs2 phosphorylation. Mol Cell Biol *25*, 5738-5751.

Chiolo, I., Saponaro, M., Baryshnikova, A., Kim, J.H., Seo, Y.S., and Liberi, G. (2007). The human F-Box DNA helicase FBH1 faces Saccharomyces cerevisiae Srs2 and postreplication repair pathway roles. Mol Cell Biol *27*, 7439-7450.

Chou, T.-C. (2014). The Molecular Role of the Saccharomyces cerevisiae DNA Helicase Srs2 during Meiosis. In Molecular Biology & Biotechnology (University of Sheffield).

Chu, S., and Herskowitz, I. (1998). Gametogenesis in yeast is regulated by a transcriptional cascade dependent on Ndt80. Mol Cell *1*, 685-696.

Clerici, M., Mantiero, D., Lucchini, G., and Longhese, M.P. (2006). The Saccharomyces cerevisiae Sae2 protein negatively regulates DNA damage checkpoint signalling. EMBO Rep *7*, 212-218.

Clift, D., and Marston, A.L. (2011). The role of shugoshin in meiotic chromosome segregation. Cytogenet Genome Res *133*, 234-242.

Cloud, V., Chan, Y.L., Grubb, J., Budke, B., and Bishop, D.K. (2012). Rad51 is an accessory factor for Dmc1-mediated joint molecule formation during meiosis. Science *337*, 1222-1225.

Cobb, J.A., Bjergbaek, L., and Gasser, S.M. (2002). RecQ helicases: at the heart of genetic stability. FEBS Lett *529*, 43-48.

Cooper, T.J., Garcia, V., and Neale, M.J. (2016). Meiotic DSB patterning: A multifaceted process. Cell Cycle *15*, 13-21.

Cromie, G.A., and Smith, G.R. (2007). Branching out: meiotic recombination and its regulation. Trends Cell Biol *17*, 448-455.

de la Torre-Ruiz, M.A., Green, C.M., and Lowndes, N.F. (1998). RAD9 and RAD24 define two additive, interacting branches of the DNA damage checkpoint pathway in budding yeast normally required for Rad53 modification and activation. EMBO J *17*, 2687-2698.

De Muyt, A., Jessop, L., Kolar, E., Sourirajan, A., Chen, J., Dayani, Y., and Lichten, M. (2012). BLM helicase ortholog Sgs1 is a central regulator of meiotic recombination intermediate metabolism. Mol Cell *46*, 43-53.

De Tullio, L., Kaniecki, K., Kwon, Y., Crickard, J.B., Sung, P., and Greene, E.C. (2017). Yeast Srs2 Helicase Promotes Redistribution of Single-Stranded DNA-Bound RPA and Rad52 in Homologous Recombination Regulation. Cell Rep *21*, 570-577.

Debrauwere, H., Loeillet, S., Lin, W., Lopes, J., and Nicolas, A. (2001). Links between replication and recombination in Saccharomyces cerevisiae: a hypersensitive requirement for homologous recombination in the absence of Rad27 activity. Proc Natl Acad Sci U S A *98*, 8263-8269.

Dupaigne, P., Le Breton, C., Fabre, F., Gangloff, S., Le Cam, E., and Veaute, X. (2008). The Srs2 helicase activity is stimulated by Rad51 filaments on dsDNA: implications for crossover incidence during mitotic recombination. Mol Cell *29*, 243-254.

Duro, E., and Marston, A.L. (2015). From equator to pole: splitting chromosomes in mitosis and meiosis. Genes Dev *29*, 109-122.

Elango, R., Sheng, Z., Jackson, J., DeCata, J., Ibrahim, Y., Pham, N.T., Liang, D.H., Sakofsky, C.J., Vindigni, A., Lobachev, K.S.*, et al.* (2017). Break-induced replication promotes formation of lethal joint molecules dissolved by Srs2. Nat Commun *8*, 1790.

Ellis, N.A., Sander, M., Harris, C.C., and Bohr, V.A. (2008). Bloom's syndrome workshop focuses on the functional specificities of RecQ helicases. Mech Ageing Dev *129*, 681-691.

Esta, A., Ma, E., Dupaigne, P., Maloisel, L., Guerois, R., Le Cam, E., Veaute, X., and Coic, E. (2013). Rad52 sumoylation prevents the toxicity of unproductive Rad51 filaments independently of the anti-recombinase Srs2. PLoS Genet *9*, e1003833.

Ferrari, S.R., Grubb, J., and Bishop, D.K. (2009). The Mei5-Sae3 protein complex mediates Dmc1 activity in Saccharomyces cerevisiae. J Biol Chem *284*, 11766-11770.

Fornander, L.H., Frykholm, K., Fritzsche, J., Araya, J., Nevin, P., Werner, E., Cakir, A., Persson, F., Garcin, E.B., Beuning, P.J.*, et al.* (2016). Visualizing the Nonhomogeneous Structure of RAD51 Filaments Using Nanofluidic Channels. Langmuir *32*, 8403-8412.

Fox, C., Zou, J., Rappsilber, J., and Marston, A.L. (2017). Cdc14 phosphatase directs centrosome re-duplication at the meiosis I to meiosis II transition in budding yeast. Wellcome Open Res *2*, 2.

Fukunaga, K., Kwon, Y., Sung, P., and Sugimoto, K. (2011). Activation of protein kinase Tel1 through recognition of protein-bound DNA ends. Mol Cell Biol *31*, 1959-1971.

Galkin, V.E., Wu, Y., Zhang, X.P., Qian, X., He, Y., Yu, X., Heyer, W.D., Luo, Y., and Egelman, E.H. (2006). The Rad51/RadA N-terminal domain activates nucleoprotein filament ATPase activity. Structure *14*, 983-992.

Gao, J., and Colaiacovo, M.P. (2018). Zipping and Unzipping: Protein Modifications Regulating Synaptonemal Complex Dynamics. Trends Genet *34*, 232-245.

Gasior, S.L., Wong, A.K., Kora, Y., Shinohara, A., and Bishop, D.K. (1998). Rad52 associates with RPA and functions with rad55 and rad57 to assemble meiotic recombination complexes. Genes Dev *12*, 2208-2221.

Gobbini, E., Cassani, C., Villa, M., Bonetti, D., and Longhese, M.P. (2016). Functions and regulation of the MRX complex at DNA double-strand breaks. Microb Cell *3*, 329-337.

Godin, S.K., Meslin, C., Kabbinavar, F., Bratton-Palmer, D.S., Hornack, C., Mihalevic, M.J., Yoshida, K., Sullivan, M., Clark, N.L., and Bernstein, K.A. (2015). Evolutionary and functional analysis of the invariant SWIM domain in the conserved Shu2/SWS1 protein family from Saccharomyces cerevisiae to Homo sapiens. Genetics *199*, 1023-1033.

Gossen, M., and Bujard, H. (1992). Tight control of gene expression in mammalian cells by tetracycline-responsive promoters. Proc Natl Acad Sci U S A *89*, 5547-5551.

Gray, S., and Cohen, P.E. (2016). Control of Meiotic Crossovers: From Double-Strand Break Formation to Designation. Annu Rev Genet *50*, 175-210.

Haber, J.E. (2002). Uses and abuses of HO endonuclease. Methods Enzymol *350*, 141-164.

Haber, J.E. (2012). Mating-type genes and MAT switching in Saccharomyces cerevisiae. Genetics *191*, 33-64.

Hassold, T., and Hunt, P. (2001). To err (meiotically) is human: the genesis of human aneuploidy. Nat Rev Genet *2*, 280-291.

Hayase, A., Takagi, M., Miyazaki, T., Oshiumi, H., Shinohara, M., and Shinohara, A. (2004). A protein complex containing Mei5 and Sae3 promotes the assembly of the meiosis-specific RecA homolog Dmc1. Cell *119*, 927-940.

Hays, S.L., Firmenich, A.A., Massey, P., Banerjee, R., and Berg, P. (1998). Studies of the interaction between Rad52 protein and the yeast single-stranded DNA binding protein RPA. Mol Cell Biol *18*, 4400-4406.

Hegde, V., and Klein, H. (2000). Requirement for the SRS2 DNA helicase gene in non-homologous end joining in yeast. Nucleic Acids Res *28*, 2779-2783.

Heude, M., Chanet, R., and Fabre, F. (1995). Regulation of the Saccharomyces cerevisiae Srs2 helicase during the mitotic cell cycle, meiosis and after irradiation. Mol Gen Genet *248*, 59-68.

Heyting, C. (1996). Synaptonemal complexes: structure and function. Curr Opin Cell Biol *8*, 389-396.

Hirano, Y., Fukunaga, K., and Sugimoto, K. (2009). Rif1 and rif2 inhibit localization of tel1 to DNA ends. Mol Cell *33*, 312-322.

Holzen, T.M., Shah, P.P., Olivares, H.A., and Bishop, D.K. (2006). Tid1/Rdh54 promotes dissociation of Dmc1 from nonrecombinogenic sites on meiotic chromatin. Genes Dev *20*, 2593-2604.

Hong, E.J., and Roeder, G.S. (2002). A role for Ddc1 in signaling meiotic double-strand breaks at the pachytene checkpoint. Genes Dev *16*, 363-376.

Honigberg, S.M., and Purnapatre, K. (2003). Signal pathway integration in the switch from the mitotic cell cycle to meiosis in yeast. J Cell Sci *116*, 2137-2147.

Hopfner, K.P., Craig, L., Moncalian, G., Zinkel, R.A., Usui, T., Owen, B.A., Karcher, A., Henderson, B., Bodmer, J.L., McMurray, C.T., *et al.* (2002). The Rad50 zinc-hook is a structure joining Mre11 complexes in DNA recombination and repair. Nature *418*, 562-566.

Hopfner, K.P., Karcher, A., Craig, L., Woo, T.T., Carney, J.P., and Tainer, J.A. (2001). Structural biochemistry and interaction architecture of the DNA double-strand break repair Mre11 nuclease and Rad50-ATPase. Cell *105*, 473-485.

Huang, M.E., de Calignon, A., Nicolas, A., and Galibert, F. (2000). POL32, a subunit of the Saccharomyces cerevisiae DNA polymerase delta, defines a link between DNA replication and the mutagenic bypass repair pathway. Curr Genet *38*, 178-187.

Huertas, P., Cortes-Ledesma, F., Sartori, A.A., Aguilera, A., and Jackson, S.P. (2008). CDK targets Sae2 to control DNA-end resection and homologous recombination. Nature *455*, 689-692.

Hulme, L. (2009). The Roles of Tel1, Srs2 and Rad6 During Meiotic DSB Repair. In Department of Molecular Biology & Biotechnology (University of Sheffield).

Humphryes, N., and Hochwagen, A. (2014). A non-sister act: recombination template choice during meiosis. Exp Cell Res *329*, 53-60.

Ira, G., Malkova, A., Liberi, G., Foiani, M., and Haber, J.E. (2003). Srs2 and Sgs1-Top3 suppress crossovers during double-strand break repair in yeast. Cell *115*, 401-411.

Jasin, M., and Rothstein, R. (2013). Repair of strand breaks by homologous recombination. Cold Spring Harb Perspect Biol *5*, a012740.

Jaspersen, S.L., Huneycutt, B.J., Giddings, T.H., Jr., Resing, K.A., Ahn, N.G., and Winey, M. (2004). Cdc28/Cdk1 regulates spindle pole body duplication through phosphorylation of Spc42 and Mps1. Dev Cell *7*, 263-274.

Kaliraman, V., Mullen, J.R., Fricke, W.M., Bastin-Shanower, S.A., and Brill, S.J. (2001). Functional overlap between Sgs1-Top3 and the Mms4-Mus81 endonuclease. Genes Dev *15*, 2730-2740.

Kamath-Loeb, A.S., Johansson, E., Burgers, P.M., and Loeb, L.A. (2000). Functional interaction between the Werner Syndrome protein and DNA polymerase delta. Proc Natl Acad Sci U S A *97*, 4603-4608.

Kang, H.A., Shin, H.C., Kalantzi, A.S., Toseland, C.P., Kim, H.M., Gruber, S., Peraro, M.D., and Oh, B.H. (2015). Crystal structure of Hop2-Mnd1 and mechanistic insights into its role in meiotic recombination. Nucleic Acids Res *43*, 3841-3856.

Kaniecki, K., De Tullio, L., Gibb, B., Kwon, Y., Sung, P., and Greene, E.C. (2017). Dissociation of Rad51 Presynaptic Complexes and Heteroduplex DNA Joints by Tandem Assemblies of Srs2. Cell Rep *21*, 3166-3177.

Keeney, S., Giroux, C.N., and Kleckner, N. (1997). Meiosis-specific DNA double-strand breaks are catalyzed by Spo11, a member of a widely conserved protein family. Cell *88*, 375-384.

Keyamura, K., Arai, K., and Hishida, T. (2016). Srs2 and Mus81-Mms4 Prevent Accumulation of Toxic Inter-Homolog Recombination Intermediates. PLoS Genet *12*, e1006136.

Klapholz, S., and Esposito, R.E. (1982). A new mapping method employing a meiotic rec-mutant of yeast. Genetics *100*, 387-412.

Klein, F., Mahr, P., Galova, M., Buonomo, S.B., Michaelis, C., Nairz, K., and Nasmyth, K. (1999). A central role for cohesins in sister chromatid cohesion, formation of axial elements, and recombination during yeast meiosis. Cell *98*, 91-103.

Klein, H.L. (1997). RDH54, a RAD54 homologue in Saccharomyces cerevisiae, is required for mitotic diploid-specific recombination and repair and for meiosis. Genetics *147*, 1533-1543.

Klein, H.L. (2001). Mutations in recombinational repair and in checkpoint control genes suppress the lethal combination of srs2Delta with other DNA repair genes in Saccharomyces cerevisiae. Genetics *157*, 557-565.

Kobayashi, W., Hosoya, N., Machida, S., Miyagawa, K., and Kurumizaka, H. (2017). SYCP3 regulates strand invasion activities of RAD51 and DMC1. Genes Cells *22*, 799-809.

Kobayashi, W., Takaku, M., Machida, S., Tachiwana, H., Maehara, K., Ohkawa, Y., and Kurumizaka, H. (2016). Chromatin architecture may dictate the target site for DMC1, but not for RAD51, during homologous pairing. Sci Rep *6*, 24228.

Kolesar, P., Altmannova, V., Silva, S., Lisby, M., and Krejci, L. (2016). Pro-recombination Role of Srs2 Protein Requires SUMO (Small Ubiquitin-like Modifier) but Is Independent of PCNA (Proliferating Cell Nuclear Antigen) Interaction. J Biol Chem *291*, 7594-7607.

Kolesar, P., Sarangi, P., Altmannova, V., Zhao, X., and Krejci, L. (2012). Dual roles of the SUMO-interacting motif in the regulation of Srs2 sumoylation. Nucleic Acids Res *40*, 7831-7843.

Kramarz, K., Mucha, S., Litwin, I., Barg-Wojas, A., Wysocki, R., and Dziadkowiec, D. (2017). DNA Damage Tolerance Pathway Choice Through Uls1 Modulation of Srs2 SUMOylation in Saccharomyces cerevisiae. Genetics *206*, 513-525.

Krasner, D.S., Daley, J.M., Sung, P., and Niu, H. (2015). Interplay between Ku and Replication Protein A in the Restriction of Exo1-mediated DNA Break End Resection. J Biol Chem *290*, 18806-18816.

Krejci, L., Altmannova, V., Spirek, M., and Zhao, X. (2012). Homologous recombination and its regulation. Nucleic Acids Res *40*, 5795-5818.

Krejci, L., Van Komen, S., Li, Y., Villemain, J., Reddy, M.S., Klein, H., Ellenberger, T., and Sung, P. (2003). DNA helicase Srs2 disrupts the Rad51 presynaptic filament. Nature *423*, 305-309.

Kusano, K., Berres, M.E., and Engels, W.R. (1999). Evolution of the RECQ family of helicases: A drosophila homolog, Dmblm, is similar to the human bloom syndrome gene. Genetics *151*, 1027-1039.

Lawrence, C.W., and Christensen, R.B. (1979). Metabolic suppressors of trimethoprim and ultraviolet light sensitivities of Saccharomyces cerevisiae rad6 mutants. J Bacteriol *139*, 866-876.

Le Breton, C., Dupaigne, P., Robert, T., Le Cam, E., Gangloff, S., Fabre, F., and Veaute, X. (2008). Srs2 removes deadly recombination intermediates independently of its interaction with SUMO-modified PCNA. Nucleic Acids Res *36*, 4964-4974.

Lee, J.Y., Qi, Z., and Greene, E.C. (2016). ATP hydrolysis Promotes Duplex DNA Release by the RecA Presynaptic Complex. J Biol Chem *291*, 22218-22230.

Leon Ortiz, A.M., Reid, R.J., Dittmar, J.C., Rothstein, R., and Nicolas, A. (2011). Srs2 overexpression reveals a helicase-independent role at replication forks that requires diverse cell functions. DNA Repair (Amst) *10*, 506-517.

Leu, J.Y., Chua, P.R., and Roeder, G.S. (1998). The meiosis-specific Hop2 protein of S. cerevisiae ensures synapsis between homologous chromosomes. Cell *94*, 375-386.

Liberi, G., Chiolo, I., Pellicioli, A., Lopes, M., Plevani, P., Muzi-Falconi, M., and Foiani, M. (2000). Srs2 DNA helicase is involved in checkpoint response and its regulation requires a functional Mec1-dependent pathway and Cdk1 activity. EMBO J *19*, 5027-5038.

Lisby, M., Barlow, J.H., Burgess, R.C., and Rothstein, R. (2004). Choreography of the DNA damage response: spatiotemporal relationships among checkpoint and repair proteins. Cell *118*, 699-713.

Liu, J., Ede, C., Wright, W.D., Gore, S.K., Jenkins, S.S., Freudenthal, B.D., Todd Washington, M., Veaute, X., and Heyer, W.D. (2017). Srs2 promotes synthesis-dependent strand annealing by disrupting DNA polymerase delta-extending D-loops. Elife *6*.

Liu, J., Renault, L., Veaute, X., Fabre, F., Stahlberg, H., and Heyer, W.D. (2011). Rad51 paralogues Rad55-Rad57 balance the antirecombinase Srs2 in Rad51 filament formation. Nature *479*, 245-248.

Liu, Y., Sung, S., Kim, Y., Li, F., Gwon, G., Jo, A., Kim, A.K., Kim, T., Song, O.K., Lee, S.E., *et al.* (2016). ATP-dependent DNA binding, unwinding, and resection by the Mre11/Rad50 complex. EMBO J *35*, 743-758.

Lohman, T.M., Tomko, E.J., and Wu, C.G. (2008). Non-hexameric DNA helicases and translocases: mechanisms and regulation. Nat Rev Mol Cell Biol *9*, 391-401.

Loidl, J., Klein, F., and Scherthan, H. (1994). Homologous pairing is reduced but not abolished in asynaptic mutants of yeast. J Cell Biol *125*, 1191-1200.

Lorenz, A. (2017). Modulation of meiotic homologous recombination by DNA helicases. Yeast *34*, 195-203.

Lorenz, A., Osman, F., Folkyte, V., Sofueva, S., and Whitby, M.C. (2009). Fbh1 limits Rad51-dependent recombination at blocked replication forks. Mol Cell Biol *29*, 4742-4756.

Lv, W., Budke, B., Pawlowski, M., Connell, P.P., and Kozikowski, A.P. (2016). Development of Small Molecules that Specifically Inhibit the D-loop Activity of RAD51. J Med Chem *59*, 4511-4525.

Lytle, A.K., Origanti, S.S., Qiu, Y., VonGermeten, J., Myong, S., and Antony, E. (2014). Context-dependent remodeling of Rad51-DNA complexes by Srs2 is mediated by a specific protein-protein interaction. J Mol Biol *426*, 1883-1897.

Manfrini, N., Guerini, I., Citterio, A., Lucchini, G., and Longhese, M.P. (2010). Processing of meiotic DNA double strand breaks requires cyclin-dependent kinase and multiple nucleases. J Biol Chem *285*, 11628-11637.

Marini, V., and Krejci, L. (2010). Srs2: the "Odd-Job Man" in DNA repair. DNA Repair (Amst) *9*, 268-275.

Martinez-Perez, E., and Colaiacovo, M.P. (2009). Distribution of meiotic recombination events: talking to your neighbors. Curr Opin Genet Dev *19*, 105-112.

Martini, E., Diaz, R.L., Hunter, N., and Keeney, S. (2006). Crossover homeostasis in yeast meiosis. Cell *126*, 285-295.

Martino, J., and Bernstein, K.A. (2016). The Shu complex is a conserved regulator of homologous recombination. FEMS Yeast Res *16*.

Masson, J.Y., and West, S.C. (2001). The Rad51 and Dmc1 recombinases: a non-identical twin relationship. Trends Biochem Sci *26*, 131-136.

Matos, J., Blanco, M.G., and West, S.C. (2013). Cell-cycle kinases coordinate the resolution of recombination intermediates with chromosome segregation. Cell Rep *4*, 76-86.

Mazin, A.V., Mazina, O.M., Bugreev, D.V., and Rossi, M.J. (2010). Rad54, the motor of homologous recombination. DNA Repair (Amst) *9*, 286-302.

McVey, M., Kaeberlein, M., Tissenbaum, H.A., and Guarente, L. (2001). The short life span of Saccharomyces cerevisiae sgs1 and srs2 mutants is a composite of normal aging processes and mitotic arrest due to defective recombination. Genetics *157*, 1531-1542.

Miller, A.S., Daley, J.M., Pham, N.T., Niu, H., Xue, X., Ira, G., and Sung, P. (2017). A novel role of the Dna2 translocase function in DNA break resection. Genes Dev *31*, 503-510.

Mimitou, E.P., and Symington, L.S. (2008). Sae2, Exo1 and Sgs1 collaborate in DNA double-strand break processing. Nature *455*, 770-774.

Mimitou, E.P., and Symington, L.S. (2009). Nucleases and helicases take center stage in homologous recombination. Trends Biochem Sci *34*, 264-272.

Mirkin, S.M. (2007). Expandable DNA repeats and human disease. Nature *447*, 932-940.

Mitchel, K., Lehner, K., and Jinks-Robertson, S. (2013). Heteroduplex DNA position defines the roles of the Sgs1, Srs2, and Mph1 helicases in promoting distinct recombination outcomes. PLoS Genet *9*, e1003340.

Miura, T., Shibata, T., and Kusano, K. (2013). Putative antirecombinase Srs2 DNA helicase promotes noncrossover homologous recombination avoiding loss of heterozygosity. Proc Natl Acad Sci U S A *110*, 16067-16072.

Moldovan, G.L., Dejsuphong, D., Petalcorin, M.I., Hofmann, K., Takeda, S., Boulton, S.J., and D'Andrea, A.D. (2012). Inhibition of homologous recombination by the PCNA-interacting protein PARI. Mol Cell *45*, 75-86.

Moreau, S., Ferguson, J.R., and Symington, L.S. (1999). The nuclease activity of Mre11 is required for meiosis but not for mating type switching, end joining, or telomere maintenance. Mol Cell Biol *19*, 556-566.

Muller, B., Koller, T., and Stasiak, A. (1990). Characterization of the DNA binding activity of stable RecA-DNA complexes. Interaction between the two DNA binding sites within RecA helical filaments. J Mol Biol *212*, 97-112.

Nakada, D., Matsumoto, K., and Sugimoto, K. (2003). ATM-related Tel1 associates with double-strand breaks through an Xrs2-dependent mechanism. Genes Dev *17*, 1957-1962.

Neale, M.J., Pan, J., and Keeney, S. (2005). Endonucleolytic processing of covalent protein-linked DNA double-strand breaks. Nature *436*, 1053-1057.

Neiman, A.M. (2005). Ascospore formation in the yeast Saccharomyces cerevisiae. Microbiol Mol Biol Rev *69*, 565-584.

Nguyen, J.H.G., Viterbo, D., Anand, R.P., Verra, L., Sloan, L., Richard, G.F., and Freudenreich, C.H. (2017). Differential requirement of Srs2 helicase and Rad51 displacement activities in replication of hairpin-forming CAG/CTG repeats. Nucleic Acids Res *45*, 4519-4531.

Nimonkar, A.V., Dombrowski, C.C., Siino, J.S., Stasiak, A.Z., Stasiak, A., and Kowalczykowski, S.C. (2012). Saccharomyces cerevisiae Dmc1 and Rad51 proteins preferentially function with Tid1 and Rad54 proteins, respectively, to promote DNA strand invasion during genetic recombination. J Biol Chem *287*, 28727-28737.

Nimonkar, A.V., Sica, R.A., and Kowalczykowski, S.C. (2009). Rad52 promotes second-end DNA capture in double-stranded break repair to form complement-stabilized joint molecules. Proc Natl Acad Sci U S A *106*, 3077-3082.

Niu, H., Chung, W.H., Zhu, Z., Kwon, Y., Zhao, W., Chi, P., Prakash, R., Seong, C., Liu, D., Lu, L., *et al.* (2010). Mechanism of the ATP-dependent DNA end-resection machinery from Saccharomyces cerevisiae. Nature *467*, 108-111.

Niu, H., and Klein, H.L. (2017). Multifunctional roles of Saccharomyces cerevisiae Srs2 protein in replication, recombination and repair. FEMS Yeast Res *17*.

Niu, H., Li, X., Job, E., Park, C., Moazed, D., Gygi, S.P., and Hollingsworth, N.M. (2007). Mek1 kinase is regulated to suppress double-strand break repair between sister chromatids during budding yeast meiosis. Mol Cell Biol *27*, 5456-5467.

Niu, H., Potenski, C.J., Epshtein, A., Sung, P., and Klein, H.L. (2016). Roles of DNA helicases and Exo1 in the avoidance of mutations induced by Top1-mediated cleavage at ribonucleotides in DNA. Cell Cycle *15*, 331-336.

Niu, H., Wan, L., Baumgartner, B., Schaefer, D., Loidl, J., and Hollingsworth, N.M. (2005). Partner choice during meiosis is regulated by Hop1-promoted dimerization of Mek1. Mol Biol Cell *16*, 5804-5818.

Niu, H., Wan, L., Busygina, V., Kwon, Y., Allen, J.A., Li, X., Kunz, R.C., Kubota, K., Wang, B., Sung, P., *et al.* (2009). Regulation of meiotic recombination via Mek1-mediated Rad54 phosphorylation. Mol Cell *36*, 393-404.

Palladino, F., and Klein, H.L. (1992). Analysis of mitotic and meiotic defects in Saccharomyces cerevisiae SRS2 DNA helicase mutants. Genetics *132*, 23-37.

Papouli, E., Chen, S., Davies, A.A., Huttner, D., Krejci, L., Sung, P., and Ulrich, H.D. (2005). Crosstalk between SUMO and ubiquitin on PCNA is mediated by recruitment of the helicase Srs2p. Mol Cell *19*, 123-133.

Parry, E.M., and Cox, B.S. (1970). The tolerance of aneuploidy in yeast. Genet Res *16*, 333-340.

Patel, D.S., Misenko, S.M., Her, J., and Bunting, S.F. (2017). BLM helicase regulates DNA repair by counteracting RAD51 loading at DNA double-strand break sites. J Cell Biol *216*, 3521-3534.

Pellegrini, L., and Venkitaraman, A. (2004). Emerging functions of BRCA2 in DNA recombination. Trends Biochem Sci *29*, 310-316.

Petes, T.D. (2001). Meiotic recombination hot spots and cold spots. Nat Rev Genet *2*, 360-369.

Petukhova, G., Sung, P., and Klein, H. (2000). Promotion of Rad51-dependent D-loop formation by yeast recombination factor Rdh54/Tid1. Genes Dev *14*, 2206-2215.

Petukhova, G.V., Pezza, R.J., Vanevski, F., Ploquin, M., Masson, J.Y., and Camerini-Otero, R.D. (2005). The Hop2 and Mnd1 proteins act in concert with Rad51 and Dmc1 in meiotic recombination. Nat Struct Mol Biol *12*, 449-453.

Pezza, R.J., Voloshin, O.N., Vanevski, F., and Camerini-Otero, R.D. (2007). Hop2/Mnd1 acts on two critical steps in Dmc1-promoted homologous pairing. Genes Dev *21*, 1758-1766.

Pfander, B., Moldovan, G.L., Sacher, M., Hoege, C., and Jentsch, S. (2005). SUMO-modified PCNA recruits Srs2 to prevent recombination during S phase. Nature *436*, 428-433.

Pierce, A.J., Hu, P., Han, M., Ellis, N., and Jasin, M. (2001). Ku DNA end-binding protein modulates homologous repair of double-strand breaks in mammalian cells. Genes Dev *15*, 3237-3242.

Potenski, C.J., Niu, H., Sung, P., and Klein, H.L. (2014). Avoidance of ribonucleotide-induced mutations by RNase H2 and Srs2-Exo1 mechanisms. Nature *511*, 251-254.

Prakash, R., Satory, D., Dray, E., Papusha, A., Scheller, J., Kramer, W., Krejci, L., Klein, H., Haber, J.E., Sung, P.*, et al.* (2009). Yeast Mph1 helicase dissociates Rad51-made D-loops: implications for crossover control in mitotic recombination. Genes Dev *23*, 67-79.

Prugar, E., Burnett, C., Chen, X., and Hollingsworth, N.M. (2017). Coordination of Double Strand Break Repair and Meiotic Progression in Yeast by a Mek1-Ndt80 Negative Feedback Loop. Genetics *206*, 497-512.

Qiu, Y.P., Anthony, E., Lohman, T., and Myong, S. (2013). Srs2 Prevents Rad51 Filament Formation by Repetitive Scrunching of DNA. Biophys J *104*, 75a-75a.

Radford, S.J., Hoang, T.L., Gluszek, A.A., Ohkura, H., and McKim, K.S. (2015). Lateral and End-On Kinetochore Attachments Are Coordinated to Achieve Bi-orientation in Drosophila Oocytes. PLoS Genet *11*, e1005605.

Refolio, E., Cavero, S., Marcon, E., Freire, R., and San-Segundo, P.A. (2011). The Ddc2/ATRIP checkpoint protein monitors meiotic recombination intermediates. J Cell Sci *124*, 2488-2500.

Robertson, R.B., Moses, D.N., Kwon, Y., Chan, P., Chi, P., Klein, H., Sung, P., and Greene, E.C. (2009). Structural transitions within human Rad51 nucleoprotein filaments. Proc Natl Acad Sci U S A *106*, 12688-12693.

Rockmill, B., Fung, J.C., Branda, S.S., and Roeder, G.S. (2003). The Sgs1 helicase regulates chromosome synapsis and meiotic crossing over. Curr Biol *13*, 1954-1962.

Rong, L., Palladino, F., Aguilera, A., and Klein, H.L. (1991). The hyper-gene conversion hpr5-1 mutation of Saccharomyces cerevisiae is an allele of the SRS2/RADH gene. Genetics *127*, 75-85.

Saponaro, M., Callahan, D., Zheng, X., Krejci, L., Haber, J.E., Klein, H.L., and Liberi, G. (2010). Cdk1 targets Srs2 to complete synthesis-dependent strand annealing and to promote recombinational repair. PLoS Genet *6*, e1000858.

Sarangapani, K.K., Duro, E., Deng, Y., Alves Fde, L., Ye, Q., Opoku, K.N., Ceto, S., Rappsilber, J., Corbett, K.D., Biggins, S.*, et al.* (2014). Sister kinetochores are mechanically fused during meiosis I in yeast. Science *346*, 248-251.

Sasanuma, H., Furihata, Y., Shinohara, M., and Shinohara, A. (2013a). Remodeling of the Rad51 DNA strand-exchange protein by the Srs2 helicase. Genetics *194*, 859-872.

Sasanuma, H., Tawaramoto, M.S., Lao, J.P., Hosaka, H., Sanda, E., Suzuki, M., Yamashita, E., Hunter, N., Shinohara, M., Nakagawa, A.*, et al.* (2013b). A new protein complex promoting the assembly of Rad51 filaments. Nat Commun *4*, 1676.

Schiestl, R.H., Prakash, S., and Prakash, L. (1990). The SRS2 suppressor of rad6 mutations of Saccharomyces cerevisiae acts by channeling DNA lesions into the RAD52 DNA repair pathway. Genetics *124*, 817-831.

Schwacha, A., and Kleckner, N. (1997). Interhomolog bias during meiotic recombination: meiotic functions promote a highly differentiated interhomolog-only pathway. Cell *90*, 1123-1135.

Senavirathne, G., Mahto, S.K., Hanne, J., O'Brian, D., and Fishel, R. (2017). Dynamic unwrapping of nucleosomes by HsRAD51 that includes sliding and rotational motion of histone octamers. Nucleic Acids Res *45*, 685-698.

Seong, C., Colavito, S., Kwon, Y., Sung, P., and Krejci, L. (2009). Regulation of Rad51 recombinase presynaptic filament assembly via interactions with the Rad52 mediator and the Srs2 anti-recombinase. J Biol Chem *284*, 24363-24371.

Sheridan, S., and Bishop, D.K. (2006). Red-Hed regulation: recombinase Rad51, though capable of playing the leading role, may be relegated to supporting Dmc1 in budding yeast meiosis. Gene Dev *20*, 1685-1691.

Shim, E.Y., Chung, W.H., Nicolette, M.L., Zhang, Y., Davis, M., Zhu, Z., Paull, T.T., Ira, G., and Lee, S.E. (2010). Saccharomyces cerevisiae Mre11/Rad50/Xrs2 and Ku proteins regulate association of Exo1 and Dna2 with DNA breaks. EMBO J *29*, 3370-3380.

Shinohara, A., and Ogawa, T. (1998). Stimulation by Rad52 of yeast Rad51-mediated recombination. Nature *391*, 404-407.

Shinohara, M., Shita-Yamaguchi, E., Buerstedde, J.M., Shinagawa, H., Ogawa, H., and Shinohara, A. (1997). Characterization of the roles of the Saccharomyces cerevisiae RAD54 gene and a homologue of RAD54, RDH54/TID1, in mitosis and meiosis. Genetics *147*, 1545-1556.

Shonn, M.A., McCarroll, R., and Murray, A.W. (2000). Requirement of the spindle checkpoint for proper chromosome segregation in budding yeast meiosis. Science *289*, 300-303.

Short, J.M., Liu, Y., Chen, S., Soni, N., Madhusudhan, M.S., Shivji, M.K., and Venkitaraman, A.R. (2016). High-resolution structure of the presynaptic RAD51 filament on single-stranded DNA by electron cryo-microscopy. Nucleic Acids Res *44*, 9017-9030.

Smith, K.N., and Nicolas, A. (1998). Recombination at work for meiosis. Curr Opin Genet Dev *8*, 200-211.

Solinger, J.A., Kiianitsa, K., and Heyer, W.D. (2002). Rad54, a Swi2/Snf2-like recombinational repair protein, disassembles Rad51:dsDNA filaments. Mol Cell *10*, 1175-1188.

Suhandynata, R.T., Wan, L., Zhou, H., and Hollingsworth, N.M. (2016). Identification of Putative Mek1 Substrates during Meiosis in Saccharomyces cerevisiae Using Quantitative Phosphoproteomics. PLoS One *11*, e0155931.

Sun, W., Lorenz, A., Osman, F., and Whitby, M.C. (2011). A failure of meiotic chromosome segregation in a fbh1Delta mutant correlates with persistent Rad51-DNA associations. Nudeic Acids Res *39*, 1718-1731.

Sung, P. (1997). Yeast Rad55 and Rad57 proteins form a heterodimer that functions with replication protein A to promote DNA strand exchange by Rad51 recombinase. Genes Dev *11*, 1111-1121.

Sung, P., and Klein, H. (2006). Mechanism of homologous recombination: mediators and helicases take on regulatory functions. Nat Rev Mol Cell Biol *7*, 739-750.

Tsubouchi, H., and Ogawa, H. (1998). A novel mre11 mutation impairs processing of double-strand breaks of DNA during both mitosis and meiosis. Mol Cell Biol *18*, 260-268.

Tsubouchi, H., and Roeder, G.S. (2002). The Mnd1 protein forms a complex with hop2 to promote homologous chromosome pairing and meiotic double-strand break repair. Mol Cell Biol *22*, 3078-3088.

Tsubouchi, H., and Roeder, G.S. (2003). The importance of genetic recombination for fidelity of chromosome pairing in meiosis. Dev Cell *5*, 915-925.

Tsubouchi, H., and Roeder, G.S. (2004). The budding yeast mei5 and sae3 proteins act together with dmc1 during meiotic recombination. Genetics *168*, 1219-1230.

Tsubouchi, H., and Roeder, G.S. (2006). Budding yeast Hed1 down-regulates the mitotic recombination machinery when meiotic recombination is impaired. Genes Dev *20*, 1766-1775.

Tsukamoto, Y., Mitsuoka, C., Terasawa, M., Ogawa, H., and Ogawa, T. (2005). Xrs2p regulates Mre11p translocation to the nucleus and plays a role in telomere elongation and meiotic recombination. Mol Biol Cell *16*, 597-608.

Tsutsui, Y., Kurokawa, Y., Ito, K., Siddique, M.S., Kawano, Y., Yamao, F., and Iwasaki, H. (2014). Multiple regulation of Rad51-mediated homologous recombination by fission yeast Fbh1. PLoS Genet *10*, e1004542.

Uringa, E.J., Youds, J.L., Lisaingo, K., Lansdorp, P.M., and Boulton, S.J. (2011). RTEL1: an essential helicase for telomere maintenance and the regulation of homologous recombination. Nucleic Acids Res *39*, 1647-1655.

Urulangodi, M., Sebesta, M., Menolfi, D., Szakal, B., Sollier, J., Sisakova, A., Krejci, L., and Branzei, D. (2015). Local regulation of the Srs2 helicase by the SUMO-like domain protein Esc2 promotes recombination at sites of stalled replication. Genes Dev *29*, 2067-2080.

Usui, T., Ohta, T., Oshiumi, H., Tomizawa, J., Ogawa, H., and Ogawa, T. (1998). Complex formation and functional versatility of Mre11 of budding yeast in recombination. Cell *95*, 705-716.

Vaze, M.B., Pellicioli, A., Lee, S.E., Ira, G., Liberi, G., Arbel-Eden, A., Foiani, M., and Haber, J.E. (2002). Recovery from checkpoint-mediated arrest after repair of a double-strand break requires Srs2 helicase. Mol Cell *10*, 373-385.

Veaute, X., Jeusset, J., Soustelle, C., Kowalczykowski, S.C., Le Cam, E., and Fabre, F. (2003). The Srs2 helicase prevents recombination by disrupting Rad51 nucleoprotein filaments. Nature *423*, 309-312.

Venclovas, C., and Thelen, M.P. (2000). Structure-based predictions of Rad1, Rad9, Hus1 and Rad17 participation in sliding clamp and clamp-loading complexes. Nucleic Acids Res *28*, 2481-2493.

Weidberg, H., Moretto, F., Spedale, G., Amon, A., and van Werven, F.J. (2016). Nutrient Control of Yeast Gametogenesis Is Mediated by TORC1, PKA and Energy Availability. PLoS Genet *12*, e1006075.

Whitby, M.C. (2010). The FANCM family of DNA helicases/translocases. DNA Repair (Amst) *9*, 224-236.

Xu, L., Ajimura, M., Padmore, R., Klein, C., and Kleckner, N. (1995). NDT80, a meiosis-specific gene required for exit from pachytene in Saccharomyces cerevisiae. Mol Cell Biol *15*, 6572-6581.

Xu, L., Weiner, B.M., and Kleckner, N. (1997). Meiotic cells monitor the status of the interhomolog recombination complex. Genes Dev *11*, 106-118.

Yang, F., and Wang, P.J. (2009). The Mammalian synaptonemal complex: a scaffold and beyond. Genome Dyn *5*, 69-80.

Zakharyevich, K., Ma, Y., Tang, S., Hwang, P.Y., Boiteux, S., and Hunter, N. (2010). Temporally and biochemically distinct activities of Exo1 during meiosis: double-strand break resection and resolution of double Holliday junctions. Mol Cell *40*, 1001-1015.

Zhu, Z., Chung, W.H., Shim, E.Y., Lee, S.E., and Ira, G. (2008). Sgs1 helicase and two nucleases Dna2 and Exo1 resect DNA double-strand break ends. Cell *134*, 981-994.

Zickler, D., and Kleckner, N. (1999). Meiotic chromosomes: integrating structure and function. Annu Rev Genet *33*, 603-754.

Zickler, D., and Kleckner, N. (2016). A few of our favorite things: Pairing, the bouquet, crossover interference and evolution of meiosis. Semin Cell Dev Biol *54*, 135-148.

Zierhut, C., Berlinger, M., Rupp, C., Shinohara, A., and Klein, F. (2004). Mnd1 is required for meiotic interhomolog repair. Curr Biol *14*, 752-762.